CENTRO INTERNACIONAL DE ESTUDOS
DE DOUTORAMENTO E AVANZADOS
DA USC (CIEDUS)

TESE DE DOUTORAMENTO

CONTRIBUTION TO WASTE VALORISATION BY PRODUCING BIOCHARS FOR DIFFERENT ENVIRONMENTAL PURPOSES

RUTH SAIZ RUBIO

ESCOLA DE DOUTORAMENTO INTERNACIONAL

PROGRAMA DE DOUTORAMENTO EN MEDIO AMBIENTE Y RECURSOS NATURALES

SANTIAGO DE COMPOSTELA

2018

USC
UNIVERSIDADE
DE SANTIAGO
DE COMPOSTELA

DECLARACIÓN DA AUTORA DA TESE

Contribution to waste valorisation by producing biochars for different environmental purposes

Dna. Ruth Saiz Rubio

Presento a miña tese, seguindo o procedemento axeitado ao Regulamento, e declaro que:

1) A tese abarca os resultados da elaboración do meu traballo.
2) De selo caso, na tese faise referencia ás colaboracións que tivo este traballo.
3) A tese é a versión definitiva presentada para a súa defensa e coincide coa versión enviada en formato electrónico.
4) Confirmo que a tese non incorre en ningún tipo de plaxio doutros autores nin de traballos presentados por min para a obtención doutros títulos.

En Santiago de Compostela, 15 de Junio de 2018

Asdo. Ruth Saiz Rubio.

USC
UNIVERSIDADE
DE SANTIAGO
DE COMPOSTELA

AUTORIZACIÓN DO DIRECTOR / TITOR DA TESE

Contribution to waste valorisation by producing biochars for different environmental purposes

D. Felipe Macías Vázquez
Dna. Marta Camps Arbestain

INFORMAN:

Que a presente tese, correspóndese co traballo realizado por D/Dna. ***Ruth Saiz Rubio****, baixo a nosa dirección, e autorizamos a súa presentación, considerando que reúne os requisitos esixidos no Regulamento de Estudos de Doutoramento da USC, e que como director desta non incorre nas causas de abstención establecidas na Lei 40/2015.*

En Santiago de Compostela, 15 de Junio de 2018

Marta Camps Arbestain
Firmado digitalmente por Marta Camps Arbestain
Fecha: 2018.06.15 09:46:55 +02'00'

Asdo. Felipe Macías Vázquez Asdo. Marta Camps Arbestain

USC
UNIVERSIDADE
DE SANTIAGO
DE COMPOSTELA

A mi familia

USC
UNIVERSIDADE
DE SANTIAGO
DE COMPOSTELA

Contents

USC
UNIVERSIDADE
DE SANTIAGO
DE COMPOSTELA

List of Figures

List of Tables

USC
UNIVERSIDADE
DE SANTIAGO
DE COMPOSTELA

List of Abbreviations

A	Absorbance
AC	Activated carbon
ADE	Anthropogenic Dark Earths
ANOVA	Analysis of variance
Av	Available
BC	Black carbon
BC_{+100}	Fraction of C in biochar that will remain stable in soil for more than 100 years
BTEX	Benzene, Toluene, Ethylbenzene, Xylene
CDB	Sodium citrate, sodium dithionite and sodium bicarbonate mixture
C_{dichro}	Carbon oxidisable with dichromate
C_{easyOx}	C easily oxidisable
CEC	Cation exchange capacity
C_{hardOx}	Carbon hardly oxidisable
C_{inorg}	Inorganic carbon
C_{nox}	Non oxidisable carbon
CO_2-C_e	Equivalent CO_2
CONCAWE	Conservation of Clean Air and Water in Europe
C_{org}	Organic carbon
Cp	C extractable with pyrophosphate
C_{per}	Permanganate oxidisable carbon
C_T	Total carbon
C_{thermo}	Thermo-degradable C fraction
CVAN	Centro de Valorización Ambiental del Norte S.L
dH	Enthalpy change for the reaction
DSC	Differential scanning calorimetry
EBC	European Biochar Certificate
EDX	Energy dispersive X-ray microanalysis

Eh	Redox potential
FAO	Food and agriculture organization of the United Nations
FB	Fluorobenzene
FixC	Fixed carbon
FO	Fuel oxygenates
FTIR	Fourier transform infrared spectroscopy
GC-MS	Gas chromatography–mass spectrometry
GDP	Gross Domestic Product
GEI	Gas de efecto invernadero
HHT	Highest heating temperature
HTC	Hydrothermal carbonization
IBI	International Biochar Initiative
IFN4	IV Inventario Forestal Nacional
IPCC	Intergovernmental Panel on Climate Change
LTA-USC	Laboratorio de Tecnología Ambiental Universidad de Santiago de Compostela
MAPAMA	Ministerio de Agricultura y Pesca, Alimentación y Medio Ambiente
NIRS	Near infrared spectroscopy
NMR	Nuclear magnetic resonance spectra
NZBRC	New Zealand Biochar Research Centre
PAHs	Polycyclic aromatic hydrocarbons
PAW	Plant-available water
PC	Principal components
PCA	Principal components analysis
PCBs	Polychlorinated biphenyls
PCM	Pyrogenic carbonaceous material
Pi	Inorganic phosphorus
Po	Organic phosphorus
ppm	Part per million
PWP	Permanent wilting point

R	Reflectance
R50	Recalcitrance Index
sBC_{+100}	Storage value
SEM	Scanning electron microscopy
SIC	Soil inorganic carbon
SOC	Soil organic carbon
Spp.	species
SSA	Specific surface area
TGA	Thermogravimetric analysis
TPH	Total petrol hydrocarbons
UKBRC	United Kingdom biochar research centre
UMSICHT	Fraunhofer Institute for Environmental, safety, and Energy technology
USBI	United States Biochar Initiative
USEPA	United Stated Environmental Protection Agency
UNFCCC	United Nations Framework Convention on Climate Change
VFOC	Volatile fuel organic compounds
VM	Volatile matter
WHC	Water holding capacity
WMO	World Meteorological Organization
WRB	World Reference Base for soil resources

List of feedstocks

AcB	Acacia bark
AcHw	Acacia heartwood
AcSw	Acacia sapwood
Cc	Corncob
Cm	Chicken manure
Cn	Chestnut
Eu	Eucalyptus
Mis	Miscanthus
Opc	Olive pomace compost
Pb	Pine bark
Pl	Plastic
Rh	Rice husk
Sd	Sawdust
Ty	Tyre
Vn	Vine shoot

List of biochars

BCc-1	Corncob (2014)
BCc-2	Corncob (2014)
BCc-3	Corncob (3 h) control low O_2 (2015)
BAcB	*Acacia melanoxylon* Bark 2h 350 °C (2014)
BAcSw-1	*Acacia melanoxylon* sapwood 3 h 350 °C (2014)
BAcSw-2	*Acacia melanoxylon* sapwood 2 h 350 °C (2014)
BAcSw-3	*Acacia melanoxylon* sapwood 2 h 300 °C (2014)
BAcHw-1	*Acacia melanoxylon* heartwood 3 h 350 °C (2014)
BAcHw-2	*Acacia melanoxylon* heartwood 2 h 300 °C (2014)
BEu-1	Eucalyptus 1 h 400 °C, 0.5 h 350 °C (2014)
BEu-2	Eucalyptus (2014)
BSd-1	Sawdust (2014)
BSd-2	Compacted sawdust 3.5 h 300 °C (2014)
BCm	Chicken manure 6h 300 °C (2014)
BOpc	Olive pomace compost 5.5 h 450 °C (2014)
BCn	Chestnut (2014)
BMis	Miscanthus (2015)
BVs	Vine shoots (2015)
BPl	Plastic wastes (2015)
BPb	Pine bark (2014)
BRh	Rice husk (2014)
BSdG	German crushed wood chip biochar
BTy	Tyre (2015)
Bbark	Pine bark commercial charcoal
Btrunk	Pine trunk commercial charcoal

USC
UNIVERSIDADE
DE SANTIAGO
DE COMPOSTELA

Resumen

La sociedad actual se enfrenta a grandes retos ambientales, como son asegurar la alimentación a una población mundial en continuo aumento sin incrementar los impactos sobre el medio ambiente, recuperar la creciente extensión de tierras contaminadas y degradadas, mejorar la gestión de residuos, y hacer frente al cambio climático global. Las diferentes políticas ambientales y la nueva concepción sobre los residuos en un ámbito de economía circular, inciden en que éstos deben ser considerados como recursos que están en un lugar o en una forma inapropiada. La valorización energética de los residuos para producción de energía y aprovechamiento de los co-productos que se generan, es una buena forma de gestionar y dar valor a los mismos.

El biocarbón o biochar es un carbón con alto contenido orgánico y altamente resistente a la descomposición que se produce a partir de la degradación térmica de biomasa en ausencia de oxígeno mediante un proceso de pirólisis. Su alto contenido en carbono recalcitrante hace que, al aplicarlo al suelo, sirva como reserva para el secuestro de carbono, ayudando a mitigar el cambio climático. Además, también posee propiedades para mejorar la calidad del suelo, aumentando la porosidad, la capacidad de retención de agua, el aporte de nutrientes y la capacidad de neutralización, entre otros. Asimismo, sirve de herramienta en gestión ambiental al presentar propiedades adsorbentes de contaminantes tanto orgánicos como inorgánicos. El concepto de biochar es reciente, sin embargo su uso se remonta a las tribus precolombinas de la Amazonía brasileña. En esta zona, a finales de siglo XIX, se encontraron suelos antrópicos oscuros, ricos en materia orgánica y C recalcitrante, conocidos como "*Terra preta"* y que eran mucho más fértiles que los suelos que les rodean. Estos suelos se formaron a partir de ferralsoles por la adición de carbón y residuos ricos en nutrientes, dando lugar a unos suelos que han

continuado fértiles durante siglos. Su elevada fertilidad se atribuye principalmente a su contenido en C pirogénico rico en estructuras condensadas aromáticas, usándose esta característica como base para el estudio de la aplicación del biochar a los suelos degradados y contaminados para mejorar sus propiedades.

Las propiedades y calidad del biochar están fuertemente influenciadas por la materia prima que se utilice para su elaboración y por las condiciones de pirólisis (temperatura, tiempo de residencia), por ello los objetivos generales de esta tesis doctoral son por un lado la producción de biocarbones a partir de residuos de distintos orígenes utilizando un reactor experimental que permita la producción a escala semi-industrial (kg por día); y por otro la caracterización de los biocarbones obtenidos para estudiar su potencial en la recuperación de diferentes problemas medioambientales como la fijación de C, la mejora de las propiedades del suelo, la descontaminación de espacios degradados o reducción de la huella de carbono del proceso de producción industrial del silicio.

Para analizar la variabilidad de las propiedades de los biocarbones producidos con gran diversidad de materias primas y establecer su potencial para solucionar distintos problemas medioambientales se plantearon los siguientes objetivos específicos:

- Estimar la temperatura de pirólisis a la que fue producido cada biocarbón mediante técnicas de espectroscopía de infrarrojo próximo.
- Determinar las propiedades y características de los biocarbones producidos, analizando su variabilidad en función de las distintas materias primas y condiciones de pirólisis. Los biocarbones producidos se clasificaron en función de su potencial como fijadores de C para luchar contra el cambio climático y por su capacidad enmendante y fertilizante.

- Establecer la capacidad de los biocarbones para inmovilizar contaminantes orgánicos derivados del petróleo, como son los compuestos orgánicos volátiles o el diésel.
- Estudiar la viabilidad de su aplicación a la industria metalúrgica, como sustituto del carbón en la producción del silicio, lo que supondría una reducción en las emisiones de C.

Las materias primas pueden suponer un importante coste para el sistema de producción de biochar, por lo que es importe buscar materiales de bajo coste, como pueden ser residuos, y que se encuentren cerca de la zona de producción o aplicación para reducir los costes derivados del transporte. Se pretende de esta forma trabajar con un sistema más eficiente, económicamente viable y tendiendo a una economía circular. En este estudio se seleccionaron materias primas de distintos orígenes que incluyen: i) plantas invasoras como la acacia, especie considerada una de las principales amenazas en los bosques gallegos y del resto de la península; ii) residuos forestales y de la industria maderera como ramas y tronco de eucalipto, corteza de pino, viruta; iii) residuos agrícolas como por ejemplo el carozo de maíz, cáscara de arroz, castañas y restos de la poda de la vid; iv) plantas herbáceas como el miscanthus, considerada cultivo energético para la producción de biocombustibles; v) residuos de origen animal y compost como son el estiércol de pollo o el compost de alperujo (subproducto que se obtiene de la producción de aceite de oliva); y vi) residuos industriales como neumáticos usados o plástico de desecho que no puede ser reciclado.

El biochar fue producido en dos reactores experimentales de bajo coste diseñados por el prof. M. Bao y la Dra. T. García-Ares situados en las instalaciones del Centro de Valorización Ambiental del Norte SL (CVAN) (Touro, Santiago de Compostela). Ambos reactores funcionan en modo discontinuo y con carga y descarga manual. Las condiciones de pirólisis varían entre los 300 y 550 °C, y un tiempo de residencia entre 1.5 y 6 h dependiendo de la humedad y propiedades de las materias primas. La temperatura máxima de pirólisis ("highest heating temperature", HHT) es

uno de los factores más importantes que condicionan las propiedades de los biocarbones. Esta temperatura es difícil de determinar con exactitud en un pirolizador experimental como el que se usó en este estudio, debido a los gradientes de temperatura que se forman dentro de la cámara. Por ello, una vez obtenidos los biocarbones, el primer objetivo específico fue estimar la HHT a la que fueron producidos los distintos biocarbones mediante espectroscopía de infrarrojo próximo (NIRS) y la aplicación de modelos matemáticos (**Capítulo 3**). Este método, además de estimar la HHT, permitió clasificar las muestras en biocarbones producidos a alta temperatura (> 400 °C) y a baja temperatura (≤ 400 °C). A temperaturas de pirólisis bajas se obtuvieron espectros de NIRS más heterogéneos, mientras que en los biocarbones producidos a alta temperatura los espectros presentan mayor absorbancia, son más planos y muestran un menor número de picos identificables. La predicción fue menos exhaustiva con las materias primas más heterogéneas y con mayor contenido en humedad como el estiércol de pollo y el compost de alperujo, ya que los distintos componentes que forman la muestra reaccionan de manera diferente a la degradación térmica, especialmente a baja temperatura. El proceso de pirólisis debe ser optimizado para cada tipo de materia prima, dependiendo de su composición y humedad original. La precisión de la estimación de la HHT se verificará en el siguiente capítulo al relacionarla con las propiedades del biocarbón que dependen de la degradación térmica, como puede ser la relación H/C, el porcentaje de C fijo o la concentración de C aromático.

En el **Capítulo 4**, se estudiaron las propiedades físico-químicas del biocarbón para determinar su potencial en la fijación de C y se clasifican las muestras en concordancia con ello. Se emplearon diferentes técnicas para determinar la estabilidad de las formas de C del biocarbón que van desde el análisis elemental, oxidación química de las formas de C, análisis termogravimétrico, resonancia magnético nuclear (NMR) y análisis infrarrojo por transformada de Fourier (FTIR).

En primer lugar se llevó a cabo el análisis elemental tanto de las materias primas como de las muestras de biocarbón obtenidas. Durante la pirólisis se produce un incremento de la proporción en C, al pasar de valores entre 29-48% en la biomasa de la materia prima a un contenido total en C del 29-89% en los biocarbones. Los biocarbones más ricos en C coinciden con los que se estimó una HHT > 400 °C. El análisis elemental permite la primera clasificación de los biocarbones, ya que cuando se obtienen valores del ratio H/C_{org} superiores a 0.7, los materiales no pueden ser considerados "biochar" según los requisitos del "International Biochar Initiative" (IBI) y el "European Biochar Certificate" (EBC), denominándose como material pirogénico carbonoso o "pyrogenic carbonaceous materials" (PCM). Según este criterio, 9 de las muestras analizadas se consideran PCM y se corresponden con las muestras cuya HHT ≤ 400 °C: biocarbón de corteza de acacia (BAcB), de tronco de acacia (BAcSw-1, BAcSw-3 y BAcHw-2), de eucalipto (BEu-1), de viruta de pino (BSd-1), de estiércol de pollo (BCm), de compost de alperujo (BOpc) y el biocarbón de plástico (BPl). Además el análisis elemental permite una segunda clasificación según el contenido de C orgánico (C_{org}). De acuerdo con la clasificación establecida por el IBI, la mayor parte de los biocarbones analizados corresponden a la Clase 1 (C_{org} ≥ 60%), mientras que los biocarbones de cáscara de arroz (BRh), de neumático (BTy) y BCm pertenecen a la Clase 2 (30% ≥ C_{org} < 60%) y BOpc fue clasificado como Clase 3 (10% ≥ C_{org} < 30%). Los biocarbones también se pueden clasificar en base a su recalcitrancia, para lo que es necesario determinar que fracción del C_{org} va a permanecer estable en el suelo más de 100 años (BC_{+100}). Siguiendo una clasificación en base al valor de almacenamiento de C total (sBC_{+100}), los biocarbones procedentes de carozo de maíz (BCc-2 y BCc-3), de eucalipto (BEu-2), miscanthus (BMis) y corteza de pino (BPb) satisfacen la mejor clase (Clase 5), con más de 600 g kg^{-1} de carbono orgánico resistente más de 100 años; BCc-1 pertenece a la Clase 4 y el resto de muestras reconocidas como biochar pertenecen a la Clase 2 (300g kg^{-1}≤ sBC_{+100} < 400g kg^{-1}).

En cuanto a las formas de C medidas por oxidación química, se observó una mayor proporción de C_{nox} en los materiales pirolizados (6-568 g C_{nox} kg^{-1}), siendo significativamente superior en los biocarbones con respecto a los PCM y las materias primas (Bonferroni post-hoc test; $p \leq 0.01$). Los biocarbones con mayor contenido en C_{nox} fueron BPb > BMis > BCc. Comparando los biocarbones según el origen de las distintas materias primas se obtuvieron mayores concentraciones de C_{nox} en los procedentes de residuos agrícolas, mientras que las menores concentraciones las presentan los derivados de estiércol y compost de alperujo. Estos resultados están en concordancia con los valores de C aromático obtenidos por NMR y los resultados de FTIR.

El análisis termogravimétrico de las muestras permitió calcular el porcentaje de carbono fijo (FixC) y la materia volátil (VM) existente, así como el cálculo del índice de recalcitrancia R50. Este índice compara la temperatura de degradación térmica de cada biocarbón con la del grafito, de tal forma que mayores valores del índice indican una mayor recalcitrancia. De acuerdo con este índice, los biocarbones de corteza de pino (BPb) y de neumático (BTy) pertenecen a la clase A, y todos los demás pertenecen a la clase B, con excepción de la muestra BCm al que se asigna a la Clase C. En cuanto al contenido en materia volátil disminuye a medida que aumenta la temperatura de pirólisis. Se encontró una correlación directa entre VM y el ratio H/C_{org} ($R^2 = 0.6988$), con valores más altos en la materia prima y PCMs. La materia volátil se relaciona con la fracción mineralizable, mientras que el C fijo se considera un indicador del valor de almacenamiento de carbono. El contenido en C fijo se incrementa con la temperatura, excepto en aquellas muestras ricas en cenizas como es el caso del biocarbón de cáscara de arroz.

De acuerdo con todas las metodologías aplicadas, se observó un incremento de la recalcitrancia al aumentar la temperatura de pirólisis, lo cual se refleja en una disminución en los ratios atómicos H/C_{org} y O/C_{org} y del contenido de materia volátil, y en un incremento de del FixC, C_{nox} y las

formas condensadas aromáticas. Así los biocarbones que favorecen una mayor fijación de C son los derivados de corteza de pino > miscanthus > carozo de maíz > eucalipto (BEu-2). En general se consideran adecuados los biocarbones producidos a partir de residuos forestales, herbáceos y agrícolas, siempre y cuando las temperaturas de pirólisis superen los 400 °C. Sin embargo, los biocarbones derivados de estiércol de pollo y compost de alperujo son menos aptos para el secuestro de C, ya que presentan menor contenido en C y son más ricos en formas lábiles.

Una vez clasificados los biocarbones con respecto a su potencial para la fijación de C, en el **Capítulo 5**, se estudió su capacidad como enmendante para la mejora de las propiedades del suelo. Para ello se analizó en los distintos biocarbones el contenido en nutrientes, tanto total como biodisponible para las plantas, la capacidad de intercambio catiónico y de retención de agua, así como la macro y microporosidad. En cuanto al potencial fertilizante de los biocarbones estudiados, en base a la disponibilidad de nutrientes para un cultivo de maíz, el biocarbón de cáscara de arroz presentó la mayor capacidad (Clase 4), seguido del biocarbón de estiércol de pollo (Clase 3) y de los biocarbones de compost de alperujo y de astilla de pino (Clase 2). Además, 10 de los 23 biocarbones analizados obtuvieron una disponibilidad de nutrientes correspondiente a la Clase 1, lo que indica que presentan capacidad para satisfacer los requisitos del cultivo de maíz para al menos uno de los nutrientes disponibles considerados. Los biocarbones derivados de madera (BEu-2 o BPb) o miscanthus, ricos en C recalcitrante, presentaron el menor potencial fertilizante. Se observó una predominancia de unos nutrientes u otros dependiendo del material de origen, así los biocarbones derivados de madera o miscanthus mostraron las menores concentraciones en nutrientes, con una predominancia de Ca, seguido de K. El contenido en nutrientes es mayor en los biocarbones derivados de estiércol, compost y residuos agrícolas, con una predominancia de K, Ca y P. Por el contrario, los biocarbones procedentes

de residuos industriales presentaron valores de nutrientes bajos, del mismo orden que los de madera, pero con un contenido mucho más alto de Fe.

Además de aportar nutrientes, los biocarbones mostraron capacidad de retención de agua, de intercambio catiónico en disolución neutra no tamponada y capacidad de aportar estructura y porosidad al suelo. Será necesario estudiar en profundidad estas propiedades y seguir sus variaciones en el suelo una vez los biocarbones sean aplicados, ya que estas propiedades pueden cambiar en su interacción con él.

En este capítulo también se estudió la toxicidad que puedan suponer los biocarbones al suelo donde se apliquen, analizando para ello su contenido en metales pesados e hidrocarburos policíclicos aromáticos (PAHs). La aplicación al suelo de biocarbones hechos con neumático se debe descartar, a pesar de su alto contenido en C recalcitrante, por ser potencialmente peligrosos debido a su contenido de metales pesados (en especial Co y Zn) y PAHs, superando los niveles establecidos por el IBI y EBC. El resto de biocarbones analizados no presentan toxicidad respecto a metales pesados o PAHs.

Aparte de la capacidad del biocarbón de fijar C y su potencial como enmendante del suelo, numerosos autores le atribuyen la capacidad de adsorber contaminantes, tanto orgánicos como inorgánicos. Actualmente se consumen aproximadamente 20 millones de toneladas de crudo y petróleo, cuyos procesos de transformación, transporte y almacenamiento provocan números vertidos que suponen un riesgo importante para suelos y aguas. Desde 1970, el CONCAWE ("Conservation of Clean Air and Water in Europe") ha registrado 674 incidentes de derrames con más de 170 m^3 de suelo afectados a lo largo de este periodo. La gasolina, el diésel y otros combustibles derivados del petróleo son mezclas complejas de compuestos orgánicos, muchos de ellos de carácter tóxico. Entre ellos se encuentran compuestos orgánicos volátiles (benceno, tolueno, etilbenceno y xilenos (BTEX)) y compuestos oxigenados (FO) como el metil *tert*-butil éter (MTBE) and etil *tert*-butil éter (ETBE). En el **Capítulo 6**, se determinó la capacidad

de los biocarbones producidos a partir de los distintos residuos para inmovilizar compuestos volátiles derivados del petróleo (BTEX y FO) y diésel, medido en forma de hidrocarburos totales del petróleo (TPH). Para ello se llevaron a cabo distintos experimentos de tipo "batch" en aguas contaminadas artificialmente con este tipo de compuestos. En primer lugar, se evaluó la capacidad de adsorción de BTEX y FO por los distintos biocarbones, utilizando para ello la cromatografía de gases de espacio de cabeza acoplada a espectrometría de masas (HS-GC-MS), sin corrección del efecto matriz. Este ensayo permitió seleccionar las muestras con mayor capacidad de retención, para después obtener con ellas las isotermas de adsorción de BTEX, FO y diésel, las cuales se describieron posteriormente mediante los modelos empíricos de Langmuir y Freundlich. Los resultaron mostraron diferencias significativas en la adsorción de BTEX y ETBE y MTBE en los distintos biocarbones, dependiendo principalmente de las propiedades físico-químicas del biocarbón, las condiciones de pirólisis y las propiedades del contaminante orgánico. Los compuestos más hidrofóbicos y apolares son inmovilizados fuertemente, mientras que por el contrario la adsorción del ETBE, MTBE y benceno, que son más hidrofílicos y polares, fue muy escasa. Además se observó un efecto de las condiciones de pirólisis sobre la capacidad de retención, siendo los biocarbones producidos a alta temperatura (HHT > 400 °C) los que presentan una mayor capacidad de retención de contaminantes orgánicos en disolución acuosa. La adsorción se ve favorecida porque estos biocarbones tienen un contenido más alto en carbono aromático y mayor superficie específica. De las muestras analizadas, el biocarbón de eucalipto (BEu-2) es el que presenta un mayor potencial para retener tolueno, etilbenceno, xilenos y TPH. Se observó un comportamiento de adsorción en multicapa. En primer lugar, los contaminantes son retenidos sobre la superficie del biocarbón hasta que se alcanza la saturación, y después aparece una segunda capa que se atribuye a la interacción de los contaminantes orgánicos entre ellos debido a su naturaleza hidrofóbica. Los modelos empíricos de Langmuir y Freundlich resultaron adecuados para describir los resultados experimentales y

detectar diferencias entre los distintos biocarbones, ajustándose mejor un modelo u otro dependiendo de la muestra. Los biocarbones producidos a baja temperatura (HHT ≤ 400 °C), como el derivado de estiércol de pollo, mostraron un comportamiento de adsorción más lineal, basado en un reparto de los contaminantes entre la materia orgánica sin pirolizar y la fase acuosa.

Y por último en el **Capítulo 7** se analizó el potencial del biocarbón para reemplazar el carbón de origen fósil que se utiliza en el proceso de producción del silicio con calidad fotovoltaica. Su posible sustitución permitiría reducir la huella de carbono del proceso y minimizar el uso de energías no renovables. Para ello el biocarbón tiene que presentar unas características específicas: un contenido en humedad por debajo del 15%; concentración estable de C fijo (~60%); y principalmente una concentración baja de fósforo, ya que este elemento compite con el silicio en la formación de las estructuras cristalinas y reduce la pureza del producto final. Para este ensayo se seleccionaron biocarbones producidos a partir de madera de eucalipto, pino y acacia. Este tipo de materia prima forestal presenta una amplia disponibilidad en Galicia, lo que asegura la demanda de la industria del silicio. Los resultados demostraron que los biocarbones producidos a partir del tronco de estos materiales cumplen los requisitos de composición y humedad cuando se producen a temperaturas superiores a los 400 °C. Se descartan los biocarbones producidos a partir de corteza, debido principalmente a su alto contenido en cenizas y en fósforo, ya que pueden interferir en la producción del silicio. Sin embargo, estos biocarbones de corteza son ricos en nutrientes, por lo que pueden ser aplicados a los suelos forestales de los que se extrae la madera, cerrando así el ciclo biogeoquímico de los elementos que contienen, mejorando las propiedades del suelo y, por consiguiente, aumentando la producción de la biomasa forestal. Es necesaria una investigación futura para establecer la influencia de la litología y el suelo en la distribución de fósforo en la

biomasa y el biocarbón. Esto permitirá seleccionar masas forestales en las que la acumulación de este nutriente sea menor.

Los distintos estudios realizados en la presente Tesis Doctoral revelan que los biocarbones presentan una composición química y física diferente en función del material de partida y las condiciones de pirólisis. En general, los biocarbones producidos a alta temperatura son ricos en formas de C recalcitrante y por tanto contribuyen al secuestro de C; aquellos con un mayor contenido en C aromático presentan elevada capacidad adsorbente de compuestos orgánicos; los biocarbones ricos en nutrientes pueden servir como fertilizantes para el suelo; y aquellos con bajo contenido en fósforo y cenizas, como los derivados de madera, se pueden utilizar en la industria del silicio. Esta variabilidad los hace adecuados para diversas aplicaciones, permitiendo resolver distintas problemáticas medioambientales. Sin embargo es necesario un análisis completo de las características de cada biocarbón con el objetivo de detectar el biocarbón más adecuado en función de la aplicación deseada. Además, siempre se tendrá en cuenta que se cumplan los valores críticos de concentración de contaminantes que aseguren la ausencia de toxicidad para el medio ambiente.

USC
UNIVERSIDADE
DE SANTIAGO
DE COMPOSTELA

Abstract

Society is currently facing serious environmental challenges such as ensuring a sufficient food supply for the ever-increasing world population (without increasing the associated environmental impact), recovering large areas of polluted/degraded land, improving waste management and confronting global climate change. Different environmental policies and the new concepts regarding the (re)use of waste in a circular economy emphasize that waste should be considered a misplaced resource or in an inappropriate form. Producing energy from waste and utilising the by-products generated are good ways of managing and adding value to waste.

Biochar is a solid material produced by the thermal decomposition (pyrolysis) of biomass in the absence of oxygen. It has a high organic C content and is highly resistant to decomposition. Biochar acts as a carbon sink when added to soil, because of its high content of recalcitrant carbon, and it can thus be used to help mitigate climate change. It can also be used to improve soil quality, by increasing the porosity, water retention capacity, nutrient supply and neutralization capacity, among other properties. It can also be used as a tool in environmental management because of its capacity to adsorb both organic and inorganic pollutants. Although the concept of biochar is relatively recent, its use can be traced back to Pre-Columbian tribes in the Brazilian Amazon. At the end of the 19th century, dark, anthropogenic soils were discovered in the area and found to be much more fertile than the surrounding soils. These soils, known as "Terra preta", are rich in organic matter and recalcitrant carbon. They were formed by the addition of carbon and nutrient-rich waste to ferralsols, giving rise to soils that have remained fertile for centuries. The high fertility of these soils is mainly attributed to the pyrogenic C that they contain, which is rich in condensed aromatic structures. This characteristic is used as the basis of

studies evaluating the potential use of biochar to improve the properties of degraded and /or polluted soils.

Biochar properties and quality are strongly influenced by the raw material used and by the pyrolysis conditions (temperature, residence time). In view of this, the general objectives of this doctoral thesis were as follows: to produce biochar from different types of waste in an experimental reactor, at a semi-industrial scale (kg per day); and to characterise the biochars thus produced in relation to their capacity to sequester C, improve soil properties, decontaminate degraded land and reduce the carbon footprint of the industrial production of silicon, thereby helping to resolve some environmental problems.

Experiments were designed with the following specific objectives in order to analyse the variability in the properties of the biochar produced from diverse types of raw material and to establish how they can be used to solve different environmental problems:

- To estimate the pyrolysis temperature at which each biochar was produced, by using near-infrared spectroscopy.
- To determine the properties and characteristics of the biochars produced, by analysing the variability in relation to the different raw materials and pyrolysis conditions. The biochars were classified on the basis of their potential use as C sinks, to mitigate climate change, and as soil amendments/fertilisers.
- To establish the capacity of biochars to immobilise organic pollutants derived from petroleum, such as volatile organic compounds and diesel.
- To study the viability of using the biochars in the metallurgical industry, specifically as a substitute for carbon in silicon production, in order to reduce the C emissions associated with the process.

The raw materials used to make biochar may represent a significant part of the overall production costs. It is therefore important to search for inexpensive materials (e.g. waste materials), which are found or generated close to the area of production or the recovery area, in order to reduce the transportation costs. The aim of using such materials is to make the system more efficient and economically viable, tending towards a circular economy. Different types of raw material were selected for study: i) invasive plants such as acacia, a species considered one of the main threats to forests in Galicia and the rest of the Iberian Peninsula; ii) forest and timber industry waste such as eucalyptus stems and branches, pine bark and pine sawdust; iii) agricultural waste such as corncob, rice husk, chestnut and vine pruning waste; iv) herbaceous plants such as miscanthus, grown as an energy crop for producing biofuel; v) animal manures and composts, such as chicken manure and olive pomace compost (a by-product of the olive oil industry); and vi) industrial waste such as used tyres and non-recyclable plastic waste.

The biochars were produced in two low-cost experimental reactors designed by Dr M. Bao and Dr T. García-Ares and located in the CVAN waste valorisation centre (Centro de Valorización de residuos del Norte SL (Touro, Santiago de Compostela). Both reactors operate in discontinuous mode with manual loading and discharge. The pyrolysis conditions vary between 300 and 550 °C, with a residence time between 1.5 and 6 h depending on the moisture content and other properties of the raw material. The maximum pyrolysis temperature ("highest heating temperature", HHT) is one of the most important factors determining biochar properties. This temperature is difficult to determine accurately in an experimental pyrolysis reactor such as that used in the present study, because of the temperature gradients that form within the chamber. Therefore, once the biochars were obtained, the main specific objective was to estimate the HHT at which each biochar was produced. This was done using near-infrared spectroscopy (NIRS) and mathematical models

(**Chapter 3**). In addition to providing an estimate of the HHT, this method enables distinguishes biochars produced at high temperatures (> 400 °C) and at low temperatures (≤ 400 °C). More heterogeneous spectra were produced as the pyrolysis temperature decreased, whereas the spectra of the biochars produced at high temperatures indicated higher absorbance, were flatter and contained fewer identifiable peaks. The prediction was less exhaustive for the more heterogeneous raw material with higher moisture contents, such as chicken manure and olive pomace compost, as the different components react differently to thermal degradation, especially at low temperature. The pyrolysis process must be optimized for each type of feedstock, depending on its composition and/or moisture content. The accuracy of estimation of the HHT was verified in the subsequent chapter by relating it to the biochar properties that depend on thermal degradation, such as the H/C ratio, the percentage of fixed C and the aromatic C content.

In **Chapter 4**, the physico-chemical properties of different biochars were determined in relation to C sequestration potential, and samples of the various biochars were classified on this basis. Different techniques were used to determine the stability of the C forms in the biochars, including elemental analysis, chemical oxidation of the C forms, thermogravimetric analysis, nuclear magnetic resonance (NMR) and Fourier transform infrared (FTIR) spectroscopy.

In the first step of this study, samples of the raw materials and of the biochars were subjected to elemental analysis. The proportion of C increased during pyrolysis, ranging from 29-48% in the raw material to 29-89% in the biochars. The biochars richest in C were those for which HHT values > 400 °C were estimated. Elemental analysis enables initial classification of the biochars. Thus, according to the requisites of the "International Biochar Initiative" (IBI) and "European Biochar Certificate" (EBC), when the value of H/C_{org} > 0.7, the material is not considered "biochar" and the material is referred to as "pyrogenic carbonaceous

material" (PCM). According to this criterion, 9 of the samples analysed were classified as PCM and corresponded to the samples for which the HHT ≤ 400 °C: acacia bark (BAcB), acacia sapwood (BAcSw-1, BAcSw-3) and acacia heartwood (BAcHw-2), eucalyptus wood (BEu-1), pine sawdust (BSd-1), chicken manure (BCm), olive pomace compost (BOpc) and plastic waste (BPl). The elemental analysis also enabled a second classification according to the organic C content (C_{org}). In accordance with the classification established by IBI, most of the biochars analysed were included in Class 1 (C_{org} ≥ 60%), whereas the biochars derived from rice husk (BRh), used tyres (BTy) and chicken manure (BCm) were included in Class 2 (30% ≥ C_{org} < 60%), and BOpc was included in Class 3 (10% ≥ C_{org} < 30%). Biochars can also be classified on the basis of their recalcitrance, by determining the proportion of C_{org} that will remain stable in the soil for more than 100 years (BC_{+100}). Following a classification based on the storage of total C (sBC_{+100}), the biochars derived from corncob (BCc-2 and BCc-3), eucalyptus wood (BEu-2), miscanthus (BMis) and pine bark (BPb) were categorised in the top class (Class 5), with more than 600 g kg^{-1} of organic carbon resistant for more than 100 years; BCc-1 was included in Class 4 and the other biochars were included in Class 2 (300g kg^{-1} ≤ sBC_{+100} < 400g kg^{-1}).

Regarding the C forms measured by chemical oxidation, the pyrolysed materials were enriched in C_{nox} (6-568 g C_{nox} kg^{-1}), and the enrichment was significantly greater in the biochars than in the PCMs and in the raw materials (Bonferroni post-hoc test; p ≤ 0.01). Biochars with the highest C_{nox} content were BPb > BMis > BCc. Comparison of the biochars according to the origin of the different raw materials revealed higher concentrations of C_{nox} in those derived from agricultural waste, whereas the lowest concentrations were found in the biochars derived from chicken manure and olive pomace compost. These results are consistent with the concentrations of aromatic C obtained by NMR and with the results of the FTIR analysis.

The thermogravimetric analysis of the samples enabled calculation of the percentage of fixed carbon (FixC) and volatile matter (VM), as well as calculation of a recalcitrance index, R50. This index compares the thermal decomposition temperature of each biochar with that of graphite, so that higher values indicate higher degrees of recalcitrance. In accordance with the index, the biochars derived from pine bark (BPb) and from used tyres (BTy) were included in Class A and all the others in Class B, except BCm, which was categorised as Class C. The volatile matter content decreased as the pyrolysis temperature increased. The VM content was directly correlated with the H/C_{org} ratio (R^2 = 0.6988) and was highest in the raw materials and PCMs. The volatile matter is related to the mineralizable fraction, whereas the fixed C is considered an indicator of the carbon sequestration potential. The fixed C content increased with the pyrolysis temperature, except in those samples with high ash contents, such as the rice husk biochar.

All of the methods applied showed that the recalcitrance of the material increased with the pyrolysis temperature, which is reflected by decreases in the atomic ratios H/C_{org} and O/C_{org} and of the volatile matter content, as well as by increases in FixC, C_{nox} and the condensed aromatic forms. Thus, the biochars can be ranked in relation to their C fixation capacity, as follows: pine bark > miscanthus > corn cob > eucalyptus (BEu-2). In general, biochars produced from forest, herbaceous and agricultural waste were considered adequate, provided that the pyrolysis temperature was higher than 400 °C. However, the biochars derived from chicken manure and olive pomace are less suitable for sequestering C as they contain less fixed C and are richer in labile forms.

Once the biochars were classified in relation to their C fixation capacity, the potential use of the biochars to improve soil properties was studied (**Chapter 5**). For this purpose, the nutrient contents of the different biochars (total and the plant available) were determined, along with the ion exchange capacity and water holding capacity. The fertiliser

potential of the biochars, which was determined on the basis of the nutrient availability for a corn crop, was highest in the rice husk biochar (Class 4), followed by the chicken manure biochar (Class 3) and the olive pomace and pine bark biochars (Class 2). Furthermore, in 10 of the 23 biochars analysed, the nutrient availability corresponded to Class 1, which indicates the capacity to satisfy the requirements of the corn crop for at least one of the nutrients considered. The miscanthus biochar and the wood-derived biochars (BEu-2 and BPb), which are rich in recalcitrant C, displayed a lower fertiliser potential. The predominance of one or other nutrients depended on the feedstock. Thus, the biochars derived from miscanthus or wood contained lower amounts of nutrients, with a predominance of Ca, followed by K. The nutrient content was higher in the biochars derived from agricultural waste, with a predominance of K, followed by Ca and P. The nutrient content of the biochars derived from industrial waste was low, of the same order as the wood-derived biochars, but with much higher Fe contents.

In addition to supplying nutrients, the biochars displayed a good water holding capacity, cation exchange capacity in unbuffered neutral solution and the capacity to improve the structure and porosity of soils. However, further, detailed study of these properties and their interactions in the soil after application of biochars is required.

In this chapter, the potential toxicity of the biochars was also studied by determining the heavy metal and polycyclic aromatic hydrocarbons (PAHs) contents. Despite containing high amounts of recalcitrant C, biochars derived from used tyres cannot be applied to soil, because of the potentially toxic levels of heavy metals (especially Co and Zn) and PAHs, which are higher than the levels established by the IBI and EBC. The other biochars analysed did not display potential toxicity in relation to heavy metals or PAHs.

Apart from the C fixation capacity of biochar and its potential use as a soil amendment, numerous authors have highlighted the capacity of biochar

to retain both organic and inorganic pollutants. At present approximately 20 million tonnes of crude oil and petroleum are consumed annually. Numerous spills occur during the transformation, transportation and storage of these products, representing an important risk to soils and water. Since 1970, CONCAWE (Conservation of Clean Air and Water in Europe) has registered 674 spills which have affected a total volume of more than 170 m^3 of soil. Petrol, diesel and other fuels derived from crude oil are complex mixtures of organic compounds, many of toxic nature. These include volatile organic compounds (benzene, toluene, ethylbenzene and xylene [BTEX]) and oxygenated compounds (fuel oxygenates, FO) such as methyl *tert*-butyl ether (MTBE) and ethyl *tert*-butyl ether (ETBE). In **Chapter 6**, the capacity of the different biochars to immobilise volatile compounds (BTEX and FO) derived from oil and diesel was measured as the total petroleum hydrocarbons (TPH). Various "batch" type experiments were carried out in samples of water artificially contaminated with these compounds. First, the capacity of the different biochars to sorb BTEX and FO was evaluated using headspace gas chromatography/mass spectrometry (HS-GC-MS), without matrix correction. This enabled the identification of those samples with the highest retention capacity. These samples were then used to obtain the sorption isotherms for BTEX, FO and diesel, which were then described by the empirical Langmuir and Freundlich models. The results showed significant differences in the sorption of BTEX and ETBE and MTBE by the different biochars, which mainly depended on the physico-chemical properties of the biochar, the pyrolysis conditions and the properties of the organic pollutant. The most hydrophobic and apolar compounds were strongly immobilised, whereas the more hydrophilic and polar, i.e. ETBE, MTBE and benzene, were scarcely sorbed. In addition, the pyrolysis conditions affected the retention capacity, and the biochars produced at high temperatures (HHT > 400 °C) showed a high capacity to retain organic pollutants in aqueous solution. The sorption was favoured by the high aromatic carbon content and large specific surface area. Of the samples analysed, the eucalyptus biochar (BEu-2) showed the highest

potential for retaining toluene, ethylbenzene, xylene and TPH. Multilayer sorption behaviour was observed, in which the pollutants were first retained on the biochar surface until reaching saturation. The second layer was attributed to the interaction between the organic pollutants due to their hydrophobic nature. The Langmuir and Freundlich isotherm models were suitable for describing the experimental results and detecting differences between the different biochars, although the model providing the best fit to the data depended on the biochar considered. Biochars produced at low temperature (HHT ≤ 400 °C), such as that derived from chicken manure, showed a more linear sorption, based on the partition of the contaminants between the unpyrolysed organic matter and the aqueous phase.

Finally, in **Chapter 7** the potential use of biochar to replace carbon in the silicon (photovoltaic quality) production process was analysed. This would reduce the carbon footprint of the process and the use of non-renewable energy. The biochar must possess some specific characteristics for this purpose: moisture content below 15%; a stable concentration of fixed C (~60%), and, above all, a low concentration of phosphorus, as this element competes with silicon in the formation of crystalline structures and reduces the purity of the final product. Biochars derived from eucalyptus, pine and acacia were selected for testing. These types of raw materials are widely available in Galicia, thereby ensuring the demands of the silicon industry. The findings demonstrate that the biochars derived from the stems of these trees meet the requirements of composition and moisture content when produced at temperatures above 400 °C. Biochars derived from bark were ruled out for this purpose, mainly because of the high ash and phosphorus contents, which may interfere in the silicon production process. However, the biochars derived from bark are rich in nutrients and could therefore be incorporated into the forest soils where the wood was extracted, thereby closing the biogeochemical cycle of the elements contained, improving the soil properties and enhancing the production of

forest biomass. Further research is required to establish the influence of the lithology on the distribution of phosphorus in biomass and biochar. This would enable identification of forest stands in which accumulation of P is lowest.

The different studies reported in this doctoral thesis revealed that the chemical and physical composition of the biochars depended on the raw starting material and the pyrolysis conditions. In general, biochars produced at high temperatures are rich in recalcitrant C forms and therefore contribute to C sequestration; those with a higher content of aromatic C show a high capacity to adsorb organic compounds; nutrient-rich biochars can be used as soil fertilisers; and those containing low amounts of phosphorus and ash, such as wood-derived biochars, can be used in the silicon industry. As result of these diverse properties, biochars can be used for many different applications, including solving various environmental problems. However, exhaustive analysis of the characteristics of all biochars considered is necessary to identify which are the most suitable for the desired application. In addition, the threshold levels of pollutants must be taken into account to minimise the risk of toxicity to the environment.

I. Introducción general

USC
UNIVERSIDADE
DE SANTIAGO
DE COMPOSTELA

CAMBIO CLIMÁTICO Y LA IMPORTANCIA DEL CICLO DEL CARBONO

A lo largo de la historia, nuestro planeta ha pasado por periodos cálidos y periodos fríos, provocados tanto por factores internos como la actividad biótica, la tectónica de placas, erupciones volcánicas o las corrientes oceánicas, como por fenómenos externos como variaciones en la radiación que la Tierra recibe del sol, impacto de meteoritos o cambios en la órbita terrestre (NASA, 2017). En los últimos 150 años, acciones humanas, como la quema de combustibles fósiles, la tala masiva de árboles, la agricultura intensiva o cambios en los usos del suelo, han producido un incremento de los gases de efecto invernadero (principalmente CO_2, CH_4, N_2O and $H_2O_{(g)}$), lo que ha conllevado una perturbación de los ciclos naturales. La composición de la atmósfera ha sido alterada, superando por primera vez la barrera de las 400 partes por millón (ppm) de CO_2 en 2015 y alcanzando un valor de 403.3 ppm en 2016 según el último informe de la Organización Meteorológica Mundial (WMO, 2017), que constituye un 145% sobre los valores correspondientes al periodo pre-industrial (anteriores a 1750). Esto se ha traducido en un incremento de temperaturas de 1.7 °C desde 1880 a la actualidad (NASA, 2017). Esta tendencia al alza de las temperaturas ha afectado considerablemente a las zonas polares y otras áreas heladas, con el correspondiente deshielo y aumento del nivel medio del mar. Otro de los efectos del cambio global es el incremento en los fenómenos meteorológicos extremos y sus impactos catastróficos alrededor de todo el mundo. Un ejemplo de ello son las inundaciones, ya que han cambiado los patrones de precipitación, tendiendo a fuertes precipitaciones en periodos cortos, incluso en zonas donde la precipitación total anual tiende a reducirse. Estos fenómenos se alternan con sequías y olas de calor cada vez más frecuentes y prolongadas, mientras los periodos fríos se reducen. Además se prevé una intensificación en la fuerza y frecuencia de los huracanes. Todos estos fenómenos parecen tener una relación directa con el aumento en las emisiones de CO_2 antropogénico

a nivel global (Figura 1.1) (IPCC, 2014) y van a afectar considerablemente a la producción de alimentos y a los sistemas humanos (Figura 1.2) (IPCC, 2014).

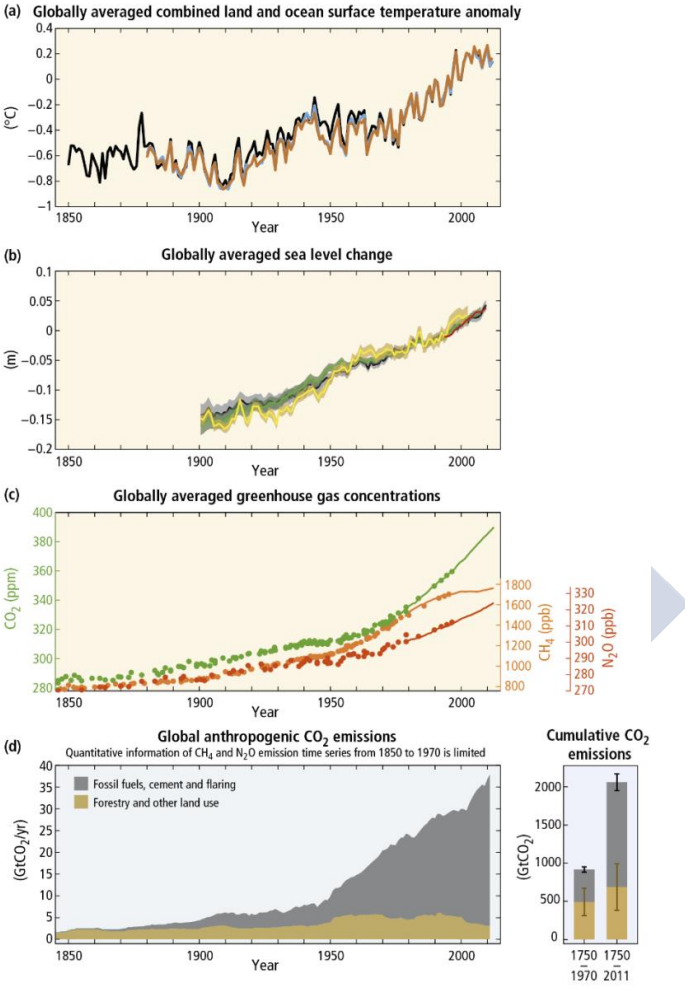

Figura 1.1 Cambios observados en el sistema climático entre 1850-2014. (a) Desde la década de 1950, tierra y océanos se han calentado; (b) ha subido el nivel medio del mar; (c) las concentraciones de gases de efecto invernadero han incrementado; (d) estos cambios tienen una relación con las emisiones de CO_2 antropogénico a nivel global. En el lado derecho (d), se representa en un gráfico de barras y bigotes las emisiones de acumuladas CO_2 y sus incertidumbres (IPCC, 2014).

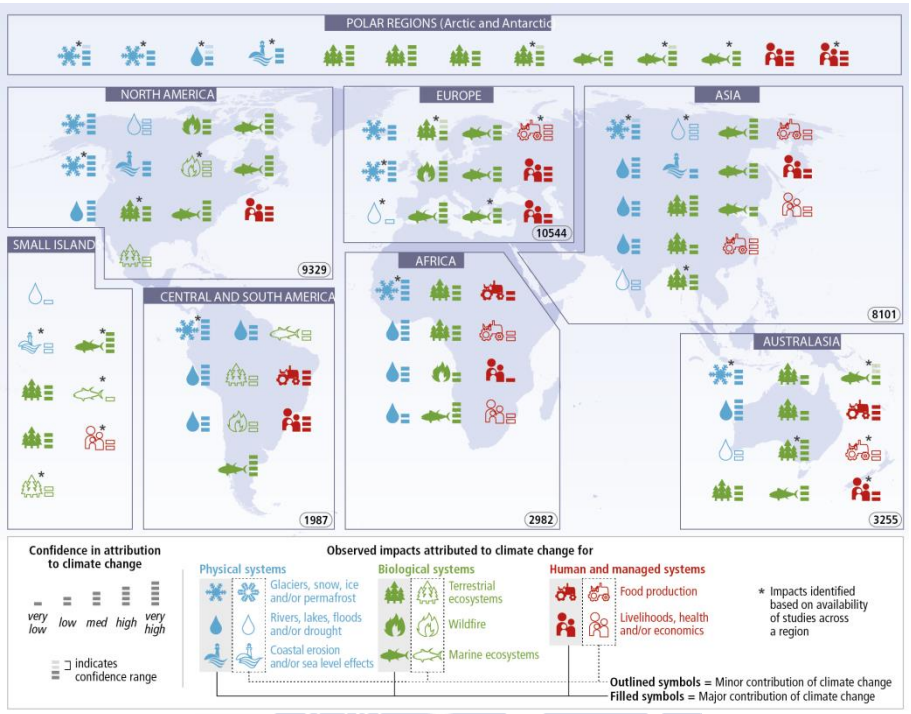

Figura 1.2 Impactos atribuidos al cambio climáticos basados en las referencias científicas disponibles (IPCC, 2014).

Cuando se firmó el protocolo de Kyoto en 1997, la mayoría de las propuestas fijadas para luchar contra el cambio climático se centraban en la reducción de los gases de efecto invernadero (GEI) con el fin de limitar el calentamiento global a 2 °C sobre la temperatura media pre-industrial. Sin embargo, la drástica reducción de las emisiones requiere una reconversión del sistema energético e industrial que no es fácil de llevar a cabo en un periodo de tiempo tan corto y que requiere importantes inversiones económicas y tecnológicas. Sólo después del Tratado de Bonn en 2001, se tuvo en cuenta como alternativa para conseguir este objetivo, el secuestro de carbono (C) de las fuentes de origen o de la atmósfera por medio de técnicas basadas en mecanismos naturales o de ingeniería (Lal, 2007).

La Convención Marco de las Naciones Unidas sobre el Cambio Climático (UNFCCC) (2009) define el "secuestro de carbono" como cualquier proceso capaz de retirar carbono de la atmósfera y depositarlo en otro compartimento geoquímico, siendo el suelo, a través de la función fotosintética y de la humificación, el sistema que más rápidamente puede actuar en las alternativas de secuestro de los sistemas terrestres. De ahí que, entre las estrategias para la mitigación y adaptación del actual forzamiento climático, se encuentra la producción de biomasa vegetal para aumentar el secuestro de CO_2 atmosférico. En el primer periodo de compromiso del Protocolo de Kyoto (artículo 3), solo las actividades de forestación y reforestación se consideraron como sumideros. Más tarde se incluyeron los suelos agrícolas y acciones en los cambios de uso del suelo como fuentes o reservorios de GEI (artículo 3.4). En 2005, el Panel Intergubernamental sobre Cambio Climático (IPCC) publicó un informe especial en el que se daban diferentes opciones de almacenamiento de CO_2 en sumideros geológicos, oceánicos, mediante carbonización mineral y usos industriales (Figura 1.3)

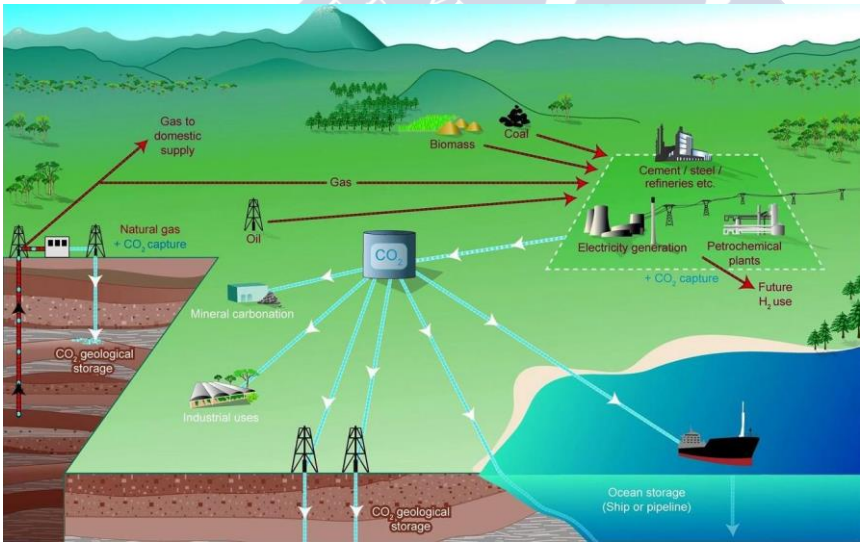

Figura 1.3 Diagrama de los posibles sistemas de captura y almacenamiento de carbono atmosférico (IPCC, 2005).

Los suelos actúan como importantes reservorios de C en la Tierra, con unos stocks de C mayores que la biota y la atmósfera juntos (Lorenz & Lal, 2016) (Figura 1.4). El stock de C en los suelos está formado por carbono inorgánico (SIC) y C orgánico (SOC). El primero de ellos está compuesto principalmente por carbonatos que derivan de la roca madre (carbonatos litogénicos) o formados por alteración química (carbonatos pedogénicos). Mientras que el segundo, SOC, deriva de distintas fuentes biológicas como plantas, microorganismos o animales y sus excrementos (Lorenz & Lal, 2016). Siendo tan importante el papel del suelo en el ciclo de C, es de vital importancia en la lucha frente al cambio climático potenciar las acciones que conserven e incrementen las reservas de carbono en el mismo.

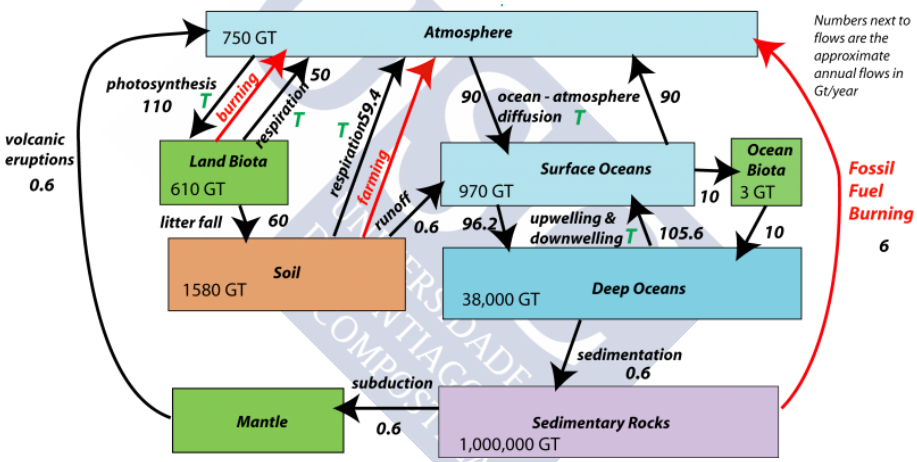

Figura 1.4. Sumideros de carbono globales y los flujos entre ellos en gigatoneladas (GT) de carbono por año. Las flechas rojas indican los flujos relacionados con las actividades humanas. Las T en verde marcan los flujos sensibles a la temperatura (Bice, n.d.).

VALORIZACIÓN DE RESIDUOS ORGÁNICOS

Desde sus orígenes, las sociedades requieren del consumo de materias y energía para su desarrollo y, como consecuencia de sus actividades, generan sustancias de desecho. Este consumo ha ido creciendo con el paso de los años, de forma que se ha llegado a generar grandes cantidades de

residuos, de composición muy heterogénea y cuya gestión, no siempre adecuada, lleva a la contaminación del medio (Macías et al., 2011).

La legislación española en materia de residuos, la Ley 22/2011, de 28 de julio, de residuos y suelos contaminados, define residuo como "cualquier sustancia u objeto que su poseedor deseche o tenga la intención o la obligación de desechar".

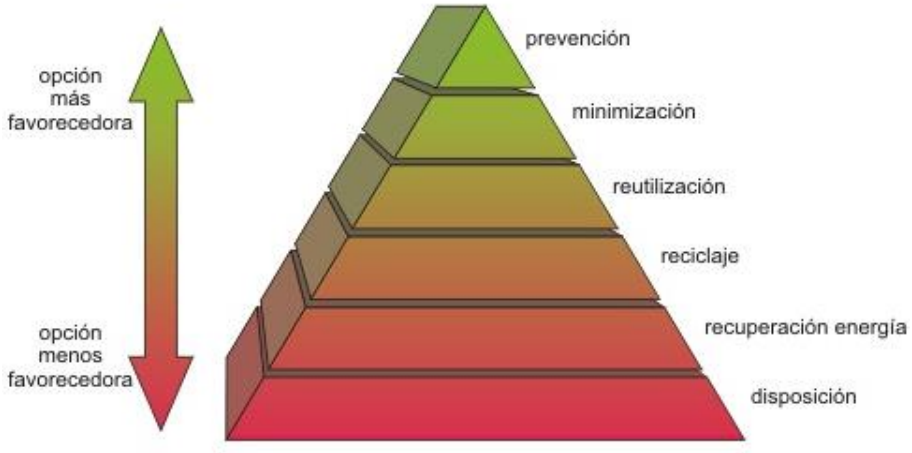

Figura 1.5 Pirámide de jerarquías en gestión de residuos (Macías et al., 2011).

Tradicionalmente, el principal destino de los residuos es su almacenamiento en vertederos controlados o incontrolados. Otros procesos a los que se someten en menor medida son de inactivación e incineración, reciclaje y recuperación de materiales útiles (Navarro-Pedreño et al., 1995). La Directiva Marco de Residuos (*Directiva 2008/98/ CE sobre los residuos*), establece una jerarquía de cinco niveles que indica la prioridad que se debe establecer en la prevención y gestión de los residuos que es: 1. Prevención; 2. Preparación para la reutilización; 3. Reciclado; 4. Otro tipo de valorización, como podría ser la energética y por último 5. Eliminación o disposición en vertederos. Sin embargo en la gestión actual de la mayor

parte de los países, incluido España, esta pirámide está invertida, siendo la acción predominante la acumulación de residuos en grandes vertederos.

A través del gobierno central se están promoviendo iniciativas para acercarnos al desarrollo sostenible; así las prioridades de la Estrategia UE 2020 son la seguridad alimentaria, el medio ambiente y el cambio climático y el equilibrio territorial, como principios rectores de la política futura (Agudo López et al., 2010). En materia de clima y energía los objetivos de esta estrategia son:

- Reducir un 20% de las emisiones de gases de efecto invernadero (respecto a los niveles de 1990)
- Incrementar en un 20% la producción de energía renovable
- Conseguir un 20% de mejora de la eficiencia energética

En las últimas décadas, las diferentes políticas ambientales y la nueva concepción sobre los residuos, inciden en que deben ser considerados como "recursos que están en un lugar o en una forma inadecuada", lo que lleva a desarrollar nuevos y más eficientes métodos de utilización y valoración de los mismos que permitan la integración de sus componentes en los ciclos biogeoquímicos de forma ambiental y sanitariamente segura. El 2 de diciembre de 2015 se hizo una propuesta de modificación de La Directiva Marco de Residuos para incorporar una serie de medidas que tiendan a una economía circular, a cerrar círculos, de forma que la gestión de residuos contribuya al desarrollo sostenible, la creación de empleo, la reducción de emisiones de gases de efecto invernadero y la mejora del medio ambiente. Uno de los objetivos que se establece es conseguir un 60% de reutilización y reciclado de los residuos municipales para 2025. Los residuos pueden ser valorizados para recuperar parte de la energía que contienen y para aprovechar sus elementos constituyentes y/o sus propiedades. La valorización de residuos para producir biocarbones reúne estos dos aspectos, siendo importante determinar las propiedades de los

materiales producidos en las diferentes condiciones de pirólisis y materiales de partida (Macías et al., 2011).

Existen numerosos tipos de residuos que se pueden clasificar de distintas formas, como por su peligrosidad: peligrosos y no peligrosos o por su procedencia: e.g., urbanos, industriales, orgánicos, inertes. Entre los residuos orgánicos encontramos los residuos agrarios y forestales que pueden ser muy variados. No existen estadísticas oficiales que permitan estimar la totalidad de restos agrarios que se generan, habiendo grandes diferencias entre los distintos estudios publicados al respecto. Según el EUROSTAT, los residuos agrícolas, forestales y de la caza suponían 11 millones de toneladas del total de 146 millones que se generaron en España en 2008. Sin embargo, una estimación independiente del 2007, indica que estos residuos fueron de 343 millones de toneladas, sin contar los residuos forestales, los derivados de la acuicultura y los subproductos de origen animal no destinados al consumo humano, lo que representaría un 72% del total de residuos sólidos generados en España (Ministerio de Agricultura, Alimentación y Medio Ambiente., 2012). Dentro de los residuos no peligrosos de origen agrícola generados y cuantificados en el año 2006, el 92% corresponden a heces animales, orina y estiércol, un 4.8% a residuos vegetales y el resto de residuos no peligrosos no representan más del 3.2% (INE, 2006).

Galicia es junto con Extremadura la región de España con mayor número de explotaciones ganaderas (bovino, avícola y porcino) (ECOREGA, 2013). En ellas se generan numerosos residuos orgánicos, tanto de origen animal como vegetal, que incluyen purines, estiércol, restos de cosechas y de poda y restos de limpieza del monte, ya que muchas explotaciones ganaderas tienen asociadas una zona forestal para el pastoreo del ganado. Además en estas explotaciones se producen importantes cantidades de plásticos procedentes de los silos e invernaderos y neumáticos en desuso procedente de la maquinaria agrícola o la compactación de silos.

Por otro lado el 69% de los usos del suelo en Galicia es forestal, según datos del IV Inventario Forestal Nacional (IFN4), que contribuyen en más del 40% a la producción forestal nacional. En España el sector de la madera generó más de 2 millones de m^3 de residuos en 2014 de acuerdo con las estadísticas de la Organización de las Naciones Unidas para la Alimentación y la Agricultura (FAO) (FAOSTAT, 2014).

En cuanto a las formas de valorización de los residuos orgánicos (biomasa y necromasa, en adelante se utilizará para ambos el término biomasa), actualmente la principal se basa en la recuperación de energía. Para ello, se han desarrollado diferentes procesos de conversión termoquímica (Tabla 1.1), de los cuales los tres procesos principales son: combustión, gasificación y pirólisis.

La combustión consiste en la oxidación completa de la materia en presencia de oxígeno, obteniendo como resultado CO_2, vapor de agua, cenizas y calor. Este último no se puede almacenar, utilizándose en la producción de energía y calor. Su tecnología está muy extendida y se han alcanzado rendimientos de hasta el 80% (Lormas et al., 2001). Sin embargo, hay que prestar atención a las emisiones a la atmósfera que produce y sus efectos en el medio ambiente, ya que se generan cenizas volantes, CO_2, CO, compuestos de azufre, óxidos de nitrógeno y, dependiendo del material que se use como combustible, pueden producirse sustancias muy tóxicas como dioxinas, furanos o hidrocarburos policíclicos aromáticos.

La gasificación es un proceso de oxidación parcial de la materia orgánica para obtener una mezcla de monóxido de carbono, dióxido de carbono, hidrógeno, metano y, en menor medida, hidrocarburos como etano o etileno. Opera a altas temperaturas y tiempos de residencia largos, obteniendo así alrededor de un 85% de gas, 10% de carbón y 5% de líquido. El proceso se puede realizar utilizando como agentes gasificantes: aire, oxígeno, vapor de agua o una mezcla de ellos. Dependiendo del agente gasificante que se use, el gas de síntesis obtenido cambiará su composición y

su poder calorífico, siendo menos energético con aire (4 - 7 MJ Nm^{-3}) y de mejor calidad con oxígeno (10 - 18 MJ Nm^{-3}) (Elias & Velo, 2005).

Por último, la pirólisis consiste en la descomposición térmica de la materia orgánica en ausencia o condiciones limitadas de oxígeno (Bridgwater, 2003). Puede operar en distintas condiciones, procesos a bajas temperaturas y tiempos de residencia largos favorecen la formación de carbón; altas temperaturas y largos tiempos de residencia incrementan la formación de gas, mientras que temperaturas y tiempos moderados favorecen la producción de líquidos, especialmente interesantes en la producción de bioaceites (Bridgwater, 2003). Dependiendo del tiempo de residencia que se mantiene durante el proceso de pirólisis, tenemos:

- Pirólisis rápida: la biomasa se calienta rápidamente y los vapores presentan tiempos de residencia cortos.
- Pirólisis lenta: es la técnica tradicionalmente utilizada en la producción de carbón vegetal, la biomasa pasa más tiempo en el reactor en ausencia de oxígeno (entre 30 minutos, varias horas o incluso días en los sistemas más primitivos) (Antal & Gronli, 2003).

Desde el punto de vista energético la pirólisis es mucho menos eficiente que la combustión, siendo la exotermicidad de la reacción de pirólisis lenta por unidad de biocarbón de 2 a 3.2 kJ g^{-1} (Boateng et al., 2015), y solo podría justificarse por la obtención de un producto, el carbón, que puede ser fácilmente almacenado y utilizado cuando conviene. Eso explica que con el tiempo, otros procesos de obtención de bioenergía han ido ganando importancia, sin embargo, esta situación ha cambiado por el forzamiento climático y la necesidad que hay de reducir las emisiones de gases de efecto invernadero a la atmósfera, principalmente CO_2 y CH_4, lo que ha llevado a la búsqueda de formas de C recalcitrante, de las que los biocarbones o biochar es la más conocida.

Klason y sus colaboradores describieron la ecuación estequiométrica de la transformación térmica de la celulosa (Klason et al., 1909) y la madera (Klason et al., 1910) durante la pirólisis a 400 °C, siendo para la celulosa:

$$C_6H_{10}O_5 \rightarrow 3.75CH_{0.6}O_{0.13} + 2.88H_2O + 0.5CO_2 + 0.25CO + C_{1.5}H_{1.25}O_{0.38} \quad [1]$$

Y para la pirólisis de madera:

$$2C_{42}H_{60}O_{28} \rightarrow 3C_{16}H_{10}O_2 + 28H_2O + 5CO_2 + 3CO + C_{28}H_{34}O_9 \quad [2]$$

Donde el primer producto de ambas ecuaciones es el biocarbón y el último el bioaceite. Más concretamente, las reacciones que se producen en un proceso general de pirolisis son las siguientes (Yan et al., 2005):

$$C + CO_2 \leftrightarrow 2CO, \qquad \Delta H_{298}^0 = +168\ MJ\ kmol^{-1} \quad [3]$$

$$C + H_2O \leftrightarrow CO + H_2, \qquad \Delta H_{298}^0 = +175\ MJ\ kmol^{-1} \quad [4]$$

$$CH_4 + H_2O \leftrightarrow CO + 3H_2, \qquad \Delta H_{298}^0 = +206\ MJ\ kmol^{-1} \quad [5]$$

$$CH_4 + 2H_2O \leftrightarrow CO_2 + 4H_2, \qquad \Delta H_{298}^0 = +165\ MJ\ kmol^{-1} \quad [6]$$

$$CO + H_2O \leftrightarrow CO_2 + H_2, \qquad \Delta H_{298}^0 = -41\ MJ\ kmol^{-1} \quad [7]$$

$$C + 2H_2 \leftrightarrow CH_4, \qquad \Delta H_{298}^0 = -75\ MJ\ kmol^{-1} \quad [8]$$

El proceso de termodegradación de la celulosa se puede resumir en tres pasos: i) un paso inicial de deshidratación y perdida de algunos volátiles; ii) la formación de un biocarbón primario; iii) la reacción del carbón primario con los gases de pirólisis para formar un biocarbón secundario (Demirbas, 2006), y el mecanismo simplificado queda ilustrado en la Figura 1.6 con las funciones predominantes en función de la temperatura (Kan et al., 2016).

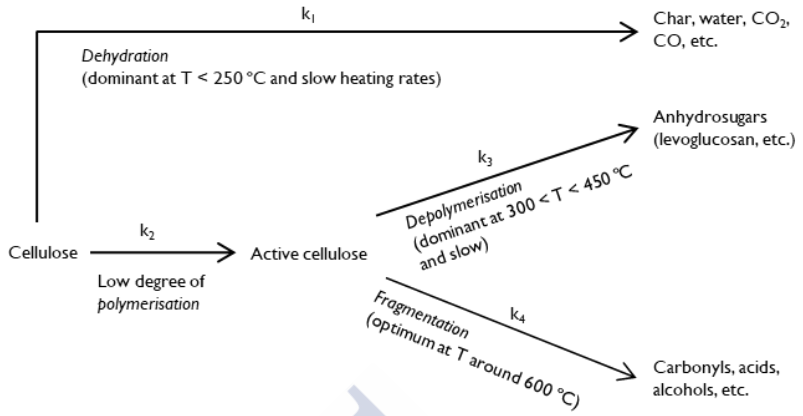

Figura 1.6 Esquema del mecanismo de Waterloo de descomposición primaria de la celulosa, donde las reacciones dominantes que se dan en función de la temperatura son la deshidrogenación, depolimerización y fragmentación (Kan et al., 2016)

Tanto en la gasificación como en la pirólisis, en la transformación termoquímica de biomasa de baja densidad, además de calor (1.5 GJ m^{-3}) (Kuppussamy et al., 2016), se generan tres subproductos que generan un valor añadido:

- Líquido denso, conocido como bioaceite (22 GJ m^{-3}) (Kuppussamy et al., 2016), con el que se producen biocombustibles, que pueden sustituir a los actuales de origen fósil.
- Gas de síntesis (syngas) (7.8 GJ m^{-3}) (Kuppussamy et al., 2016), consiste en una mezcla de gases, principalmente hidrógeno, monóxido de carbono, dióxido de carbono, metano e hidrocarburos, que generalmente es usado como fuente de energía. También puede ser refinado para producir biodiesel o como producto intermedio en la producción de otros productos químicos (Sparkes & Stoutjesdijk, 2011).
- Residuo carbonoso sólido (23.3 GJ m^{-3}) (Kuppussamy et al., 2016), que se puede utilizar para aplicarlo al suelo para mejora de sus propiedades o como sumidero de carbono (biochar) o como fuente de energía por combustión completa.

Dependiendo del tipo de producto que se quiera priorizar, se establecerán unas condiciones de operación u otras (Figura 1.7). Diferentes estudios determinan cuales son los parámetros óptimos para favorecer la producción de biocarbón o bioaceites (Yoder et al., 2011). Por lo general, las bajas temperaturas favorecen la formación de biocarbón mientras que las altas producen mayores cantidades de bioaceites (Mašek et al., 2011).

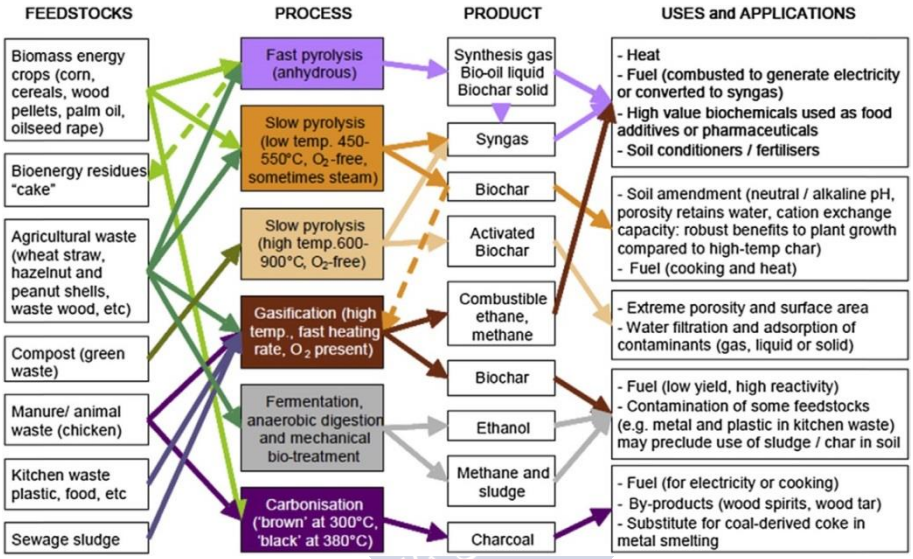

Figura 1.7 Resumen de los procesos de conversión termoquímica en relación con las materias primas más frecuentes, los productos obtenidos y potenciales usos y aplicaciones (Komang Ralebitso-Senior & Orr, 2016; Sohi et al., 2010).

Tabla 1.1 Tecnologías de conversión termoquímica de la biomasa y distribución de los productos (Boateng et al., 2015).

Proceso termoquímico	Temp. (°C)	Otros parámetros	Gas %	Líquido %	Sólido %	Principal producto buscado
Carbonización	300-1200	Estanqueidad, tiempo de residencia, material	60-75	3-5	10-35	Carbón ("charcoal"); combustible sólido y uso industrial
Pirólisis (para bioaceites)	400-600	Tasa de calentamiento, tiempo de residencia, tamaño de partícula, flujo de gas	20-40	40-70	10-25	Bioaceite; productos químicos y biocombustibles
Pirólisis (para biocarbón)	300-700	Tiempo de residencia, tasa de calentamiento	40-75	0-15	20-50	Biochar; enmendante de suelos, secuestro de carbono y bioremediación
Gasificación	500-1500	Medio oxidante, ratio equivalente	85-95	0-5	5-15	Syngas; combustible gaseoso para calor y energía, y gas para líquido
Proceso hidrotermal	200-400	Elevadas presiones, tipo de solvente y ratio (ej. agua)	0-90	0-80	0-60	Varios productos químicos
Combustión	1000-1500	Exceso de aire para la completa combustión	95	0	5	Energía convertida a calor y potencia

BIOCARBÓN o "BIOCHAR"

El biocarbón o "biochar" en la nomenclatura inglesa, es un producto de la pirólisis rico en carbono que se obtiene de la transformación termoquímica de biomasa en ausencia o condiciones limitadas de oxígeno. Puede utilizarse como producto en sí mismo o un ingrediente de una mezcla en una serie de aplicaciones como enmienda para la mejora de las propiedades del suelo, remediación y/o protección contra la contaminación ambiental y como agente para mitigar el efecto invernadero (Lehmann & Joseph, 2009; IBI, 2015; Lehmann & Joseph, 2015). Además debe cumplir unas propiedades que aseguren su calidad y seguridad. Cuando estos requisitos no se cumplen, el producto se denomina material pirogénico carbonoso o "Pyrogenic Carbonaceous Material" (PCM) (EBC, 2012; IBI, 2015), término más genérico aplicable a todos los materiales producto de una conversión termoquímica que contienen algo de C orgánico (Lehmann & Joseph, 2015). También se puede utilizar el término "torrefactado", que indica que el proceso de calentamiento ha sido insuficiente para llegar a las exigencias de formación de biocarbón o biochar, pero que ya se han producido determinados cambios en el material inicial, de los que la pérdida de agua y cambios en la concentración de las formas más lábiles de C son los más significativos.

El biochar es rico en carbono recalcitrante. El IPCC (2007) define "recalcitrante" como el material orgánico que resiste la descomposición. Su recalcitrancia se debe a que en el proceso de transformación de la materia prima, se consigue una forma de C más aromática y con menos grupos funcionales hidrofílicos, lo que le confiere menor degradabilidad, pudiendo permanecer en el suelo miles de años (Lehmann et al., 2015; Lehmann, 2007). Esto ha llevado a que se realicen numerosas investigaciones para su uso como sumidero de carbono frente a la lucha contra el cambio climático y la reducción en la emisión de gases de efecto invernadero.

En castellano, no existe una terminología que diferencie los distintos tipos de biocarbones o carbón vegetal según su finalidad; sin embargo el término anglosajón biochar se diferencia de otros productos carbonosos en que su objetivo es la aplicación al suelo o su uso en gestión ambiental (Lehmann & Joseph, 2009). Se diferencia de otros términos como "*charcoal*", que se utiliza cuando su uso es la producción de energía (para generar calor, cocinar o en procesos industriales) o "*char*" referente al material generado por la combustión incompleta en fuegos naturales o provocados. Cuando el proceso de producción es la carbonización hidrotermal (HTC) o hidrólisis química al producto sólido resultante se le denomina "hydrochar", que suele tener mayores ratios H/C y menor aromaticidad que el biochar (Schimmelpfennig & Glaser, 2012; Fuertes et al., 2010). Otra terminología relacionada es "black carbon" que Lehmann & Joseph (2015) definen como PCMs dispersos en el medio ambiente procedentes de fuegos y la combustión de combustibles fósiles. El IPCC lo define en la atmósfera como un aerosol primario con gran capacidad de absorber la radiación solar, contribuyendo enormemente al calentamiento global (IPCC, 2007). El carbón activo o "activated carbon" (AC) es otra forma de PCM que ha sufrido una activación superficial, bien sea química o física (i.e. térmica). Su uso es muy extendido como adsorbente, ya que contiene una gran cantidad de microporos que le confieren una elevada superficie específica.

El biochar puede producirse de una gran variedad de materias primas que van desde la biomasa forestal y agrícola o cultivos energéticos, a una amplia variedad de residuos orgánicos como restos de poda, cortezas, paja, lodos de depuradoras, residuos ganaderos como el estiércol, residuos sólidos urbanos o residuos de industrias como la papelera o alimentarias (EBC, 2012). La materia prima utilizada afectará, junto con el sistema de producción, a las propiedades físicas y químicas del biochar, condicionando las posibles aplicaciones ambientales del mismo (Amonette & Joseph, 2009; Sparkes & Stoutjesdijk, 2011; Lehmann & Joseph, 2015; McBeath et al., 2014). Elegir una materia prima fácilmente disponible y de bajo coste va a

influir en el potencial de aplicación a gran escala y la eficiencia económica del sistema (Bruckman et al., 2016).

Antecedentes

El término biochar puede parecer relativamente nuevo, sin embargo el concepto tiene su origen en la "Terra Preta" de la amazonia brasileña. Los ecosistemas de la cuenca del Amazonas tradicionalmente se han caracterizado por una baja fertilidad y suelos altamente evolucionados, alterados y erosionados, donde se llevaba a cabo una agricultura de rotación con fuego, cultivo y abandono (Glaser & Birk, 2012).

Las condiciones de temperatura y humedad que se dan en los suelos de climas tropicales, hacen que la materia orgánica se descomponga y degrade rápidamente. Ello, junto con el predominio de arcillas 1:1, conduce a una escasa capacidad de intercambio catiónico del suelo. Sin embargo, alrededor de la década de 1870, varios científicos que investigaban la Amazonia por separado, descubrieron zonas con suelos oscuros y ricos en C orgánico con un horizonte superficial de más de 60 cm de espesor, que se describieron como los mejores suelos de la Amazonía (Haefele, 2007). Estos suelos son conocidos como "*Antropogenic Dark Earths*" (ADE), "*Terra preta do Indio"* o simplemente Terras pretas (englobando suelos con menor expresión de estas características a los que se denominan Terras mulatas) y presentan unas propiedades totalmente distintas a los suelos que los rodean (Figura 1.8). A pesar de tener una composición mineralógica y textura similar, se caracterizan por su color oscuro y su gran cantidad de materia orgánica estable y altos niveles de nutrientes (Glaser & Birk, 2012; Glaser et al., 2001; Hung Chia et al., 2010; Sombroek et al., 2002). Estos suelos son de origen antropogénico, se formaron principalmente a partir de Ferralsoles, Acrisoles y Arenosoles, por adición de carbón y residuos ricos en nutrientes (Glaser & Birk, 2012). Fueron creados por las poblaciones precolombinas hace entre 500-2500 años (Haefele, 2007). Se caracterizan por la presencia de carbón y cenizas, trozos de cerámica, heces, huesos y

restos de animales y otro tipo materiales de desecho. Se pone en duda si su origen fue intencionado o como resultado de la ocupación humana, lo que sí se sabe es que a pesar de la agricultura continuada y condiciones climáticas desfavorables (abundantes lluvias y altas temperaturas), han continuado fértiles durante milenios (Glaser, 2007).

Figura 1.8 Comparación de dos perfiles de suelo: a la izquierda podemos ver un oxisol, suelo típico en la Amazonía, pobre en nutrientes, y a la derecha un oxisol transformado en Terra preta (Glaser et al., 2001).

La fertilidad de la Terra preta se atribuye principalmente a su contenido en C pirogénico con estructuras condensadas aromáticas (i.e. Black Carbon (BC)) (Glaser et al., 2000). Las concentraciones de BC son del orden de 70 veces superiores a las de los suelos adyacentes, se midieron valores de 150 g C kg^{-1} de suelo en la Terra preta frente a los 20-30 g C kg^{-1} de los suelos adyacentes (Glaser et al., 2001). La materia orgánica que contienen los suelos Terra preta no se degrada tan rápidamente como la de los suelos de su entorno. La oxidación lenta del

biochar a lo largo del tiempo produce grupos carboxilo en los bordes de los compuestos aromáticos, lo que aumenta la capacidad de retención de nutrientes, presentando tres veces más nitrógeno y fósforo disponible, que contribuye al desarrollo de una elevada biodiversidad microbiana y alta actividad biótica (Glaser et al., 2001). Además las formas de C recalcitrantes permiten el mantenimiento estable de la estructura y un claro efecto de secuestro de C durable, al tiempo que originan una elevada estabilidad estructural que reduce los procesos de erosión.

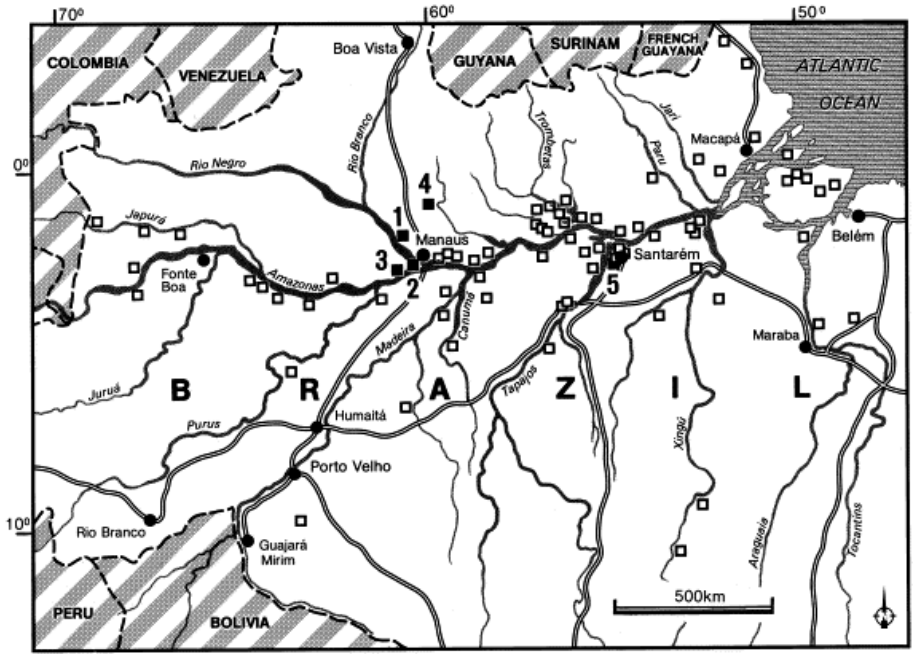

Figura 1.9 Mapa de distribución de las zonas de Terra preta conocidas en la Amazonía brasileña (cuadrados blancos) y zonas de Terra preta investigadas (cuadrados oscuros) rodeadas de Oxisoles (Glaser et al., 2000).

Podemos encontrar Terra preta a lo largo de la cuenca del Amazonas (Figura 1.9), en un principio se localizaron estos suelos a orillas de los principales ríos, pero hoy también se conocen en zonas interfluviales (Eden et al., 1984). Estos suelos se extienden por la Amazonia de Brasil, pero también se han encontrado en partes de la Amazonia de Perú, Colombia, el

sur de Venezuela y en Guayanas, aunque en menor densidad. La extensión de los parches de Terra preta descritos por diferentes autores tienen una extensión desde menor a una hectárea hasta varios kilómetros cuadrados (Glaser & Birk, 2012), representado en conjunto un porcentaje superficial inferior al 3% del total del área ferralítica.

Algunos autores diferencian entre distintos tipos de tierras oscuras: Terra preta (suelos negros) y Terra mulata (suelos marrones oscuros resultantes de la aplicación intencionada de materiales vegetales carbonizados y con apenas artefactos pero igualmente ricos en materia orgánica) (Sombroek et al., 2002). Wim Sombroek (2002) puso en marcha un proyecto para desarrollar de forma sostenible suelos antropogénicos enriquecidos que replicaran a los Terra preta de las tribus indias pre-colombinas, de forma que tanto las tribus indígenas de la Amazonía como granjeros de otras partes del mundo contribuyeran al secuestro de CO_2 mediante la gestión y mejora de las propiedades del suelo. Este proyecto se denominó Terra preta nova, con su visión del suelo como elemento clave para luchar contra el cambio global (Woods et al., 2009). El Laboratorio de Tecnología Ambiental de la Universidad de Santiago (LTA-USC) pretende seguir con esta idea mediante la elaboración de "Tecnosoles Terra preta", tomando las características de la Terra preta como modelo para el desarrollo de biocarbones y de los procesos de pirólisis como forma de obtener nuevos compuestos orgánicos con propiedades de alto interés ambiental e industrial.

La Base Referencial Mundial del Recurso Suelo (WRB) (WRB, IUSS Grupo de Trabajo, 2007) definió en 2006 un nuevo grupo de suelos de referencia en el que se describe Tecnosol como "un suelo fuertemente influenciado por material hecho, modificado o cambiado de sitio por el hombre, que contenga un 20 por ciento o más de artefactos (en volumen o peso)". Son suelos derivados de residuos como escombreras, cenizas, lodos u otros desechos de las actividades humanas. Estos suelos antropogeomórficos si son correctamente formulados pueden evolucionar

mediante los procesos edáficos, cumpliendo alguna o varias de las funciones propias del suelo, pudiendo aplicarse para solucionar problemas ambientales como la rehabilitación de suelos o espacios contaminados o degradados (Camps-Arbestain et al., 2008).

Sistemas de producción de biochar

Las formas de producción del biochar son muy variables, desde hornos tradicionales en forma de montículo o en hoyos en el suelo, hasta eficientes plantas industriales (Brown, 2009). Desde hace miles de años se ha producido carbón en hornos temporales construidos con tierra, rocas o madera. Éstos todavía se usan hoy en día, sobre todo en países en vías de desarrollo, ya que el coste y la tecnología que requieren son bajos. Sin embargo, esta forma de pirólisis es poco eficiente porque no se aprovecha la energía en forma de calor que se genera ni los co-productos. Además pueden ser altamente contaminantes si no se lleva un control de la temperatura (Pratt & Moran, 2010), ya que como consecuencia de los procesos termoquímicos se pueden generar, a ciertas condiciones de temperatura, tóxicos como hidrocarburos policíclicos aromáticos (PAHs), dioxinas, furanos, bifenilos policlorados (PCBs), etc. (Cordella et al., 2012). Los procesos de producción con control de la contaminación pueden llegar a reducir en un 80% las emisiones de CO, material particulado y compuestos orgánicos volátiles (Brown, 2009). Por ello, para que la producción de biochar sea eficiente y sostenible es necesario el uso de tecnologías más avanzadas, que requieren mayor inversión económica, pero presentan un mayor rendimiento, sistemas de depuración de gases y control de la contaminación (Brown, 2009).

Según Brown (2009) un pirolizador para la producción eficiente de biochar debe cumplir con los siguientes objetivos: alimentación continua para aumentar la eficiencia energética y reducir las emisiones contaminantes; operación exotérmica sin infiltraciones de aire; optimizar la reutilización de los co-productos que se generan para reducir las emisiones y mejorar el

rendimiento económico; control de las condiciones de operación lo que permite mejorar las propiedades del biochar y flexibilidad en la materia prima que se pueda carbonizar.

Algunas de las tecnologías desarrolladas que permiten cumplir estos objetivos son el pirolizador de tambor, los hornos rotatorios, pirolizador de tornillo, de lecho fluidizado, reactores de pirólisis rápida, gasificadores, reactores de proceso hidrotermal y estufas madera-gas.

El proceso de producción se puede optimizar para biochar a diferentes escalas, desde miligramos por hora en ensayos de laboratorio, a nivel local, en granjas o pequeñas industrias, como a nivel regional y de grandes industrias, pudiéndose llegar a producir toneladas por hora (Kuppussamy et al., 2016). Existen incluso pirolizadores móviles (Sparkes & Stoutjesdijk, 2011).

Desarrollo de la investigación en *biochar*

A pesar del escaso tiempo de desarrollo del concepto de biochar en la forma propuesta por Lehmann y colaboradores (Lehmann & Joseph, 2009; Lehmann & Joseph, 2015) se han realizado numerosos estudios para determinar las propiedades y características del mismo, así como comprobar los efectos de su aplicación en el suelo y otras aplicaciones ambientales. El número de publicaciones que incluyen el término biochar ha crecido notablemente en la última década (Figura 1.10), como indicativo del creciente interés en la comunidad científica. Ello se debe al gran potencial del biochar para solventar los grandes retos que afronta el mundo actual, como son la gestión de residuos, las energías renovables, la pérdida de suelos y el cambio climático (Shareef & Zhao, 2017) La base de datos bibliográfica *ISI Web of Knowledge* recoge hasta finales del 2017 casi 6000 publicaciones relacionadas con el término biochar, con un importante incremento del número de artículos de revista desde 2010 (Figura 1.10). El interés por los biocarbones se ha desarrollado a nivel global, adaptándose en cada región a las necesidades a nivel local. Si bien a principios de 2015

Estados Unidos contaba con el mayor número de publicaciones en el tema (601 artículos) (Rajapaksha et al., 2015), a finales de 2017 China se pone a la cabeza en publicaciones sobre biochar (Figura 1.11).

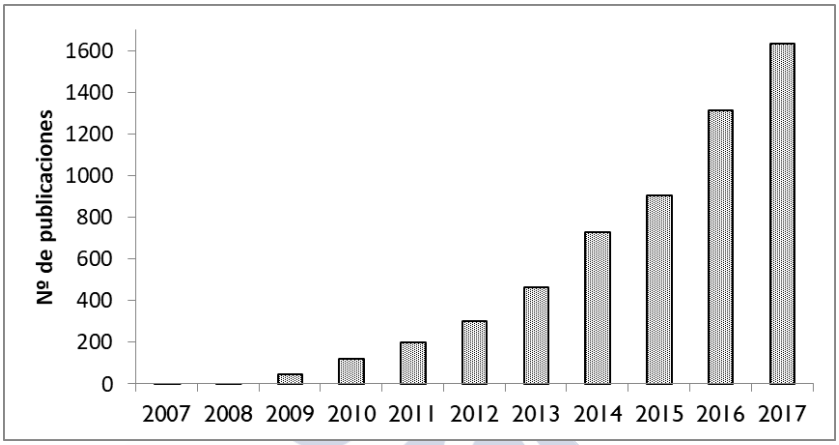

Figura 1.10 Número de publicaciones en revistas científicas enumeradas en el ISI Web of Knowledge (https://apps.webofknowledge.com) con el término "biochar" tanto en el título como en palabras clave o contenido, a fecha de 01/01/2018.

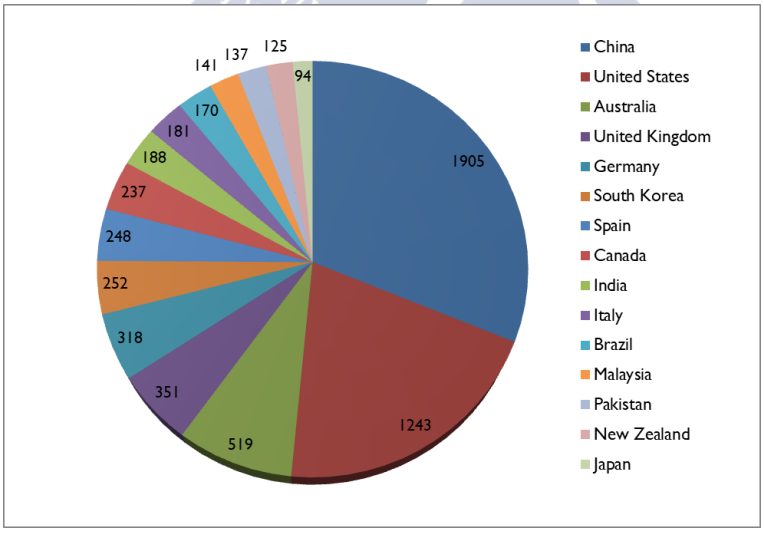

Figura 1.11 Número total de publicaciones en "Biochar" en el periodo 2007-2017 para los 15 primeros países que más publican sobre el tema (Basado en los datos de www.webofknowledge.com con acceso de 01/01/2018).

El biochar es muy versátil y presenta un gran potencial en aplicaciones para la sostenibilidad ambiental. Se han publicado artículos relacionados con infinidad de áreas de investigación, predominando las aplicaciones en ciencias ambientales y ecología, seguidos de agricultura, ingeniería, y energía (Figura 1.12).

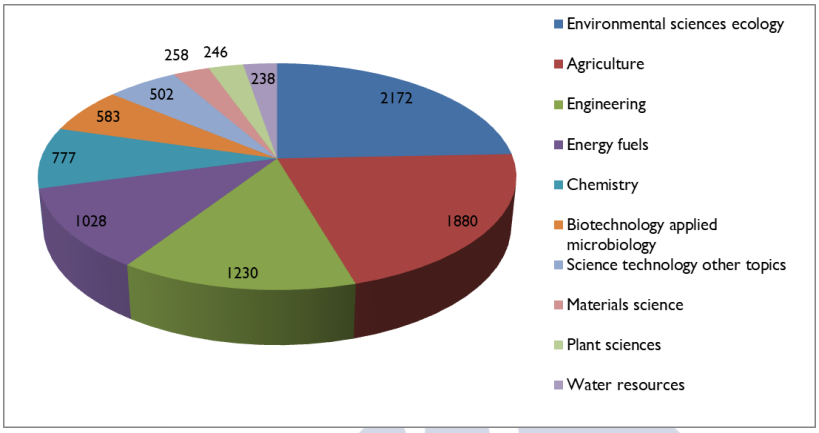

Figura 1.12 Principales áreas de investigación en las que se publica sobre biochar (Basado en los datos de ISI Web of Knowledge con acceso de 01/01/2018).

Además de la producción científica, dado el interés suscitado por esta nueva herramienta, y la necesidad del desarrollo de estándares y guías para su producción y aplicación han surgido diversos organismos reguladores en todo el mundo como el "International Biochar Initiative" (IBI), la "European Biochar Foundation/ Certification" (EBC), el "British Biochar Foundation" (BBF), el "UK Biochar Research Centre" (UKBRC), el "European Cooperation on Science and Technology Action on Biochar / European Biochar Research Network", el "United States Biochar Initiative" (USBI), el "Australia and New Zealand Biochar Researchers Network" y el "China Biochar Network" (Tabla 1.2) (Komang Ralebitso-Senior & Orr, 2016). Cada uno presenta diferentes enfoques con estrategias y declaraciones más o menos formales, con el fin de informar y asegurar un producto de calidad y seguridad a mercados y consumidores, ya que en ningún país existe una política o marcos legislativos sobre el uso y aplicaciones del biochar.

Uno de los principales cuerpos es el IBI, que se fundó en el año 2006 en el Congreso Mundial de la Ciencia del Suelo en Filadelfia, con tres objetivos principales: apoyar la investigación en biochar, aportar información fiable sobre todos los aspectos relacionados con él y crear estándares y políticas para guiar a los usuarios a escala local, regional y global.

Tabla 1.2 Ejemplos de normativas sobre el biochar de diferentes cuerpos o iniciativas y sus fundamentos principales hasta febrero de 2016. Traducida de Komang Ralebitso-Senior & Orr (2016).

Institución	Documento normativo	"Política" fundamental o parámetros	Comentarios	Localización del documento
International Biochar Initiative (IBI)	IBI Biochar Standards – Standardised Product Definition and Product Testing Guidelines for Biochar That is Used in Soil	Categoría A (Propiedades básicas de utilidad, requeridas para todos los biochars); Categoría B (Evaluación de sustancias tóxicas, requerido para todos los biochars); Categoría C (Análisis avanzados y mejora de las propiedades del suelo, opcional)	Desarrollados mediante la consulta a un amplio rango de marcos/organismos/métodos, como por ej. OECD, USEPA, ASTM, AOAC. Los estándares para el biochar del IBI se basan en revisiones de las políticas	http://www.biochar-international.org/sites/default/files/IBI_Biochar_Standards_V2%200_final_2014.pdf
European Biochar Foundation/ Certificate (EBC)	European Biochar Certificate—Guidelines for a sustainable production of biochar	Biochars clasificados en "básicos" y "premium"; la certificación depende de la materia prima, el método de producción, características físico-químicas, y los métodos/ objetivos de aplicación; nueve requisitos clave estipulados para las propiedades del biochar	-	http://www.europeanbiochar.org/en
British Biochar Foundation (BBF)	Biochar Quality Mandate		Se centra especialmente en la adicción de biochar al suelo; El mandato se basa en el conocimiento de expertos investigadores, de las fuentes de financiación de UK y los cuerpos políticos	http://www.britishbiocharfoundation. org/

UK biochar Research Centre (UKBRC)	N/A	N/A	Elabora el UKBRC Standard Biochar; Repositorio para informes comisionados y la Agencia de Protección Ambiental Escocesa publica el "Interim Regulatory Position Statement on Biochar"	http://www.biochar.ac.uk/index.php https://www.sepa.org.uk/media/134422/wst-ps-031-manufacture-and-use-of-biochar-from-waste.pdf
European Commission Environmetn, eg, Wastes Framework Directive	N/A. Registro de proyectos financiados y artículos de investigación	Biochar debe cumplir con, por ejemplo, la Directiva 2001/95/EC y 2009/31/EC en producción segura y "almacenamiento geológico de dióxido de carbono", respectivamente	Biochar clasificado como residuo, por lo tanto tiene implicaciones en seguridad y uso en suelos agrícolas y otros ecosistemas inalterados	http://ec.europa.eu/environment/index_en.htm
UK Environment Agency	N/A. Modelos de deliberación incluyendo: Product comparators for materials applied to land: non-waste biochar Report-SC130040/R6	Lista de materias primas que no son residuos; biochar aplicado al secuestro de carbono y a la mejora de las condiciones del suelo; requisitos para biochar derivados de N en "zonas vulnerables por nitratos"; identificados parámetros físico-químicos analizables y certificables; se establecen límites para Metales pesados/metaloides, PAHs, dioxinas/furanos and PCBs	Documento basado, en parte, en la literatura científica publicada	https://www.gov.uk/government/organisations/environment-agency

PAHs, Hidrocarburos policíclicos aromáticos; PCBs, bifenilos policlorados; OECD, Organización para la Cooperación Económica; USEPA, Agencia de Protección Ambiental de Estados Unidos; ASTM, Metodologías de estandarización Americana; AOAC, Asociación de Comunidades Analíticas

Biochar como sistema

El biochar puede ser producido a partir de innumerables materias primas de distintos orígenes que dan lugar a productos diferentes, cada uno con sus oportunidades y restricciones. En general, presenta un gran potencial y versatilidad dependiendo de la materia prima y las condiciones de producción; su uso puede extenderse a diferentes sectores y escalas, con objetivos y resultados diferentes (Lehmann & Joseph, 2009). Por otro lado hay que tener en cuenta que otros factores como las propiedades del suelo donde se aplique el biocarbón, las condiciones climáticas o el régimen de aplicación también van condicionar los efectos del mismo en el sistema receptor. Para aprovechar todo su potencial, el biochar debe ser considerados como un sistema "win-win" en el que, según Lehmann & Joseph (2009), hay cuatro objetivos complementarios y sinérgicos que justifican su aplicación en la gestión medioambiental: mejora de las propiedades del suelo, mitigación del cambio climático, gestión de residuos y producción de energía, en cuya combinación o individualmente producen beneficios sociales y económicos, con menos riesgos y costes que otras opciones disponibles (Cowie et al., 2015).

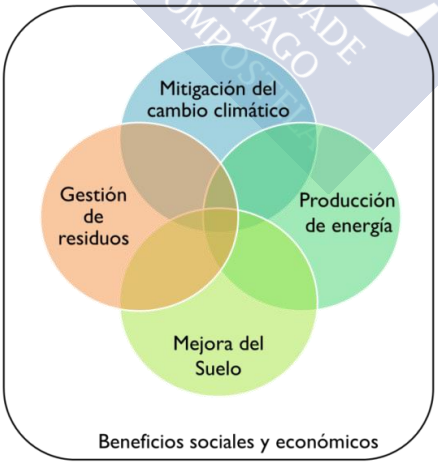

Figura 1.13 Motivación para la aplicación de biochar como sistema (Lehmann & Joseph, 2015).

Mejora de las propiedades del suelo

El biochar ofrece una forma de mejorar la calidad del suelo y el uso eficiente de los nutrientes utilizando fuentes locales y renovables de una forma sostenible, siempre y cuando se aplique el biochar adecuado para cada tipo de suelo y en la dosis acertada. En países subdesarrollados, el aumentar la fertilidad del suelo es una cuestión vital para asegurar la alimentación de una población creciente. En los países desarrollados las tasas de pérdida de suelos por sobrexplotación y contaminación están siendo cada vez más alarmantes, el biochar puede contribuir no solo a aumentar la productividad del suelo, sino también a reducir el impacto medioambiental que se está produciendo sobre el suelo y las aguas. Autores como Xie et al. (2010), Galinato et al. (2011), Spokas et al. (2012), Jeffery et al. (2015), Qian et al. (2015), Kuppussamy et al. (2016), Shareef & Zhao (2017) recogen datos sobre algunos de los estudios que se han realizado, resumiendo los distintos tipos de materias primas que se utilizan para su producción, tipos y condiciones de pirólisis, los resultados de los experimentos llevados a cabo y sus efectos sobre el suelo y las cosechas, etc. De los estudios recogidos en Spokas et al. (2012), el 50% presentan resultados positivos a corto plazo en el rendimiento o crecimiento de las cosechas, un 30% indican que no hay diferencia entre la aplicación de biocarbón y el control y un 20% reportan impactos negativos en el crecimiento o rendimiento de la producción. Entre las propiedades positivas que se atribuyen a la aplicación de biochar en el suelo no sólo se ha conseguido aumentar la producción de las cosechas (Zhang et al., 2012; Shareef & Zhao, 2017), sino que también se ha observado un incremento de la capacidad de intercambio catiónico (CEC) (Liang et al., 2006); aumento de la capacidad de retención de agua y mejora del drenaje (Case et al., 2012; Karhu et al., 2011); el biochar presenta capacidad neutralizante en suelos ácidos (Novak et al., 2009); aumenta la concentración de nutrientes disponibles para las plantas (Sohi et al., 2010); hace más eficiente el uso de fertilizantes al reducir las pérdidas por filtración (Laird et al., 2010; Sparkes

& Stoutjesdijk, 2011) y proporciona condiciones favorables para el desarrollo de los microorganismos del suelo, incluyendo los fijadores de N y los hongos micorrícicos (Ahmad et al., 2016; Steiner et al., 2016).

Además, el biochar ayuda a mejorar la calidad del suelo actuando como adsorbente de contaminantes tanto en el suelo como en el agua (Qian et al., 2015). Se han probado su efectividad en la retención de contaminantes inorgánicos, como metales pesados; y de contaminantes orgánicos, como derivados de hidrocarburos, pesticidas, tintes, etc. Ahmad et al. (2014), Zhang et al. (2015) y Kuppussamy et al. (2016) entre otros, resumen los números trabajos publicados sobre la capacidad adsorbente de distintos tipos de biochar.

Gestión de residuos

A partir de la revolución verde, en agricultura y ganadería se generan grandes cantidades de residuos de naturaleza variada (Ministerio de Agricultura, Alimentación y Medio Ambiente., 2012). Estos desechos suponen una fuente de contaminación de suelos y de las aguas; sin embargo, la mayoría de ellos, se pueden considerar junto con otros residuos orgánicos, como un recurso para la obtención de biofuel o su transformación en biochar. El uso de residuos para la producción de biochar hace que se reduzca la competencia con otras materias primas que puedan tener competencia alimentaria o con otros sectores productivos como la industria maderera. Además, la conversión en biochar reduce el peso y el volumen de la materia prima inicial y el potencial patógeno de los residuos (Sparkes & Stoutjesdijk, 2011). Los residuos con alto contenido en humedad pueden resultar menos atractivos al requerir más energía en su transformación (Lehmann & Joseph, 2015). El tratamiento local de los residuos, supone asimismo, un ahorro en energía de transporte y una buena alternativa en lugares donde no hay vertederos. Por otro lado, una correcta gestión de los residuos orgánicos puede ayudar a mitigar el efecto invernadero indirectamente, mediante la reducción de emisiones de CH_4 de los vertederos (Ackerman, 2000). Sin embargo es necesario realizar

controles exhaustivos del biochar que asegure unos estándares de calidad previos a la aplicación al suelo, ya que algunos residuos como los lodos de depuradora pueden contener metales pesados. Si bien, autores como Méndez et al. (2012) demostraron que la pirólisis de estos residuos reduce la movilidad y biodisponibilidad de algunos de elementos (Ni, Zn, Cd y Pb).

Producción de energía

Durante el proceso de pirólisis además de biochar se produce calor, que puede ser utilizado en el propio proceso para el secado de las materias primas o como sistema de calefacción. Además se generan otros subproductos líquidos y sólidos de alto valor en la producción de biocombustibles (Lehmann & Joseph, 2015). Tanto la captura de energía durante el proceso de producción de biochar, como la aplicación en el suelo del biochar que se genera en la producción de biocombustibles, aumentan los beneficios y rentabilidad del sistema y justifican la producción de biomasa (Gaunt & Lehmann, 2008). Hay que tener en cuenta que aunque la bioenergía, y más concretamente la pirólisis, no van a solucionar la crisis energética por si solas, sin embargo pueden contribuir significativamente, ya que se reduce el consumo de combustibles fósiles que en general han de ser importados. Por lo tanto, se disminuye la dependencia energética exterior y se apuesta por la generación y distribución de energía local, que a su vez generará puestos de trabajo y dinamizará la economía de la zona (Shareef & Zhao, 2017). Pueden ser una oportunidad importante para zonas rurales cuya principal fuente de energía es la biomasa, haciéndola más eficiente mediante la pirólisis, menos contaminante y utilizando además de la madera, otras materias primas como los residuos de las cosechas, dada la versatilidad en las materias prima que acepta (Lehmann & Joseph, 2009).

Mitigación del cambio climático

La producción y el uso de biochar para la mejora de los suelos, junto con la producción de bioenergía, reduce la emisión de gases de efecto invernadero, ya que el CO_2 es fijado por las plantas mediante la fotosíntesis

y transformado mediante la pirólisis en una forma de C más estable que el material orgánico del que procede, por lo que se descompone lentamente (Lehmann & Joseph, 2009). Wang et al. (2016) concluyeron que el 97% del C contenido en el biochar no está disponible para los microorganismos, siendo una contribución directa al secuestro de carbono a largo plazo en el suelo. Por otro lado los co-productos que se generan en la pirólisis, calor, gases y bioaceites, reemplazan a fuentes de energía de origen fósil (Figura 1.14) (Woolf et al., 2010). Además del potencial del biochar en el secuestro de carbono, diferentes estudios han demostrado que se reducen las emisiones del suelo de otros gases de efecto invernadero como metano (CH_4), probablemente debido a cambios en la aireación del suelo (Karhu et al., 2011) y óxido nitroso (N_2O) por la acción de varios mecanismos que afectan a los microorganismos del suelo, a la denitrificación o incluso la adsorción de NO_2 por el biochar (Sparkes & Stoutjesdijk, 2011; Cayuela et al., 2014; Cornelissen et al., 2013), siempre teniendo en cuenta que los efectos dependerán de las propiedades del biochar y su interacción con el suelo (Jeffery et al., 2015). Woolf et al. (2010) estimaron que el uso de biochar puede suponer una reducción de las emisiones de CO_2, metano y óxido nitroso de 1.8 Pg CO_2-C equivalente (CO_2-C_e) por año, lo que supone un 12% de las emisiones de CO_2-C_e antropogénicas en el año de la publicación, sin comprometer la seguridad alimentaria, los hábitats o la conservación del suelo. Además la aplicación de biochar a suelos previamente infértiles, proporciona una retroalimentación positiva, incrementando la productividad del suelo.

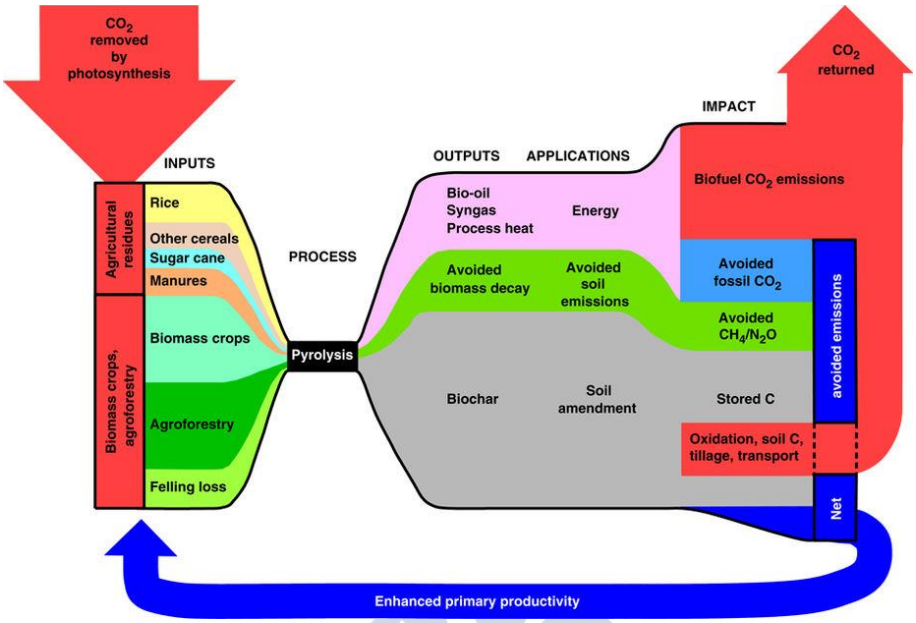

Figura 1.14 Descripción general del concepto de biochar sostenible. En la figura se muestran las entradas, procesos, productos, aplicaciones e impactos del biochar en el calentamiento global. Fuente: (Woolf et al., 2010).

Algunas limitaciones

A pesar de los innumerables beneficios demostrados de la aplicación de biochar en distintos ámbitos de la gestión medio ambiental, existen todavía numerosas incertidumbres sobre los efectos de su aplicación, toxicidad y sus impactos que hacen necesaria más investigación (Kuppussamy et al., 2016). En primer lugar la mayoría de los ensayos se realizan a corto plazo (desde meses a unos pocos años) por lo que existe incertidumbre sobre sus efectos a largo plazo y a veces es difícil determinar cuantitativamente las mejoras que su aplicación produce en el suelo. Además, es necesario profundizar en los estudios sobre la tasa de aplicación de biochar en diferentes tipos de suelo y condiciones climáticas, ya que las propiedades del sistema receptor y su interacción con el biochar van a condicionar sus efectos, pudiendo ser adversos en algunos casos (Galinato et al., 2011; Spokas et al., 2012). Por ejemplo, algunos autores no consiguieron ningún

efecto o vieron reducida la producción de las cosechas (Van Zwieten et al., 2010; Chan et al., 2007) y también se registraron efectos negativos en la biota del suelo (Lehmann et al., 2011). Por otro lado existe incertidumbre sobre el efecto del biochar en la eficacia y biodisponibilidad de agroquímicos como pueden ser fertilizantes, pesticidas o herbicidas (Sparkes & Stoutjesdijk, 2011). La aplicación de biochar puede tener dos efectos potenciales sobre ellos: inactivarlos uniéndose los productos químicos orgánicos al biochar, este es el caso observado por Graber et al. (2012) con herbicidas aplicados en suelos con biochar, obteniendo una reducción de la eficiencia de los mismos; o en segundo lugar, inhibir la degradación microbiana de los compuestos orgánicos (Kookana, 2010), alterando por tanto la permanencia de los compuestos en el suelo.

La aplicación del biochar al suelo puede tener efectos en el albedo del suelo ya que su aplicación supone un oscurecimiento del mismo, que hace que absorba más energía, y reduzca el albedo del suelo, luego puede tener una implicación en el cambio climático (Sparkes & Stoutjesdijk, 2011). Esto supondría un aumento en la temperatura del suelo que puede alterar los ciclos de nutrientes (Sohi et al., 2010). Por tanto sería necesario cuantificar la contribución del cambio de albedo producida por el biochar al calentamiento global, si bien hay que tener en cuenta que si el suelo presenta una cubierta vegetal, la influencia del biochar en el albedo será mínima.

Otro factor a considerar es que tanto la superficie de tierra productiva, como el agua, son finitas, lo que supone una competencia directa con la producción alimentaria, que puede traer efectos negativos y positivos (Muler et al., 2008). Por otro lado, los métodos de producción y transporte se deben refinar para hacerlos más eficientes y reducir al máximo las distancias.

Por lo tanto, dado el creciente interés por el biochar, es necesario un estudio exhaustivo de sus propiedades y posibles efectos en el medio de aplicación para reducir cualquier tipo de riesgo ambiental.

2. General objectives

USC
UNIVERSIDADE
DE SANTIAGO
DE COMPOSTELA

OBJETIVOS

Actualmente, nos encontramos bajo un contexto de cambio global, con una población mundial creciente en continua demanda de alimento y energía y con una gran tasa de generación de residuos, de los cuales la mayor parte no se gestiona de forma adecuada. Esto lleva al agotamiento de los recursos y al incremento de la contaminación de suelos y aguas. El uso de residuos para producir biocarbón o biochar supone una alternativa innovadora que permite dar solución de forma integral a varios de estos problemas en base a una economía circular. El biocarbón permite en primer lugar la estabilización de C fijado fotosintéticamente, y al mismo tiempo la reducción de residuos y la producción de energía. Además su aplicación al suelo aporta otros beneficios económicos al mejorar las propiedades del suelo y permitir la remediación de áreas contaminadas. Sin embargo, las condiciones de producción y materias primas utilizadas determinarán las propiedades del biocarbón así como su aplicabilidad y sostenibilidad.

Teniendo en cuenta esta situación, el principal objetivo de este trabajo es la producción y caracterización de materiales carbonosos (biochar) generados a partir de distintos tipos de residuos mediante procesos de pirólisis en un reactor experimental de bajo coste, capaz de producir biocarbón a escala semi-industrial. Además se evaluará su potencial para utilizarlos en la remediación de diferentes problemas medioambientales como mitigar el cambio climático, la mejora de las propiedades del suelo, la descontaminación de espacios degradados o la reducción de la huella de carbono de procesos industriales, entre otros. Para ello se desarrollaron una serie de ensayos con los siguientes objetivos particulares:

- Estimar la temperatura de pirólisis a la que fue producido cada biocarbón mediante técnicas de infrarrojo próximo.
- Determinar las propiedades y características de los biocarbones producidos, analizando su variabilidad en función de las distintas condiciones de pirólisis y materias primas. Los biocarbones

producidos se clasificaron en función de su potencial como fijadores de C para luchar contra el cambio climático global y por su capacidad enmendante y fertilizante.

- Establecer la capacidad de los biocarbones para inmovilizar contaminantes orgánicos derivados del petróleo que contaminen aguas y suelos, como son los compuestos orgánicos volátiles o el diésel.
- Estudiar la viabilidad de su aplicación en la industria metalúrgica, como sustitutivo del carbón en la producción del silicio, que supondría la reducción de las emisiones de C.

Todo ello, con un enfoque adecuado de gestión y valorización de residuos, que utilice recursos locales, permita una economía circular y una tecnología de bajo coste, aplicable tanto en proyectos de recuperación ambiental como de mejora productiva de suelos agrícolas y silvícolas.

OBJECTIVES

Within the context of global change, the growing world population is placing ever-increasing demands on food and energy resources while also generating huge amounts of waste that are not usually managed properly. This leads to depletion of the resources and increased contamination of soil and water. The use of waste to produce biochar is an innovative option that potentially provides a solution to several of these problems, supporting a circular, bio-based economy. Thus, biochar production enables stabilisation of photosynthetically fixed C, generation of energy and reduction of waste. In addition, the application of biochar to soils provides other economic benefits by improving soil properties and allowing the remediation of contaminated areas. However, the properties of the biochar produced, as well as its applicability and sustainability, depend on the pyrolysis conditions and feedstock used, and these variables must therefore be studied in detail.

Within this context, the main objectives of the present study are as follows: (i) to characterise biochars produced in a low-cost experimental reactor on a semi-industrial scale, and (ii) to evaluate the potential use of biochar to resolve different environmental problems, with the aim of mitigating global climate change, improving soil properties, decontaminating degraded areas and reducing the C footprint of industrial process.

Different studies were carried out with the following specific objectives:

- To estimate the highest heating temperature reached during pyrolysis of different types of biochar by using near infrared spectroscopy and applying mathematical models to the data.
- To determine the properties and characteristics of the different types of biochar produced, by analysing how they vary in relation to pyrolysis conditions and feedstock. Biochar types were classified according to their C sink potential and fertiliser value.

- To determine the capacity of biochar to adsorb and retain fuel organic pollutants such as volatile organic compounds and diesel, which contaminate water and soils.
- To study the viability of using biochar as an alternative to coal in the metal industry to produce high quality silicon, which would imply a reduction in C emissions and an improvement of the sustainability of the entire process.

The use of biochar as outlined above will enable the creation of a circular economy with low-cost technology that will be applicable to the environmental recovery of damaged areas and the improvement of agricultural and forestry soils, together with an adequate approach towards waste management and valorisation and use of local resources.

3. Biochar production and prediction of the highest pyrolysis temperature by Near-Infrared Spectroscopy (NIRS)

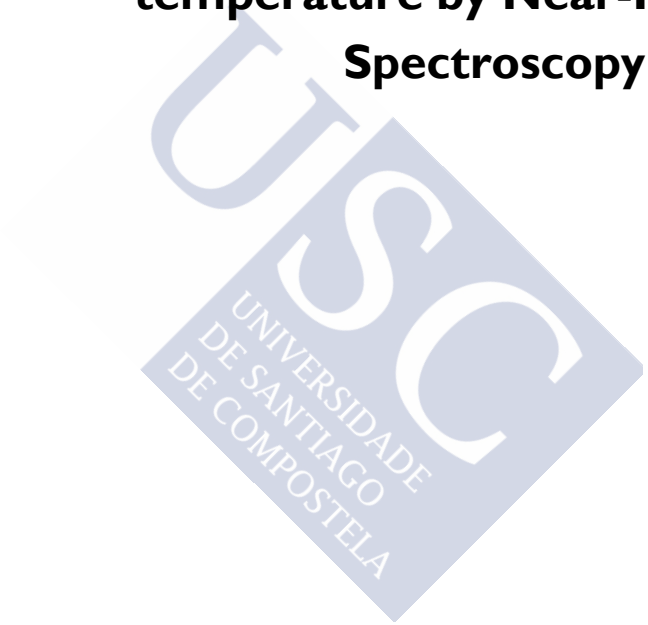

USC
UNIVERSIDADE
DE SANTIAGO
DE COMPOSTELA

INTRODUCTION

The highest heating temperature (HHT), feedstock composition and pyrolysis conditions are known to affect the properties that will ultimately determine the persistence of biochar in soil and/or its fertiliser value (Brewer et al., 2012; Calvelo Pereira et al., 2011; Lehmann & Joseph, 2009; Lehmann et al., 2015; Antal & Gronli, 2003). Among the variety of thermochemical conversion technologies currently used to produce biochar, pyrolysis is the most common. A wide range of HHTs (varying from 200 to 900 °C) have been tested in biochar research for application in the pyrolysis process (Ahmad et al., 2014; Spokas et al., 2012). Importantly, the reaction conditions must be tightly controlled to achieve consistently good quality products. The main methods used to regulate the heating conditions during pyrolysis are (i) measurement and control of the temperature inside the reactor, and (ii) examination of the colour of the vapours produced (Boateng et al., 2015). The latter is used in simple pyrolysis reactors such as brick kilns, in which the colour of the smoke is monitored. At the beginning of the carbonisation process, the smoke is white and it then turns bluish white and finally transparent blue. Once the transparent colour is stable, the air inlet is closed and the pyrolysis process stops (FAO, 1987). Even in high technology reactors, which have multiple thermocouples inside the pyrolysis kiln for monitoring the temperature, accurate measurement of the HHT reached during the process can be complicated by the existence of temperature gradients (Van de Velden et al., 2010; Guerrero, 2010). Several techniques have been proposed for determining the HHT reached in carbonised materials, such as Raman spectroscopy, in which characteristic bands (1340 and 1590 cm^{-1}) observed in the spectra of pyrolysed samples are linked to variations in HHT (McDonald-Wharry et al., 2013; Yamauchi & Kurimoto, 2003). Nevertheless, this technique requires a powerful laser to yield high quality signals. There is also a risk that the samples could be burned with high energy radiation, and preliminary testing must therefore

be carried out before measurements are made, which results in high maintenance costs of the instrument (Jestel, 2010).

The use of Near Infrared Spectroscopy (NIRS) to determine biochar properties has recently been proposed. NIRS, which is based on the interaction between electromagnetic radiation (780-2500 nm wavelength) and molecules, is a rapid, inexpensive technique relative to the previous approaches. Although less specific than mid infrared spectroscopy, NIRS can provide quantitative information about molecules with C-H, N-H, S-H, C=O and O-H bonds in organic and inorganic compounds, and it is also very useful for determining the chemical composition of samples (Guerrero, 2010). Empirical approaches are used to obtain the maximum benefit from the information generated in the NIRS spectrum, and models are constructed using a statistical technique known as chemometrics. This approach has been widely used in different fields (e.g. the petrochemical industry, the food industry, medicine, and the environment). It has been used to predict physical, chemical and biological soil properties (Kusumo et al., 2011) as well as to estimate the maximum temperature reached in burned soils (Guerrero, 2010). Recently, NIRS has also been shown to be a valid technique for predicting biochar properties related to carbon preservation (Kusumo et al., 2011) and HHT (Mahmud et al., in preparation).

The vast majority of research on biochar uses experimental material produced on a small scale under laboratory conditions or biochar produced on an industrial scale (in high tech ovens) by commercial companies. The first objective of the present study was to generate biochar in a low-cost pyrolysis reactor, to enable production of biochar on a semi-industrial scale (kilograms per day), in a cheap and effective process. The biochar thus produced will be further used as an ingredient of Technosols to help solve environmental problems and to recover damaged areas in projects developed by the Environmental Technology Laboratory at the University of Santiago de Compostela (LTA-USC). This experimental reactor will also

serve as the basis for a future development of a technology that could be used by farmers or local communities to valorise their own waste simply and economically and obtain a product that can then be added to their soils. This will contribute to fulfilling the "dream" of Wim Sombroek, who claimed that every farmer in Amazonia (and in other parts of the world) would be able to create their own sustainable soils by adding biochar as a replication of Amazonian dark earths (Sombroek et al., 2002).

The feedstock may represent an important part of the cost of biochar production systems (Shackley et al., 2015), and it is therefore important to obtain a supply of low-cost materials. The types of feedstock selected for analysis in the present study were bio-wastes potentially generated during different human activities (agriculture, forestry and industry), as well as invasive plants or energetic crops. Moreover, all of the materials included in this study were produced locally (or close to a recovering area) and thus did not require long distance transportation, making the system even more efficient and economically viable. In 2012, the European Biochar Certificate (EBC) established a maximum distance of 80 km as the distance allowed for transportation of feedstock to produce biochar (longer distances are only admissible for scientific purposes).

As controlling the pyrolysis temperature may be challenging with a simple reactor, the second objective of the study was to estimate the HHT during pyrolysis by applying the NIR spectroscopic method developed by Mahmud et al. (in prep.) at the New Zealand Biochar Research Centre (NZBRC).

MATERIALS AND METHODS

Feedstock

Eleven different types of feedstocks were used to produce biochar:

- Invasive plants: *Acacia melanoxylon* bark, sapwood and heartwood (AcB, AcSw, AcHw, respectively). This material was tested as a

feedstock, as acacia is considered one of the most important invasive plants in Portugal and Spain. It is included in the Global Invasive Species Database, because of its fast growth and wide ecological tolerance, which lead to the displacement of autochthonous vegetation. Controlling expansion of this species is expensive and ineffective. Pyrolysing acacia wood before the seeds are disseminated may be a novel approach to preventing further propagation and reducing the population of the species.

- Agricultural residues: corncob (Cc), chestnut (Cn), vine shoot (Vn) and rice husk (Rh), all waste residues from common crops grown in the region or other parts of the country.
- Forestry residues: eucalyptus wood (Eu), pine sawdust (Sd) and pine bark (Pb). These species were selected as the most representative of those used in the Galician forestry industry and considering that small branches, sawdust, bark and other residues from the forestry industry could be used to produce biochar, in addition to excess forest biomass (small trees and bushes), the presence of which may increase the risk of forest fires.
- Herbaceous plants: miscanthus grass (Mis), which is traditionally grown as an energy crop for biofuel production. Miscanthus rapidly adapts to new environments and is resistant to low temperatures (Speller, 1993).
- Animal residues and compost: chicken manure (Cm) and olive pomace compost (Opc). Galicia and Extremadura are the regions of Spain with the largest number of livestock farms (ECOREGA, 2013). Olive mill pomace is one of the by-products of olive oil production, an important business in eastern and southern Spain that generates considerable amounts of organic waste.
- Industrial waste: tyres (Ty) and plastic (Pl). The plastic used in this study was wasted material dumped in yellow recycling containers, but comprising small pieces or types of plastic that cannot be recycled. The tyres were removed from abandoned vehicles. Both

of these are abundant waste products that are difficult to manage and, often, end up in landfills or are burnt in uncontrolled fires. Therefore, the pyrolysis of Ty and Pl is an interesting option that requires further investigation, even though these materials are not included in the list published by the EBC (2012) as feedstock approved for producing biochar.

Figure 3.1 Different types of feedstock tested for producing biochar.

Biochar production

Biochar was produced by F. Macías-García between 2014-2016 in two experimental low-cost biomass pyrolysis units designed by Prof. M. Bao and T. García-Ares (Garcia-Ares, 2015) and based at the CVAN ("Centro de Valorización Ambiental del Norte SL") installations in the Touro mine (Santiago de Compostela, Spain). The first reactor designed (Figure 3.2A) consisted of two iron stoves connected with a tube. In the first stove, wood was burned to produce heat, and the hot gases generated without oxygen moved to the other stove to pyrolyse the feedstock. A second reactor was later designed with the intention of increasing the biochar production capacity (volume 2500 L) (Figure 3.2B). Both reactors are operated in batch mode with manual charging of feedstock and discharging of biochar. Temperature sensors were placed in the reactors to control pyrolysis conditions. The operational settings in both systems were varied between 300 and 550 °C and the residence time, between 1.5 and 6 h, depending on moisture content and other feedstock properties. The different types of biochar produced were designated the name of the original feedstock, with the prefix "B". Some biochars included in the research were produced in other experimental reactors and were included in this study for purposes of comparison: pine bark (BPb) and rice husk biochar (BRh), which were produced in an experimental reactor in Bordeaux; a pine sawdust biochar (BSdG) produced at the Fraunhofer Institute for environmental, safety, and energy technology (UMSICHT) in Germany, and tyre biochar (BTy), which was produced in an industrial oven in Galicia, under controlled conditions of pyrolysis to prevent emission of contaminants. All samples were ground and sieved to 2 mm or 0.1 mm, depending on the requirements of the characterization method.

Figure 3.2 Low-cost experimental pyrolysis reactors (Garcia-Ares, 2015).

UV-Visible NIR Spectral acquisition and pre-processing

UV-Visible NIR spectral reflectance was obtained with a soil contact probe (supplied by ASD) attached by fibre optic cable to the spectrometer-ASD FieldSpec 3 V-NIR Spectrometer (Analytical Spectral Device, Boulder, CO) located at the Landcare Research facilities in Palmerston North (New Zealand). The spectrometer provides spectra from 350 to 2500 nm with 1 nm resolution. Thirty spectra acquisitions were recorded per sample and the average was assigned as the final spectrum. Indico Pro version 6.0 software was used for splice correction in the spectrum.

Chemometric ParLeS software was used for spectral pre-processing and to identify significant peaks (Viscarra Rossel, 2008). Data were transformed from reflectance (R) to absorbance (A) by applying the relation A= log (1/R); the data were pre-processed using wavelet detrending (with 0.2 and 5, trend and decomposition level, respectively). A Savitzky–Golay filter with a third-order polynomial algorithm and a window size of 7 nm was used to reduce the noise. The smoothed data were thereafter processed to the first derivative and finally treated using mean centring

(Savitzky & Miller, 1964). Only pre-processed NIR spectral data at selected wavelength ranges of 780-2450 nm were used, rather than the full-recorded bands of 350-2500 nm, to minimise noise.

The maximum pyrolysis temperature of biochar samples was estimated using the NIR calibration model developed by Mahmud, et al. (in prep.). Briefly, the NIR calibration model was built using Partial Least Square Regression (PLSR) analysis by correlating the pre-processed NIR spectral data (780-2450 nm) of 82 biochar samples produced from different types of feedstock and under different pyrolysis conditions to the reference data, i.e. the recorded highest heating temperature (HHT). The model performance was assessed by the leave-one-out cross validation (LOO-CV) technique and with an external prediction set (n = 20), before it was used to estimate the HTT of biochar samples in this study.

Five samples of pine biochar produced under controlled conditions (at 300, 400, 500, 550 and 600°C) at Massey University (New Zealand) were also measured and used for technical purposes.

Principal Components Analysis (PCA), implemented in Minitab software (Minitab Inc., State College, Pennsylvania), was applied to the pre-processed NIRS data to examine the accuracy of predicted temperatures, to produce the sample distribution patterns and determine any outliers.

RESULTS

Range of types of biochar produced

A total of 23 carbonised materials were analysed in this study, including those produced at LTA-USC (19 samples) and those produced in other reactors (4 samples) (Figure 3.3 and Table 3.1). The degree of carbonisation of the samples varied widely due to the variability of feedstock composition and production conditions. In some of the biochar samples, unburned particles were visible to the naked eye, e.g. in one eucalyptus biochar (BEu-1), biochar produced from chicken manure (BCm) and the olive pomace

compost biochar (BOpc) (Figure 3.3). The heterogeneous carbonisation of the biochar in a single batch reflects the differences in heat distribution in the combustion chamber. By contrast, other types of biochar, e.g. the corncob biochar, were uniformly carbonised.

Accurate determination of the exact yield from each feedstock was not possible, as the moisture content of the raw material varied greatly depending on the origin of feedstock and meteorological conditions. However, the overall yield was approximately 25-30% in volume. With corncob, which has a density of 0.3 kg L^{-1}, around 240 kg of biochar was produced per run in the biggest reactor.

Figure 3.3 Biochar obtained from each feedstock grouped by origin.

Table 3.1 Feedstock and description of the 23 biochar samples analysed.

Sample Code	Lab. code	Source	Feedstock and description
BCc-1	14-0991	LTA-USC	Corncob (2014)
BCc-2	14-1301	LTA-USC	Corncob (2014)
BCc-3	15-0605	LTA-USC	Corncob (3 h) control low O_2 (2015)
BAcB	14-0258	LTA-USC	*Acacia melanoxylon* Bark 2h 350 °C (2014)
BAcSw-1	14-0260	LTA-USC	*Acacia melanoxylon* sapwood 3 h 350 °C (2014)
BAcSw-2	14-0261	LTA-USC	*Acacia melanoxylon* sapwood 2 h 350 °C (2014)
BAcSw-3	14-0263	LTA-USC	*Acacia melanoxylon* sapwood 2 h 300 °C (2014)
BAcHw-1	14-0259	LTA-USC	*Acacia melanoxylon* heartwood 3 h 350 °C (2014)
BAcHw-2	14-0262	LTA-USC	*Acacia melanoxylon* heartwood 2 h 300 °C (2014)
BEu-1	14-0264	LTA-USC	Eucalyptus 1 h 400 °C, 0.5 h 350 °C (2014)
BEu-2	14-1300	LTA-USC	Eucalyptus (2014)
BSd-1	14-0265	LTA-USC	Sawdust (2014)
BSd-2	14-0464	LTA-USC	Compacted sawdust 3.5 h 300 °C (2014)
BCm	14-0467	LTA-USC	Chicken manure 6 h 300 °C (2014)
BOpc	14-0600	LTA-USC	Olive pomace compost 5.5 h 450 °C (2014)
BCn	14-1218	LTA-USC	Chestnut (2014)
BMis	15-0046	LTA-USC	Miscanthus (2015)
BVs	15-0435	LTA-USC	Vine shoots (2015)
BPl	15-1016	LTA-USC	Plastic wastes (2015)
BPb	14-0577	Bordeaux	Pine bark (2014)
BRh	14-0578	Bordeaux	Rice husk (2014)
BSdG	15-0470	Germany	German crushed wood chip biochar (2015)
BTy	15-0410	Industrial	Tyre (2015)

Spectral absorbance of the biochar samples and HHT estimation

The NIR absorbance spectra of the 28 biochar samples analysed (23 samples + 5 biochars for technical purposes) are shown in Figure 3.4 and Figure 3.5. Spectra were used to estimate the highest heating temperature as described in Table 3.2. Overall, there was a good correlation between the estimated temperatures and those measured using the probe in the reactor and the visual inspection of the samples. Biochars produced at higher temperatures displayed high absorbance, and the spectra were flat and lacked recognisable peaks (Figure 3.5) due to loss of thermolabile compounds during the thermal process and the effect of dark colours, which absorb more radiation. By contrast, the spectra of low temperature biochars (≤ 400°C) showed significant absorption bands (Figure 3.4). The direct interpretation of NIR spectra is, however, difficult due to the overlapping of absorption bands of different molecules in the same region. Nevertheless, a clear peak appeared at ~1940 nm, corresponding to moisture (De Muñiz et al., 2013). The OH absorption was identified at ~1400 nm (Kusumo et al., 2011) and the peak around 2380 nm was attributed to holocellulose (De Muñiz et al., 2013).

Inconsistencies were found between measured and estimated temperatures of acacia bark biochar (BAcB), chicken manure (BCm) and olive pomace compost (BOpc). The estimated temperature was lower than that measured in the reactor during pyrolysis. The estimated temperature is probably more accurate as even uncharred material was discernible in these samples on visual inspection, which was a clear sign that the target temperature was not reached. Moreover, the original Cm and Opc feedstocks had a high moisture content and were very heterogeneous, which contributed to the lack of uniform carbonisation. The differences between the temperature measured in the pyrolysis chamber and that estimated in the sample suggest that, at least in some cases, the temperature in the combustion chamber was not the same as that inside the sample, due to the presence of heat gradients.

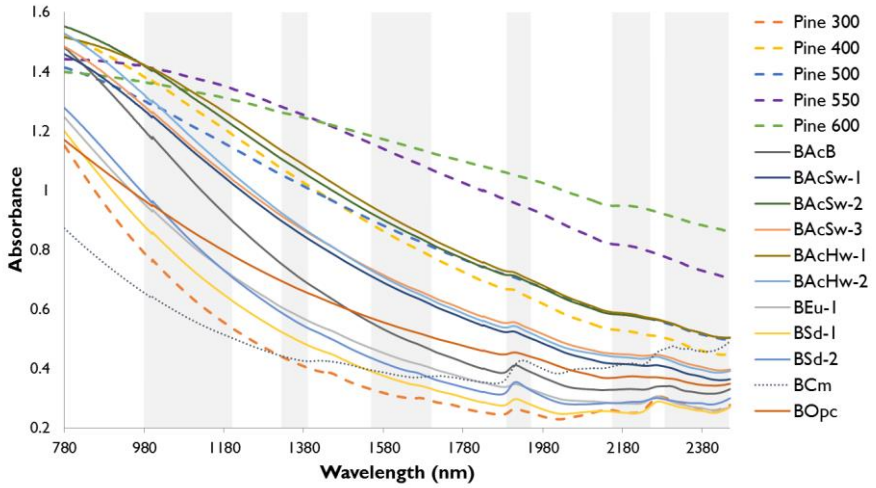

Figure 3.4 NIR spectral absorbance of biochar samples with an estimated HHT ≤ 400 °C; absorbance = log(1/reflectance). Shaded areas represent bands regions associated with variations in the samples. The discontinued lines represent the five samples used for technical purposes in the prediction model.

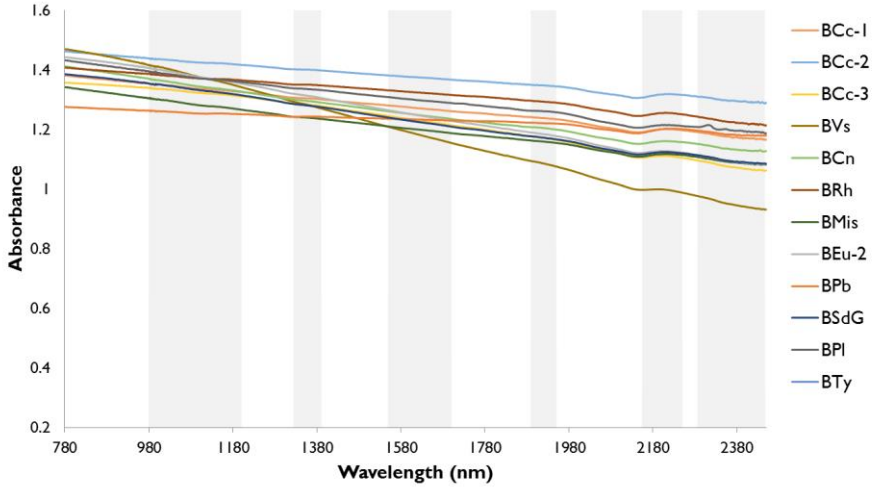

Figure 3.5 NIR spectral absorbance of different samples with an estimated HHT > 400 °C; absorbance = log(1/reflectance). Shaded areas represent bands regions associated with variations in the samples.

Table 3.2 Estimated maximum pyrolysis temperature obtained by NIRS analysis.

Sample	N° code PCA	Temperature measured during pyrolysis	NIRS Estimated Temperature ± 50 °C
BAcB	4	350	< 300
BAcSw-1	6	350	350
BAcSw-2	7	350	400
BAcSw-3	9	300	300
BAcHw-1	5	350	400
BAcHw-2	8	300	350
BEu-1	10	400	400
BEu-2	20	-	500
BSd-1	11	-	300
BSd-2	12	300	400
BCm	14	300	< 300
BOpc	17	450	350
BCc-1	18	-	500
BCc-2	21	-	500
BCc-3	26	-	500
BCn	19	-	500
BMis	22	-	500
BVs	24	-	450
BPl	27	-	450
BPb	15	-	550
BRh	16	-	600
BSdG	25	-	450
BTy	23	-	550

Information about the temperature at which the biochar was produced was only available for 10 of the 23 original samples analysed. Thus, the accuracy of this prediction could not be evaluated using statistics such as RPD (ratio of prediction to deviation) or RMSEP (root mean squared error of prediction) due to the insufficient reference data. As an alternative approach, PCA was used to group the different biochars under study. Ten principal components (PC) represented 94.7% of the total variation of NIRS data obtained from all 23 samples, with PC 1 and PC 2 accounting for 58.4% and 13.3% of the variation, respectively (Figure 3.6). The distribution of samples in the score plots showed a clear trend from PCA scores plot based on HHT. The biochar samples produced at temperatures > 400 °C were included together in the IV quadrant (Figure 3.6), tightly clustered together regardless of feedstock type, with the exception of the samples produced from tyres (BTy n°. 23) and plastic waste (BPl n°. 27), probably because of the different chemical constituents. The samples of biochar produced at the lowest temperature (≤ 400 °C) were more variable, as shown by the spectral absorbance of biochar samples in Figure 3.4 and the PCA score plot (Figure 3.6). All biochar produced at lower temperature (≤ 400 °C) tended to spread out more than the biochar produced at higher temperatures (> 400 °C). The PCA confirmed the existence of an outlier or sample with unsual characteristics (the sample plotted at the bottom left – Quadrant III – was clearly isolated from other biochar samples; which was not adequately predicted using the NIR calibration model, and whose special characteristics could be inferred by visual inspection of the spectra. This was the chicken manure biochar (BCm, sample n°. 14), which had a different spectrum from those of the other samples (dotted line in Figure 3.4). The type of feedstock used strongly influenced the biochar samples produced at low temperatures, with woody pyrolysed material (acacia, sawdust and eucalyptus) appearing in the positive area of PC 2, and chicken manure and olive pomace compost (BOpc sample n°. 17) appearing on the negative side of the axis.

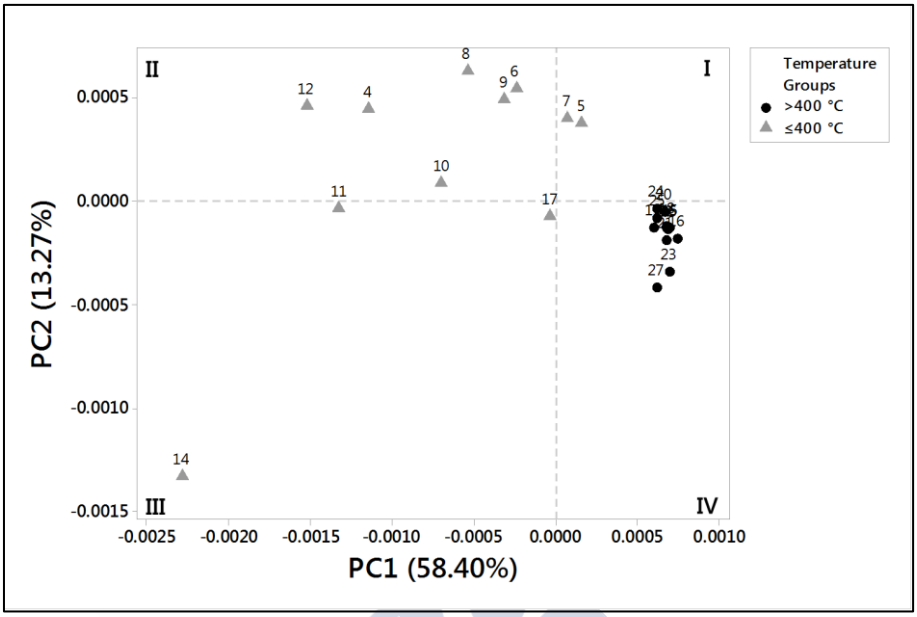

Figure 3.6 PCA used to estimate pyrolysis temperatures. Samples are classified according to production temperatures, > 400 °C represented as circles and ≤400°C as triangles. The reference number of samples is indicated in Table 3.2.

DISCUSSION

Most of the biochar samples analysed in this study were produced in two experimental reactors at LTA-USC. Although both reactors included a probe to measure temperature and to control pyrolysis conditions, in practice, the process was mainly regulated by visual observation of the variation in pyrolysis gases, colour and smell. Pyrolysis was considered optimal when the gases were almost transparent and the entire surface of the kiln was as hot as if water was spilled on the wall of the kiln, it immediately evaporated, causing a spitting sound. This simple, apparently imprecise method was defined (a few decades ago) as a way of producing charcoal, with satisfactory results (FAO, 1987). The degree of carbonisation of the different biochar samples varied, which is consistent with their different HHT, as estimated by NIRS. Some of the differences observed in biochars produced from the same specific feedstock and identical HHT can

be explained by optimization of the pyrolysis process over time. This is the case of BEu-1 compared with BEu-2. Acacia and sawdust biochars were also produced before optimisation of the process. Once pyrolysis was optimised, replicability improved and fluctuated only slightly when the feedstock was changed.

The type of feedstock, as it is well known, also contributed to the variability. The woody materials contained different proportions of cellulose, hemicellulose and lignin, which degrade at different temperatures, thus affecting the physico-chemical properties of biochar as well as the yield (Ripberger, 2016). Hemicellulose begins to decompose at 220°C and its decomposition is completed at 315°C. At that point, the degradation of cellulose is maximal (Yang et al., 2007). Of the three principal components of wood biomass, lignin is the most thermo-stable. It degrades slowly and steadily between 160°C and 900°C, so that the use of lignin-rich biomass (e.g. wood) will increase the yield (Sparkes & Stoutjesdijk, 2011). Furthermore, the yields obtained in this study are consistent with those previously published in the literature (Antal & Gronli, 2003; FAO, 1987; Brown et al., 2015).

The moisture content also affected the degree of carbonisation of the feedstock. For example, chicken manure contained more water than woody feedstocks, and this consumes energy during evaporation. The moisture content was also dependant on weather conditions, as the raw materials were stored outside when obtained in large amounts. For optimal outcome, the feedstocks should contain less than 10-20% of moisture to make the reaction more efficient (Kurchania, 2012; Riuji Lohri et al., 2016). Storing the raw material under cover and drying over-moist samples may also help to improve the efficiency of the process.

Variations in NIR spectra were also caused by changes in the HHT. However, the process of converting the feedstock into biochar and the resulting properties of the material produced are also influenced by feedstock type and other pyrolysis conditions (Brown, 2009), which in turn

affect the predicted outcomes. Other researchers have found that, even when the same plant species are used as feedstock, different soil or climatic conditions also contribute to the variability, as well as the part of the plant pyrolysed and the particle size (Sparkes & Stoutjesdijk, 2011; Brown et al., 2015). The prediction was therefore less accurate for more heterogeneous samples, such as manure and compost, which may explain the existence of an apparent outlier. Manure consists of a mixture of seeds, hair or feathers, proteins, digested food, bedding material and minerals (Joseph et al., 2010), which react differently to heat treatment, particularly at lower temperature. Similarly, olive pomace compost consists of soil, olive bones, peel and small pieces of wood, among other elements, all of which degrade at different temperatures. Hence, the production conditions in a specific pyrolyser must be optimised for each feedstock, depending on its composition and moisture content.

In addition to the visual inspection of the NIR spectra, followed by the PCA, the estimated pyrolysis temperature was also related to other biochar properties associated with their thermal degradation, i.e. the increase in C content and decrease in molar H/C_{org} ratio with increasing pyrolysis temperature (data shown in Chapter 4), which supports the accuracy of the prediction.

FUTURE PLANS

Future directions include improvement of the pyrolysis reactor in order to make the process more efficient and easier to manage. Some required modifications had already been proposed by García-Ares (2015), including the use of a chain hoist as a way to facilitate the charge/discharge of feedstock and biochar. In addition, a new mobile pyrolyser has been designed (by M. Bao and T. García-Ares) to include a recovery gas system (to allow the gases to recirculate within the pyrolysis chamber and also to take advantage of the heat) and a drier unit for drying the feedstock material prior to pyrolysis.

CONCLUSIONS

This study demonstrated that it is possible to produce biochar in a low-cost experimental pyrolysis reactor with various types of waste, including industrial, agriculture and forestry residues, as well as invasive plants, manure, compost and energy crops. Satisfactory results in relation to yield, visual aspect and homogeneous carbonisation of the biochar were obtained after optimisation of the pyrolysis process. However, further optimization of the process is required to improve its use for some heterogeneous materials such as manure and compost, in order to produce high quality biochar.

The HHT was accurately estimated by NIRS, a simple, quick and cheap inexpensive method (if the equipment is available). The differences between the experimentally measured temperature during pyrolysis and the predicted temperature may be at least partly attributed to the existence of a thermal gradient inside the kiln. As the temperature decreased, the heterogeneity of the spectra increased. The use of non-homogenous feedstock affected the process, especially for low temperature biochar.

ACKNOWLEDGEMENTS

I would like to acknowledge CVAN for producing the biochar samples analysed in this study.

4. Characterisation and classification of biochar in relation to carbon sequestration potential

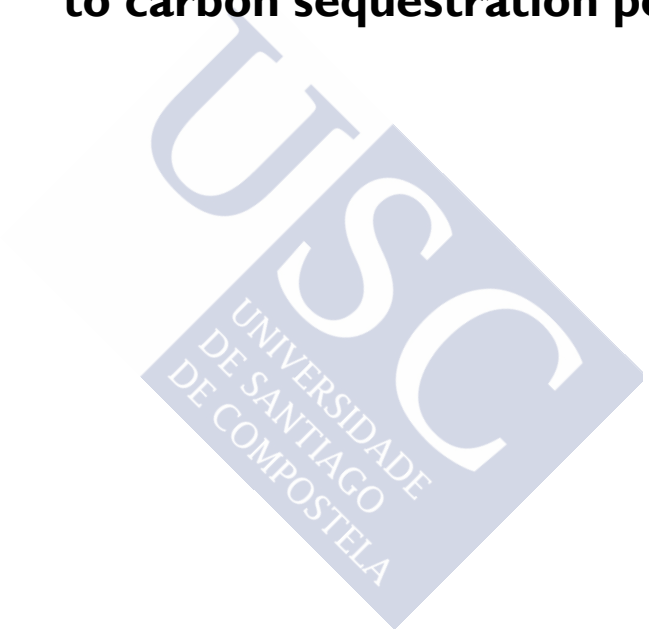

USC
UNIVERSIDADE
DE SANTIAGO
DE COMPOSTELA

INTRODUCTION

Organic matter in soil and biomass is originally created by photosynthetic fixation of atmospheric carbon dioxide, which takes place under strongly reducing conditions (Eh ~−600 mV). The soil redox potential generally varies between -300 and +900 mV, and is usually in the range +300 to +500 mV under aerobic conditions. Fresh organic matter is therefore thermodynamically unstable in soils, especially the most reduced fraction, followed by necromass and most of the soil organic matter (Figure 4.1A) (Macías & Camps Arbestain, 2010). Environmental Eh-pH conditions determine the thermodynamic stability of C forms (Figure 4.1B).

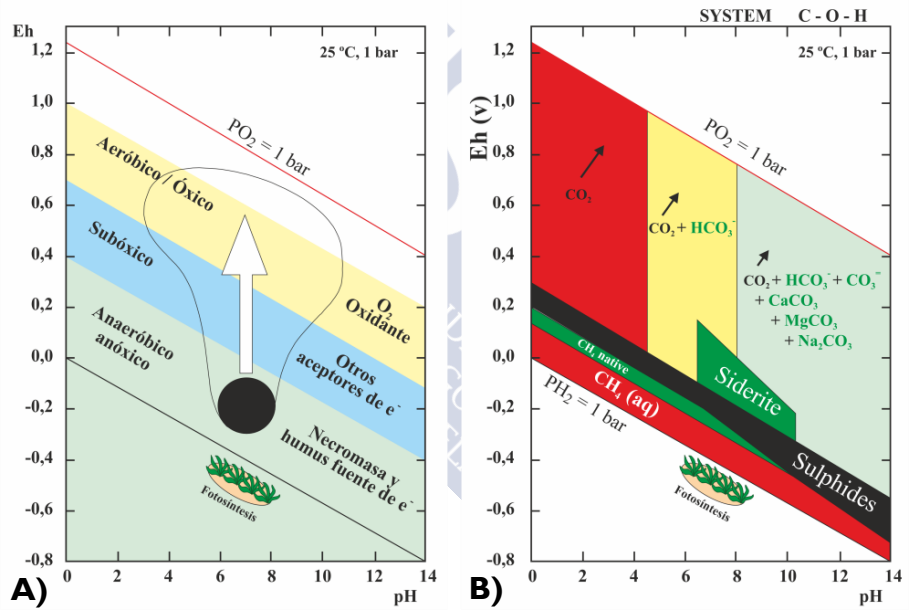

Figure 4.1 A) Eh-pH conditions during photosynthesis and necromass in soils under different redox conditions: anaerobic (green), suboxic (blue) and aerobic conditions (yellow). The mushroom-shaped area represents the prevailing conditions in most soils. B) C forms depending on Eh-pH conditions (Macías & Camps Arbestain, 2010).

Organic matter decomposes at a faster rate under oxidizing conditions than under reducing conditions; however, organic C can be meta-stabilised by different mechanisms and remain stable in soils for centuries or millennia (Macías et al., 2004; Macías et al., 2005). The stability of C in soils will depend on the origin, climate, topography, lithology, type of soil and human actions associated with land-use changes, and the persistence (recalcitrance) of C will vary widely depending on the biogeochemical conditions of the system in which is located and, above all, on the mechanisms of meta-stabilisation (Macías et al., 2004; Macías & Camps Arbestain, 2010). As charred organic materials has been described as a key component of the long-term stability of organic matter in Terra preta soils (Glaser et al., 2000), pyrogenic C and its preservation in soils have been widely studied. Black carbon (pyrogenic C) appears in the environment as the result of human activity, but also as a consequence of naturally occurring forest and vegetation fires (Masiello, 2004). However, black carbon is not a single compound and Hedges et al. (2000) referred to "the black carbon continuum" (Figure 4.2) to describe the different black carbon forms present in environment derived from thermo-chemical conversion of biomass, with all components rich in carbon and dominated by aromatic structures (Masiello, 2004). The continuum ranges from slightly charred biomass, char, charcoal to soot and graphite, as the most stable carbon form. The term biochar extends across all divisions.

Biochar could potentially play an important role in addressing climate change. Biochar is produced by transforming biomass that is readily decomposable and generates gases (CO_2, CH_4, NO_x, H_2O, NH_4^+, HS_2, CO…), into a more chemically and biologically stable C form (Lehmann et al., 2015). The stability of biochar is derived from its ability to resist degradation. The C stability in biochar and the concentrations of aromatic C structures are highly dependent on the thermochemical conditions. The aim of the research reported in this chapter was to characterise the samples described in Chapter 3 (Table 3.1) by using different methods to

assess the stability of biochar and its potential as C sink and to determine the quality of the biochars.

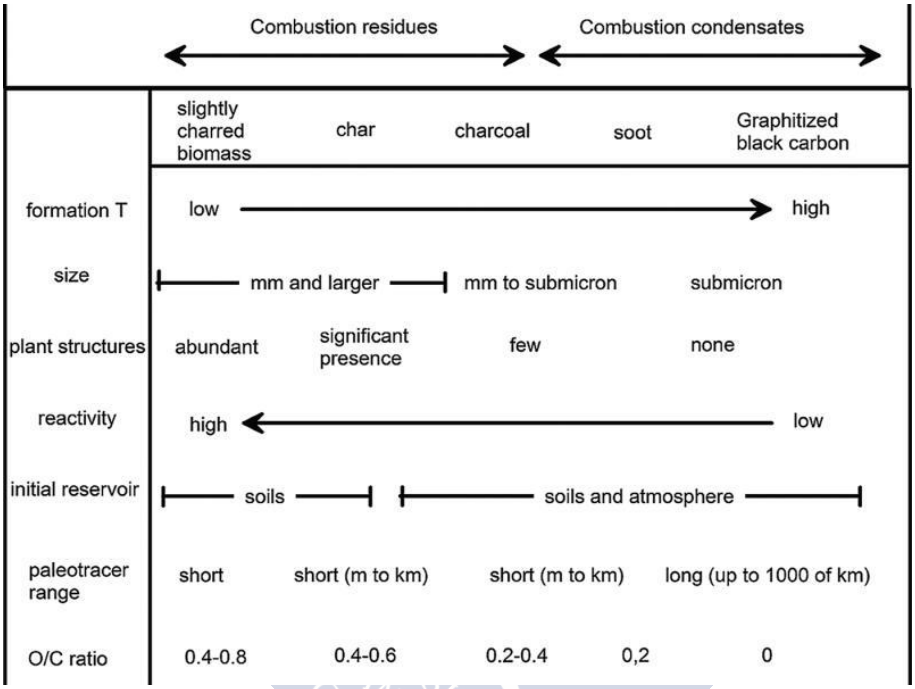

Figure 4.2 Spectrum of the combustion product continuum as a result of the thermochemical conversion of biomass (Schimmelpfennig & Glaser, 2012).

MATERIALS AND METHODS

Elemental analysis

Biochar samples and feedstock were characterised using different analytical techniques. Total C (C_T), H and N were determined in a TruSpec CHN analyser and S was determined in a LECO SC-144DR analyser. The ash content was determined by combustion at 1000 °C for 4 h. Oxygen content was estimated as follows: O = 100 – C + N + H + S + ash. The inorganic C (C_{inorg}) content was determined from the weight loss associated with the endothermic peak between 600-900 °C under air atmosphere in TGA analysis (Wang et al., 2014) in a simultaneous thermal analyser

(STA6000 PerkinElmer). A calibration curve constructed with oven-dried $CaCO_3$ as a standard was used to correct concentration of CO_3-C in biochars. Organic C (C_{org}) was calculated by subtraction, as $C_{org} = C_T - C_{inorg}$.

Methods of determining C stability

Thermogravimetric analysis and differential scanning calorimetry (TGA-DSC)

TGA-DSC scanning of samples was conducted in triplicate in a Simultaneous Thermal analyser (STA6000 PerkinElmer) in: (i) air atmosphere, according to the procedure of Harvey et al. (2012) for calculating the recalcitrance index (R50), or (ii) N_2 (plus air atmosphere once temperature reached 900 °C), following UNE 32-019-84 Standards for volatile matter content determination in combustible mineral solids. The thermo-degradable fraction (C_{thermo}; ash-free, dry basis) is defined as the fraction of volatile matter (VM) relative to the sum of volatile matter and fixed C content (Calvelo Pereira et al., 2011). Fixed carbon (FixC) was calculated as the solid material remaining after loss of moisture and VM minus the ash (Donahue & Rais, 2009).

$$FixC(\%) = 100 - moisture\ (\%) - ash(\%) - VM(\%)$$

The TGA thermograms obtained in procedure (i) were corrected for moisture and ash contents following the method described by Harvey et al. (2012). The R_{50} Index was then calculated to estimate the recalcitrance potential of biochar, as follows:

$$R_{50} = \frac{T_{50\,x}}{T_{50\,graphite}}$$

where $T_{50\,x}$ and $T_{50\,graphite}$ are the temperatures corresponding to 50% weight loss by respectively oxidation/volatilisation of biochar and graphite, and are obtained from the corrected thermograms. $T_{50\,graphite}$ was assumed to be 886 °C (Harvey et al., 2012).

Oxidative Differential Scanning Calorimetry (DSC) was carried out at the same time as TGA in order to calculate the heat flow and enthalpy of the reaction. Peak temperatures, peak heights and total heat reaction were recorded for subsequent correlation with the stability of the carbonised materials (Leifeld, 2007). Heat flow was calibrated by melting indium and silver.

Chemical oxidation

The oxidability of biochar was determined by wet oxidation with potassium dichromate ($K_2Cr_2O_7$) (Walkley & Black, 1934) and potassium permanganate ($KMnO_4$) (Tirol-Padre & Ladha, 2004). Potassium dichromate-oxidisable organic carbon (C_{dichro}) was determined following a modification of the Walkey-Black oxidation method. Briefly, 0.1 g of biochar (dry and milled) was oxidised in duplicate with 20 mL of 1.8 N $K_2Cr_2O_7$, 5 mL of H_3PO_4 and 20 mL of concentrated H_2SO_4 for 2 h at 110 °C. At the end of the reaction, excess dichromate was determined by titration against 0.033 M $FeSO_4$. Control samples without biochar were also analysed and used as reference samples. The equivalence used to determine the oxidisable C was 1 meq $K_2Cr_2O_7$ = 3 mg C. The difference between total C_{org} and C_{dichro} has been used to calculate the non oxidisable C (C_{nox}), which is associated with black carbon content and recalcitrance.

Potassium permanganate-oxidisable organic C (C_{per}) was determined using 25 mL of 33 mM $KMnO_4$ solution added to 50 mL centrifuge tubes containing an amount of dry biochar (< 2 mm) equivalent to 15 mg organic C (Tirol-Padre & Ladha, 2004). The tubes were shaken for 24 h and centrifuged for 15 min at 3000 rpm. The supernatant was removed and diluted in distilled water (1:25 v/v), and the absorbance was measured at 565 nm with a spectrophotometer (Jasco V-630). Blanks without biochar were analysed before each run. For calculation purposes, it was assumed that three moles of C (e.g. carbohydrates) are oxidised for every four moles of Mn^{+7} reduced (Tirol-Padre & Ladha, 2004).

Sodium pyrophosphate was used as extractant to obtain the extractable C (Cp) (Bascomb, 1986), as an estimate of the most labile C fraction. The sample was extracted with $Na_4P_2O_7$ overnight. An aliquot of pyrophosphate extract was pipetted into an Erlenmeyer flask and evaporated to dryness. The C was determined by dichromate digestion with a 0.1 N solution of Mohr's salt ($(NH_4)2Fe(SO_4)_2 \cdot 6H_2O$) in a similar process to that described for C_{dichro}.

To better understand the "oxidability" of C in biochar, we considered different C fractions, as follows:

I. Non oxidisable C (C_{nox}): calculated as the difference between C_{org} and C_{dichro}.
II. Hardly oxidisable C (C_{hardOx}): calculated as the difference between C_{dichro} and C_{per}. The organic C oxidised with dichromate (C_{dichro}) in warm and acid medium represents the potentially oxidised forms, although only under artificial conditions (Eh ≈1200 mV) that do not exist in soils (prevalent range of Eh in soils between +300 and +500mV (Macías & Camps Arbestain, 2010)), and this type of C will therefore also remain stable in nature for a long time, being scarcely oxidisable.
III. Easily oxidisable C (C_{easyOx}): the fraction of C oxidised with potassium permanganate (C_{per}). Permanganate is less aggressive than dichromate (Eh ≈600 mV), and the oxidising conditions are more similar to natural conditions in soils, and thus the fraction obtained is associated with readily oxidisable C. The $KMnO_4$ promotes oxidation of carbohydrate products, mainly compounds containing glycol groups (Tirol-Padre & Ladha, 2004; Suárez-Abelenda et al., 2014)
IV. Labile C (Cp): this form of C corresponds to the C extracted with pyrophosphate and represents the labile fraction that can interfere in the biochemical processes providing energy to the microorganisms on their transformation (Macías et al., 2004).

Nuclear magnetic resonance spectra (CP-MAS ^{13}C-NMR)

Solid NMR measurements were made in an Agilent (Varian) VNMRS-500-WB spectrometer equipped with a "pencil" probe (5 mm tip). he measurements were made at a proton resonance frequency of 500 MHz and using a zirconia rotor of an outer diameter of 5 mm with a sample capacity of 160 µL. Carbon chemical shifts were referenced to the carbon methylene signal of solid adamantane at 28.92 ppm. This sample was also used for calibration of the ^{13}C Cross Polarisation Magic Angle Spinning (1D ^{13}C CPMAS) experiments. Proton chemical shifts were referenced to the 1H MAS spectrum of adamantane at 1.87 and 1.75 ppm.

The 1D ^{13}C CPMAS spectrum of the samples was obtained using linearly ramped cross polarization with a contact time of 1 ms. During cross polarization, the field strength of the carbon pulse was held constant at 41 kHz and that of the 1H pulse was linearly ramped with a 20 kHz ramp near the matching sideband during 10% of the contact time. The inter-scan relaxation delay was 0.6 s; the MAS rate was 11 kHz. Heteronuclear decoupling during acquisition of the FID was performed with SPINAL-64 with proton field strength of 33 kHz. The number of scans was 16000 and the total measurement time of the spectrum was 3 h.

The spectra obtained were processed and integrated with MestreC software. For quantification of the different C forms, the ^{13}C NMR spectra obtained from feedstock and biochars were divided into different chemical shift regions (Table 4.1) (Knicker, 2011; Suárez-Abelenda et al., 2014; Kupryianchyk et al., 2016).

Table 4.1 Chemical shift assignment in solid-state ^{13}C NMR spectrum.

ppm		Assignment
0-45		Alkyl-C
45-110		O- and N-alkyl
	45-60	N-alkyl C, methoxyl C
	60-110	O-alkyl C
110-160		Sp2-hybridized C
	110-140	C-H Aromatic C
	140-160	COR Aromatic C
160-220		Carboxyl C, amide C
220-245		Ketone C, aldehyde C

Fourier Transform Infrared Spectroscopy (FTIR)

Fourier transform infrared spectroscopy (FTIR) has been extensively used to analyse functional groups in biochar. FTIR analysis of both, biochars and feedstocks, was performed using a Jasco FT/IR-4200typeA spectrophotometer equipped with a MIRacle Single Reflection ATR accessory. Spectral data were obtained in the range 4000-600 cm^{-1} at 4 cm^{-1} resolution and a scanning speed of 2 mm sec^{-1}. Samples were corrected from CO_2 and a 15-point moving average smoothing algorithm was applied prior to peak analysis. The samples were ground finely, mixed homogeneously and placed on a Diamond/ZnSe crystal for attenuated total reflection.

Data Analysis

Box plots of the different C fractions were constructed using the statistical software IBM SPSS Statistics version 24. One-way ANOVA was use to search for significant differences between the different biochars, which were grouped on the basis of the origin of feedstock and H/C_{org} ratio. Normal distribution of the data was confirmed by a Kolmogorov-Smirnov test, and a Bonferroni post hoc test was used to analyse differences between groups.

Principal component analysis (PCA) was applied using CANOCO software (for Windows version 4.5) (ter Braak and Smilauer, 2002).

RESULTS

Feedstocks

The results of biomass characterisation are shown in Table 4.2. Biomass was characterised by a pH of around 3.7 - 6.2, a total carbon content (C_T) of between 29-48%, and by being rich in volatile matter (on average, 75%) and poor in FixC (less than 30%). The N content of the different raw materials was generally low, although it varied widely in the different feedstocks (0.2-2.6%), with manure and compost being the richest. The variance of the atomic ratio H/C_{org} was low (1.5-1.7).

Biochar

Most of the biochars analysed were alkaline (pH 7-10), although the pH of BSd, BEu-1, BAcHw-1 and BPl was low (pH ~ 5) (Table 4.3). After pyrolysis, both $\%C_T$ and %N increased, while %H decreased. The C content of the biochars was higher than in the corresponding feedstocks, ranging from 29-89%. Pine bark, miscanthus and corncob were the biochars richest in C_T. The N content ranged between 0.2 and 3% and depended on the characteristics of the raw material rather than on the pyrolysis conditions (Ahmad et al., 2014). The highest values corresponded to chicken manure and olive pomace compost, and the lowest to wood-derived biochars. The %H varied between 1 and 5.2% in all biochars. In addition, the ash content was always higher in the biochars than in the corresponding feedstocks, and the C content tended to be lower in samples with high ash contents. The %S varied between 0 and 2.5%, and the lowest values corresponded to wood-derived biochars (BAc, BEu, BSd), whereas the highest value corresponded to BTy. The S concentration was generally lower in all pyrolysed samples than in the corresponding feedstocks.

In general, the inorganic C (C_{inorg}) content of all samples was low, although it was higher in biochar than in feedstock and ranged between 0 and 1.7%. The biochar with the highest carbonate content was BOpc, sample that included both biomass and also soil. BAcB, BAcSw, BEu-2 and BCm also contained a notable amounts of C_{inorg} (0.33-0.59%).

The values of the H/C_{org} ratio varied between 0.14 and 1.46, and those of the O/C_{org} ratio between 0 and 0.52 (Table 4.3). The variations in these ratios, along with dehydration and decarboxylation trends, are depicted in a Van Krevelen Diagram (Figure 4.3). The H/C-O/C ratios of other materials were also plotted side by side for purposes of comparison. Feedstocks were located in the upper right corner of the diagram, close to cellulose and wood ($H/C_{org} \approx 1.6$). On the other hand, pyrolysed material was located on the left side of the graph. Biochars, which by definition have a $H/C_{org} \leq 0.7$ (IBI, 2015; EBC, 2012), appeared close to the position of anthracite and bituminous coals, whereas pyrogenic carbonaceous materials (PCMs) with a $H/C_{org} > 0.7$ (EBC, 2012), were located between biochars and feedstocks. The lowest ratios obtained corresponded to BPb, BTy, BEu-2, BMis, BRh, BSdG and all Bcc samples (ranging between 0.1-0.4). The values for BVs, BCn and some acacia samples were between 0.5 and 0.7. Similar values were previously reported by Chun et al (2004) and Chen et al (2011) for wood and wheat biochars pyrolysed at low temperatures. The O/C_{org} ratios were less variable, ranging between 0 and 0.4 in most of the samples, although the value for BOpc was higher.

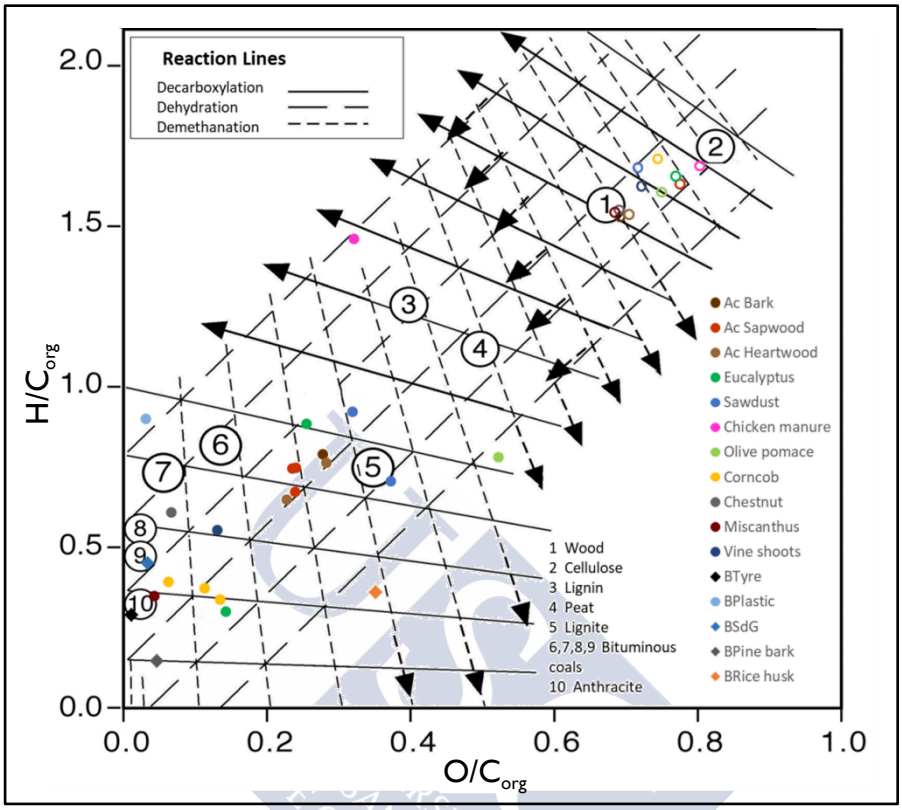

Figure 4.3 Van Krevelen Diagram of the biochars produced from different feedstocks. The biochars (solid coloured dots) and the corresponding raw materials (empty coloured circles) are represented for each feedstock. The ratios in other materials (wood, cellulose, coal, etc.) are also represented (numbered circles) for reference purposes. Reaction lines represent decarboxylation, dehydration and demethanation processes. Adapted from Fuertes et al. (2010).

Table 4.2 Characterisation of raw materials.

Sample	%C	%N	%H	%S	%O	% Ash	H/C_{org}	O/C_{org}	%VM	%FixC	pH
Acacia Bark	46.75	1.69	5.94	0.2	42.69	2.74	1.52	0.68	68.22	28.33	5.1
Acacia Sapwood	45.40	0.34	6.18	0.01	46.67	1.40	1.63	0.77	80.54	14.22	5.8
Acacia Heartwood	47.90	0.31	6.13	0.02	44.69	0.95	1.54	0.7	81.05	18.83	5.3
Eucalyptus	44.97	0.43	6.18	0.026	45.67	2.72	1.65	0.76	83.13	14.91	4.9
Sawdust	47.00	0.38	6.60	0.026	44.67	1.33	1.68	0.71	83.64	15.45	4.9
Chicken Manure	31.41	2.57	4.39	0.31	33.19	28.13	1.70	0.81	57.2	11.3	6.1
Olive Pomace Compost	29.15	2.07	3.90	0.92	28.96	35.00	1.61	0.74	37.33	10.02	6.1
Corncob	46.00	0.38	6.56	0.06	45.38	1.62	1.71	0.74	82.57	16.08	6.2
Chestnut	44.84	0.72	5.8	0.06	41.08	7.51	1.55	0.69	71.63	22.44	3.7
Miscanthus	47.99	0.25	6.18	0.03	43.58	1.96	1.54	0.68	92.81	6.6	4.7
Vine shoot	46.24	0.89	6.27	0.08	44.26	2.26	1.63	0.72	78.15	20.03	5.5

Table 4.3 Main physico-chemical characteristics of the different types of biochar. The biochar samples are highlighted in grey, while the PCMs are shown in white (classified according to the H/C_{org} values).

Sample	%C	%N	%H	%S	% Ash	%O	$\%C_{inorg}$	O/C_{org}	H/C_{org}	C/N	pH
BAcB	64.5	2.2	4.2	0.128	5.5	23.5	0.52	0.28	0.79	34	6.8
BAcSw-1	69.9	0.6	4.3	0.010	3.5	21.6	0.49	0.23	0.74	126	7.3
BAcSw-2	70.0	0.7	3.9	0.021	3.6	21.9	0.59	0.24	0.67	119	7.1
BAcSw-3	69.7	0.6	4.3	0.004	3.5	22.0	0.28	0.24	0.75	140	7.6
BAcHw-1	71.9	0.4	3.9	0.053	2.3	21.4	0.26	0.22	0.65	209	5.0
BAcHw-2	68.0	0.4	4.3	0.010	2.0	25.3	0.21	0.28	0.76	223	7.2
BEu-1	69.3	0.4	5.1	0.005	1.9	23.2	0.17	0.25	0.88	196	5.2
BEu-2	79.0	0.6	1.9	0.036	3.8	14.7	0.36	0.14	0.30	163	9.4
BSd-1	65.8	0.7	5.0	0.065	0.7	27.7	0.12	0.32	0.92	107	5.5
BSd-2	62.7	0.7	3.7	0.035	2.1	30.8	0.06	0.37	0.70	109	4.9
BCm	32.6	3.0	3.9	0.319	46.4	13.7	0.33	0.32	1.46	13	7.2
BOpc	28.6	1.6	1.8	0.139	49.3	18.7	1.66	0.52	0.78	21	9.9
BCc-1	77.2	0.8	2.1	0.032	6.3	13.6	0.09	0.13	0.33	117	9.7
BCc-2	80.2	0.5	2.5	0.030	5.1	11.7	0.05	0.11	0.37	208	9.8
BCc-3	82.6	1.0	2.7	0.050	7.2	6.6	0.10	0.06	0.39	101	9.2
BCn	67.3	1.7	3.4	0.080	21.8	5.7	0.05	0.06	0.61	47	7.9
BMis	83.3	0.3	2.4	0.042	9.5	4.4	0.05	0.04	0.34	311	6.7
BVs	75.4	1.5	3.4	0.122	6.7	12.8	0.07	0.13	0.55	58	10.3
BPl	69.8	2.3	5.2	0.113	19.9	2.6	0.05	0.03	0.90	35	5.4
BPb	88.7	0.6	1.0	0.059	4.4	5.2	0.15	0.04	0.14	167	8.8
BRh	49.6	2.3	1.5	0.358	23.3	23.0	0.05	0.35	0.36	25	8.4
BSdG	73.0	1.0	2.7	0.100	20.2	3.0	0.20	0.03	0.45	88	10.5
BTy	53.3	0.2	1.3	2.472	42.2	0.7	0.05	0.01	0.28	301	8.9

TGA-DSC

The results of the thermo-degradability analysis (procedure (i)) are summarised in Table S A.1, which provides integrated information from variables obtained from TGA curves, and by DSC. On the one hand, the weight loss was used to determine the recalcitrance index, R50, as described by Harvey et al, (2012), which ranged from 0.46 to 0.74 in biochars and PCM, and from 0.36 to 0.42 for feedstocks ranged. The thermogravimetry curves of biochar corrected for water and ash content used to calculate the index are shown in Figure S A.1. The temperature at which half weight loss was reached ranged between 335 and 393 °C for feedstocks and 409 and 657 °C for biochars. The lowest R50 value corresponded to BCm, while the highest ratios included BTy > BPb > BPl >

BMis > BCc-2 > BVs and BEu-2, BRh and BCn with the same ratio. The recalcitrance of the material increases as the value of the ratio increases.

Heat flow curves were also obtained for all the samples (weight loss curves, as well as heat flow curves are provided in the Supporting Information for feedstock (Figure S A.2 to Figure S A.12) and pyrolysed materials (Figure S A.13 to Figure S A.35)). At first sight, there was only one exothermic peak in biochars (e.g. of BMis in Figure 4.4A), while there were two peaks in PCM (Figure 4.4B) - the first corresponding to the degradation of uncharred materials (cellulose and hemicellulose) and the second to the degradation of pyrolysed material. The total heat of the reaction dH varied from around 7.6 kJ g^{-1} in BCm and BOpc to 21.1 kJ g^{-1} in BCc-2, which was the sample with the highest amount of energy. The position of individual peaks was also significant, as shown in Table S A.1. The highest temperature peak and its contribution to the total heat evolved are particularly important, as these are associated with the most thermally stable compounds (Leifeld, 2007). The highest temperature ranged from 466 °C in BSd-1 to around 785 °C in BTy and BPl. The contribution of the highest temperature peak to the total heat was less than 10% in most cases, although it was sometimes difficult to define as it appeared as a wide peak. The highest contribution was in BMis, for which a single peak appeared at 612 °C. As most of the samples presented other peaks due to their heterogeneous composition, the temperature at which the first main peak was reached was also registered, varying from 315 °C in BOpc to 616 °C in BTy. Temperatures were lower in PCM, associated with unstable material.

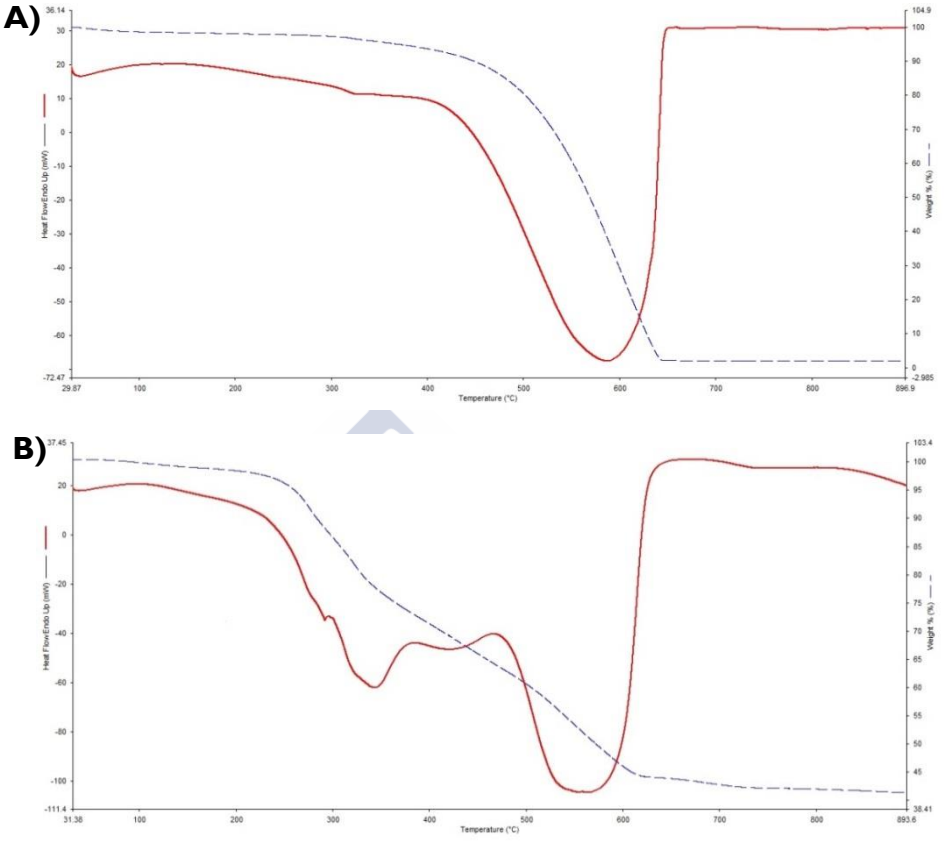

Figure 4.4 TGA curve (blue) and DSC curve (red) for (A) a biochar (BMis) and (B) a PCM (BCm).

Data obtained from thermo-degradability of method UNE 32-019-84 (procedure ii) are summarised in Table S A.2 and an example of the curves obtained is represented in Figure S A.36. The first weight loss corresponded to water loss, which includes free and hygroscopic water (up to 200°C). The loss varied between 1.1 and 5.5%. Ash content varied significantly depending on feedstock, ranging from 0.77-50%. It was lower in wood-derived biochars such as Eu, Sd and Ac. When the different parts of acacia trunk were taken into account, the results indicated that bark was richer in ash, and the value decreased towards the centre of the trunk (heartwood). Large amounts of ash were detected in four biochars (BTy,

BRh, BCm and BOpc), which was related to the high concentration of minerals in the feedstock (Table 4.2). Volatile matter (VM) per unit dry weight ranged from 10% to 52%. The lowest value corresponded to BTy, followed by BPb, BRh and BCc. The highest values corresponded to the uncharred samples, such as BSd, BEu-1 and BCm. FixC contents, which varied from 14%-84%, were lowest in BCm and BOpc and highest in BPb, BCc, BMis and BEu-2.

Carbon forms

The results regarding the different oxidisable C fractions (expressed in g kg^{-1}) are represented in box plots in Figure 4.5. Samples were grouped according to the H/C_{org} ratio and whether they corresponded to feedstock, pyrogenic carbonaceous materials (PCM) or biochars. Biomass was characterised by low C_{nox} content (4 - 64 g kg^{-1}) and a large amount of easily oxidisable C. By comparison, the C_{nox} content of the biochar was much higher (69 - 568 g kg^{-1}). Moreover, there was a significant difference between C_{nox} in biochar and feedstock and in biochars and PCM (Bonferroni test; $p \leq 0.01$). By contrast, there were no significant differences between feedstocks and PCMs. The lowest C_{nox} values corresponded to BCm, BOpc, BEu-1 ($C_{nox} < 50$ g kg^{-1}). The biochars richest in C_{nox} were BPb > BMis > BCc. The hardly oxidisable C content in feedstocks varied between 180 g kg^{-1} and 400 g kg^{-1}. After pyrolysis, the values for biochar ranged between 170 and 530 g kg^{-1}. The values varied considerably depending on feedstock, and no significant differences were found between groups (Bonferroni test; $p > 0.05$). The easily oxidisable C of the raw materials varied between 37 and 152 g kg^{-1}, while after pyrolysis, the values ranged from 1 g kg^{-1} in BMis to 114 g kg^{-1} in BEu-1. Although C_{easyOx} values were higher in PCM than in biochar, there was no significant difference between them; though both were significantly different from feedstocks (Bonferroni test; $p \leq 0.05$).

The mean value of Cp was significantly higher in biomass than in pyrolysed materials (Bonferroni test; $p \leq 0.01$), ranging between 4 and

92 g kg^{-1} in the feedstocks, with the lowest value corresponding to Ac wood and the highest to chestnut. Biochars were characterised by low Cp values (< 10 g kg^{-1}). Once again, intermediate values were found in PCM and were generally < 2% of the total C content, except in BCm and BOpc (with 16.2 and 7.3% of C_T, respectively).

Samples were also grouped according to the origin of feedstock, and the mean values for each C fraction were calculated (Figure 4.6). The percentage of C_{nox} in biochars derived from agricultural waste differed significantly from that in biochars derived from manure/compost (Bonferroni test; $p \leq 0.05$).

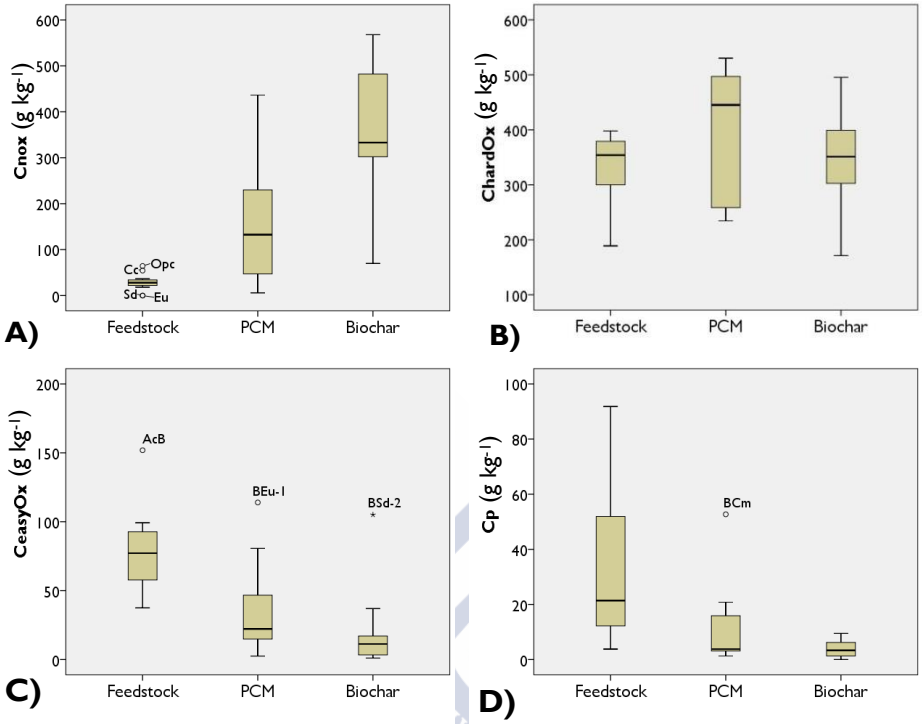

Figure 4.5 Box plot of different C forms for the samples grouped as feedstock, PCM and biochars expressed in g of C per kg of biochar (g kg^{-1}). (A) C_{nox}, (B) C_{hardOx}, (C) C_{easyOx} and (D) Cp. The line across the boxes indicates the median value. The lower boundary of the box shows the 25th percentile (i.e. first quartile, Q1), and the upper boundary shows the 75th percentile (i.e. third quartile, Q3). The whiskers indicate the minimum and maximum values, excluding outliers, which are shown as open circles (>1.5 times of the length of the interquartile range from the lower and upper edges of the box).

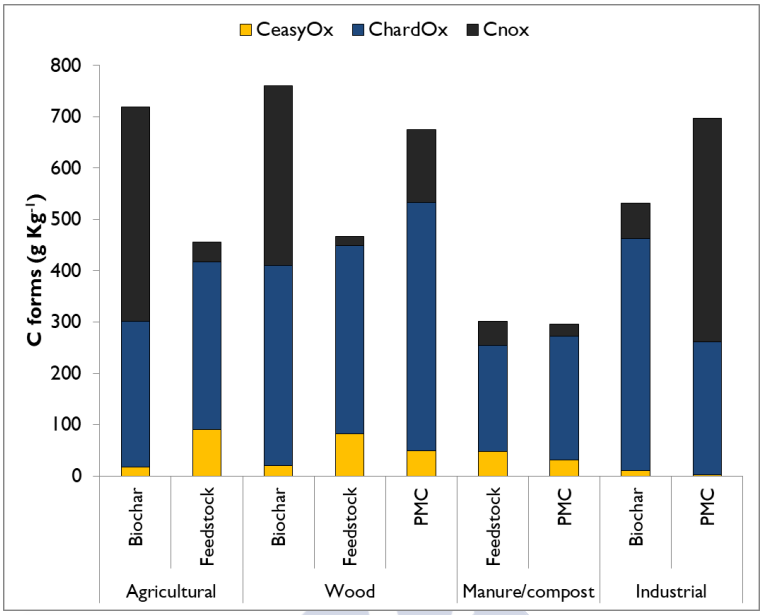

Figure 4.6 Carbon forms in biochars and the corresponding feedstocks grouped by categories depending on the origin of feedstock (expressed as averages in g kg^{-1}). Miscanthus, acacia and forestry residues are included in wood-derived biochars.

NMR

Solid state ^{13}C NMR spectra for feedstocks and pyrolysed materials are shown in Figure 4.8, Figure 4.9 and Figure 4.10. Integration of the signal area for each spectrum in the different chemical shift regions, as defined in Table 4.1, are provided in Figure 4.7 (averaged for feedstock, PCM and biochar). They were expressed in terms of relative signal intensity (i.e. the signal of each region as a fraction of the total signal area). The presence of large amounts of iron and/or other para-magnetic compounds in samples BCc-1, BCc-2, BEu-2, BPb and BTy hindered their characterisation. A notable difference between feedstocks and biochar was detected. The predominance of the O-alkyl C peak observed in feedstock (varying between 39 and 72% depending on feedstock) was attributed to the presence of cellulose (Calvelo Pereira et al., 2011) and a low amount of aromatic C (aggregate of C-H Aromatic C and COR aromatic C varied

between 8.5-23.5%). On the other hand, biochars showed a large peak in the aromatic region (110-160 ppm), ranging from 44% to 77%, with a broad band in the alkyl-C region (0-45 ppm). Overall, carbonised materials (both biochar and PCM) showed a significant increase in C-H and COR aromatic C relative to the corresponding feedstock materials (Bonferroni test; $P \leq 0.05$). The carboxyl C was also significantly higher in biochar samples than in the feedstock. In the PCMs, the alkyl C content differed significantly between biochar and feedstocks. Only moderate structural differences between feedstock and biochar were observed for BCm, in which the content of O-alkyl (43%) was higher than that of aromatics (18%), indicating incomplete pyrolysis. This finding is consistent with the low pyrolysis temperature of this biochar (< 300 °C), as estimated by NIRS.

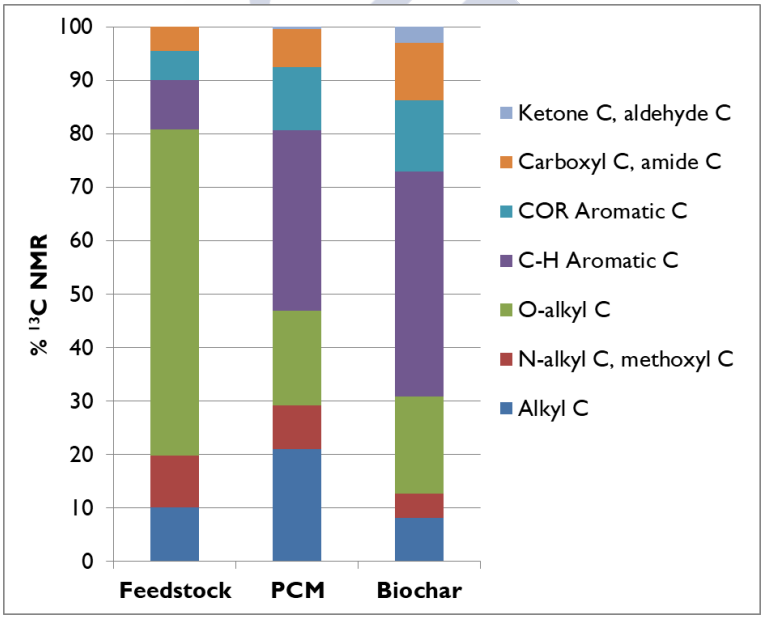

Figure 4.7 Results of integrating the solid state ^{13}C NMR signal area expressed in terms of relative signal intensity with the signal of each region as a fraction of total signal area, for the different samples. The samples were classified as feedstock, PCM and biochar according to the H/C_{org} ratio. The mean values are plotted in the bar graph.

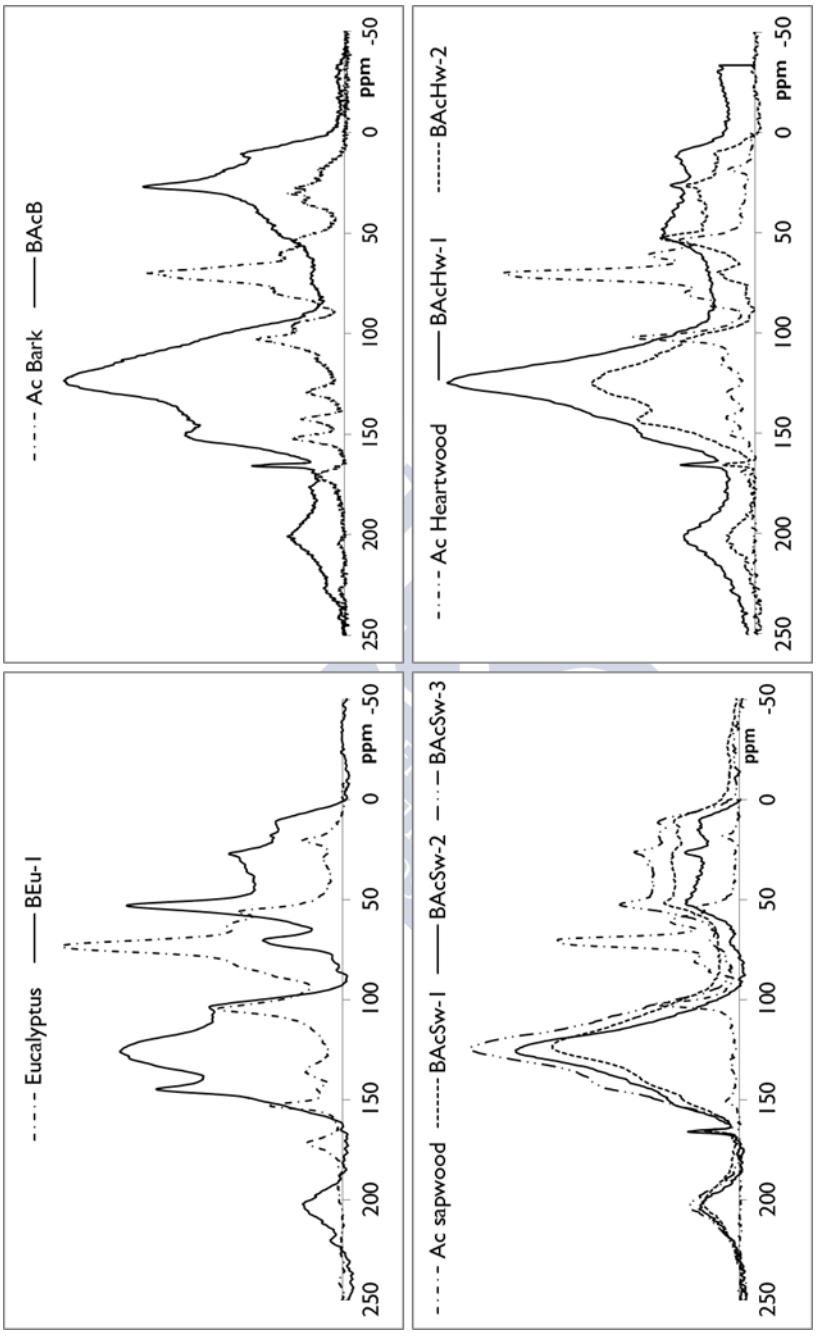

Figure 4.8 Solid state ^{13}C NMR spectra for eucalyptus, acacia bark, sapwood and heartwood and the pyrolysed materials derived from each.

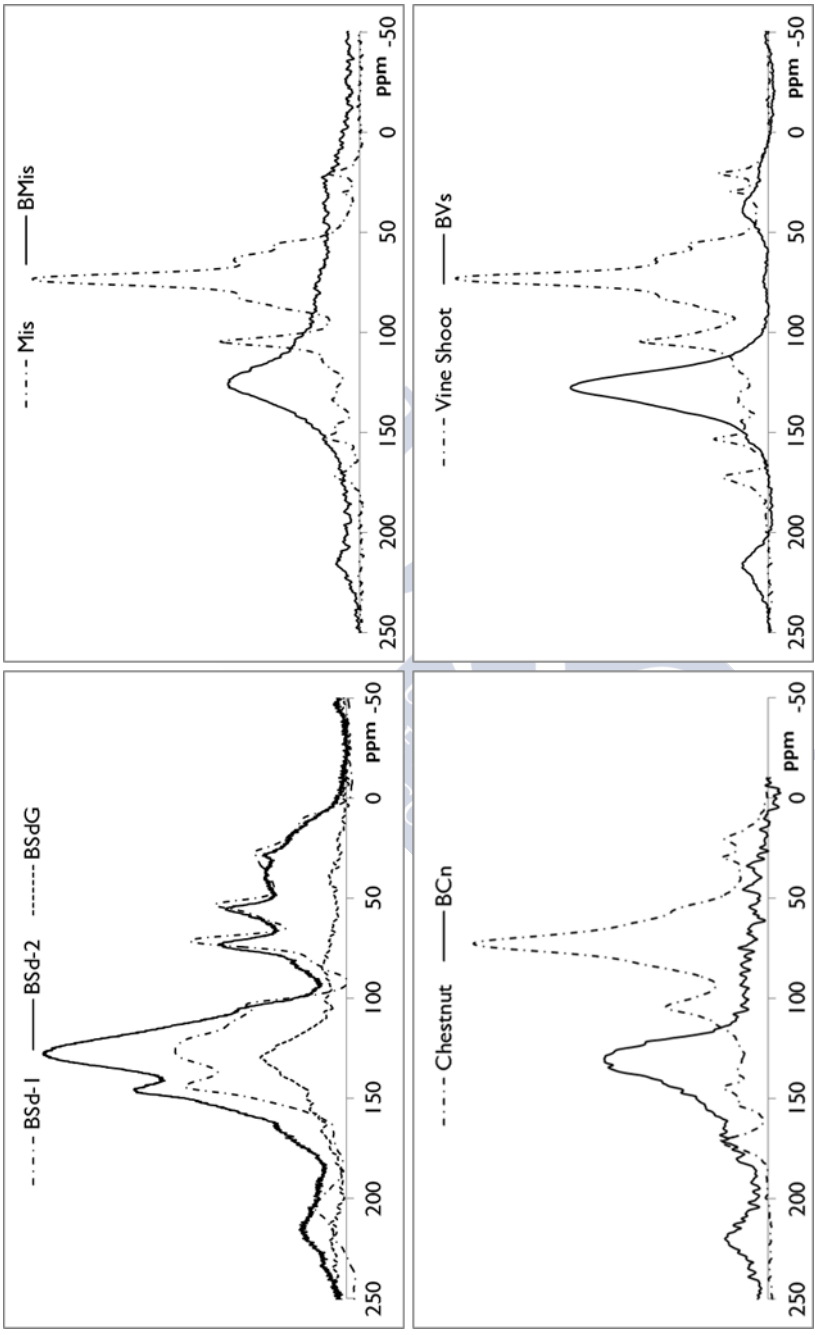

Figure 4.9 Solid state ^{13}C NMR spectra for sawdust, miscanthus, chestnut, vine shoot and the pyrolysed material produced from each.

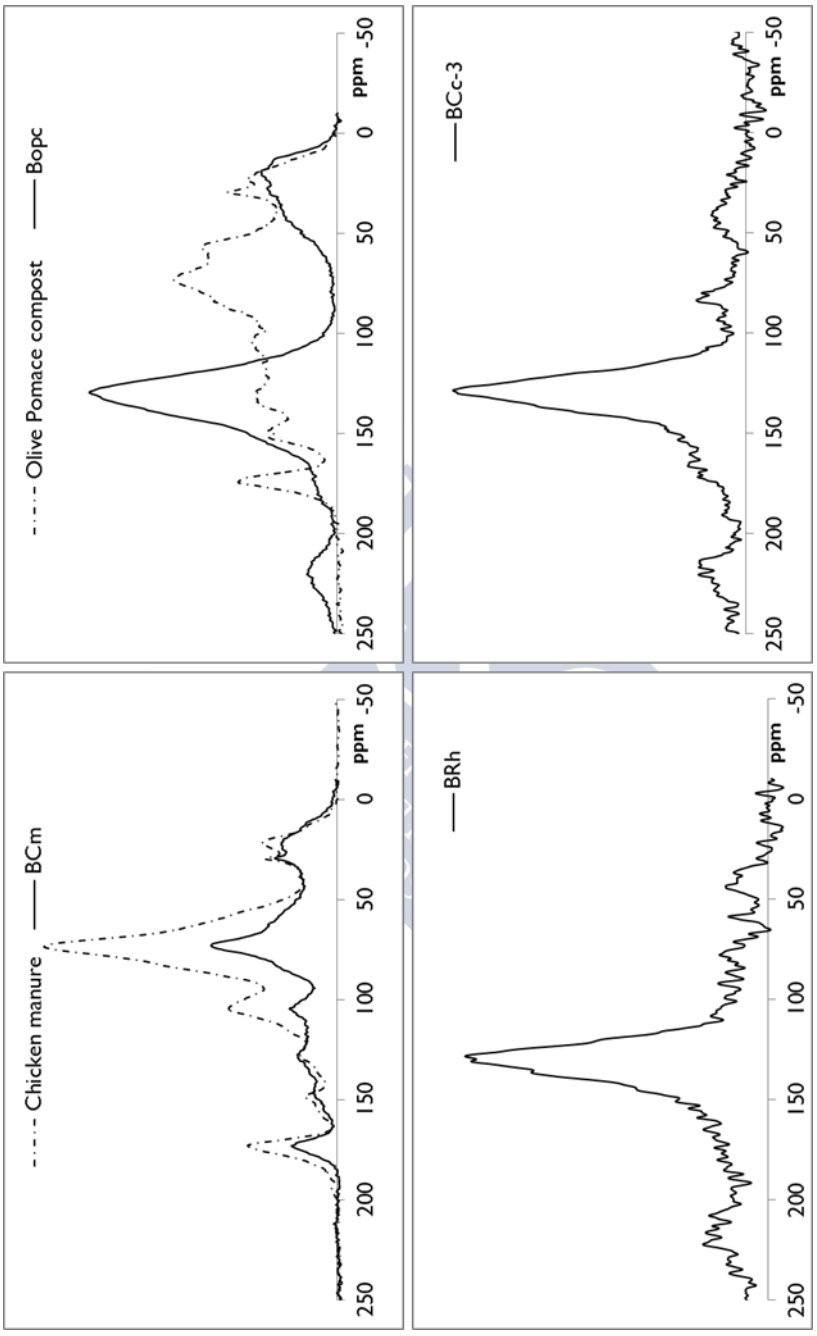

Figure 4.10 Solid state ^{13}C NMR spectra for chicken manure and olive pomace compost and the pyrolysed material produced from each and rice husk and corncob biochars.

FTIR

FTIR spectra were obtained for feedstock (Figure 4.11) and the resulting pyrolysed materials, PCM and biochar samples, (Figure 4.12 and Figure 4.13, respectively) and were characterised by the presence of different bands. In feedstock, a wide band was observed at 3400–3200 cm^{-1}, corresponding to OH vibrations of hydroxyl groups (Brewer et al., 2011; Yang et al., 2007). There was a prevalence of aliphatic ethers (C-O-C) and alcohols –OH bands (1110-1030 cm^{-1}) and $–CH_2$ and $-CH_3$ groups of long-chain aliphatic components (2950-2850 cm^{-1}). The peaks are characteristic of cellulose and hemicellulose (Yang et al., 2007; Chen et al., 2011). The poorly carbonised samples, but not biochar samples, conserved these peaks. In the latter, a peak detected at 1600 cm^{-1} was assigned to C=O of carboxyl and ketone groups or C=C of aromatic components (Hina et al., 2010; Cao & Harris, 2010). Carboxylic bonds appeared at around 1700 cm^{-1}. A band identified between 1500 and 1400 cm^{-1} was attributed to the presence of C-C bonds in aromatic rings. The band around 1000 cm^{-1} was attributed to the presence of phosphate (Cao & Harris, 2010). Stretching between 700-900 cm^{-1} corresponded to C-H bonds of aromatic compounds (Yang et al., 2007).

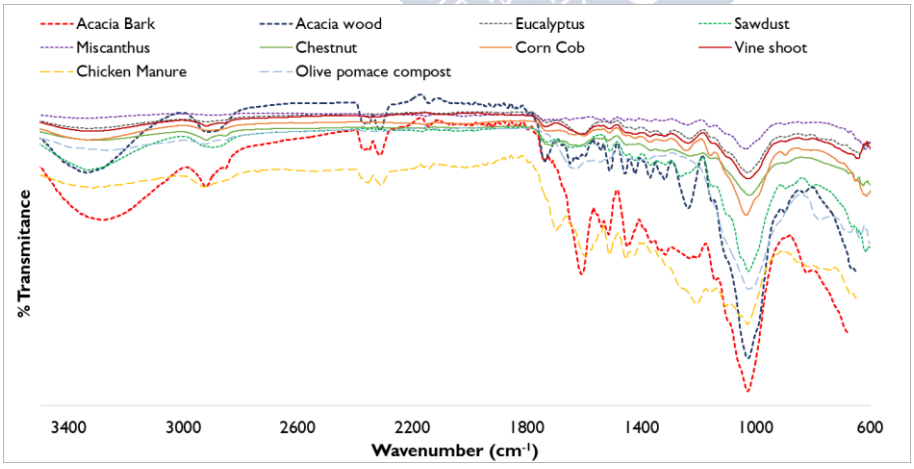

Figure 4.11 FTIR spectra of feedstock.

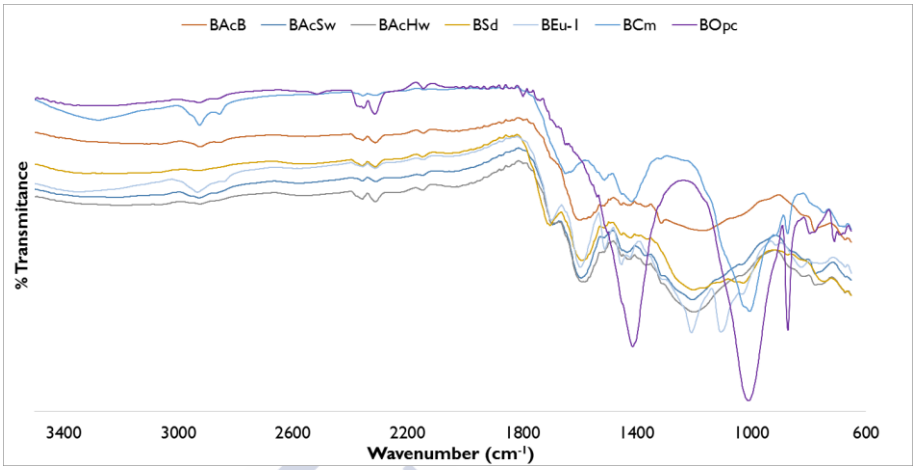

Figure 4.12 FTIR spectra of PCM produced at low temperatures (estimated HHT by NIRS ≤ 400 °C).

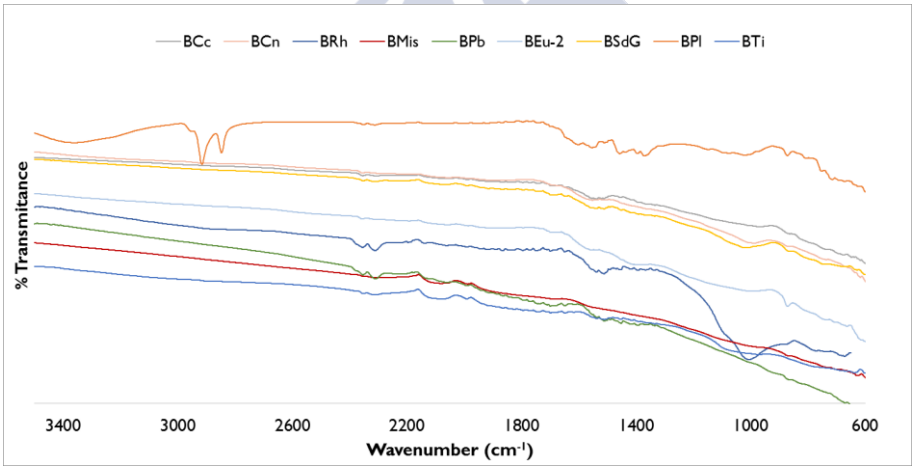

Figure 4.13 FTIR spectra of biochar samples generated at high temperatures (estimated HHT by NIRS > 400 °C).

Principal Component Analysis (PCA)

The first four principal components accounted for 92.5% of the total variability in physico-chemical properties, with PC1 and PC2 accounting for 56.8% and 25.9%, respectively (Figure 4.14 and Figure 4.15). Feedstocks appeared on the positive side of PC1 space, and biochars on the negative side. As expected, PCM was located between biochars and feedstocks. The narrow angle between R50, C_{nox} and FixC vectors implies a high correlation between these biochar properties (Figure 4.14). These three vectors were also closely related to production temperature in biochars. Although the vector angle was greater, it was also correlated with pH, consistent with the alkalinity recorded in biochar. Temperature and pH appeared in the same quadrant of ash content, indicating an increase in ash with increasing temperature. By contrast, the H/C_{org}, O/C_{org}, VM, Cthermo and C easily oxidisable are located in the PC1 positive area, with feedstocks. This is consistent with the high values of these properties in feedstocks and low values in biochar (ex. $H/C_{org} < 0.7$ for biochars and >1.5 in biomass). Furthermore, the positive space of PC2 was related to high values of ash, N, S and C_{inorg} content. Distribution of samples according to this second component was more closely related to the origin of feedstock than to pyrolysis conditions (Figure 4.15). The distribution of two samples, BCm and BOpc, was very different from that of the other samples. These biochars appeared separately from the others, with very little difference between each biochar and the raw material. Still in the positive space of PC2, but with smaller loadings, biochars derived from agricultural waste appeared along with industrial biochars, all of which are rich in ash and have a high inorganic C content. Herbaceous and wood-derived biochars appeared in the negative space of PC2, consistent with their low ash and N contents, and high organic C concentration.

As condensed aromatic C, measured by NMR, was not available for all samples, we repeated the PCA without the samples for which these data were lacking to enable evaluation of relationship between this variable and

the other properties. The first four principal components accounted for 87.0% of the total variability in physico-chemical properties, with PC1 and PC2 accounting for 46.3% and 21.3% of the variability, respectively. Results are shown in Figure 4.16. Samples were distributed in the same space of PC1 and PC2 as in the previous analysis (Figure 4.15). The proximity between aromatic C, C_{nox}, R50 and Fix C vectors confirmed the close correlation between aromatic C forms estimated by NMR, thermogravimetric techniques and chemical oxidation. The estimated pyrolysis temperature was closely correlated with all the parameters related to biochar recalcitrance. These properties were also related to total C content. In addition, the analysis revealed a relationship between increasing ketone C content and carboxyl groups in biochars with these properties and production temperature. By contrast, the properties characteristic of the feedstock such as high values of O/C_{org} and H/C_{org} ratios, labile C forms (Cp and C easily oxidisable), VM and the predominance of different forms of alkyl C appeared in the positive PC1 area, showing an inverse relationship with production temperature.

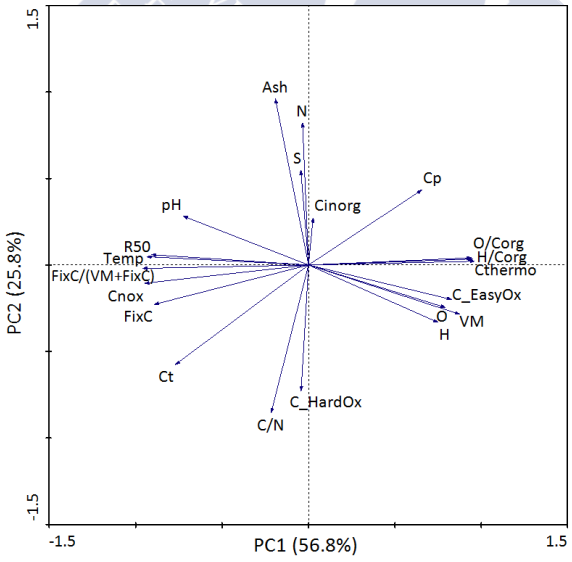

Figure 4.14 Loadings of biochar and feedstock properties in PC1-PC2 space for the samples under study.

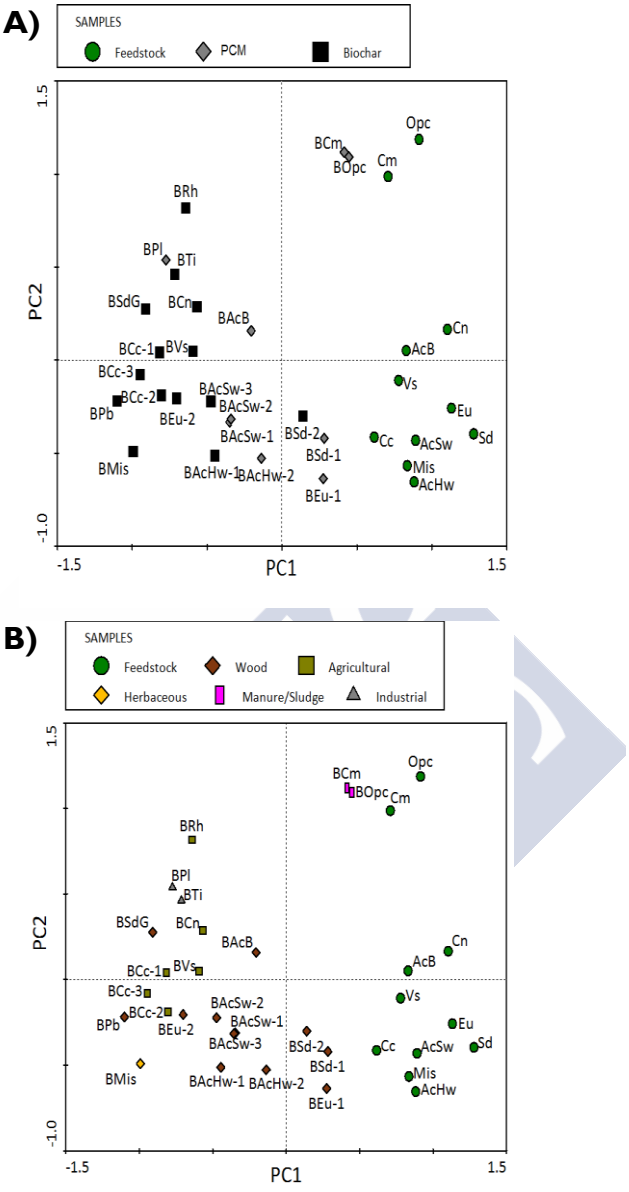

Figure 4.15 Factor scores of the samples in the PC1-PC2 space obtained for the samples, classified by (A) type (i.e. feedstock, PCM and biochar) and (B) original material (i.e. feedstock, wood, agricultural wastes, herbaceous, manure/sludge and industrial waste).

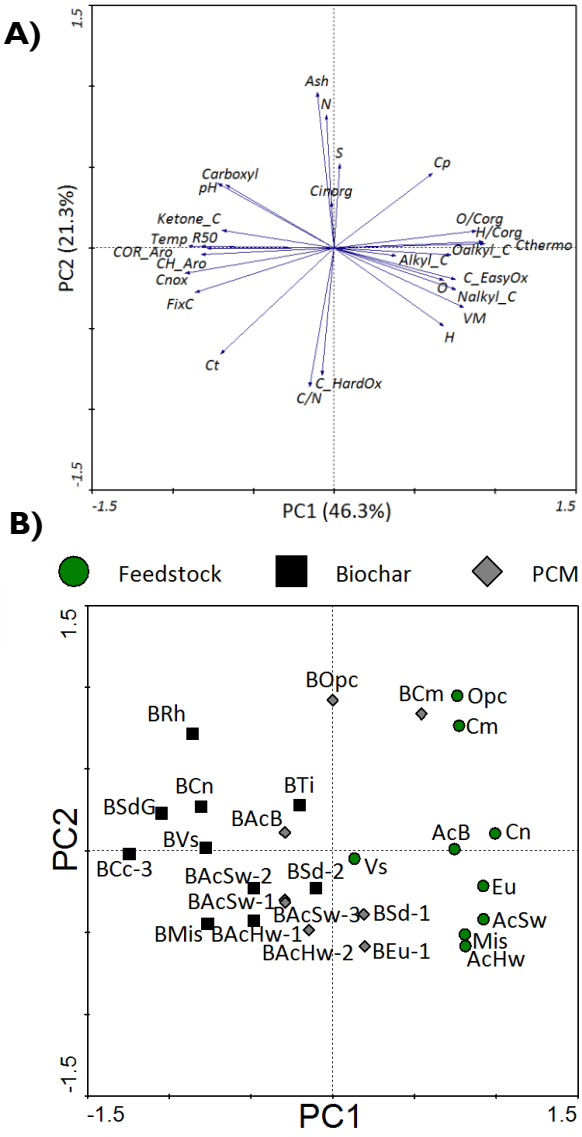

Figure 4.16 (A) Loadings of biochar and feedstock properties in PC1-PC2 space for the samples with NMR data; (B) factor scores of the samples in PC1-PC2 space obtained for the samples, classified by type (i.e. feedstock, PCM and biochar).

In order to identify the relationships between the different methods used to estimate persistent C and labile C forms, the following indexes/properties were considered: H/C_{org}, FixC, C_{nox}/C_T, R50 and aromatic C (AromC, as the sum of C-H Aromatic C and COR aromatic C). Regression analysis was applied to the data from raw materials and that of biochars (Table 4.4).

Table 4.4 Pearson's correlation coefficients between main variables associated with recalcitrant C.

	Temp	H/C_{org}	VM	FixC	R50	C_{nox}	AromC
Temp	1						
H/C_{org}	-0.96**	1					
VM	-0.91**	0.90**	1				
FixC	0.88**	-0.93**	-0.81**	1			
R50	0.92**	-0.92**	-0.88**	0.84**	1		
C_{nox}	0.81**	-0.79**	0.74**	0.87**	0.71**	1	
AromC	0.39*	-0.42*	-0.38*	0.36*	0.31	0.23	1

* Correlation significance at $p < 0.05$

** Correlation significance at $p < 0.01$

The H/C_{org} ratio was negatively and significantly correlated ($p < 0.01$) with %FixC, R50, and $\%C_{nox}$ and was slightly less well correlated with % condensed aromatic C ($p < 0.05$). By contrast, there was a positive significant correlation with VM, i.e. materials rich in volatile matter had a higher H/C_{org} ratio, as expected. All properties related to the persistence of biochar (R50, FixC, C_{nox} and Aromatic C), were positively and significantly related and were, in turn, highly dependent on pyrolysis temperature ($p < 0.01$ for all except for aromatic C which is $p < 0.05$). For BOpc, aromatic C was considered an outlier, as a substantial amount of the aromatic C was not related to the R50 or FixC content.

DISCUSSION

Assessment of biochar stability and sequestration potential

The techniques used to characterise the biochars and feedstocks provided detailed and essential information about the biochar properties, enabling identification of the best type of biochar for carbon sequestration. The five different procedures used to compare biochar stability revealed that recalcitrance of the product increased with pyrolysis temperature, with concomitant decreases in H/C_{org} and O/C_{org} ratios and in VM content and an increases in FixC, C_{nox} and condensed aromatic C.

During pyrolysis of biomass, dehydration and depolymerisation reactions led to the loss of H and a reduction in the H/C ratios from >1.5 in the raw materials to ≤ 0.7 in biochar. The values of both ratios, H/C_{org} and O/C_{org} decreased with the duration and intensity of heat treatment (Kleber et al., 2015). The H/C ratio is often used as a proxy for aromaticity (Crombie et al., 2013), while the O/C ratio is an indicator of biochar stability (Spokas, 2010). A decrease in H/C and O/C ratios reflects an increase in condensed aromatic C and a decrease in its polarity (and O-based functional groups) as carbonisation increases (Ahmad et al., 2014), biochars will be more stable with fewer O-based functional groups. Ratios > 0.7 are associated with the predominance of non-condensed aromatic structures possibly originating from the feedstock, i.e. lignin (Schimmelpfennig & Glaser, 2012). This was observed in the PCMs, such as BEu-1, BSd-1 BAcHw-2 or BAcB, in which the higher ratio may be a consequence of low temperatures during pyrolysis, as all of these samples were classified by NIRS as being produced below 400 °C (Chapter 3), and thus uncharred materials were present. The aforementioned findings are consistent with previously reported data on low-temperature biochars (Krull et al., 2009). Therefore, these results showed the influence of the production process on the chemical composition of biochar and the formation of condensed aromatic C. This was particularly evident in the comparison between samples produced with the same feedstock, but at

higher temperature and enough residence time (for example BEu-2) and others produced from the same material, but poorly charred (BEu-1). In addition to the effect of low pyrolysis temperature, samples not containing lignocellulosic compounds, such as BCm and BOpc, did not undergo depolymerization (Ahmad et al., 2014), which may explain the higher H/C_{org} ratio (1.5 and 0.8, respectively). It is also possible that H from inorganic constituents contributed to the higher ratio. This has been observed for H in Al oxyhydroxides in biochars produced from biosolids (Wang et al., 2012a). Low O/C_{org} values are characteristic of low polar black carbon. When this ratio ranges between 0 and 0.2, the biochar properties are similar to those of soot or active carbon, and when it varies between 0.2 and 0.4, the properties are similar to those of charcoal (Schimmelpfennig & Glaser, 2012; Chun et al., 2004). Only BOpc had a higher O/C_{org} ratio, which indicates a low degree of carbonization and high degree of polarity. Schimmelpfennig & Glaser (2012) obtained similar results with analogous feedstocks. Spokas et al. (2010) proposed that biochar with an O/C ratio < 0.2 will have a half-life > 1000 years, and an O/C of 0.2 – 0.6 will indicate a half-life of 100-1000 years. According to this, all the samples classified as biochars, except BRh, BSd-2 and BAcSw, were included in the first group, while the other of the pyrolysed samples under study will remain stable for 100-1000 years.

Biochars with low organic C content were rich in ash contents (20-60%) and thus contained an abundant inorganic fraction. It is well known that organic compounds tend to be lost in preference to inorganic compounds during thermal conversion, thus leading to an increase in ash content, although this is highly dependent on the feedstock (Enders et al., 2012; Krull et al., 2009). The biochars richest in ash were BCm and BOpc, which were those produced from manure and sludge, as found in previous studies (Zhao et al., 2013; Wang et al., 2012a).

Thermal degradation of the samples under study indicated that the main decrease in mass occurred between 250 and 600 °C. This range

corresponds to the thermal degradation of hemicellulose (200-350 °C), cellulose (315-400 °C) and lignin decomposition (150-900 °C) (Yang et al., 2007). The direct relationship between VM and H/C_{org} observed (R^2 = 0.6988) is consistent with the findings of other authors (Brewer et al., 2012). The values of VM were higher in feedstock and PCM. VM tends to decrease with increasing pyrolysis conditions, temperature and heating rate and it is associated with the readily mineralisable fraction in biochar, which is consistent with previous findings (Brewer et al., 2012; Uchimiya et al., 2011). By contrast, FixC increases in biochars as temperature increases, and is an indicator of carbon storage value (Enders & Lehmann, 2017), except in ash-rich biochars such as rice husk (Enders & Lehmann, 2017; Cowie et al., 2015).

The R50 values for the biochars under study were consistent with those obtained by Zhao et al. (2013), who concluded that thermal production conditions determine the persistence of biochar, especially when the holding time was sufficiently long. This was apparent for eucalyptus biochar samples, BEu-1 and BEu-2, which differed in the holding time (1.5 h in the former and 3 h in the latter), with R50 values of 0.52 and 0.60, respectively.

The results obtained by thermal degradation (FixC and R50) were consistent with those obtained by chemical oxidation, i.e. C_{nox}, which as for the former, are associated with persistent C (Macías et al., 2004). All are closely related with the estimated content of condensed aromatic C and low H/C_{org} and O/C_{org} ratio, as previously reported (Zhang et al., 2011; Calvelo Pereira et al., 2011). FTIR analysis also confirmed the increase in persistence from raw material to biochar. Furthermore, all the parameters used to establish biochar stability were closely related to HHT, estimated by NIRS, thus confirming the accuracy of the estimation method.

The different techniques used to estimate the persistence of organic C in biochar had several advantages and disadvantages. Elemental analysis is a rapid, simple method that enables the determination of H/C and O/C ratios,

which have been widely studied to estimate the persistence of biochar C (Baldock & Smernik, 2002; Krull et al., 2009; Spokas, 2010; Enders et al., 2012). TGA-DSC provides valuable information about biochar properties with no need for pre-treatment of the sample, is simple to manage and the results are easy to interpret. The disadvantage of both techniques is that the sample processing is destructive, which may be problematical when the amount of sample is limited and further analysis is required. By contrast, NMR and FTIR required minimal sample preparation and quantity and they are non-destructive methods. However, the presence of paramagnetic compounds in biochars interferes with NMR measurements. In the FTIR analysis, we faced limitations associated with the use of diamond/ZnSe crystal due to the refractory nature of black samples, resulting in strong optical absorption. This problem can be solved by the diluting the samples in KBr. All of the abovementioned techniques require specialised equipment, which is not always available in laboratories, and analysis of the samples can therefore be expensive. Regarding chemical oxidation, dichromate oxidation is traditionally used to study the C stability in soils and provides useful information about C oxidability. However, this method generates substantial amounts of Cr-rich residues, which must be treated as hazardous waste, as they can potentially affect public health and the environment.

According to the results obtained with the different procedures, the best biochars for C storage in a new strategy for addressing global change are BPb > BMis > BCc > BEu-2. In general, forestry residues, as well as agricultural waste and herbaceous biochars, could be used for C storage due to their high contents of recalcitrant organic C, although the pyrolysis conditions must be controlled to ensure complete transformation of the feedstock into a stable organic C form. On the other hand, manure-derived biochars and BOpc contained low amounts of organic C, mainly oxidisable C.

Biochar classification

Different authors and institutions involved in biochar research and development have established standards and classification systems to ensure a sustainable production and to minimise any hazards associated with use of the materials when applied to soil or the environment. In this chapter, the biochars studied were classified using different systems according to their stability and carbon storage potential.

One of the first properties of a biochar established is the organic C content (C_{org}). The IBI Guidelines set three classes of biochar in relation to C_{org} content, as follows:

C_{org} (%)	**Classification**
≥ 60%	Class 1
≥ 30% - < 60%	Class 2
≥ 10% - < 30%	Class 3
<10%	Not biochar

Most of the biochars under study here were classified as Class 1. Chicken manure, rice husk and tyre biochars were included in Class 2 and only olive pomace mill compost was considered Class 3 biochar.

The European Biochar Foundation is another important institution that has established biochar standards, i.e. the European Biochar Certificate (EBC). In this case, the first requirement to be considered for a biochar is a total C content ≥50% (EBC, 2012). According to this, all the samples studied are classified as biochars, except BCm and BOpc, which are classified by EBC as Pyrogenic Carbonaceous Material (PCM).

In addition to the $\%C_T$ and $\%C_{org}$, an estimatimation of the stable C fraction in biochar is required. For this, both IBI and ECB established that the molar H/C_{org} ratio should be ≤ 0.7 to be considered as such (IBI, 2015; EBC, 2012). Once again, not all of the pyrolysed materials complied with

this criterion. Samples with higher ratios were those pyrolysed at low temperatures (≤ 400 °C) (Table 4.5), referred to as PCM.

Budai et al. (2013) took a further step in the biochar classification by considering the C fraction in biochar that will remain stable in soil for more than 100 years (BC_{+100}). This index is based on extrapolations of medium-long term incubation experiments and their relationship with molar H/C_{org} values. In a conservative scenario, the IBI Stable C Protocol considered that values of $H/C_{org} \leq 0.4$ would retain at least 70% of C_{org} after a century. When $0.4 > H/C_{org} \leq 0.7$, this was considered to be $BC_{+100} = 50\%$.

As the total C storage value will not only depend on the assigned BC_{+100} value but also on the amount of C_{org} it holds, Camps Arbestain et al (2015) referred to the storage value as stock of BC_{+100} (sBC_{+100}), expressed in g kg^{-1} and obtained as follows:

$$sBC_{+100} = C_{org} \times BC_{+100}$$

These authors thus defined five C storage classes:

sBC_{+100}	**Class**
$sBC_{+100} \geq 600$ g kg^{-1}	5
500 g $kg^{-1} \leq sBC_{+100} < 600$ g kg^{-1}	4
400 g $kg^{-1} \leq sBC_{+100} < 500$ g kg^{-1}	3
300 g $kg^{-1} \leq sBC_{+100} < 400$ g kg^{-1}	2
$sBC_{+100} < 300$ g kg^{-1}	1

According to the method developed by Camps-Arbestain et al. (2015), the biochars under study were categorised as follows: (i) BCc-2, BCc-3, BEu-2, BMis and BPb biochars were included in Class 5, the best class (Table 4.5); (ii) BCc-1 was classify as Class 4, and (iii) the other materials were included in Class 2. Pyrolysed samples with $H/C_{org} > 0.7$ were not considered in this group as they do not fulfil the definition of biochar based

on the IBI Standards (IBI, 2015) and the European Biochar Foundation Certification (EBC, 2012).

Apart from the classifications already described, Harvey et al, (2012) established another method of estimating the stability of biochar with a simple Recalcitrance Index (R50) based on the relative thermal stability of biochar relative to graphite (considered highly recalcitrant). According to this index, biochars can be classified according to their recalcitrance/carbon sequestration as Class A ($R50 \geq 0.70$), Class B ($0.50 \leq R50 < 0.70$) or Class C ($R50 < 0.50$), where Class A biochars are highly resistant to decomposition, Class B has an intermediate value and Class C has a carbon sequestration potential similar to uncharred plant biomass. On this basis, BPb and BTy were included in Class A (Table 4.5) and the other samples studied were classified as Class B, with the exception of BCm, which was considered Class C.

Table 4.5 Carbon storage classification according to $\%C_{org}$, H/C_{org} ratio, R50 Index and sBC_{+100}.

Biochar	$\%C_{org}$	H/C_{org}	R50	Class	$\%BC_{+100}$	sBC_{+100} (g kg^{-1})	Carbon Storage
BAcB	Class1	PCM	0.57	B	-	-	-
BAcSw-1	Class1	PCM	0.56	B	50	349	-
BAcSw-2	Class1	Biochar	0.56	B	50	349	Class2
BAcSw-3	Class1	PCM	0.58	B	50	348	-
BAcHw-1	Class1	Biochar	0.59	B	50	359	Class2
BAcHw-2	Class1	PCM	0.57	B	-	-	-
BEu-1	Class1	PCM	0.52	B	-	-	-
BEu-2	Class1	Biochar	0.60	B	70	551	Class5
BSd-1	Class1	PCM	0.52	B	-	-	
BSd-2	Class1	Biochar	0.54	B	50	313	Class2
BCm	Class2	PCM	0.46	C	-	-	-
BOpc	Class3	PCM	0.55	B	-	-	-
BCc-1	Class1	Biochar	0.55	B	70	540	Class4
BCc-2	Class1	Biochar	0.64	B	70	561	Class5
BCc-3	Class1	Biochar	0.55	B	70	577	Class5
BCn	Class1	Biochar	0.60	B	50	336	Class2
BMis	Class1	Biochar	0.65	B	70	583	Class5
BVs	Class1	Biochar	0.61	B	50	377	Class2
BPl	Class1	PCM	0.66	B	-	-	-
BPb	Class1	Biochar	0.70	A	70	619	Class5
BRh	Class2	Biochar	0.60	B	70	345	Class2
BSdG	Class1	Biochar	0.54	B	50	365	Class2
BTy	Class2	Biochar	0.74	A	70	372	Class2

CONCLUSIONS

The research reported here involved the detailed characterisation of biochar produced from a wide range of waste materials and under different pyrolysis conditions, with particular emphasis on the stability of organic C.

Pyrolysis transforms readily degradable C forms in biomass into recalcitrant forms that can remain stable in soils for centuries. The wide variability in the properties of the resulting materials depend on feedstock and pyrolysis conditions. The C content of the biochar was generally higher than that of the feedstock, and it was lower in PCM than in biochar, i.e. in the samples produced at low temperatures (≤ 400 °C) such as most of the acacia samples, chicken manure and olive pomace compost. Low H/C_{org} and O/C_{org} ratios indicated increased aromaticity and stability after pyrolysis, particularly at high temperatures. This is consistent with the results of the other methods used to determine biochar stability (C oxidised with dichromate, TGA-DSC, NMR and FTIR). Although PCMs were richer in labile C than biochars, the C was more stable than in feedstock, with potentially beneficial effects on soil.

Overall, the best biochars for C storage were those classified as Class 5 according to the C storage value: BPb> BMis > BCc > BEu-2. The other biochar samples considered had a moderate C storage potential (Class 2). Manure and compost derived biochars were less suitable for use as C sinks.

Production of carbonised materials from industrial waste material, such as plastic and tyres (BPl and BTy, respectively), should be considered as they may be rich in C_{nox} when pyrolysed at appropriate temperatures, although environmentally-related problems associated with their production must first be evaluated.

USC
UNIVERSIDADE
DE SANTIAGO
DE COMPOSTELA

5. Characterisation and classification of biochars according to their potential for soil amendment

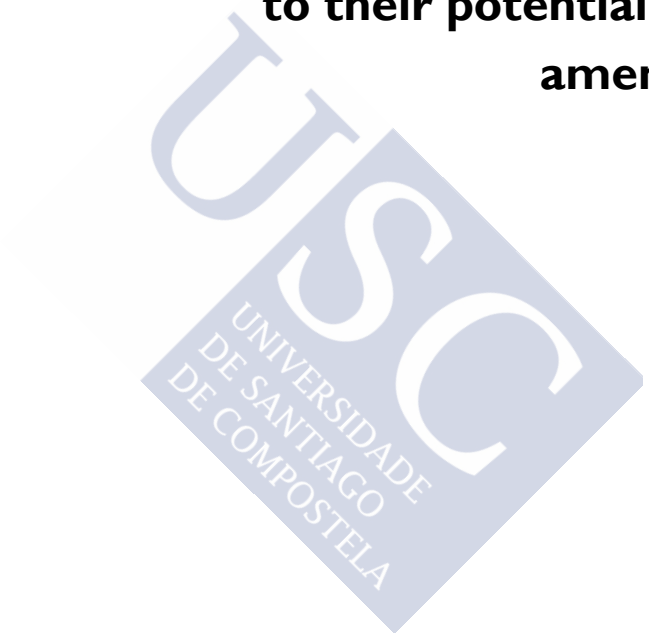

USC
UNIVERSIDADE
DE SANTIAGO
DE COMPOSTELA

INTRODUCTION

According to the United Nations World Populations Prospect report (2015), the world population is continuing to rise and is estimated to reach more than one billion in the next 15 years. This will lead to a greater demand for food and therefore greater pressure on land productivity and on the environment. Furthermore, increased interest has recently been shown in the use of energy crops or co-crops (such as corn or wheat stover) to produce biofuels. In these new approaches, crop residues are not usually returned to the land, leading to the loss of nutrients and C from soils (Laird, 2008). At the local level, Galician soils are characterised by being shallow, acidic (pH 4.5-5), with a sandy to loam texture and a low capacity to retain water and nutrients, factors that tend to limit crop yields (Macías & Calvo de Anta, 2001; Fernádez Marcos et al., 1994).

Biochar is proposed as a potential ameliorator of soil properties, contributing to the stable C pool and, in some instances, providing some benefits to the soil, by e.g. returning nutrients and enhancing soil properties, increasing the pH, improving CEC and the water holding capacity (Syuhada et al., 2016). Most of the available nutrients and heavy metals in biochar are found in the ash fraction and determining and understanding the inorganic composition of biochar is important because this will ultimately affect plant nutrition and soil contamination (Enders et al., 2012). Various studies involving the application of biochar to soil have produced satisfactory, negative and uncertain results, depending on the type of biochar, application rate, crop and soil properties, among other factors (Galinato et al., 2011; Spokas et al., 2012; Visioli et al., 2016).

The source of feedstock and pyrolysis temperature used to produce biochar determine the concentration and availability of nutrients in the final product (Ippolito et al., 2015; Camps-Arbestain et al., 2015). The elemental composition is largely dependent on feedstock and to a lesser extent on pyrolysis conditions (Camps-Arbestain et al., 2017), although slow pyrolysis generally increases the concentrations of N, S and available P, Ca and Mg, as

well as the surface area. This is attributed to the loss of volatile compounds and residual concentration of nutrients (Ippolito et al., 2015). Regarding the type of feedstock, manure-derived biochars tend to be richer in nutrients than plant-based biochars, which usually have higher C content. The total nutrient concentration, however, cannot be used as an indicator of the fertiliser value of biochar, because the availability of the nutrients will depend on the nature of their constituents and how they are adsorbed in pores (Camps-Arbestain et al., 2017). Available nutrients are defined as those present in the correct chemical form that can be taken up by plants for growth. The six major nutrients that plants generally require are N, P, K, S, Mg and Ca.

Nitrogen availability is one of the major factors that limits plant growth. During pyrolysis, aromatic and heterocyclic N-rings are formed while amide N decreases. These forms are difficult for microbes to decompose, and the availability of N in biochar is often limited. Nonetheless, biochars may contain a fraction of hydrolysable N, especially if derived from animal-based feedstock pyrolysed at low temperature. However, huge amounts will be required in a realistic application scenario according to the crop requirements (Camps-Arbestain et al., 2015; Camps-Arbestain et al., 2017).

Phosphorus (P) is another macronutrient highly demanded by crops, and million tonnes of P are added as fertilisers to agriculture soils annually to increase the supply of P to plants (Wang et al., 2012b). The fertilisers are mainly derived from rock phosphate mining, which is a non-renewable, rapidly depleting source (Zwetsloot et al., 2016). It is important to recycle P from waste to achieve for a more sustainable use of this source. Phosphorus in biochars is generally found as amorphous phosphate salts and the concentration mainly depends on feedstock (Camps-Arbestain et al., 2015), as it is only volatilised at temperatures > 700 °C (De Luca et al., 2009). During pyrolysis, organic P forms tend to be converted into inorganic forms at temperatures above 350 °C (Camps-Arbestain et al., 2017). Potassium (K) is also absorbed in high amounts by plants (second

only to nitrogen) (Camps-Arbestain et al., 2017). It is readily soluble in water and occurs in biochar when present in the original feedstock. Calcium (Ca) and magnesium (Mg) are less readily volatised during pyrolysis than K and Na, and they therefore remain in biochar when the pyrolysis temperature is < 500 °C. Sulphur is also an essential plant nutrient that is susceptible to chemical and biological oxidation reduction reactions in soils. It can be found in biomass as C-bound S, ester-S and sulphate-S. The first form tends to disappear at temperatures below 450-500 °C. Ester-S may accumulate or be transformed to sulphate-S, which is the most thermally stable form. Sulphate-S decomposes at temperatures around 500-600 °C (Camps-Arbestain et al., 2017).

Although the addition of nutrients can improve soil fertility, overabundance of micronutrients, such as Mn, Zn, Cu, Mo, B and Cl, can have toxic effects (Enders et al., 2017). Some toxic elements such as heavy metals may be present, which is dangerous for humans and also for the environment. Moreover, during the pyrolysis reaction, other pollutants such as polycyclic aromatic hydrocarbons (PAHs) may be co-generated together with biochar. Although these contaminants are dangerous if released into the environment, they are usually strongly retained in biochar at hydrophobic surfaces. Nonetheless, knowledge of the potential contribution of PAHs to the environment is needed before biochar is applied to the soil (Cornelissen & Hale, 2017).

Selection of the initial feedstock greatly influences the elemental composition of biochar. This chapter describes how the biochars and PCMs studied in Chapter 3 were characterised by different methods, to assess their potential benefits to soils as soil amendments in relation to their fertiliser value. The presence of pollutants was also evaluated with the aim of minimising any detrimental effects of biochar on the environment.

MATERIALS AND METHODS

The pH and electrical conductivity were measured in a suspension of biochar in deionised water (1:5). Macronutrient and heavy metal concentrations were determined by atomic absorption spectroscopy, in a Perkin Elmer Atomic Absorption Spectrometer (1100B), after wet acid digestion (3 mL HNO_3 + 9 mL HCl) in a microwave (Milestone Ethos Plus with HPR-100/10s). The concentrations of As, Cd and Sb were measured in a Graphite Camera, Perkin Elmer spectrophotometer, model 4110 ZL. Total P content was determined by the molybdenum blue method (Murphy & Rley, 1962). Available nutrients (K, Ca, Mg and SO_4-S) were determined following the method proposed by Camps-Arbestain et al. (2017), which involves extraction with 1M HCl and measurement of the cations in a microwave plasma AE spectrophotometer (Agilent 4200 MP-AES). The concentration of SO_4-S was determined in a Technicon AutoAnalyser. Available P was extracted with 2% formic acid, following the procedure of Wang et al. (2012c) and measured in the same way as Total P. Soluble ions were extracted with a non-buffered solution and determined according to the method of Peech et al. (1947). The concentrations of Ca^{+2}, Mg^{+2} and Al^{+2} were determined by atomic absorption spectroscopy after addition of 1% of lanthanum to prevent interferences. The concentrations of Na^{+} and K^{+} were measured by atomic emission spectroscopy. When the extract pH was below 4.2, exchangeable protons (H^{+}) were determined by titration, with phenolphthalein as an indicator.

Water holding capacity

The water holding capacity of biochar (WHC) was measured following the method of M.A.P.A. (1986). Samples were placed in a container with water for two weeks until saturation. They were then transferred to a special ring with a porous membrane and different pressures were applied. Field capacity was determined after applying a pressure of 0.1 atm (many authors associate this value with the WHC (Masiello et al., 2015)) and the permanent wilting point (PWP) was determined after applying a pressure of

15 atm. Plant-available water (PAW) was calculated as the difference between these values.

Scanning electron microscopy (SEM)

In order to elucidate the microtextural structure, pore properties and elemental concentration at the surface of biochars, images were obtained by scanning electron microscopy (SEM) (Zeiss EVO LS15) and energy dispersive X-ray Microanalysis (EDX) (OXFORD detector). The operating voltage was 20 kV.

Polycyclic aromatic hydrocarbons (PAHs)

The United States Environmental Protection Agency (USEPA) includes 16 PAHs in the Toxic Pollutant List (USEPA, 2013). For extraction of PAHs in biochar samples, 1 – 4 g of each sample was extracted with pressurised fluids in an accelerated solvent extractor (ASE 200 Dionex), with hexane at 100 °C, 2000 psi. The extracts were pre-concentrated by evaporation in an N_2 evaporator in a water bath (TurboVap®LV, Caliper Lifesciences Inc.) until a very small volume was reached. This residual volume was then made up to 5 mL with hexane.

Extracted samples (2 µL) were analysed by gas chromatography (Model 450 GC, Agilent Technologies) coupled to mass spectrometry (Model 220 MS, Agilent Technologies) (GC/MS). The injector was operated at 280 °C in splitless mode. The column oven temperature program was 1 minute at 60 °C, with a temperature ramp of 10 °C min^{-1} until 250 °C (isothermal for 5 minutes) and temperature ramp of 5 °C min^{-1} until 300 °C (isothermal 5 minutes).

Biochar classification according to the fertiliser value

The biochars were classified on the basis of their fertiliser value, as proposed by Camps-Arbestain et al. (2015). The system is based on the hypothetical requirements of corn for P, K, S and Mg. It does not consider N, due to its low availability, or Ca, which is usually present in high amounts. The classification system considers that biochar should be able to provide a

nutrient value when applied at a maximal application rate of 10 t ha^{-1}. The minimum concentrations of each nutrient in biochar, based on corn requirements (expressed as a percentage of total weight), are as follows: available P_2O_5 = 1%, available K_2O = 0.5%, available S = 0.15% and MgO = 0.35%. If the nutrient concentrations are below these values, the biochar is not considered to have a fertiliser value. However, such biochars could possibly fulfil nutrient requirements if applied at higher rates or used with crops with lower requirements.

The following classes were established:

Class	Condition
Class 0	All available nutrients contents are below values established for corn
Class 1	Fertiliser value for one nutrient
Class 2	Fertiliser value for two nutrients
Class 3	Fertiliser value for three nutrients
Class 4	Fertiliser value for four nutrients

RESULTS

Total nutrient content

Although the feedstock composition cannot be used to predict the total nutrient content of biochar, it strongly influences the biochar properties. The total elemental analysis of raw materials pyrolysed at LTA-USC is shown in the Supporting Information in Table S B.1, in which it can be seen that Cm and Opc are richer in nutrients than the other feedstocks. Regarding the pyrolysed materials (Table S B.2), the total nutrient contents varied widely: P (0.02-17.2 g kg^{-1}), Ca (0.79-124.2 g kg^{-1}), Mg (0.34-8.6 g kg^{-1}), Na (0.11-4.70 g kg^{-1}), K (0.29-35.92 g kg^{-1}) and S (0.04-24.72 g kg^{-1}). Other elements, such as Fe (0.03-211.96 g kg^{-1}) and Al (0.07-14 g kg^{-1}), were also measured. Comparison of the nutrient contents (on a dry weight basis) before and after pyrolysis revealed a slight enrichment in P, Ca, K, Mg

and Ca, while the Fe and Al contents remained unaltered (Supporting Information Figure S B.1).

Overall, four groups of biochars were distinguished according to the macronutrient concentration:

- Forestry residues and herbaceous-derived biochars (BAc, BEu, BSd, BMis). These biochars contained the lowest concentration of nutrients. Ca was the most predominant nutrient, followed by K. The biochar containing the smallest amounts of nutrients was BMis, and the biochar richest in nutrients was BSdG, followed by BAcB and BEu-2. The nutrient concentrations of the acacia samples decreased from the bark to the heartwood. The pyrolysis conditions also affected the nutrient concentrations and increased with increasing temperature, e.g. the nutrient contents were higher in BEu-2 than in BEu-1, with estimated HHTs of 500 °C and 400 °C, respectively.
- Agricultural residues (BCc, BCn, BRh, BVs): the nutrient concentrations were much higher than in the previous group. In this case, the most abundant nutrient was K, followed by Ca and P. The highest values corresponded to BRh.
- Manure and compost (BCm, BOpc): the nutrient concentrations were particularly high in these carbonaceous materials, and BOpc was the most nutrient-rich biochar. Both of these PCMs were abundant in Ca, and also contained high amounts of K and P.
- Industrial (BTy, BPl): the nutrient content of BPl was in the same range as woody biochar, with a predominance of Ca, while that of BTy was much lower, although it contained high amounts of Fe.

Available nutrients

Not all nutrients in biochar are available to plants, and in this section, the available fractions of nutrients were determined. The concentrations of available nutrients in biochar varied widely: P_{Av} (0.00 - 11.66 g kg^{-1}), Ca_{Av} (0.38 - 93.40 g kg^{-1}), Mg_{Av} (0.02 - 7.62 g kg^{-1}), Na_{Av} (0.08 - 4.36 g kg^{-1}), K_{Av} (0.16 - 49.77 g kg^{-1}) and S_{Av} (0.01 - 3.78 g kg^{-1}) (Figure 5.1). BRh contained the highest amounts of all available nutrients, except Ca, which was present at highest concentrations in BOpc. The wood derived biochar, especially BAcHw, contained the lowest amounts of available nutrients, as expected due to the low total content.

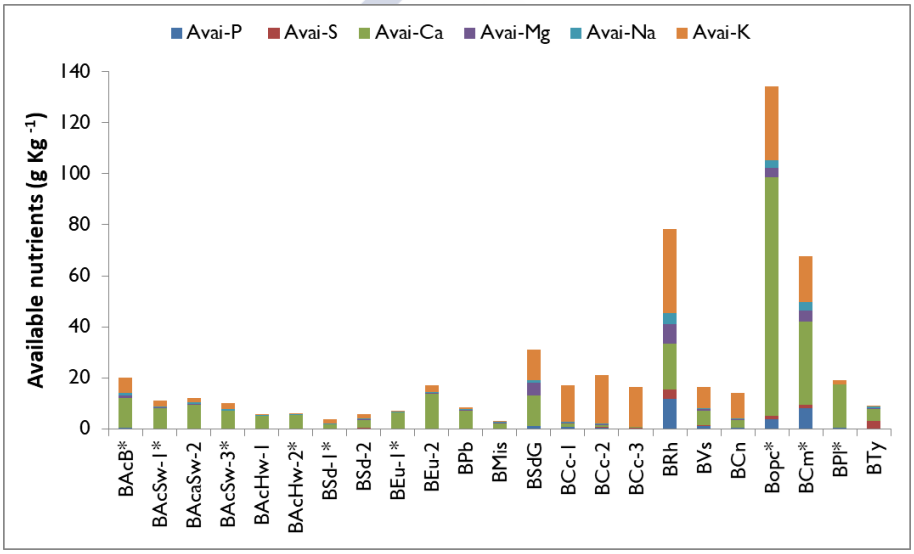

Figure 5.1 Available nutrients in biochar and PCM. PCMs marked with an asterisk (*).

The available nutrient content was also expressed as a proportion of the total nutrient concentration and again varied greatly, from 1% to 100%, depending on the nutrients and type of biochar considered. The proportion of available P, S and Mg was around 30% on average, while the proportions of available Ca, Na and K varied between 60 and 77%.

Available-P, expressed as % P_2O_5, varied between 0 and 2.67% (Table 5.1). The highest value corresponded to BRh, followed by BCm. The P_2O_5 content of the other samples was below 1%. The available K, expressed as % K_2O, ranged from below detectable levels in BAcHw to 12% in BRh. Of the 23 biochars analysed, 13 had fertiliser value for K, according to the values established by Camps-Arbestain et al. (2015). The proportion of available MgO varied from below detection limits to 1.26%, with the highest value corresponding to BRh and the lowest value to the wood-derived biochars, except BSdG, which contained a high amount of K. In this case, only 4 of the biochars studied had fertiliser value for Mg: BRh > BSdG > BCm > BOpc, in decreasing order. The last nutrient taken into account in the biochar fertiliser classification was SO_4-S. The values of available S were below detection limits in some of the biochars studied (wood derived biochar). The highest value, expressed as % of SO_4-S, was 0.38, corresponding to BRh. BTy also fulfilled the requirement of fertiliser value for S.

Table 5.1 Available nutrients in biochar expressed as percentage of P_2O_5, K_2O, MgO and SO_4-S. The values shaded in green are higher than the levels established by Camps-Arbestain et al. (2015).

Sample	%P_2O_5	%K_2O	%MgO	%SO_4-S	Class
BAcB	0.07	1.45	0.18	0.02	1
BAcSw-1	0.03	0.57	0.03	0.00	1
BAcSw-2	0.03	0.36	0.04	0.00	0
BAcSw-3	0.02	0.56	0.03	0.00	1
BAcHw-1	0.00	0.05	0.00	0.00	0
BAcHw-2	0.00	0.04	0.00	0.00	0
BEu-1	0.01	0.11	0.03	0.00	0
BEu-2	0.04	0.64	0.04	0.01	1
BSd-1	0.00	0.36	0.02	0.00	0
BSd-2	0.02	0.39	0.05	0.02	0
BPb	0.01	0.23	0.03	0.01	0
BCm	1.85	4.39	0.70	0.14	3
BOpc	0.88	6.96	0.62	0.12	2
BRh	2.67	12.00	1.26	0.38	4
BCc-1	0.19	3.43	0.06	0.01	1
BCc-2	0.13	4.58	0.03	0.01	1
BCc-3	0.05	3.73	0.02	0.01	1
BCn	0.08	2.42	0.09	0.01	1
BVs	0.25	2.05	0.12	0.03	1
BMis	0.02	0.12	0.06	0.00	0
BSdG	0.27	2.85	0.84	0.00	2
BTy	0.03	0.13	0.07	0.31	1
BPl	0.07	0.49	0.05	0.03	0

Exchangeable and soluble ions in unbuffered, neutral solution

The soluble ions extracted with a non-buffered solution were measured in the feedstock and the resulting pyrolysed materials (Figure 5.2 and Figure 5.3, respectively). The highest concentrations (in units of cmoles (+) kg^{-1} biochar) were mainly found for K (0.08 - 127), Ca (0.7 - 37.5) and

Mg (0.02 – 18.1), with lower amounts of Na (0.2 - 15.6) and Al (0.02 - 1.21). In BAcSw-2, BACSw-3 and BSd-1, the pH of the solution was below 4.2 so extractable protons (H^+) were also measured, ranging between 0.14 and 3.94 cmoles(+) kg^{-1}. In general, the concentration of soluble ions was higher in biochars derived from manure and compost, followed by the biochars produced from agricultural residues, and the lowest values were detected in biochars derived from wood and herbaceous materials. The concentration of soluble ions was highest in BRh followed by BOpc > BCm > BCc. The initial concentration of the soluble ions extracted from the feedstocks varied enormously in comparison with those determined after pyrolysis, and a considerable increase was observed in corncob biochar, BEu-2 and BSd-2, while in other samples such as BCm, BMis and BVs it did not vary or even decreased slightly. A decrease in concentration in PCM, such as BSd-1 and BEu-1, was also observed, so that although the concentration was mainly dependent on the feedstock, the pyrolysis conditions also had some influence.

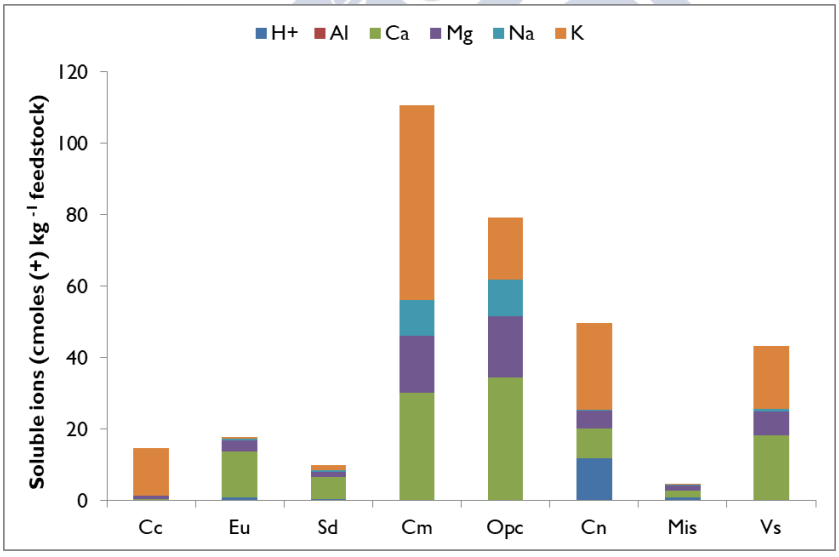

Figure 5.2 Soluble ions extracted with a non-buffered solution expressed in cmoles(+) per kg of feedstock.

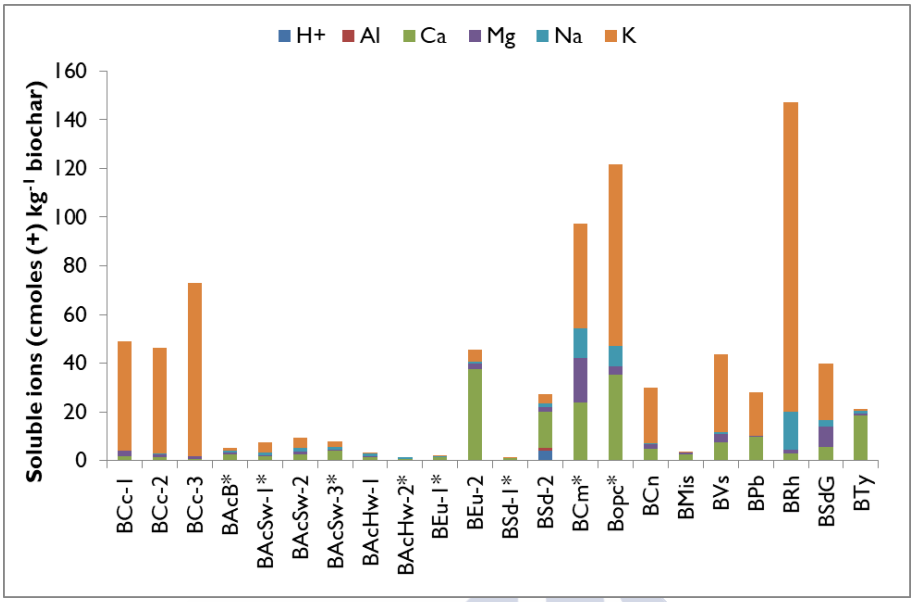

Figure 5.3 Soluble ions extracted with a non-buffered solution from the different types of biochar and PCM under study. PCMs are marked with an asterisk (*).

SEM-EDX

All samples were examined by SEM with magnifications of 30 – 500 µm used to observe biochar morphology and structure: Figure 5.4 (for biochars derived from corncob, rice husk, olive pomace compost and chicken manure) and Figure 5.5 (woody derived biochars). The cell structure was maintained in the wood- and plant-derived biochars, providing the material with an organised morphology and a considerable degree of macro and microporosity. The cell wall was well defined with small pores. Interestingly, stoma structures were distinguished in the rice husk biochar (Figure 5.4B). In trunk samples of both eucalyptus and acacia (Figure 5.5B, C and D), different size tubes (around 50 µm in diameter) were observed, corresponding to the phloem and the xylem. Accumulations of inorganic constituents were also distinguished as white spots arranged in regular bands that tended to diminish closer to the trunk centre. Bark samples were more irregular in form and richer in inorganic constituents than trunk

samples (Figure 5.5A and F). The morphology of BCm and BOpc (Figure 5.4C and D, respectively) was also irregular and rougher. Although some vegetal structures were identified in the samples, pores were not easily recognisable in these highly heterogeneous matrixes, with a predominance of mineral phase.

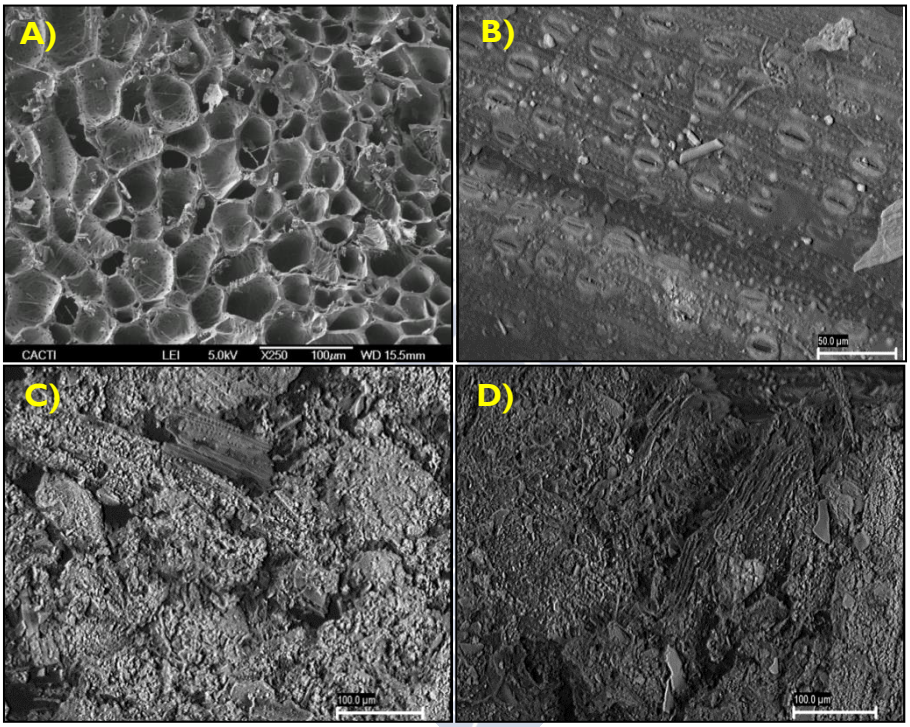

Figure 5.4 SEM image of different types of biochar: A) Corncob; B) Rice husk; C) Olive pomace compost; D) Chicken manure.

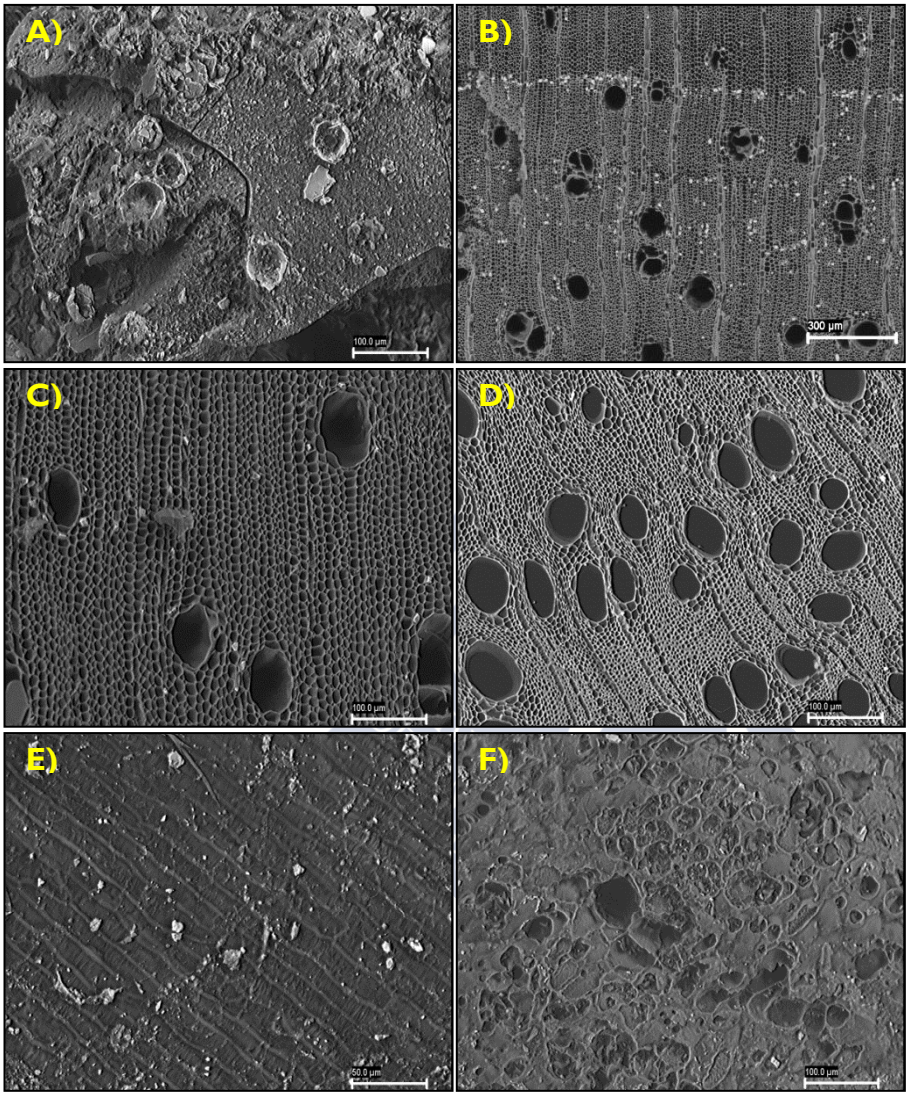

Figure 5.5 SEM image of different types of wood-derived biochar: A) Acacia Bark; B) Acacia Sapwood; C) Acacia heartwood; D) Eucalyptus; E) Sawdust; F) Pine bark.

Energy dispersive X-ray analysis (EDX) was also used to analyse the surface composition of the biochars. For example, the carbonaceous matrix of BRh comprised many inorganic constituents (shown in light colour) (Figure 5.6). The composition of one of these (marked in Figure 5.6 as Spectrum 3) revealed C, O and K as the major constituents (23.3 wt%, 25 wt% and 20 wt%, respectively). This sample was also rich in P and Mg, along with other minor elements such as Fe, Si and Ca. The same composition was also found in the total analysis, as expected.

EDX can also be combined with beam scanning electron microscopy to generate an area map that shows the distribution of a specific element in a defined surface area. An example can be seen in Figure 5.7 in the same area of BRh as the specific analysis, in which the distribution of phosphorus, magnesium and potassium is revealed in the same particles, with that of other minor elements, as in the specific analysis.

More examples of SEM-EDX analysis are shown in Supporting Information B for BSd (Figure S B.3), BEu (Figure S B.4), BAcB (Figure S B.5), BAcSw (Figure S B.6), BCc (Figure S B.7). BOpc (Figure S B.8) and BCm (Figure S B.9). The inorganic constituents incrusted in pores present in biochar derived from acacia trunk included Ca as a major inorganic element, while biochar made from bark of the same species, and also the biochar samples made from chicken manure and olive pomace compost are more heterogeneous and richer in different elements. Once again, this is consistent with the results obtained for the total nutrient content.

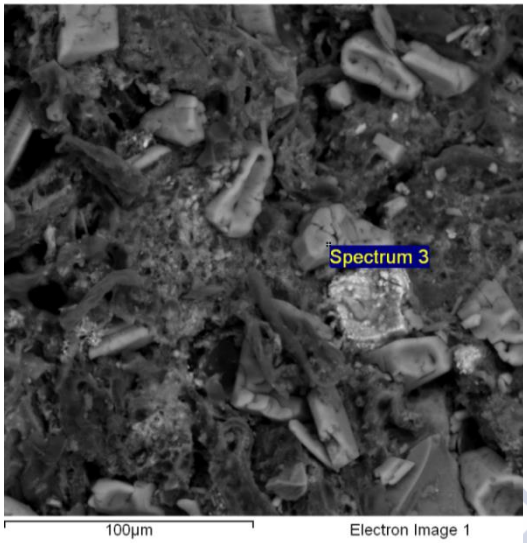

Element	Weight%	Atomic%
C K	23.29	37.94
O K	24.98	30.54
Mg K	10.34	8.32
Si K	0.80	0.56
P K	18.72	11.83
K K	20.56	10.29
Ca K	0.46	0.22
Fe K	0.86	0.30

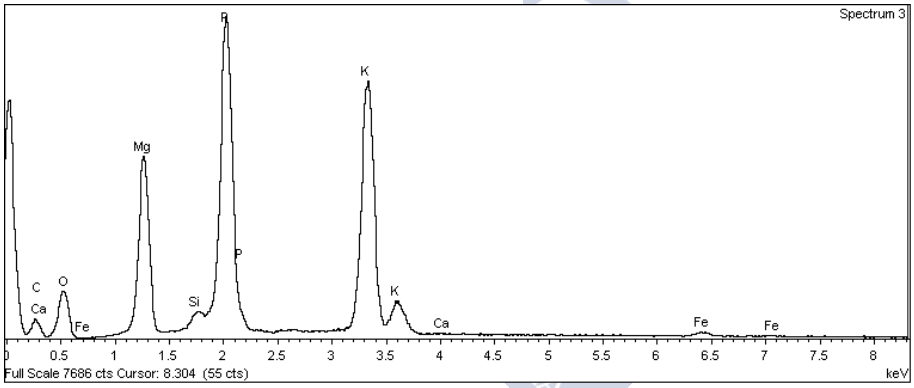

Figure 5.6 SEM-EDX with specific microanalysis of the BRh sample taken in the particle marked as Spectrum 3. The table shows the elemental composition as well as the spectrum.

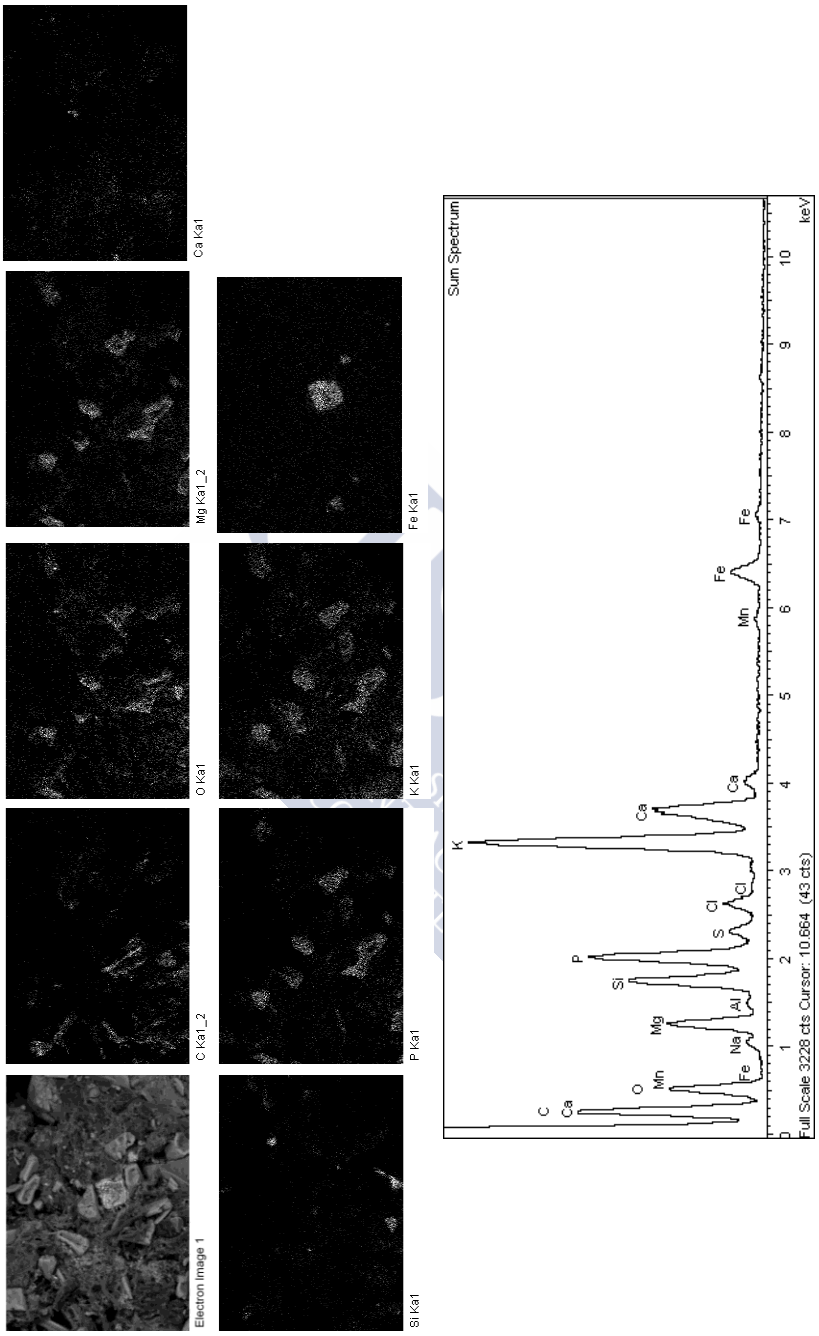

Figure 5.7 Backscattered electron image of BRh biochar/mineral complex, and EDX elemental maps for carbon, oxygen, magnesium, calcium, silicate, phosphorus, potassium and iron.

Water holding capacity

The values of the water holding capacity of some biochars are shown in Figure 5.8 and Table S B.4 (in Supporting Information). In general, the biochars samples were highly hydrophobic and had to be submerged in water for a long time before becoming saturated. BSd-1 and BEu-2 were the most hydrophobic samples and even after two weeks in water they were not completely saturated. This may have increased the variability of the measures. The WHC varied between 43 and 177% (expressed as % of dry sample), with the highest capacity corresponding to BEu-2 biochar and the lowest, to BAcB. The WHC of BEu-2 was significantly higher than those of all of the acacia samples, BCm and BOpc ($p < 0.05$). The WHC tended to increase with the pyrolysis temperature (R^2=0.3889). The plant-available water (PAW) was even more important than the WHC and ranged from 8% in BCm to 80% in BEu-2. The PAW was statistically significantly higher ($p < 0.05$) in BEu-2 than in all the other samples except sawdust- and pine bark-derived biochar. There was large variability in the PAW of biochars depending on the type of feedstock, which may be associated with biochar porosity. As seen with SEM, Eu was richer in macro and microporosity with a well-defined structure, while BAcB, BCm and BOpc were more amorphous.

In addition to the ability of specific types of biochar to retain water, the hydrological effect of biochar in soils is highly dependent on soil water properties, the particle size of the biochar and the interactions between soil and biochar (Kinney et al., 2012). Thus the WHC of biochar alone cannot be used to estimate its behaviour in soil mixtures.

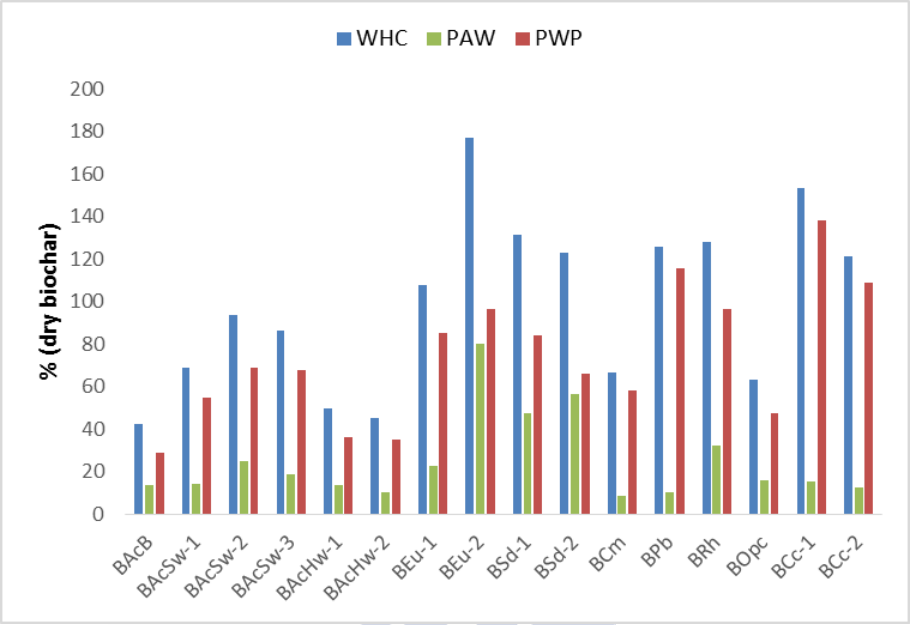

Figure 5.8 Water holding capacity (WHC), plant available water (PAW) and permanent wilting point (PWP) in different types of biochar and PCM (expressed as % of dry sample).

Potential toxicity of biochar

The potential toxicity of biochar must be determined before the material is applied to soil, as soil amendments should not affect soil health or generate environmental impacts (Monlau et al., 2016). Pollutants can be divided into two categories: (i) those present in the original feedstock (i.e. trace metals) and (ii) those generated during the production process by thermochemical conversion (polycyclic aromatic hydrocarbons (PAHs)) (IBI, 2015). It is important to establish threshold levels for both of these categories of pollutants to ensure that application of biochar to soil is free of risks.

The following values were established by IBI for metal concentrations in biochar: Arsenic (As) 13 - 100 mg kg^{-1}, cadmium (Cd) 1.4 - 39 mg kg^{-1}, chromium (Cr) 93 - 1200 mg kg^{-1}, cobalt (Co) 34 - 100 mg kg^{-1}, copper (Cu)

143 - 6000 mg kg^{-1}, lead (Pb) 124 - 300 mg kg^{-1}, nickel (Ni) 47 - 420 mg kg^{-1}, selenium (Se) 2 - 200 mg kg^{-1} and zinc (Zn) 416 - 7400 mg kg^{-1}.

The metal concentrations in biochars are shown in Table S B.3. Importantly, the values were below the limits established by IBI in all the biochars, except BTy. In this biochar, the concentration of Co was three times the maximum allowed, and that of Zn was almost five times higher than the maximum allowed. The metal concentration varied in the other biochars: Co (<5 - 11 mg kg^{-1}), Cr (<5 - 62 mg kg^{-1}), Cu (<5 - 108 mg kg^{-1}), Mn (<5 - 800 mg kg^{-1}), Ni (<5 - 140 mg kg^{-1}), Pb (<25 - 48 mg kg^{-1}), Zn (5 - 860 mg kg^{-1}). The concentration of As, Se, Cd and Sb were below the detection limits in all samples except for BTy (3.124 mg kg^{-1} Sb, 1.021 mg kg^{-1} Se, 6.589 mg kg^{-1} As and 1.055 mg kg^{-1} Cd), with all values below the threshold values established by IBI Standards. Wood derived biochar contained the lowest amounts of heavy metals, which in most cases were below the detection limits. After pyrolysis, an increase in the concentration of metals was observed relative to that in the corresponding feedstocks (Table S B.1), which was attributed to the residual concentration during the thermal process. The metal content increased with increasing pyrolysis temperature in BEu-1 (HHT ≤ 400 °C) and BEu-2 (HHT around 500 °C).

Regarding the PAHs content (expressed as the sum of 16 USEPA PAH) of the biochars and PCMs varied between 0.32 and 16.45 mg kg^{-1} (Table S B.5). The highest values corresponded to the biochar made from tyres, followed by BPl and BCm with 3.98 and 3.11 mg kg^{-1}, respectively. The IBI Standards establish the threshold range at between 6 and 300 mg kg^{-1}, and thus the values for the samples under study were well below this limit. By contrast, the requirements established by the EBC are more restrictive, with a threshold of 12 mg kg^{-1} for basic grade biochar and of 4 mg kg^{-1} for premium grade biochar. In this case, the level in the biochar made from tyres was higher than the most restrictive threshold (16.45 mg kg^{-1}). The other biochars contained low concentrations of PAHs (average 0.79mg kg^{-1}), of < 4 mg kg^{-1}. Overall, the most abundant of the 16 PAHs were

Benzo(a)pyrene, Naphthalene, Dibenzo(a,h)anthracene, Chrysene and Indene(1,2,3-cd)pyrene. By contrast, Phenanthrene, Acenaphthylene, Acenaphthene, Benzo(a)anthracene were found at concentrations below the detection limits in various samples, mainly those derived from wood.

Finally, no relationship between pyrolysis temperature and PAH content was observed; the concentration was mainly related to the feedstock and was highest in plastic and tyre due to the nature of these materials.

DISCUSSION

Diverse physical and chemical biochar characteristics were determined for evaluation of potential value of adding the biochar to the soil. First, the feedstock source was found to be an important factor determining the nutrient content of biochars. The nutrients contained in feedstock become concentrated during the process of pyrolysis (Brewer et al., 2012). Our results are consistent with those of previous studies (Ippolito et al., 2015; Camps-Arbestain et al., 2015; Brewer et al., 2012), in which the nutrient content in plant-based biochars was found to be lower than in animal-based biochar. Moreover, nutrient concentration was closely related to the percentage of ash (r^2 = 0.8282) (Figure S B.2 A). In addition, the nutrient concentration was inversely related to total C content (r^2 = 0.5449) (Figure S B.2 B), due to an increase in the latter as the ash fraction increases (Ippolito et al., 2015). Considering the predominant elements, biochars derived from herbaceous or wood material are richer in Ca and K, while biochar made from agricultural residues is dominated by K, followed by Ca and P. These results are consistent with those of Oleszczuk et al (2016), who also found that miscanthus biochar was richer in Ca and K than in other nutrients.

However, the total nutrient content of biochar does not provide information about the short-term availability to crops. The methods traditionally used to determine available nutrients in soils or vegetables are

not always adequate for biochar (Steiner, 2016). In this study, available nutrients in biochar were determined by the methods developed by Camps-Arbestain et al. (2017). The results were then used to classify the samples according to their fertiliser value following the method proposed by Camps-Arbestain et al. (2015). According to this, rice husk biochar is potentially the most useful, as it fulfilled the minimal available nutrient content requirement for four elements. In addition, it was shown to be rich in phosphorus, one of the most limiting elements for plants growth. Chicken manure was the second best pyrolysed material, based on its fertiliser value, as it was classified as Class 3. This was followed by olive pomace compost, as Class 2. All biochar derived from agricultural residues, as well as BEu-2, BAcB, BAcSw-1, BAcSw-3 and BSdG, were classified as Class 1, contributing K. Interestingly, BMis, which was one of the best biochars for C storage, had the lowest fertiliser value. This demonstrates that a biochar it is not universally good or bad, as its potential value will depend on the proposed use. Even samples belonging to Class 0 could be used to fertilise crops with less requirements than corn or when applied in higher quantities.

SEM-EDX microanalysis confirmed the results of the total analysis of the samples, showing that wood-derived biochar contained less nutrients than biochar derived from agricultural, manure and compost. The images also showed a higher degree of heterogeneity and higher concentrations of inorganic elements in bark than in trunk samples. By contrast, plant-derived biochar had a well-defined structure and porosity.

In addition, biochar with the highest concentration of available nutrients contained the highest amounts of soluble and exchangeable ions. There was no clear relationship between soluble ion content and pyrolysis temperature. The relationship reported so far in the literature is also inconsistent, as the authors sometimes obtained better exchange capacity in biochar produced at lower temperatures, while the opposite was found with other types of feedstock (Yuan et al., 2011).

It must be noticed that a nutrient-rich biochar is not always adequate for use as a soil amendment. Soil properties and their requirements must always be taken into account, as if disproportionate amounts of nutrients are applied to a soil with a low ability to retain nutrients, this may affect the surface and ground water quality (Novak & Busscher, 2013). A micronutrient deficiency may also occur at a high pH value and biochar may contribute to liming the soil (Novak et al., 2009).

Regarding the hydrological behaviour of biochar, the results obtained for the different pyrolysed materials were variable. As well as the effect on nutrient content, the WHC of biochars will vary greatly depending on the type of soil to which they are applied and the interactions between biochar-soil and the interparticle space, as well as the particle size of the biochar. A preliminary, detailed study of the soil-biochar system would be necessary prior to each application, as cases of improved, reduced and no-effect have been reported depending on the type of soil (Kinney et al., 2012).

Another important characteristic of biochar in relation to its use as a soil amendment is the alkalinity, which is related to the presence of ash. The high pH values measured in biochar were associated with the content and nature of the ash. According to previous studies, at pyrolysis temperatures above 300 °C, the nutrients in inorganic salts separate from the organic matrix and, as alkali salts dominate and acidity is lost in the volatile compounds, the pH tends to increase (Cao & Harris, 2010). In the present study, the pH values of some PCMs (Sd, Eu-1 and Ac biochars) were low. This was attributed to the fact that these materials were pyrolysed at low temperatures. As a result, cellulose and hemicellulose, which can be decomposed at around 200-300 °C, thus producing organic acids and phenolic substances with a common pH between 2-3, that were not evolved, remain in the system and cause a decrease in the pH of the samples (Cao & Harris, 2010; Sipilä et al., 1998). Other authors have reported the low pH of biochar produced from wood at low temperatures (≤ 300 °C) (Calvelo Pereira et al., 2011). As most types of biochars are

basic (pH > 7), they can be used as liming agents to ameliorate acidic soil conditions (Ippolito et al., 2015), as in Galician soils.

Finally, the potential toxicity of biochar was studied by measuring the concentrations of heavy metals and PAHs. The concentrations of these pollutants are within the established threshold values, except for biochar made from tyres, which presented some risk due to the high concentrations of Co and Zn. Elevated PAHs levels were also found in BTy and BPl, which can be explained by the nature of the feedstock. The PAHs content does not seem to be related to any other property of biochar. Previously published data did not provide a satisfactory explanation regarding the relationship between PAH concentration in biochar and pyrolysis temperature or residence time (Buss et al., 2016; Bucheli et al., 2015). The results obtained in this study demonstrated that even in a simple pyrolysis system with poorly controlled production conditions, the PAHs content was below existing environmental quality standards in soils in almost all types of biochar. Even biochars with higher values may not present a considerable risk, as other authors (e.g. Hale et al. 2012), have previously shown that only 1-10% of the total PAHs content was bioavailable, due to the ability of biochar (and other black carbon materials) to retain organic compounds. The associated environmental risk is therefore low (Cornelissen & Hale, 2017).

Overall, the biochars showing the best potential as soil conditioners according to their properties were BRh, BCm, BOpc and all BCc. This can be attributed to the nutrient availability, soluble ion concentration, potential water holding capacity, high pH and lack of potential toxicity. As claimed by Lehmann (2009), biochar should be considered a soil conditioner, rather than a fertiliser, and it can be used to improve the essential soil functions over long periods, although the effects will ultimately depend on soil type and properties.

CONCLUSIONS

In this chapter, the potential value of different types of biochar as soil amendment was evaluated by considering nutrient availability, soluble ions concentrations, structure and water holding capacity, as well as the associated environmental risks. The biochars presented a wide variety of behaviours and properties depending on the feedstock used. Samples rich in ash (and thus poorer in organic C) were richer in nutrients. For the application of biochar as soil amendment, the best options were manure- or compost-derived pyrolysed materials, such as BCm or BOpc, and agricultural waste-derived biochars, such as BRh and BCc. Wood-derived biochars were less suitable as they contained low amounts of available nutrients. However, the biochar properties must be studied in greater depth as the soil-biochar interaction may alter some of these properties. The choice of a particular biochar will depend on soil requirements or deficiencies. Tyre-derived biochar should be completely disregarded for use as a soil amendment due to the high concentrations of heavy metals (Co and Zn) and PAHs. Considering the EBC requirements for PAHs content, plastic-derived biochar cannot be applied to soils. Overall, the production of biochars and PCMs with fertiliser value is possible, even with a low-cost pyrolysis reactor. This approach could thus be presented to farmers as a low-cost tool for disposing of waste and improving their land, while also capturing C from atmosphere.

USC
UNIVERSIDADE
DE SANTIAGO
DE COMPOSTELA

6. Use of biochar as a sorbent for the removal of fuel-derived organic compounds from contaminated water

USC
UNIVERSIDADE
DE SANTIAGO
DE COMPOSTELA

INTRODUCTION

Approximately 20 million tonnes of oil and petroleum products are used worldwide every day (Fingas, 2012). Petroleum is transformed in refineries and transported and stored in different locations (e.g. petrol stations, industrial sites, heating plants). The fuel compounds produced during this process are thus potentially important sources of environmental contamination due to accidental spills, poor management of the waste products and leakage from underground storage tanks and transportation pipes (Kim et al., 2011) (Figure 6.1).

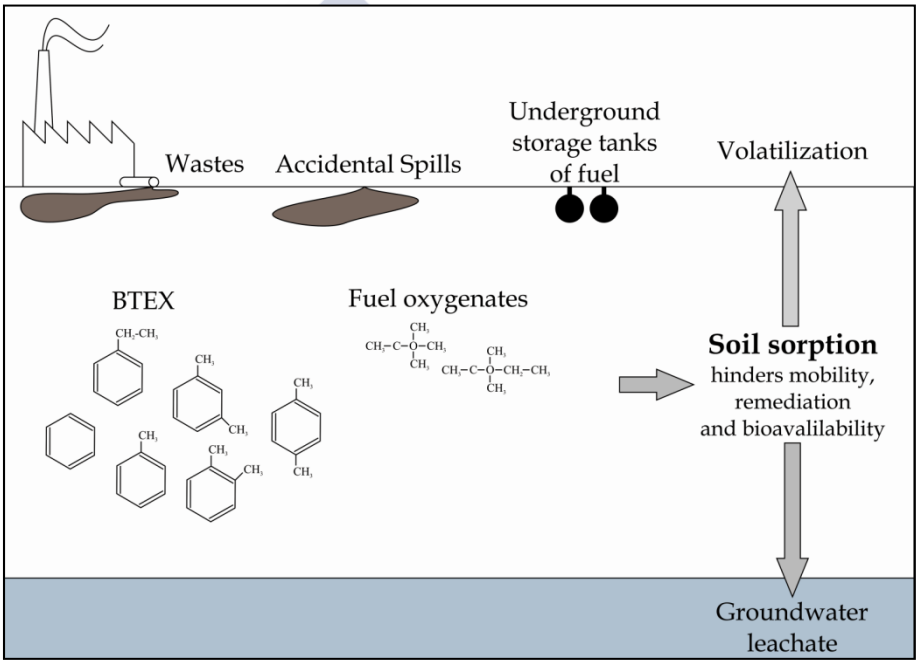

Figure 6.1 Main sources of fuel compounds in the environment, from Balseiro-Romero et al. (2012).

Since 1970, almost 10000 oil spill incidents involving tankers have been reported worldwide, with most (81%) categorised as small spills (< 7 tonnes) (ITOF, 2017). Furthermore, CONCAWE (Conservation of Clean Air and Water in Europe) recorded data on spills from European pipelines

during the period 1971 – 2015, registering 674 incidents with an average of 170 m³ per spill (CONCAWE, 2017). Although the environmental damage caused by a spill depends on the amount of fuel released (Figure 6.2), small spills may sometimes affect large areas due to dispersal of the pretroleum by wind, groundwater and surface water flows (CONCAWE, 2017).

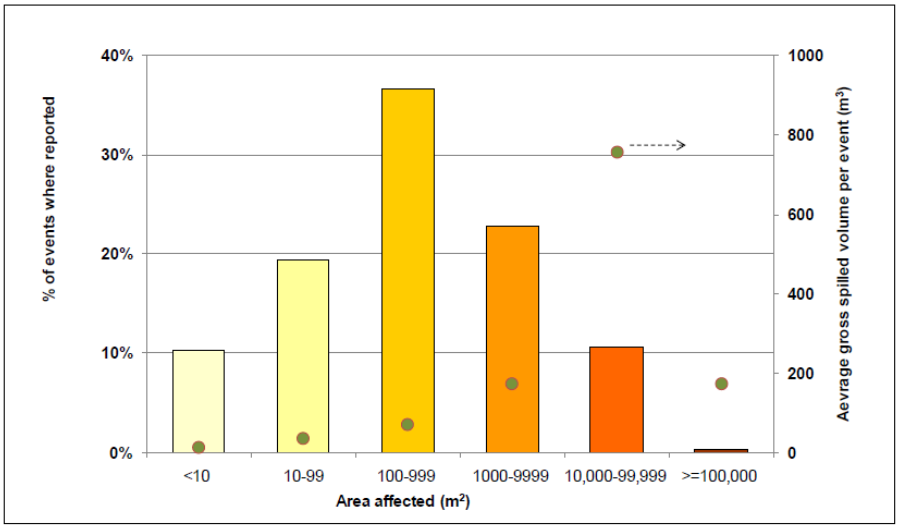

Figure 6.2 Ground area (m²) affected by oil spills (% of number reported) (CONCAWE, 2017).

Despite the increase in the production and consumption of petroleum, the number of spills has decreased over the years (Figure 6.3). Nevertheless, spill incidents continue to occur, causing considerable environmental and economic damage.

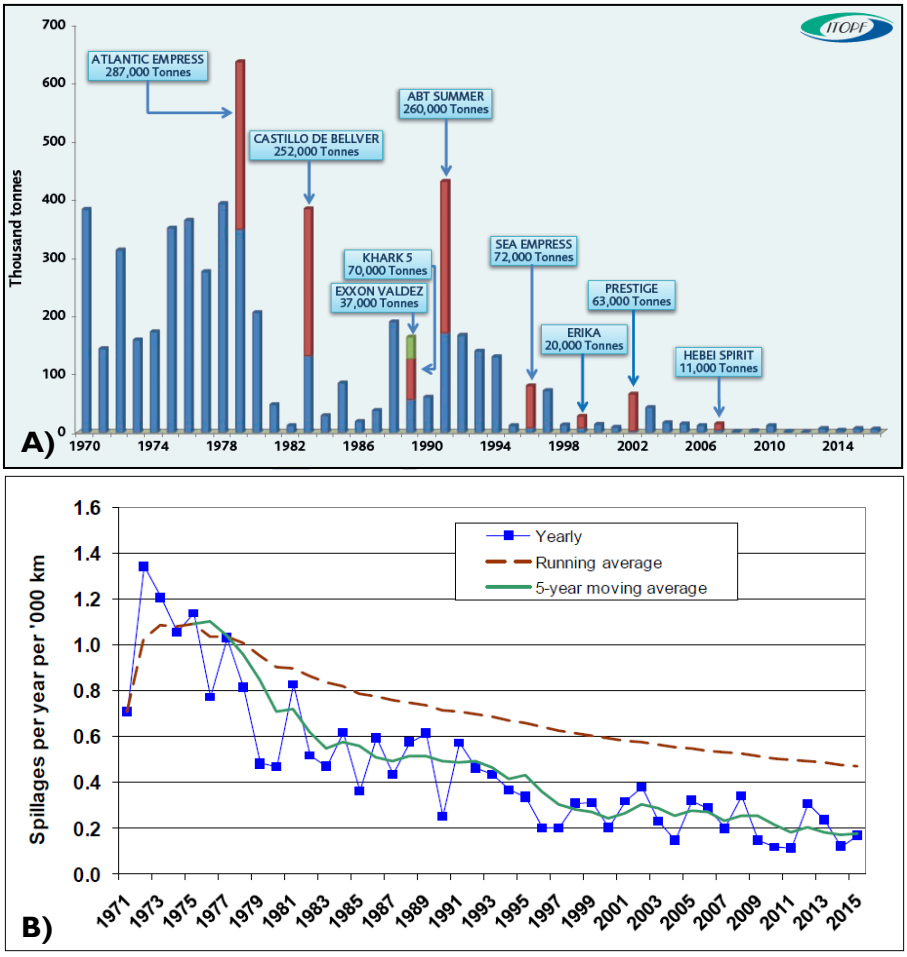

Figure 6.3 (A) Number of oil spills of 7 tonnes or over (rounded to nearest thousand) and the most significant events between 1970 and 2016 (ITOF, 2017); (B) Spill frequency involving European pipelines during the 45 year period, excluding theft, expressed as spills per year and per 1000 km of pipeline (CONCAWE, 2017).

Diesel, gasoline and other fossil fuels are complex mixtures of organic compounds, most of which are toxic and included in the United States Environmental Protection Agency (USEPA) priority pollutant list. Diesel fuel is mainly composed of *n*-alkanes, *iso*-alkanes, cycloalkanes and aromatic compounds (Farrell et al., 2007). BTEX (benzene, toluene, ethylbenzene and

m-, *p*- and *o*-xylene isomers) is a group of organic aromatic compounds commonly present in petroleum products, mainly in gasoline (USEPA, 2010). Gasoline formulations also include fuel oxygenates (FO) as additives to enhance the octane number and to reduce emissions. Methyl *tert*-butyl ether (MTBE) and ethyl *tert*-butyl ether (ETBE) are the most commonly used FO (Kanai et al., 1994). These compounds are the most volatile and water-soluble components of fuel and can migrate from the contamination source and cause serious environmental problems (Fries et al., 1994). They also pose a threat to human health as they can cause skin and sensory irritation, affect the nervous system and are considered haematotoxic and carcinogenic (Wilbur & Bosch, 2004).

For all of the above reasons, the development of rapid, simple handling remediation plans with effective tools or materials are required in order to minimise the negative consequences of petroleum spills (Silvani et al., 2017). This can be done by removing, degrading, immobilising or transforming the pollutants into less dangerous forms in situ or ex situ by physical, chemical or biological processes (Morillo & Villaverde, 2017; Rao et al., 2017). Some of the techniques conventionally used to remove organic compounds from water include de-oiling, chemical oxidation and precipitation, photocatalysis, electrodialysis, sand filtration, membrane-based separation and adsorption (Zaib et al., 2014; Fakhru'l-Razi et al., 2009). Other technologies are based on bioremediation, which uses microorganisms to degrade the contaminants (Jecu et al., 2008; Compton et al., 2003). More specifically, among the physical methods developed, air/steam stripping combined with organic-vapour membrane has been reported to be effective for enhancing the recovery of the pollutants from water (Wijmans et al., 2006). In particular, the use of different sorbents (such as activated carbon, diatomite and zeolite) to remove these contaminants from the environment has been previously evaluated (Zadaka-Amir et al., 2012; Aivalioti et al., 2010; Cornelissen et al., 2005). Recently developed sorbents, such as carbon nanotubes and polydimethylsiloxane nanoparticles, have been used to retain

BTEX (Gupta & Kulkarni, 2011; Zaib et al., 2014). Activated carbon has been widely applied in wastewater treatment due to its high adsorption capacity; however, it is difficult to regenerate/reactivate and its application on a large-scale is expensive (Ali & Gupta, 2007). Therefore, research must focus on finding novel and efficient materials: biochar and pyrogenic carbonaceous materials (PCMs) are low-cost, suitable alternatives that will also contribute to a more efficient waste management and to creating a circular economy. Moreover, biochar can be produced with local and/or wastes materials (produced close to a recovery area), thus avoiding the need for long distance transportation and enhancing the efficiency of the system, by making it economically viable and closing cycles. The potential use of biochar as a soil amendment and in C sequestration has been widely investigated (Chen et al., 2018; Kuppussamy et al., 2016; Lehmann et al., 2015). Another important property attributed to biochar is its capacity to act as a sorbent, especially for organic compounds (Smernik, 2009). The physico-chemical properties of biochars, i.e. elemental composition, aromaticity, specific surface area or microporosity, are important properties that determine the sorption capacity of biochar (Kookan et al., 2017; Kupryianchyk et al., 2016; Xiao et al., 2016; Ahmad et al., 2014;). In addition, the nature of the contaminant will also affect the efficiency of removal, as observed by many authors (Chen et al., 2008; Sander & Pignatello, 2005).

Within this context, the objective of the present study was to evaluate the potential use of biochars and PCMs to remove petroleum-derived organic compounds, such as BTEX, FO and diesel fuel (measured as Total Petroleum Hydrocarbons, TPHs) from aqueous solutions. The effect of feedstock material and pyrolysis conditions on the sorption capacity of biochar was also assessed. For this purpose, batch-based sorption experiments were designed to characterise the sorption of fuel-derived volatile compounds and the sorption behaviour of diesel fuel, a more complex mixture.

MATERIALS AND METHODS

Reagents

The following reagents were used in the study: benzene (purity, 99.8%; grade, PAI-ACS (UV-IR-94 HPLC-GPC)), toluene (purity, 99.8%; grade, PAI-ACS (UV-IR-HPLCGPC)), ethylbenzene (purity, 99%; grade, PS), *o*-xylene (purity, 99%; grade, PA (Reag.USP. Ph. Eur)), *m*-xylene (purity, 99%; grade, PA (Reag. Ph. Eur)), *p*-xylene (purity, 99%; grade, PA (Reag.USP)), MTBE (purity, 99.7%; grade, PAI (PAR)) and ETBE (purity, 99%; grade, PA (Reag.USP)). Fluorobenzene (purity, 99%) was used as internal standard for calibration. All reagents were purchased from Panreac Química, S.L.U. (Barcelona, Spain), except fluorobenzene, which was purchased from Sigma-Aldrich Co, LLC (China). The spiking solutions were prepared in methanol (purity, 99.9%; grade, PAI (PAR)) with each of the reagents (BTEX and FO) at concentrations of 100 mg L^{-1} (Experiments 1) and 10000 mg L^{-1} (Experiments 2). Another standard solution was prepared with fluorobenzene (FB) at a concentration of 100 mg L^{-1}.

In order to determine the capacity of different biochars to sorb TPHs, commercial diesel fuel was purchased from a local petrol station (Repsol). Extractions, dilutions and standards were prepared in hexane (purity, 99.9%; grade, PAI (PAR)).

All other chemicals used in the experiments were of Merck p.a. quality.

Sorption experiments

Experiment 1: A headspace-analytical approach to assessing the sorption of fuel-derived volatile compounds on biochars

HeadSpace-Gas Chromatography-Mass Spectrometry analysis (HS-GC-MS) without matrix effect correction was used to evaluate the performance of biochar for sorbing BTEX and FO following the optimised method reported by Balseiro-Romero & Monterroso (2013). The technique is

simple, fast and requires limited handling, making it appropiate as a first approach to determining the sorption capacity of different biochars.

A wide variety of previously characterised biochars (16 samples) were selected for this experiment. The biochars were derived from acacia (BAcB, BAcSw-1, BAcSw-2, BAcSw-3, BAcHw-1 and BAcHw-2), eucalyptus (BEu-1 and BEu-2), pine sawdust (BSd-1), pine bark (BPb), chicken manure (BCm), olive pomace compost (BOpc), rice husk (BRh), corncob (BCc-1 and BCc-2) and used tyres (BTy). The main properties of these materials are shown in Table 4.3 (Chapter 4). A slurry was prepared with 0.5 g of biochar mixed with 2 mL of distilled water in 10 mL-HS analytical vials to which 100 µL of spiking solution was added. The total spiking concentration in the experiment was 40 mg kg^{-1} for ∑FO (the sum of ETBE and MTBE) and 120 mg kg^{-1} for ∑BTEX (the sum of benzene, toluene, ethylbenzene and xylene isomers). The slurry facilitated the homogeneous distribution of the organic contaminants in the biochar and reduced loss by evaporation (Serrano & Gallego, 2006). Fluorobenzene was added to all samples at the same concentration (5000 µg kg^{-1}). Once the biochar samples were spiked with the contaminants, the headspace (HS) vials were hermetically sealed and statically incubated at 4 °C for 7 days. Experiments were carried out in triplicate and the concentration of volatile fuel organic compounds (VFOC) was analysed by HS-GC-MS (See section "Instrumental and Analytical procedure").

Experiment 2: Sorption isotherms of BTEX and FO for selected biochars

Four biochars produced from different feedstock materials were chosen for batch sorption experiments to determine the sorption isotherms for BTEX and FO. The biochars were produced from acacia bark (BAcB), chicken manure (BCm), corncob (BCc-2) and eucalyptus (BEu-2). BAcB and BCm were produced by low-temperature pyrolysis, and BCc-2 and BEu-2 were obtained at high-temperature pyrolysis (> 400 °C). The main physico-chemical properties of these samples are summarised in

Table 6.1. The specific surface area (SSA) was determined by applying the Brunauer-Emmett-Teller (BET) method to N_2 adsorption with a Micromeritics Gemini 2360 V2.01 instrument.

Batch experiments were conducted using deionised water containing 5 mM $CaCl_2$, to simulate natural conditions, and 5 mM NaN_3, to inhibit bacteria degradation (Chen & Yuan, 2011; Xiao et al., 2014). The contaminant stock solution (10000 mg L^{-1}) was diluted to yield an initial range of concentrations of between 2 and 600 mg L^{-1} for each individual compound: specifically 2, 15, 30, 60, 90, 120, 200, 300, 400 and 600 mg L^{-1}. Aliquots of 10 mL of these solutions were added to glass vials containing 0.1 g of biochar and were shaken for 36 h (Chen & Yuan, 2011; Xiao et al., 2014). The headspace in the tubes was minimised to reduce the volatilisation of any contaminants during shaking. After equilibrium was reached, solid and aqueous phases were separated by centrifugation at 2100 rpm for 15 min and a 2 mL-aliquot of supernatant was transferred to HS analysis vials. Finally, 50 µL of FB solution was added, and the vials were quickly sealed to prevent evaporation of the contents.

Experiments were conducted in triplicate and the concentrations of BTEX and FO were analysed by HS-GC-MS following the same method as in Experiment. 1. The amount of contaminant sorbed was calculated as the difference between the total amount spiked and the amount remaining in the final solution.

Table 6.1 Main physico-chemical properties of selected biochars and PCMs.

Sample	BAcB	BCm	BEu-2	BCc-2
HHT (°C)	<300	<300	500	500
pH	6.84	7.15	9.38	9.79
%C	64.48	32.59	79.02	80.22
%N	2.23	3.02	0.57	0.45
%H	4.20	3.94	1.94	2.47
%S	0.13	0.32	0.04	0.03
%Ash	5.48	46.44	3.75	5.09
%O	23.48	13.70	14.69	11.74
%C_{inorg}	0.52	0.33	0.36	0.05
O/C_{org}	0.27	0.32	0.14	0.11
H/C_{org}	0.78	1.49	0.30	0.37
(O+N)/C	0.30	0.39	0.15	0.11
% FixC	51.83	36.69	73.91	78.90
% VM	42.92	46.08	22.17	15.78
R50	0.57	0.46	0.60	0.64
C_{nox} (g kg^{-1})	132.46	41.58	287.97	482.15
P (g kg^{-1})	1.13	15.35	1.25	2.78
Ca (g kg^{-1})	21.70	47.80	23.26	1.30
K (g kg^{-1})	7.33	16.82	3.08	21.84
Mg (g kg^{-1})	2.20	7.20	1.07	0.63
Na (g kg^{-1})	1.05	3.97	0.34	0.19
Fe (g kg^{-1})	0.20	14.58	0.99	5.20
Al (g kg^{-1})	0.24	14.00	0.50	0.40
CEC (cmoles(+) kg^{-1})	5.03	97.22	45.50	46.27
SSA (m^2 g^{-1})	0.06	1.27	205.60	8.89

HHT, Highest Heating Temperature; FixC, Fixed Carbon; VM, Volatile Matter; R50, Recalcitrance Index; Cnox, non oxidisable Carbon

Experiment 3: Diesel sorption on biochars

Another batch experiment was conducted with diesel to determine the sorption capacity of biochar, as evaluated by TPH analysis. According to the results obtained in the previous experiments, as well as to the sample availability, eucalyptus (BEu-2) and corncob (BCc-2) biochars were selected for this experiment. Batch sorption experiments were conducted by mixing 0.25 g of biochar with 25 mL of a solution of deionised water, 5 mM $CaCl_2$ and 5 mM NaN_3 (Chen & Yuan, 2011; Xiao et al., 2014). Samples were spiked in triplicate with 1, 2, 5, 7.5, 10, 13, 15, 20 and 30 µL of commercial diesel. After 3 days with continuous stirring, each sample was centrifuged at 2300 rpm for 15 min. The supernatant (25 mL) was separated from biochar and ultrasonically extracted with 25 mL hexane for 1 h. Trace amounts of water in hexane extracts were removed with anhydrous sodium sulphate. TPHs in the extracts were measured by gas chromatography coupled to mass spectrometry (GC-MS). The biochar sorption capacity was determined as the difference between the total concentration spiked and the concentration measured in the equilibrium solution.

Instrumental and analytical procedure

Analysis of BTEX and FO by HS-GC-MS

The analytical system consisted of an autosampler (Agilent-Varian Combi PAL) with HS injection, an oven, a gas chromatograph (Agilent-Varian 450-GC) and a mass spectrometer with ion trap (Agilent-Varian 220-MS). Cycle Composer software (Version 1.5.4; CTC Analytics AG) was used to control the Combi PAL autosampler and MS Workstation software (Version 6.9.3; Varian, Inc.) was used to control the GC-MS system and to process the data.

The operating conditions were established according to Balseiro-Romero & Monterroso (2013). Vials were heated in the oven at 80 °C for 15 minutes with constant stirring (500 rpm) to achieve equilibrium between phases. When equilibrium was achieved, 1 mL of HS gas was injected in the

chromatograph for analysis. Note that in the preliminary experiment (Experiment 1), three phases were present in the tubes (biochar, water and HS), and sorption of the analytes onto biochar reduced their movement to the HS (Figure 6.4).

A FactorFour VF-5ms EZ-Guard chromatographic column of 30m x 0.25 mm x 0.25 µm (supplied by Agilent Technologies) was used in the experiment. The column oven temperature varied as follows: 35 °C (held for 5 min), 10 °C min^{-1} up to 80 °C and 25 °C min^{-1} up to 200 °C (held for 0.7 min). The carrier gas, helium, was supplied at a constant flow rate of 1 mL min^{-1}. The injector was operated at 250 °C and in split 1/10 mode. The mass spectrometer was operated in full scan mode. The molecules were ionised by electron impact, and the ion trap temperature was fixed at 220 °C (Balseiro-Romero et al. 2016). *m*- and *p*-xylene were quantified as single compounds, because they appeared as single peaks in the chromatograms.

Calibration standards were prepared in 2 mL of distilled water containing 100-10000 µg L^{-1} of each individual contaminant and a constant concentration of fluorobenzene (2.5 mg L^{-1}) as internal standard. The same concentration of FB was added to the supernatants in the batch experiment (Experiment 2), but not in the first experiment. The latter type of calibration without matrix effect correction enable quantification of the matrix effect and the biochar sorption process. The results of the HS-GC-MS analysis of samples corresponded to the amount of contaminant recovered that

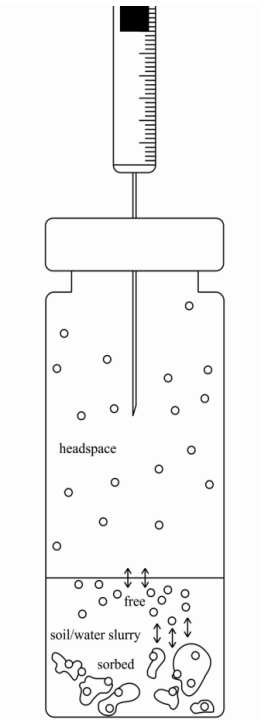

Figure 6.4 Simplification of the equilibrium process in HS vials in Experiment 1 (Balseiro-Romero, 2014).

is free of sorption and participates in the slurry-HS equilibrium (Figure 6.4) (Balseiro-Romero & Monterroso, 2013).

Analysis of TPH by GC-MS

The concentration of diesel in solution was determined by GC-MS. The TPH calibration standards were prepared in hexane by diluting the same commercial diesel used to contaminate samples to yield several concentrations: 10, 25, 50, 75, 80, 100, 125, 175, 200 mg L^{-1}. Chromatographic separation was performed on the same column used in HS-GC-MS method, which was operated with the following oven temperature program: 40 °C (held for 10 min) to 320 °C at 10°C min^{-1}. The carrier gas, helium, was supplied at a constant flow of 1 mL min^{-1}. The injector was operated using a temperature ramp from 60 to 320 °C (held for 47 min) at 200 °C min^{-1}, and samples (1 µL extract) were injected in split/splitless mode. The mass spectrometer was operated in full scan mode. The molecules were ionised by electron impact, and the ion trap temperature was fixed at 220 °C (Balseiro-Romero et al., 2016). The TPH contents were calculated as total ion count, by integrating the peak area obtained in the chromatogram.

Empirical adsorption models

Data from BTEX and diesel adsorption assays (Experiments 2 and 3) were described by the two empirical models most commonly used in the descriptive analysis of adsorption processes:

Langmuir model (L): $q_e = \frac{Q_{max}(K_L C_e)}{1+(K_L C_e)}$

Freundlich model (F): $q_e = K_F C_e^{1/n}$

where: q_e is the concentration of each contaminant sorbed per unit of mass of biochar (g kg^{-1}); C_e is the concentration of each organic compound in the solution (mg L^{-1}); Q_{max} is the maximum adsorption capacity of each biochar (g kg^{-1}); K_L is the Langmuir equilibrium constant which is related to the binding strength (L mg^{-1}); K_F is a constant related to the adsorption capacity (g $L^{1/n}$ $mg^{-1/n}$ kg^{-1}); and n is a constant related to the intensity of adsorption and the heterogeneity of the binding sites.

The fitting of the sorption models was conducted using OriginPro 8 SR0 software, with minimisation of the residual sum of squares (RSS) as a fitting criterion. Several statistics (R^2, χ^2) were used to assess the model results.

Statistical analysis

The data were analysed using IBM SPSS Statistics 24.0 software. The normality of the data from Experiment 1 was tested with a Kolmogorov-Smirnov test. When the data were not normally distributed, a non-parametric test (Krustal-Wallis test) was used to determine the differences in the recovery of VFOC between the samples and contaminants. One-way ANOVA was used to assess whether the nature of biochar significantly affects the recovery of the contaminants (after confirmation of the normal distribution of the data). A post hoc Bonferroni test was used to compare the sorption behaviour of biochar samples (again after confirmation that the data were normally distributed). Pearson correlation analysis was used to compare the FO and BTEX recovery and biochar properties in all the samples. Principal component analysis (PCA) was applied using CANOCO 4.5 software (Ter Braak & Šmilauer, 2002), to correlate the sorption capacity determined in Experiment 2 with the physico-chemical characteristics of the biochar samples. A significance level of $p< 0.05$ was applied in all statistical analyses.

RESULTS

Recovery of BTEX and FO from biochar and PCM (Experiment 1)

HS-GC-MS analytical data were used to compare the recovery of the amounts of pollutants not sorbed by the biochar samples. An example of the chromatograms obtained is shown in Figure 6.5, where peaks corresponding to the different pollutants present are clearly distinguished. The recovery from each sample varied widely.

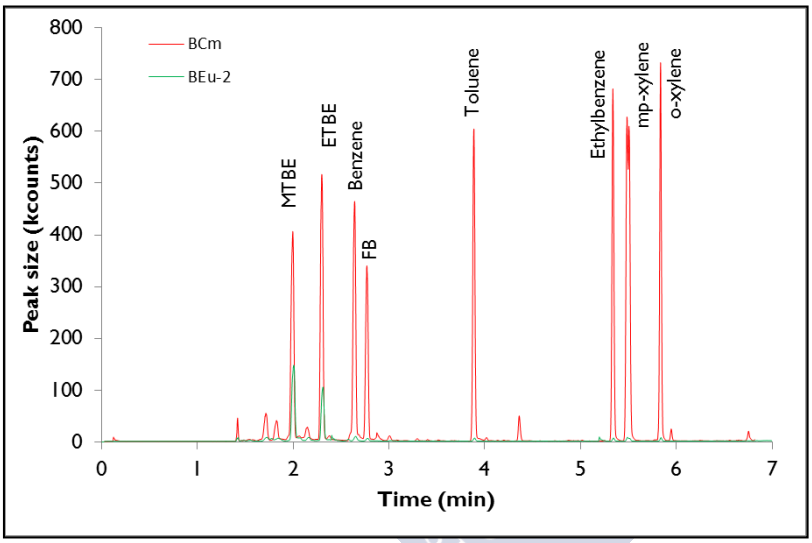

Figure 6.5 HS-GC-MS chromatogram of eucalyptus biochar (green) and chicken manure biochar (red) obtained in Experiment 1. The peaks correspond to FO, BTEX and FB.

HS-GC-MS data for Experiment 1 are shown in Figure 6.6, and are expressed as the percentages of ∑BTEX and ∑FO recovered in solution from the total amount initially spiked in the system. Significantly more FO than BTEX were recovered from all samples ($p < 0.05$). Recovery of ∑FO varied from 4 to 39 mg kg^{-1}, while that of ∑BTEX ranged between 0.14 and 54 mg kg^{-1} (the initial spiking concentration was 40 mg kg^{-1} for ∑FO and 120 mg kg^{-1} for ∑BTEX). Recovery of ∑FO was maximal in systems containing PCM ($H/C_{org} > 0.7$), i.e. BSd-1 (97% from the total spiked),

followed by BAcHw-2 and BCm (~73%). By contrast, recovery of ∑FO was lowest in BEu-2 and BCc-1 (indicating the higher sorption capacities of these), with 10 and 13 % recovery of the initial amount of FO spiked, respectively. Regarding ∑BTEX, BCm showed the lowest sorption potential (recovery of 45% of the total BTEX spiked), whereas BEu-2 and BCc-2 showed the highest sorption capacity (0.1 and 0.9% recovery, respectively). The recovery of all contaminants from BEu-2 was significantly lower ($p < 0.05$) than from all biochars produced at low temperature (HHT ≤ 400 °C), such as all acacia samples, BEu-1, BOpc and BCm.

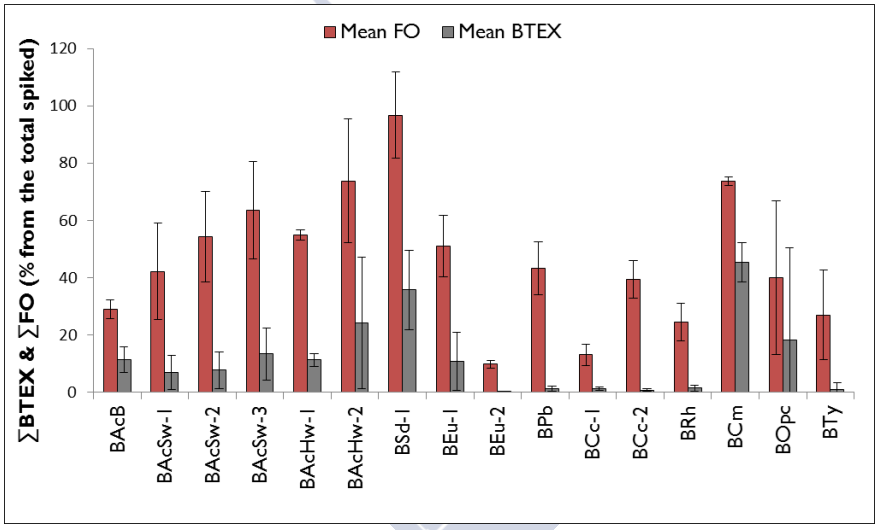

Figure 6.6 Amount of ∑BTEX and ∑FO recovered from the slurry of each type of biochar, after HS-GC-MS analysis for an initial spiked concentration of 100 mg kg^{-1}. The results are expressed as means (bars) ± the standard deviation (whiskers) (n=3).

Individual comparison of each contaminant revealed a relatively high recovery of MTBE. The recovery was highest in systems containing BAcHw-2 and BCm (~77.5%) (Figure 6.7A) and lowest in BEu-2 (~ 12.3%). The degree of recovery for MTBE and ETBE was not significantly different ($p > 0.05$). However, the difference between the recovery of each of these and each BTEX contaminant was statistically significant ($p < 0.05$). Nevertheless,

differences between recovery of the BTEX compounds were not significant ($p > 0.05$) (Figure 6.7B).

Pearson's correlation analysis was used to determine the relationship between the adsorption of organic compounds (BTEX and FO) and biochar properties (Table 6.2). The recovery of BTEX and FO was inversely correlated with the highest heating temperature (HHT) ($p < 0.01$), indicating that sorption capacity increased substantially with increasing HHT. The degree of recovery (of both BTEX and FO) was closely and positively correlated ($p < 0.01$) with H/C_{org} ratio and volatile matter (VM). In this case, the sorption decreased as H/C_{org} and VM increased. In general, the biochar properties had a greater effect on BTEX sorption than FO sorption. Although biochar pH was correlated with FO sorption ($p < 0.01$), it did not significantly affect the BTEX sorption. BTEX sorption was positively correlated ($p < 0.01$) with stable carbon forms (C_{nox} and FixC), which in turn are good indicators of the aromaticity of biochar samples. On the other hand, the recovery of BTEX increased significantly with the content of easily oxidisable C forms ($p < 0.05$).

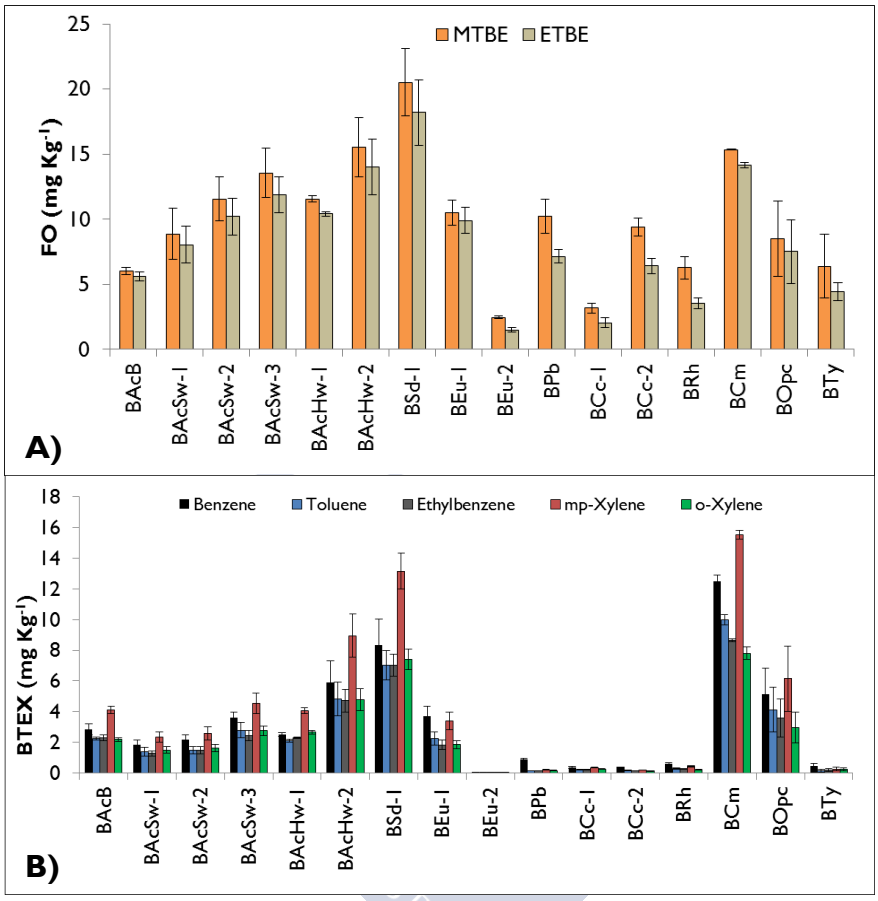

Figure 6.7 Recovery of (A) the individual FO compounds (MTBE and ETBE) and (B) BTEX compounds (benzene, toluene, ethylbenzene, *mp*-xylene and *o*-xylene) in the presence of different pyrolysed materials. Results are expressed as the mean recovery of BTEX or FO mg kg^{-1} ± standard deviation (n = 3).

Table 6.2 Pearson's correlation coefficients for the comparison between ∑BTEX and ∑FO recovery and main properties of all biochar and PCM samples.

	HHT	∑FO	∑BTEX	C	N	H	O/C_{Org}	H/C_{Org}	pH	VM	Ash	FixC	C_{EasyOx}	Cnox	Cp
HHT	1														
FO	-.626**	1													
BTEX	-.797**	.808**	1												
C	.390	-.152	-.531*	1											
N	-.350	-.007	.434	-.668**	1										
H	-.751**	.683**	.570*	.047	-.031	1									
O/C_{Org}	-.515*	.353	.565*	-.686**	.547*	.339	1								
H/C_{Org}	-.897**	.678**	.886**	-.553*	.486	.736**	.633**	1							
pH	.509*	-.641**	-.467	-.049	.039	-.824**	-.227	-.571*	1						
VM	-.859**	.734**	.740**	-.181	.148	.940**	.542*	.858**	-.800**	1					
Ash	.052	-.170	.186	-.875**	.571*	-.503*	.386	.133	.417	-.306	1				
FixC	.619*	-.393	-.733**	.944**	-.655**	-.257	-.771**	-.779**	.229	-.486	-.683**	1			
C_{EasyOx}	-.383	.598*	.535*	-.081	-.094	.669**	.258	.566*	-.631**	.656**	-.194	-.313	1		
Cnox	.647**	-.404	-.636**	.707**	-.273	-.448	-.576*	-.696**	.404	-.618*	-.377	.822**	-.531*	1	
Cp	-.521*	.299	.689**	-.693**	.641**	.075	.376	.694**	.028	.262	.577*	-.726**	.155	-.418	1

** Correlation significance at level p < 0,01

* Correlation significance at level p < 0,05

BTEX sorption isotherms (Experiment 2)

After preliminary assessment of the general sorption capacities of a wide variety of biochars (Experiment 1), four of the biochars (i.e. BEu-2, BCc-2, BAcB and BCm) were selected for detailed study of their sorption capacities. This experiment confirmed the low capacity of biochar to retain MTBE, ETBE and benzene. The four biochars tested only sorbed these pollutants at the first three or four spiking concentrations tested (2, 15, 30, 60 mg L^{-1}) (Figure S C.2 in the Supporting Information), making it impossible to simulate the data with any empirical model. MTBE was the least well sorbed pollutant: the biochars sorbed between 1 and 60% of this compound present at low concentrations (≤ 30 mg L^{-1}). BCm displayed the highest sorption capacity for this compound (0.386 g kg^{-1} from an initial spiking concentration of 30 mg L^{-1}). Considering ETBE, BEu-2 retained 90% of this compound present at the lowest initial spiking concentration (2 mg L^{-1}), but BAcB showed the highest sorption capacity (0.837 g kg^{-1} were retained from an initial spiking concentration of 30 mg L^{-1}). Finally, considering benzene, BEu-2 sorbed 80 % of the compound present at a relatively low concentration (≤ 60 mg L^{-1}), whereas BCm immobilised ~50% of the initial amount.

Hence, the fitting of the sorption models was evaluated for toluene, ethylbenzene and xylene isomers. The experimental data reflected multilayer sorption behaviour; an example can be seen in Figure 6.8, in which the concentration of toluene sorbed, q_e (g kg^{-1}), was plotted against the equilibrium concentration in aqueous solution, C_e (mg L^{-1}), for the four biochars studied. Initially, in the first layer, BTEX were sorbed to the surface of biochars, until surface saturation was achieved. The subsequent appearance of a second sorption layer may be attributed to the interaction between layers of organic compounds following surface saturation, due to their hydrophobic nature (Limousin et al., 2007; Sposito, 1984; Breus & Mishchenko, 2006). Although differences in sorption between materials

were observed in the first layer, these differences were minimised in the second layer.

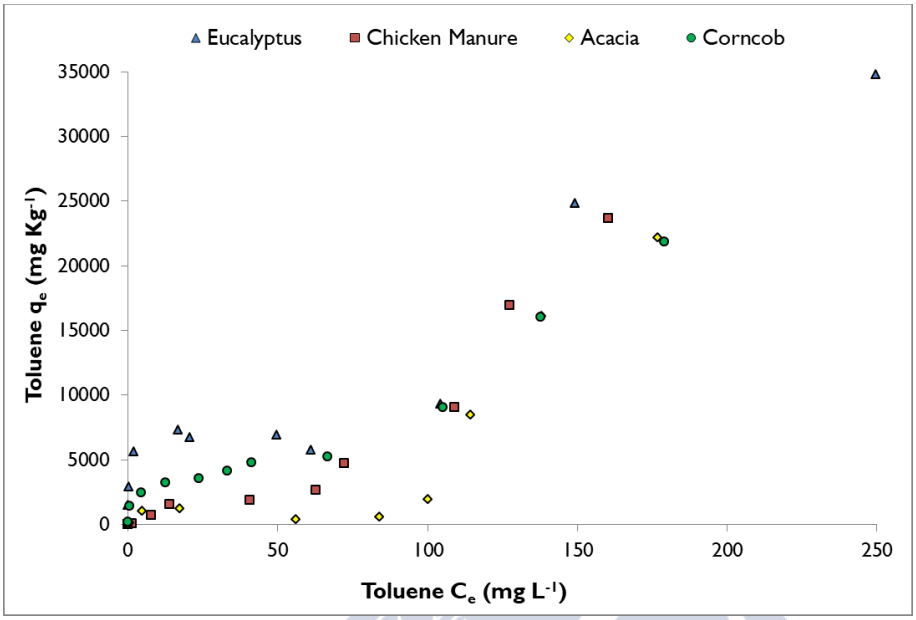

Figure 6.8 Experimental results for toluene sorption on the different biochars. Data are expressed as the average concentration for the three replicates (with standard deviations varying between 0.00001-39.79 for C_e and 0.002-4.04 for q_e).

Accordingly, the fitting of the empirical sorption models was conducted considering only the first layer, which involved the biochar surface. Langmuir and Freundlich isotherms were fitted to the experimental data for each sorbent, and the fitting model parameters and their corresponding errors are shown in Table 6.3. The Langmuir model provided the best fit to the experimental data (Figure 6.9 and Figure 6.10). This is supported by the higher correlation coefficients (R^2) and the lower reduced chi-square values (χ^2) obtained for the Langmuir model, which ranged from 0.72 to 0.98 and from 0.05 to 1.47, respectively. R^2 values for the Freundlich model ranged between 0.46 and 0.95, while χ^2 ranged between 0.09 and 3.46. For the five contaminants studied, the Langmuir model provided the best description of

the eucalyptus biochar (BEu-2) performance, and the poorest description for acacia bark biochar (BAcB), especially with *o*-xylene (R^2 = 0.72). However, the sorption of toluene, ethylbenzene and xylenes on corncob biochar (BCc-2) was best described by the Freundlich model.

Comparing the different sorbent materials, BEu-2 yielded the highest Q_{max} value for all the organic compounds studied, followed by BCc-2, BCm and BAcB (Table 6.3). The Langmuir constant, K_L, varied from 0.02-0.05 for all the organic pollutants on BCm to ~6 for *o*-xylene sorption on BEu-2. This constant is related to binding strength, indicating a lower affinity of the organics pollutants for BCm. The value of K_L varied depending on the physico-chemical properties of the pollutant (Table S C.1), following the general trend ethylbenzene > *o*-xylene > toluene > *mp*-xylene.

For the Freundlich model, n ranged from ~1.4-1.7 for BCm, to values higher than 5 for BEu-2. The constant 1/n was below the unit in all cases, resulting in a downward-curved isotherm (L-type isotherm) and indicating less competition for sorption sites and a decrease in sorption energy with increasing surface concentration (Site, 2001). The 1/n value was highest for BCm and lowest for BEu-2 (0.71 and 0.17, respectively), indicating a reduction in linearity to strong non-linearity. Regarding the Freundlich constant, K_F, the highest values were obtained for BEu-2 and BCc-2, which is consistent with the results obtained for the Langmuir constant and reflects the higher sorption capacity of these samples. The K_F values followed a trend depending on the organic pollutants and biochar type, which was ethylbenzene > toluene > *mp*-xylene > *o*-xylene in BCc-2 and BEu-2 biochars; however K_F value for *o*-xylene was higher than that for *mp*-xylene in the BCm and BAcB PCMs.

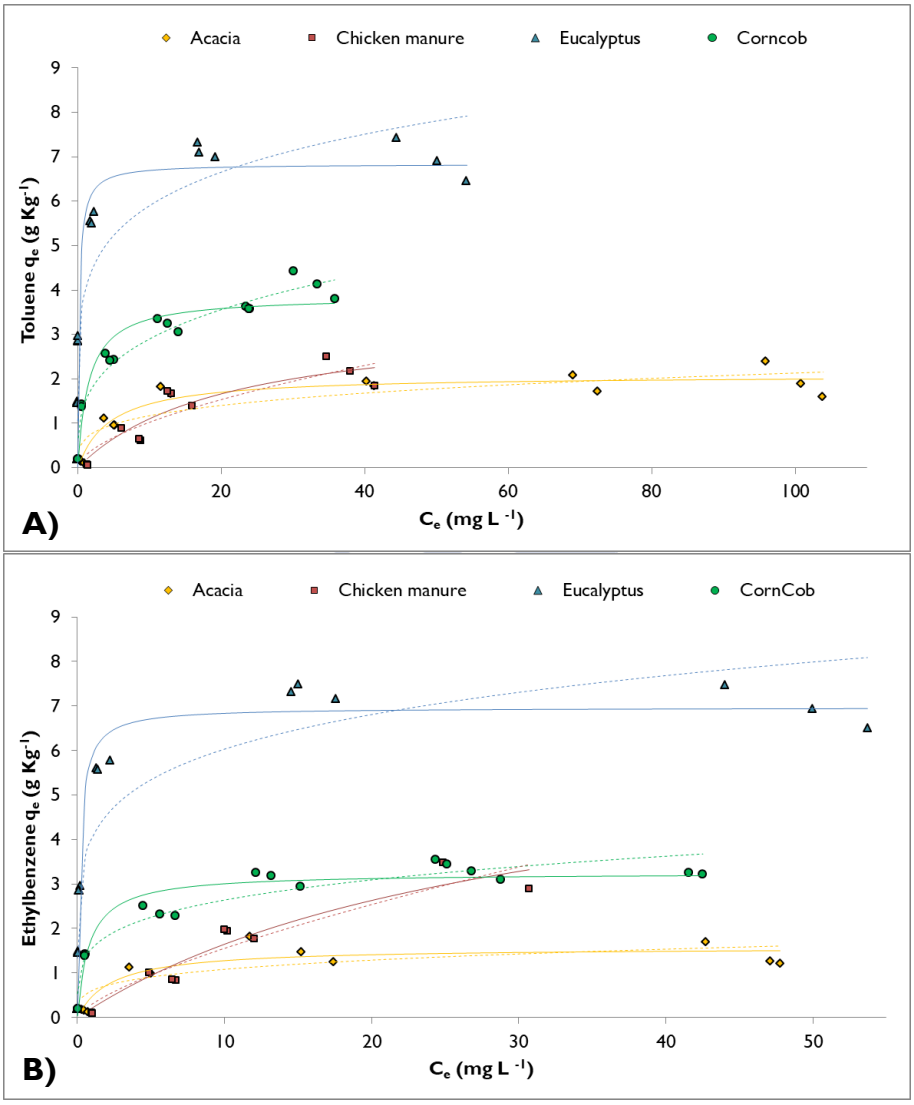

Figure 6.9 Sorption isotherms for (A) Toluene and (B) Ethylbenzene for the four biochars. Experimental data are represented by symbols. The solid lines represent the fitting of the Langmuir model and the dashed lines the fitting of the Freundlich model.

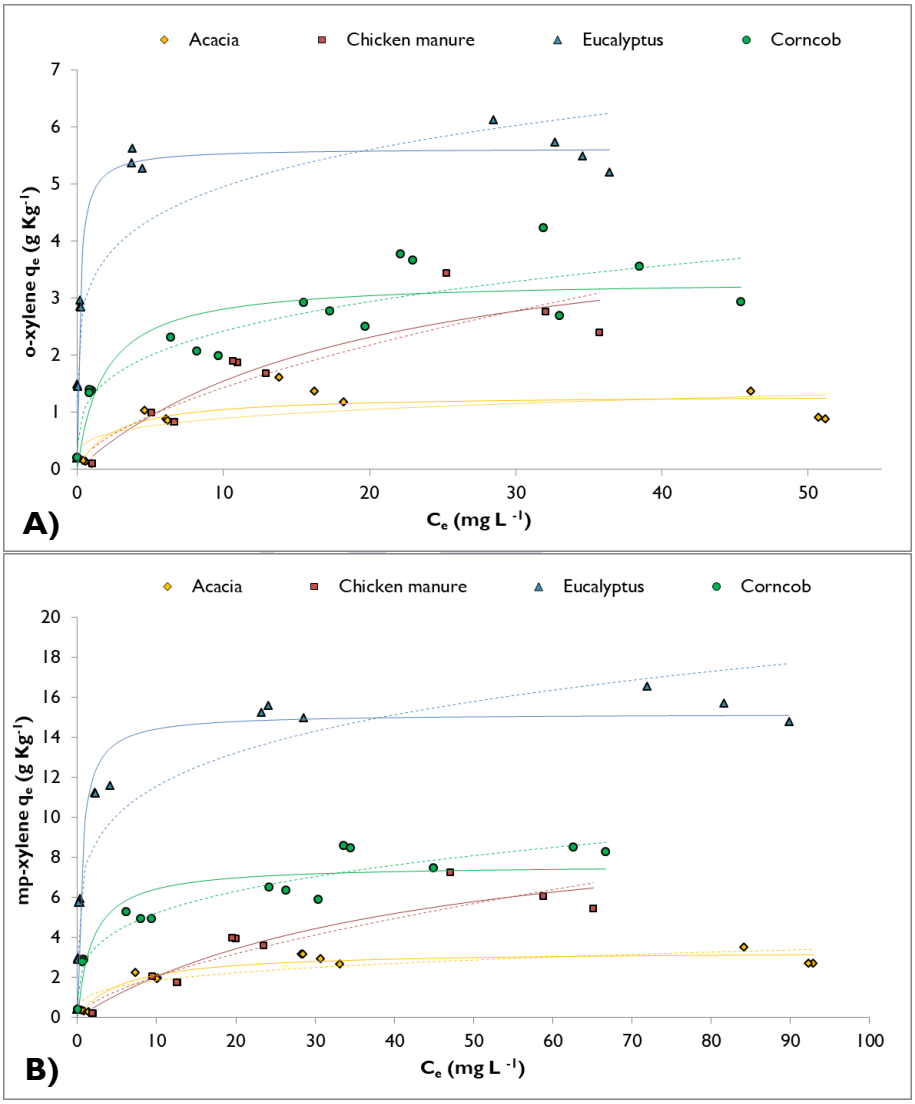

Figure 6.10 Sorption isotherms for (A) *o*-xylene and (B) *mp*-xylene for the four biochars. Experimental data are represented by symbols; solid and dashed lines to the fitting to the Langmuir and Freundlich models, respectively.

Table 6.3 Comparison of Langmuir and Freundlich model parameters for the different adsorbates studied (corncob and eucalyptus biochar and acacia bark and chicken manure PCM).

Adsorbate	Langmuir Model				Statistics		Freundlich Model				Statistics	
	Q_{max} (g kg^{-1})		K_L (L mg^{-1})		χ^2	R^2	K_F (g $L^{1/n}$ $mg^{-1/n}$ kg^{-1})		n		χ^2	R^2
Corncob												
Toluene	3.86	± 0.16	0.65	± 0.16	0.1237	0.9361	1.47	± 0.11	3.38	± 0.29	0.0975	0.9496
Ethylbenzene	3.25	± 0.10	1.24	± 0.27	0.0747	0.9472	1.56	± 0.11	4.37	± 0.47	0.0995	0.9297
mp-Xylene	7.63	± 0.40	0.53	± 0.19	0.9159	0.8925	2.79	± 0.26	3.68	± 0.37	0.4890	0.9426
o-xylene	3.32	± 0.23	0.55	± 0.23	0.2651	0.8294	1.27	± 0.18	3.57	± 0.59	0.2205	0.8581
Eucaliptus												
Toluene	6.84	± 0.18	4.66	± 0.77	0.2387	0.9687	3.95	± 0.25	5.75	± 0.65	0.7164	0.9062
Ethylbenzene	6.97	± 0.20	5.28	± 0.92	0.2719	0.9657	4.03	± 0.29	5.72	± 0.73	1.0040	0.8732
mp-xylene	15.18	± 0.48	1.88	± 0.36	1.4727	0.9602	7.40	± 0.56	5.16	± 0.56	3.4643	0.9063
o-xylene	5.62	± 0.14	5.70	± 0.76	0.1129	0.9775	3.28	± 0.26	5.60	± 0.81	0.7332	0.8538
Chicken Manure												
Toluene	3.38	± 0.74	0.05	± 0.02	0.1009	0.8642	0.27	± 0.10	1.71	± 0.34	0.1346	0.8189
Ethylbenzene	6.52	± 1.78	0.03	± 0.01	0.1013	0.9230	0.30	± 0.09	1.41	± 0.21	0.1336	0.8984
mp-xylene	10.64	± 2.37	0.02	± 0.01	0.5609	0.9015	0.48	± 0.19	1.58	± 0.27	0.7727	0.8643
o-xylene	4.60	± 1.04	0.05	± 0.02	0.1482	0.8790	0.36	± 0.13	1.65	± 0.32	0.2044	0.8331
Acacia												
Toluene	2.08	± 0.11	0.22	± 0.06	0.0522	0.9065	0.64	± 0.14	3.85	± 0.80	0.1359	0.7567
Ethylbenzene	1.57	± 0.14	0.43	± 0.19	0.0582	0.8287	0.61	± 0.15	3.97	± 1.24	0.1316	0.6128
mp-Xylene	3.33	± 0.21	0.18	± 0.05	0.1108	0.9151	0.98	± 0.24	3.64	± 0.85	0.3410	0.7386
o-xylene	1.31	± 0.15	0.40	± 0.24	0.0704	0.7232	0.52	± 0.16	4.31	± 1.78	0.1368	0.4620

Principal Components Analysis (PCA) was applied to the Langmuir and Freundlich parameters obtained for toluene and the physico-chemical properties of the biochars used as sorbent material. The first 3 principal components accounted for 100% of the total variability in the physico-chemical properties, with PC1 and PC2 accounting for 70.9% and 25.0%, respectively (Figure 6.11). As expected, the samples were dispersed through the score plot, as they were produced from different feedstock material and were characterised by different physico-chemical properties. Otherwise, biochar samples can be separated into those produced at a low highest heating temperature (HHT ≤ 400 °C), plotted in the negative area of PC1, and those produced over 400 °C, in the positive area. Biochars were plotted from the negative to the positive PC1 area according to the sorption capacity and aromaticity following the order BCm < BAcB < BCc-2 < BEu-2. Properties related to biochar aromaticity, such as H/C_{org}, total C and C_{nox}, as well as the Freundlich parameters scored mainly in component 1. The presence of a narrow angle between SSA, Langmuir parameters and Freundlich constant indicated that these factors were closely correlated, while n was more closely correlated with biochar aromaticity and hydrophobicity, showing a narrow angle with C_{nox} and an inverse correlation with H/C_{org}, O/C_{org} and (O+N)/C ratios (located in the opposite quadrant). The correlation between K_F and H/C_{org} was highest for toluene (R^2 = 0.87) and lowest for *o*-xylene (R^2 = 0.76), which is the least volatile organic compound (boiling point 144.5 °C). PCA of the data on the other contaminants produced similar results and correlations as for toluene (data not shown).

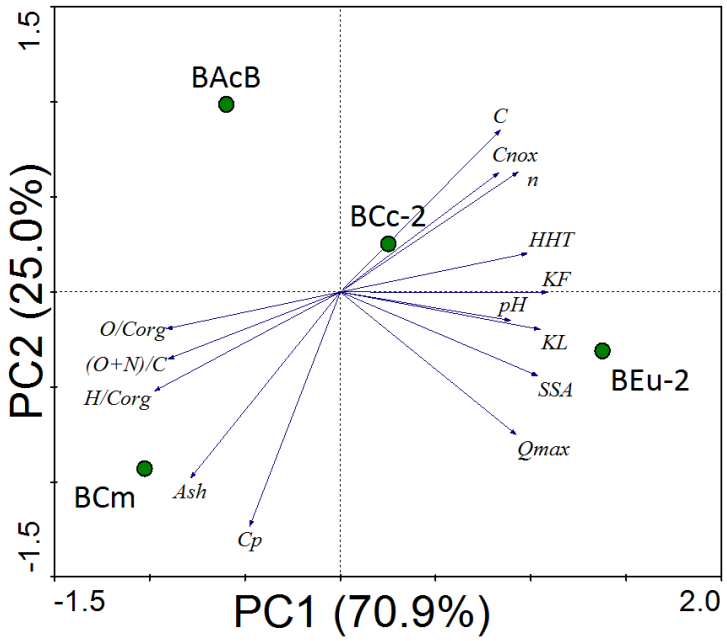

Figure 6.11 Principal Components Analysis (PCA) score plot for the Langmuir and Freundlich parameters for toluene and biochar properties.

Diesel adsorption isotherms (Experiment 3)

The capacity of eucalyptus and corncob biochars (BEu-2 and BCc-2) to retain TPH was assessed, as these biochars showed the highest capacity to sorb BTEX. The TPH content at each equilibrium concentration (Ce) was calculated as the total ion count, by integrating the whole peak area obtained in the chromatogram. An example of a chromatogram is shown for eucalyptus in Figure 6.12.

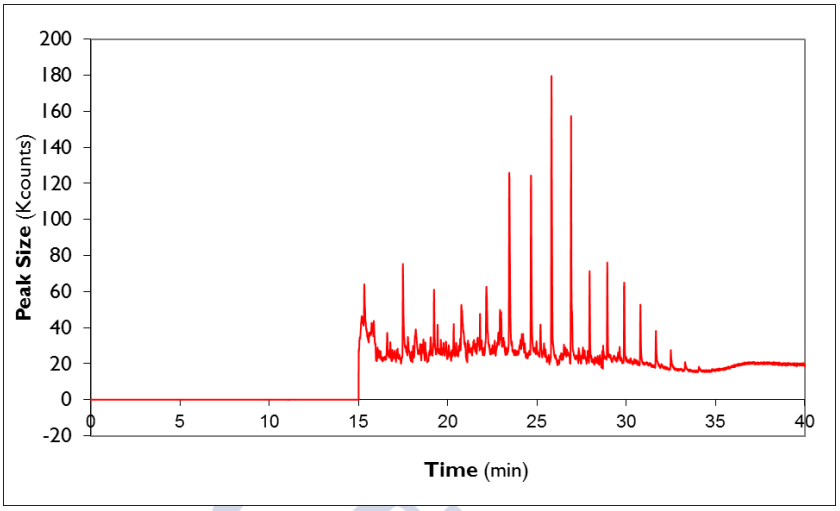

Figure 6.12 GC-MS chromatograph for TPH sorption on eucalyptus biochar (BEu-2) for an initial spiking concentration of diesel of 480 mg L^{-1}.

Experimental data of the sorption of diesel onto BCc-2 and BEu-2 biochars along with the fits for the adsorption isotherm models are shown in Figure 6.13. In this case, only one sorption layer was observed and all experimental data points were considered when fitting the isotherm models. The Freundlich or Langmuir models provided similar fits, although there were slight variations in the R^2 and χ^2 coefficients. The Freundlich isotherms better represented the sorption capacity of BEu-2, whereas the Langmuir isotherm better described that of the BCc-2 biochar. As for BTEX, eucalyptus biochar showed a higher capacity to sorb diesel than corncob biochar. The Q_{max} and K_F values for BEu-2 were almost three times higher than those for BCc-2 (Table 6.4). On the other hand, the n values were similar for both materials, with $1/n < 1$, indicating that both biochars were capable of adsorbing diesel. By contrast, the K_L values were low for both BCc-2 and BEu-2, indicating weak binding strength.

Table 6.4 Langmuir and Freundlich model parameters for TPH sorption by eucalyptus (BEu-2) and corncob (BCc-2) biochars.

	Value	Error	Value	Error	Statistics	
Langmuir	Q_{max} (g kg^{-1})		K_L (L mg^{-1})		χ^2	R^2
BEu-2	180.38 ±	19.76	0.008 ±	0.002	52.56	0.941
BCc-2	62.44 ±	13.53	0.006 ±	0.003	50.10	0.749
Freundlich	K_F (g kg^{-1}) (L mg^{-1})		**n**		χ^2	R^2
BEu-2	3.57 ±	0.49	1.48 ±	0.07	44.19	0.951
BCc-2	1.27 ±	0.62	1.59 ±	0.24	53.11	0.733

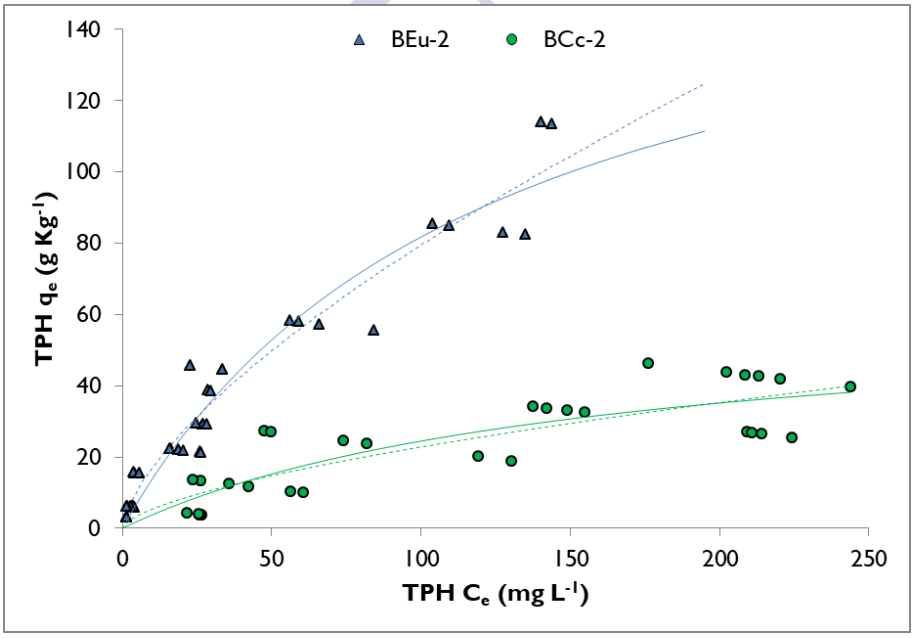

Figure 6.13 TPH adsorption isotherms on eucalyptus biochar (BEu-2 in blue) and corncob biochar (BCc-2 in green). Solid and dashed lines represent the fitting of the Langmuir and Freundlich models, respectively.

DISCUSSION

Effect of contaminant properties on sorption by biochar

The general capacity of different carbonaceous materials to immobilise volatile compounds, BTEX and FO, was assessed. The results varied widely depending on the properties of the organic compounds and the sorbent matrix, which in turn was strongly affected by the feedstock material (Zhang et al., 2015) and the pyrolysis conditions (Bornemann et al., 2007). Overall ∑BTEX and ∑FO sorption differed significantly, with higher recovery of the FO compounds in all the samples. This may be related to the nature and physico-chemical properties of the contaminants (Table S C.1 in the Supporting information). Fuel oxygenate compounds are the most volatile (boiling points of MTBE and ETBE are 55 and 69 °C, respectively), highly soluble in soluble in water (solubility of MTBE and ETBE in water at 25 °C are 51.6 and 26 g L^{-1}, respectively, and for BTEX between 0.14 and 1.80 g L^{-1}), and highly hydrophilic (based on their octanol-water coefficient log values of 1.06 and 1.48 for MTBE and ETBE, respectively). The higher solubility and volatility of FO compounds is related to a higher degree of mobility in soils and aqueous systems (Balseiro-Romero, 2014). Similarly, the recovery of benzene and xylene isomers varied significantly, and the degree of recovery increased according to the volatility of the organic compound (BTEX volatility varied in the order benzene > toluene > ethylbenzene > *mp*-xylene > *o*-xylene (Table S C.1). Biochar materials tend to be hydrophobic and non-polar, and thus BTEX molecules displayed a higher affinity for these materials: non-polar compounds tend to be attracted by non-polar phases (Goss & Schwarzenbach, 2003). The FO compounds thus showed a lower affinity for biochar materials and were poorly sorbed by biochar. In a study of the sorption of BTEX and MTBE onto thermally modified diatomite Aivalioti et al. (2010) also observed differences between adsorbates, with higher sorption for BTEX, especially xylenes, than for MTBE. Xiao et al. (2014) attributed the lower adsorption of MTBE than of benzene to differences in

the kinetic diameter. The molecular size of MTBE is 0.62 nm (Sano et al., 1995), while for benzene it is ~ 0.35 nm (Xiao et al., 2014). Therefore, benzene may be strongly sorbed onto biochar micropores as a result of a pore-filling mechanism.

Influence of biochar characteristics on the sorption of organic compounds

Recovery of the contaminants varied widely depending on the biochar, ranging from 2 to 53%, reflecting the contribution of different sorption mechanisms depending on the physico-chemical properties of the sorbents. Several authors have established that the sorption of organic compounds onto biochar is mainly governed by two processes: adsorption onto carbonised fractions and partition into non-carbonised fractions (Zhang et al., 2017; Zhang & Lu, 2015; Chen et al., 2008). The sorption forces that determine the interaction between biochar surfaces and organic pollutants are ionic electrostatic attraction, hydrogen bonding, hydrophobic interaction and π-π electron–donor–acceptor interaction (π-π EDA) (Zhang & Lu, 2015; Sander & Pignatello, 2005). The latter is related to the observed increase in the aromaticity of the studied biochars with the increase in pyrolysis temperature, which may favour the formation of a graphene-like surface. These structures are capable of interacting with both electron donors and electron acceptors (Sun et al., 2012). The results obtained in Experiment 1 showed that BTEX and FO sorption are directly correlated with pyrolysis temperature (Table 6.2). A significantly lower recovery was found for biochars produced at high temperatures (HHT >400 °C), such as BEu-2 and BCc. This may be due to the loss of O- and H-containing functional groups with increasing temperature, which is reflected in biochar with a less polar character and higher degree of aromaticity (Ahmad et al., 2014; Uchimiya et al., 2011; Antal & Gronli, 2003). Moreover, the recovery of BTEX from PCMs increased with the O/C molar ratio, which is an indicative of higher surface hydrophilicity (Chun et al., 2004). On the other hand, the low O/C values in biochar (O/C < 0.1) are indicative of surface

water repellency and similar behaviour to that observed for active carbon. These biochars therefore displayed greater attraction for hydrophobic compounds such as BTEX. This is also in consistent with the (O+N)/C ratio, which is an indicator of polarity (Xiao et al., 2014) and decreases with increasing pyrolysis temperature. The sorption rates associated with the biochars under study increased as the (O+N)/C ratio decreased.

In addition to the pyrolysis conditions and physico-chemical characteristics of the contaminant, sorption process will be affected by the feedstock material used to prepare the biochars. The recovery of BTEX and FO was highest from materials rich in ash and inorganic compounds, such as BCm, BOpc and BAcB. The hydrophilic character of the samples is increased by a high proportion of inorganic compounds (caused by the nature of these particles), thus decreasing the sorption of hydrophobic compounds (Bornemann et al., 2007). Other authors have observed that the biochar mineral content has an indirect effect on the sorption capacity of organic compounds, as the mineral fraction also affects the formation of aromatic structures during pyrolysis (Smernik, 2009). This was also observed by Balseiro-Romero & Monterroso (2013) in a study of the sorption of BTEX and FO on different soil samples, with lower sorption levels in soils containing higher concentrations of inorganic elements. Differences in the sorption capacity of eucalyptus and corncob biochars, which were pyrolysed at a similar temperature (~500 °C), were observed, possibly due to the feedstock composition (Zhao et al., 2013) and to the large difference in SSA. The aromatic carbon content is often associated with lignin content. Eucalyptus is richer in lignin as the hardwood has about 35% of lignin (Anderson & Tillmann, 1977), while the content in corncob is ~12% (Pointner et al., 2014). Furthermore, determination of the water holding capacity of the eucalyptus biochar revealed the high hydrophobicity of this biochar (Chapter 5), which also explained the strong interaction with hydrophobic organic compounds.

Variability in the isotherm parameters

The sorption isotherms for BTEX and FO confirmed the competition among the different pollutants for these pyrolysed materials. The compounds with a more polar and hydrophilic nature, i.e. ETBE, MTBE and benzene, were less well retained on biochar. It is noteworthy that despite the significantly higher hydrophobicity of ethylbenzene and xylenes than of toluene (K_{OW} = 1412.5 for ethylbenzene, *o*-xylene and *p*-xylene; K_{OW} = 1584.9 for *m*-xylene; K_{OW} = 489.8 for toluene), the Q_{max} was in the same order of magnitude for all the adsorbates. Similar results were obtained by Bornemann et al. (2007) for adsorption of toluene and benzene onto different wood-derived biochars. This behaviour was attributed to a pore filling mechanism, so that when an identical volume of the sorbates is added into the system, sorption of these compounds onto the biochar may be similar (Bornemann et al., 2007; Chiou et al., 2000).

Traditional Langmuir and Freundlich models were adequate for detecting general differences in the sorption of volatile organic compounds (BTEX and FO) and TPHs by different biochars. Sorption of BTEX on three of the four sorbent materials studied was described by the Langmuir model (BEu-2, BCm and BAcB), although the fit was less accurate for BCm and BAcB (lower R^2 values than for BEu-2). This may be because these biochars were less homogeneous, i.e. the feedstock material was a mixture of different compounds such as feathers, proteins, digested food, bedding material and minerals in the case of BCm. By contrast, BTEX sorption on corncob biochar exhibited Freundlich sorption behaviour. Bornemann et al. (2007) obtained different fits to Langmuir and Freundlich models depending on the characteristics of the biochar used. Nevertheless, each model contributed with relevant information for helping to understand the sorption process; e.g. the Langmuir model is useful for determining the maximum sorption capacity (Q_{max}), thus enabling the comparison of the biochars studied and helping in the selection of the best sorbent material. The values of Q_{max} obtained for the four biochars tested were four orders

of magnitude higher than those obtained for the same pollutants with diatomite as adsorbent (Aivalioti et al., 2010). Moreover, Q_{max} is highly correlated with the SSA of each biochar, which in turn is associated with the HHT and the aromatic character of biochar, e.g. larger surface areas in BEu-2 and BCc-2, samples which were pyrolysed at temperatures above 400 °C. Both samples showed a higher degree of aromaticity and lower degree of polarity and hydrophilicity than BCm and BAcB, as reflected by the molar ratios of H/C, (O+N)/C and O/C, which resulted in a higher sorption capacity. This is consistent with the finding reported by Xiao et al. (2014). Comparison of the Q_{max} values of BCc-2 and BEu-2 for BTEX and TPH reveals that the sorption capacity was found highest for TPH, although it must be taken into account that multilayer sorption was observed for BTEX and not all data were considered in the fitting. By contrast, the K_L values indicated a lower binding strength for TPH, probably due to the complexity of diesel and the competition of the different components for sorption sites.

Finally, information about the linearity of the sorption process was obtained from the Freundlich model fit. The 1/n parameter decreased following the sequence BCm > BCc-2 > BAcB > BEu-2, indicating a higher degree of non-linearity and a sorption mechanism based on adsorption onto carbonised material porous in the latter three biochars (Chen et al., 2008; Lattao et al., 2014). BCm showed 1/n values close to 0.7, indicating a more linear behaviour than the other samples and therefore some partitioning into the non-carbonised parts of the sample (Lattao et al., 2014). This is consistent with the HHT estimated by NIRS for this sample (Chapter 3), which was the lowest of all the biochars studied, indicating that this sample was the richest in non-carbonised organic matter. Both Freundlich and Langmuir parameters were highly correlated with the H/C_{org} ratio, as shown in the PCA (Figure 6.11). The log K_F was correlated with H/C, as observed by Xiao et al. (2016) for naphthalene.

CONCLUSIONS

The study revealed that all the biochars tested can be considered low-cost sorbents for organic compounds, including both volatile organic contaminants and TPHs. As expected, not all biochars displayed the same sorption capacity, and the characteristics of the organic contaminant, the pyrolysis conditions (especially HHT) and the nature of the feedstock material were the main factors affecting the sorption capacity.

The most volatile and hydrophilic compounds, i.e. MTBE, ETBE and benzene, were poorly sorbed on biochar. Non-polar and hydrophobic compounds were more strongly sorbed. The results showed that biochar obtained at high pyrolysis temperatures (HHT > 400 °C), i.e. BEu-2, performed better for the removal of organic compounds from aqueous solution: sorption was favoured by higher aromatic carbon content and specific surface area. Other physico-chemical properties of the biochar related to the feedstock material, such as ash content, pH and nutrient content, also affected the sorption behaviour.

The sorption of fuel organic compounds on biochar reflected a multilayer mechanism and a relatively high sorption capacity of the biochar produced at high temperature (HHT > 400 °C). Langmuir and Freundlich models adequately described the experimental data and reveal general differences in the sorption behaviour of volatile organic compounds and TPHs by the different biochars. Biochars produced at low temperatures (HHT ≤ 400 °C), such as BCm, showed more linear sorption behaviour due to the presence of non-carbonised organic matter. In the case of TPH, the Freundlich model best described the sorption on BEu-2, whereas the Langmuir model did so for sorption on BCc-2.

7. Potential use of biochar in the silicon industry

USC
UNIVERSIDADE
DE SANTIAGO
DE COMPOSTELA

INTRODUCTION

The silicon and ferrosilicon production process

In the last few years, there has been an increase in technologies that require silicon for use in emerging applications (e.g. battery production, renewable energy and nanotechnology), thus intensifying the demand for high quality silicon. One of the areas in which the increase in demand for silicon has been greatest is the production of lithium-ion batteries, in which silicon replaces carbon and improves the characteristics of the batteries. These batteries are used extensively in mobile devices and laptops due to their extended operational autonomy; however, the forecasted increase in the use of electric vehicles will require batteries with higher capacity and sophisticated features. An overview of the Silicon carbide (SiC) market estimates that demand for SiC power devices will grow, generating over US$ 3000 million by 2025, predominantly caused by the expansion of hybrid/electric vehicles (Figure 7.1) (IHS Markit, 2016).

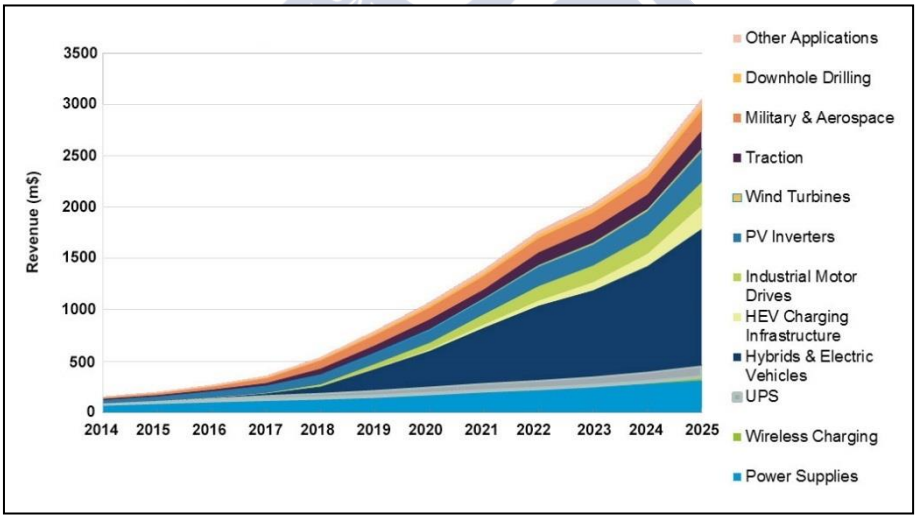

Figure 7.1 Silicon carbide (SiC) market forecast. Source: IHS Markit (2016).

The company Ferroatlántica S.A. (now Ferroglobe), located in the province of A Coruña, in Galicia (NW Spain), specialises in producing silicon metal and ferrosilicon for use as a raw material in the aluminium, steel and chemical industry. In 2008, this company implemented a new project to produce photovoltaic-grade silicon metal (Solar-Si), which requires greater purification of the final product (99.9999%). This is achieved by using metallurgical processes to purify the standard-quality silicon metal (purity of 99.00-99.99%). The feedstocks used to produce silicon are high purity quartz from the Serrabal mine (A Coruña), sub-bituminous coal, mainly from the Cerrejón mine (Colombia) (about 60000 tons per year), and wood, coming from several different countries, mostly from Latin America (around 60000 tons per year). Silicon production takes place in electric arc furnaces at high temperatures (around 2000 °C), and coal is used as a chemical reducing agent to transform silica. Spanish coal production has decreased in the past few decades (Figure 7.2), and most coal is now imported from overseas, thus increasing the carbon footprint associated with the long transport.

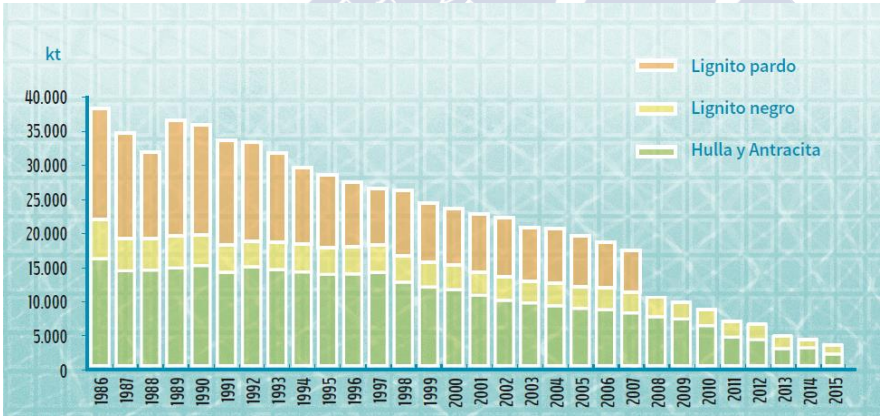

Figure 7.2 Changes in coal production in Spain between 1986 and 2015 (Carbunion, 2015).

The quality (i.e. purity) of silicon is highly dependent on the quality of the raw materials used, i.e. on the presence of low levels of aluminium,

titanium, phosphorus and other residual elements. Replacement of coal with charcoal or biochar produced from sustainable biomass obtained from Spanish forests would reduce CO_2 emissions by preventing the need for the material to be transported over long distances.

Galician forest characteristics

Spain has a woodland area of around 18.5 million ha, and a productive volume of more than 1000 million m^3 of wood, according to the results of the IV National Forestry Inventory (IFN4) reported by the Spanish "Ministerio de Agricultura y Pesca, Alimentación y Medio Ambiente" (MAPAMA). The Galician forestry sector is the ninth most important in Europe and leads the sector at a national level (Confemadera Galicia & UVigo, 2015). Almost 70% of the total area of the region (around 2 million ha) is covered by forest, with more than 65% considered woodland (tree canopy cover fraction > 10%: MAPAMA, 2008) and the rest (600000 ha) considered unproductive land (scrubland, grassland, felled or open areas). Lugo and A Coruña have the largest areas of woodland in the region (Figure 7.3).

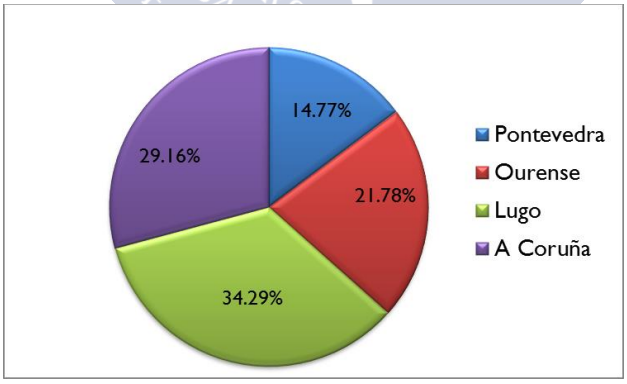

Figure 7.3 Distribution of woodland by province in Galicia. Data from IFN4.

Galician woodlands are mainly composed of pine trees (Figure 7.4), with a predominance of *Pinus pinaster*, the characteristic species in the Atlantic area, although the presence of *Pinus radiata* is increasing. These

species are followed in abundance by eucalyptus (*Eucalyptus globulus* and *Eucalyptus nitens*) and oak (*Quercus robur*).

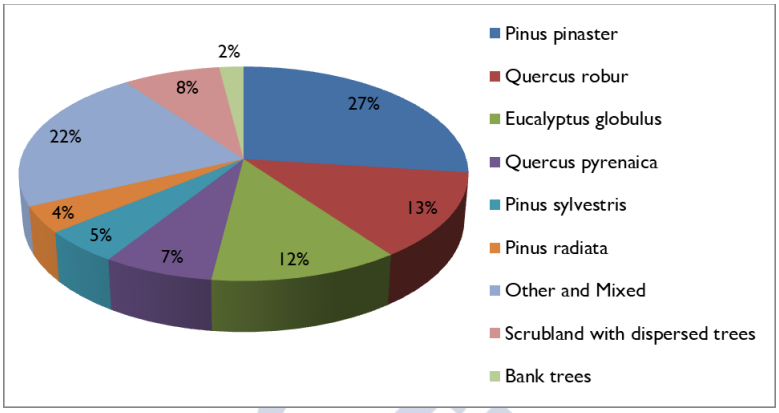

Figure 7.4 Relative abundance of the main forest species in Galicia (Carballo & Picos, 2009)

Galicia produces around 50% of the timber in Spain, although with only 7.6% of Spanish woodland (Miramontes, 2009). The forestry sector contributes 3.5% to the Gross Domestic Product (GDP) in Galicia, generating about 70000 jobs, considering direct and indirect employment (González Laxe, 2013). By contrast, the area considered unproductive (around 30%) is significantly higher than in other European forestry powers such as Finland or Sweden, where such areas cover between 10 and 20% of the land (González Laxe, 2013). Galician forest is characterised by a predominance of private ownership (68%), followed by around 30% of communal woodlands and only a small percentage of state-owned/public property (Miramontes, 2009). Each owner has on average 2 ha of land divided into different plots. The predominance of small privately owned properties, together with the geographically disperse and ageing population, and the phenomenon of rural exodus, has led to inadequate forest management. Thus, in some areas, pruning and clearing are not carried out, leading to a high risk (and occurrence) of wildfires and a reduction in forest productivity.

Another important aspect to be taken into account in forestry systems is the increasing spread of invasive plants, with *Acacia* spp. dominating in Galicia (Alberdi et al., 2012; Sanz et al., 2004). The most abundant allochthonous species in the region are *Acacia melanoxylon* and *Acacia dealbata* (Figure 7.5); the first is common in the provinces with Atlantic influence, while *Acacia dealbata* is found in some sites (5%) in Ourense (Alberdi et al., 2012). *Acacia* spp. are most abundant in the province Pontevedra and the increase in abundance of these species between the III and IV National Forestry Inventory (IFN3 and IFN4, respectively) was most notable in the province of A Coruña (Alberdi et al., 2012).

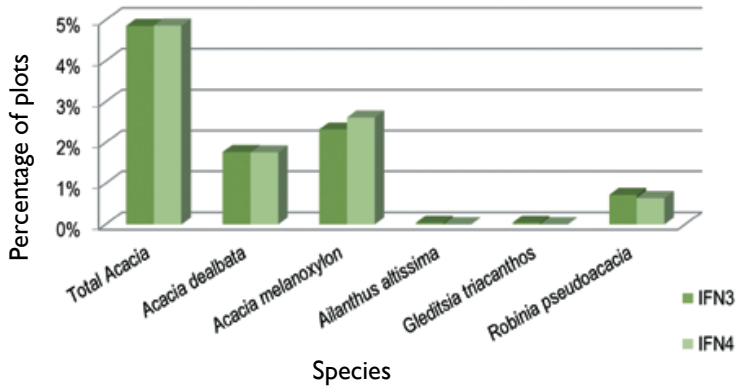

Figure 7.5 Change in the abundance of invasive species observed between the III and IV National Forestry Inventories (IFN3 and IFN4) in Galicia. Source: Alberdi et al. (2012).

Both of these species of Acacia are originally from Australia and were generally introduced in Europe as ornamental plants and, to a lesser extent, to stabilise sand dunes or slopes in civil engineering projects (Sanz et al., 2004). The high capacity of these species to adapt to different environments has led to their proliferation in Galicia and the north of Portugal, and the displacement of many autochthonous species. Invasion by these species causes a reduction in available light at inferior levels, alteration of soil nutrient content (C, P, NH_4^+, NO_3^-) and acidification, which ultimately affects soil microbial communities and enzymatic activities (Lorenzo &

Rodríguez-Echeverría, 2015; Lorenzo et al., 2016). Moreover, *Acacia dealbata* spreads more widely in pine forest than in scrublands (Rodríguez et al., 2017).

Invasive plants have many impacts on native ecosystems, displacing local species and directly and indirectly affecting biodiversity and ecosystem functions (Weidenhamer & Callaway, 2010). Their presence can lead to economic problems and health hazards (due to toxicity, allergies, etc.) (Liao et al., 2013), and it is therefore important to develop tools to minimise their proliferation. So far, numerous technologies and management systems have been used to reduce the expansion of invasive plants, including mechanical (burning, pruning), chemical (herbicides) and biological (competitive species) methods, not all of which have been successful. Pyrolysis of these plants to produce biochar before seeds germination is a potentially good method of reducing their expansion.

Objective

The general aim of the project led by Ferroatlántica S.A. was to improve the silicon production process to yield a high quality product (>99.99% purity) that fulfils the requirements of new technologies by using local resources, reducing the C footprint of the process and favouring a circular economy (Figure 7.6). The specific objective of the study reported in this chapter was to evaluate the potential use of biochar as an alternative to coal to produce high quality silicon. This would enable the replacement of a non-renewable feedstock, with a high contribution to global change, with a renewable form of carbon produced from local resources. Different biochars were characterised and evaluated in relation to the quality requirements for silicon production. The study mainly focused on the phosphorus forms present in the biochars, as the tetrahedral structure of P is similar to that of Si, which interferes with the crystallisation of silicon and reduces the purity of the final material. The concentrations of other elements (e.g. aluminium, iron, titanium), which can also generate impurities, were also determined.

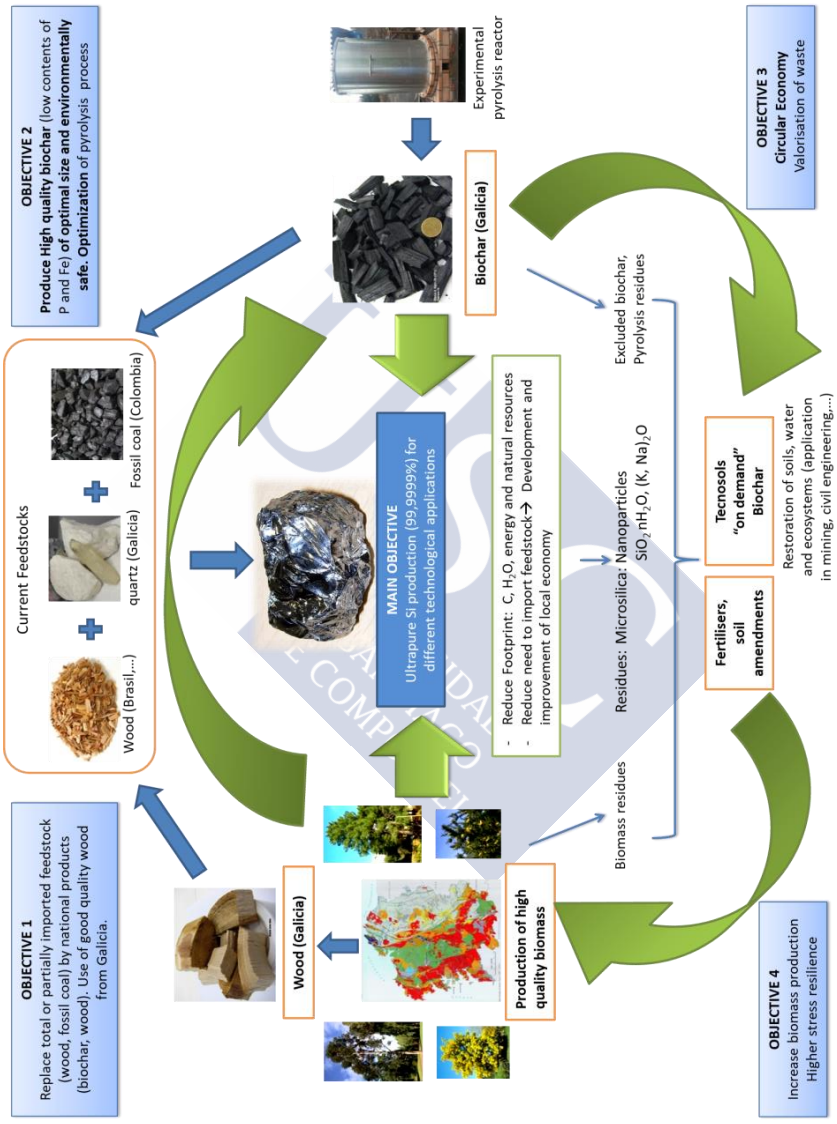

Figure 7.6 Summary of the objectives of the overall project. This chapter focuses on objective 2.

MATERIALS AND METHODS

Materials

Eight different carbonaceous materials were evaluated in this study as potential alternatives to coal:

i) sub-bituminous coal (hereinafter referred to as coal), as the material traditionally used in the silicon production process;

ii) five biochars produced in the LTA-USC experimental reactor: three *Acacia melanoxylon* samples, divided into bark, sapwood and heartwood (BAcB, BAcSw-1, BAcHw-1, respectively), eucalyptus branches (BEu-1) and pine sawdust (BSd-1). These biochars were selected for the following reasons: acacia is an abundant invasive plant; eucalyptus is one of the predominant fast-growing species in Galicia; and pine sawdust is a waste product generated by the forestry industry. The materials were pyrolysed at around 300-400 °C for between 1.5 – 3 h depending on the moisture content;

iii) two commercial biochars derived from pine wood (from trunk (Btrunk) and bark (Bbark)), for purposes of comparison.

Samples characterisation

All of the samples were characterised using different analytical techniques. The pH and conductivity were measured in a solution of biochar and water (1:5). Elemental analysis (C, H, N and S) was performed in a TruSpec CHN analyser and S was determined in a LECO SC-144DR analyser. Ash content was determined after combustion at 1000 °C for 4 h. Oxygen was estimated as follows: O = 100 – C + N + H + S + ash. Total nutrient and heavy metal concentration were determined by atomic absorption spectroscopy after wet acid digestion (in a Perkin Elmer Atomic Absorption Spectrometer 1100B). Fixed C (FixC) and volatile matter (VM) were determined by TGA-DSC scanning of samples in a Simultaneous Thermal analyser (STA6000 PerkinElmer) following UNE 32-019-84

Standards for determining the volatile matter content in combustible mineral solids. DSC thermographs were obtained at air atmosphere following the procedure described by Harvey et al. (2012).

Phosphorus analysis

The total P content was determined by the molybdenum blue method (Murphy & Riley, 1962) after wet acid digestion. Available P was extracted with 2% formic acid, following the procedure of Wang et al. (2012c) and its concentration was measured in the same way as total P. In order to explore inorganic P forms, the fractionation procedure described by Zhang & Kovar (2009) for non-calcareous soils, based on the procedure of Chang & Jackson (1957), was used. This method is based on the selective solubility of phosphates in various extractants and considers the presence of P in the following states: soluble and loosely bound P, Al-P, Fe-P, reductant-soluble P, Ca-P and occluded P. Initial extraction was carried out with ammonium chloride (1 M NH_4Cl) to remove soluble and loosely bound P. The Al-P was then separated from Fe-P with 0.5 M NH_4F and the Fe-P was removed with 0.1 M NaOH. A mixture of sodium citrate (0.3 M $Na_3C_6H_5O_7 \cdot 2H_2O$), sodium dithionite (1 g $Na_2S_2O_4$) and sodium bicarbonate (1M $NaHCO_3$) (CDB) was used to extract reductant soluble-P from within the matrices of retaining aggregates/minerals. The next step involved the addition of 1 M NaOH for 17h to determine occluded P (Gil-Sotres, 1980). Finally, the Ca-P was removed with sulphuric acid (0.25 M H_2SO_4) because Ca-P is insoluble in CDB (Zhang & Kovar, 2009). The procedure is illustrated in Figure 7.7. All P extracts were measured spectrophotometrically at 880 nm following the same procedure used for total P. The organic P (Po) content was calculated as the difference between the total P content and the sum of the inorganic fractions.

In order to elucidate the distribution of phosphorus at the surface of biochar particles, Scanning Electron Microscope (SEM) images were obtained with in a Zeiss EVO LS15 scanning electron microscope with

energy dispersive X-ray Microanalysis (EDX) (OXFORD detector). The operating voltage was 20 kV.

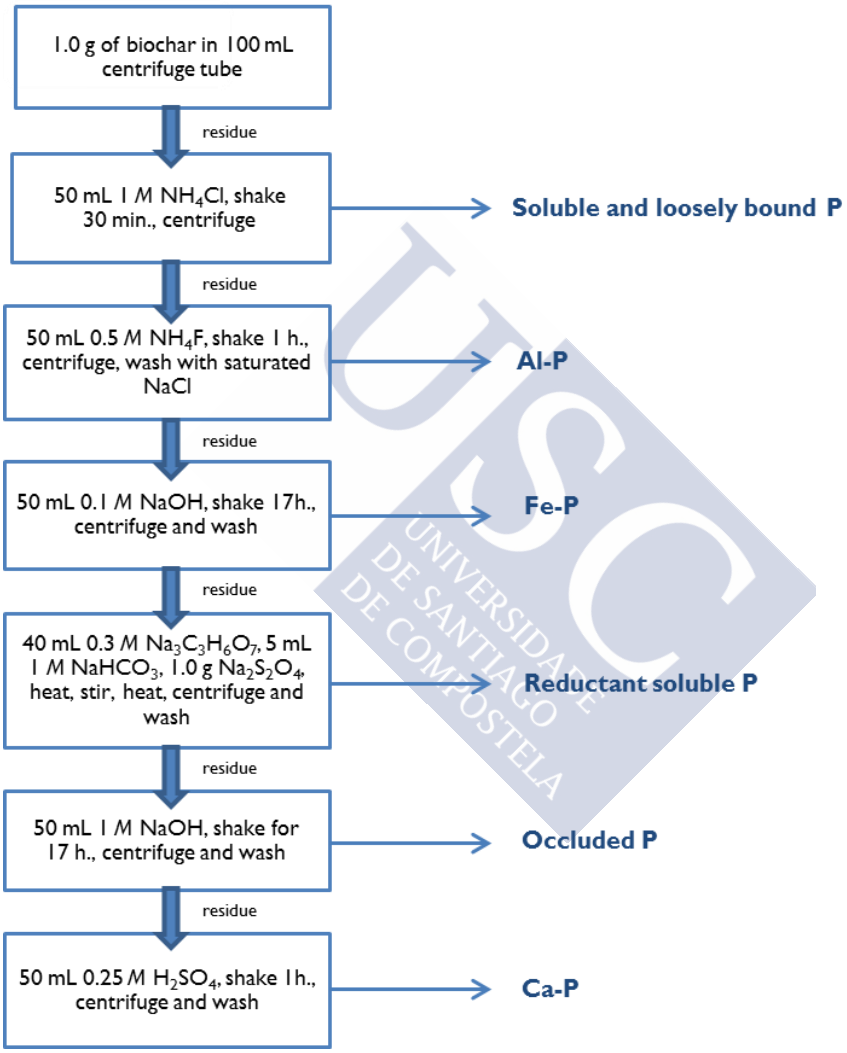

Figure 7.7 Sequential fractioning of inorganic P.

RESULTS

The elemental composition of the eight samples selected for this study is summarised in Table 7.1. The initial moisture content of the samples was between 1 and 5% (and was the highest in BAcB). These values corresponded to the amount of moisture that the samples take up from the surrounding air, which was well below the current limit of 15% for the use of charcoal in the silicon industry. Overall, the samples were rich in C, which varied between around 38% in Bbark and 78% in Btrunk. The C content of LTA-USC biochars was around 68%, i.e. lower than in coal, although it was not very low considering that all biochars were pyrolysed at low temperatures (≤ 400 °C as estimated by NIRS analysis in Table 3.2). The C content of BAcB was almost twice that of commercial bark charcoal. The molar H/C_{org} and O/C_{org} ratios were represented in a Van Krevelen diagram (Figure 7.8). The coal occupied a position closer to sub-bituminous coals in the diagram (Fuertes et al., 2010). The biochars appeared between bituminous coals and lignite, with the exception of Bbark, in which the H/C_{org} ratio was lower and the O/C_{org} value was higher. The sulphur content was much lower in biochars (0.01-0.13%) than in coal (0.67%). Another important parameter to be considered in the use of biochar in the silicon industry is the ash content, which can interfere in the production process. The ash content of trunk-derived samples ranged between 0.77 and 2.65%, being in the same order of magnitude as coal (1.74%). By contrast, the ash content of the bark-derived biochars was larger, and that of commercial bark charcoal was more than 50%.

The FixC is another significant parameter affecting the silicon production process, which must be stable and >60%. In the biochars analysed, FixC varied between 32.7% and 69.2%; the lowest value corresponded to the Bbark sample and the highest value to the Btrunk sample, whereas that of coal was around 61%. The energy emitted by the samples was measured by DSC: coal emitted around 18.60 kJ g^{-1} (Figure S D.1), while the biochars produced in the laboratory emitted around 13kJ g^{-1}

of energy. The lowest exothermic peaks were detected in commercial biochars, with values of 12 and 7 kJ g^{-1} for Btrunk and Bbark, respectively. Two exothermic peaks were distinguished in the heat flow curve of all the samples. The first corresponded to the degradation of non-carbonised organic matter and the second, more energetic one, corresponded to the charred material (Cao & Harris, 2010) (thermograms are included in Supporting Information A for biochars produced at LTA-USC at Figure S A.2, Figure S A.3, Figure S A.6, Figure S A.8 and Figure S A.10 and in Supporting Information D for coal and commercial biochars at Figure S D.1, Figure S D.2 and Figure S D.3).

Table 7.1 Elemental composition of different type of carbonaceous materials.

Sample	Coal	Btrunk	Bbark	BAcB	BAcSw-1	BAcHw-1	BEu-1	BSd-1
%C	73.26	77.78	38.35	64.48	69.93	71.92	69.32	65.75
%N	1.41	0.6	0.37	2.23	0.65	0.40	0.41	0.72
%H	6.11	4.05	1.60	4.20	4.30	3.86	5.09	5.04
%S	0.67	0.04	0.04	0.128	0.01	0.053	0.005	0.07
%O	17.67	15.24	6.8	23.48	21.57	21.44	23.24	27.72
O/C	0.18	0.15	0.16	0.27	0.23	0.22	0.25	0.32
H/C	1.00	0.62	0.50	0.78	0.74	0.64	0.88	0.92
%moisture	2.68	2.69	1.16	5.05	3.01	3.17	2.14	2.39
%VM*	37.47	29.45	14.41	42.92	39.37	37.63	47.62	52.10
%FixC*	60.79	69.18	32.74	51.83	57.98	60.76	51.61	46.53
% Ash*	1.74	1.37	52.84	5.25	2.65	1.61	0.77	1.37
dH (kJ g^{-1})	18.60	11.90	7.30	13.80	13.10	12.40	13.40	10.50

* Dry Basis

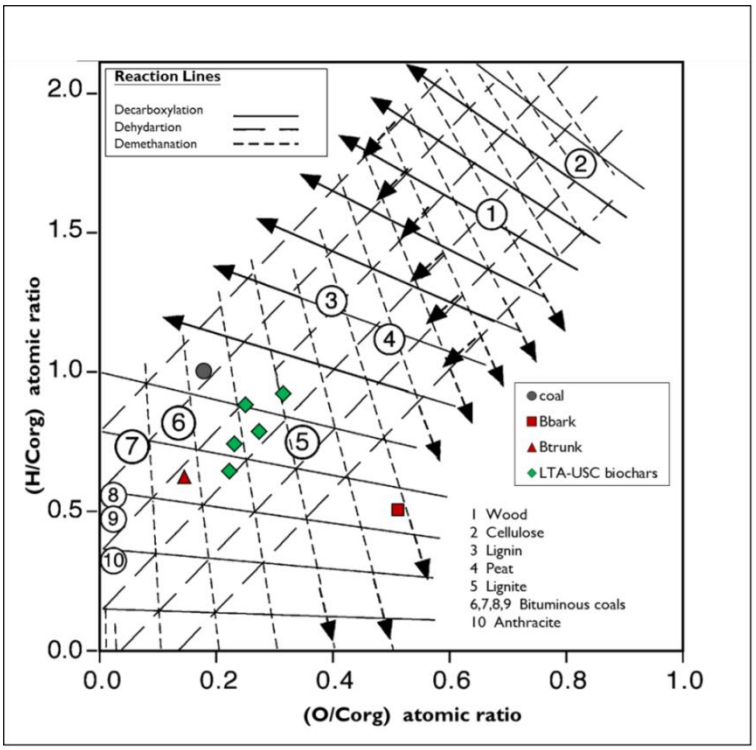

Figure 7.8 Van Krevelen diagram for subbituminous coal, commercial charcoals (Bbark and Btrunk) and biochars produced in LTA-USC. Adapted from (Fuertes et al., 2010).

The total nutrient and heavy metal contents were also determined as some of these can interfere in the silicon production process, e.g. P and Fe (Data can be seen at Table 7.2). The concentrations of Ca, Mg, Na and K in the biochars were one or two orders of magnitude higher than in coal, with Ca being the predominant cation. Biochars produced from bark were richer in nutrients than those produced from trunk. The concentrations of Fe and Al were much lower in biochars, with the exception of Bbark, than in coal. The concentrations of Fe and Al were lowest in the biochar produced from acacia trunk. Heavy metals content such as Co, Cu, Ni and Pb were below detection limit in most of the biochars. Overall, all the samples met the threshold values established by the International Biochar Initiative (IBI) for

heavy metals in biochar (IBI, 2015) (IBI standards for heavy metals in mg kg^{-1} are: Cr 64-1200; Co 40-150; Cu 65-1500; Pb 70-500; Ni 47-600).

Table 7.2 Nutrient and heavy metal contents of the different carbonaceous materials analysed, expressed in mg kg^{-1}.

Sample	Coal	Btrunk	Bbark	BAcB	BAcSw-1	BAcHw-1	BEu-1	BSd-1
P	151.7	652.6	1204.1	1129.9	677.8	32.9	272.8	396
Ca	636	6240	2360	21700	16000	11740	4520	4340
Mg	79	380	5200	2200	800	420	440	460
Na	75	184	541	1053	756	608	204	265
K	47	2520	5180	7325	3101	387	498	1611
Fe	1200	94	9480	201.3	51.7	29.7	255.2	455.4
Al	824	105	11680	240	n.d.	n.d.	136	435
Co	n.d.	n.d.	10	n.d.	n.d.	n.d.	n.d.	n.d.
Cr	n.d.	n.d.	15	n.d.	n.d.	n.d.	n.d.	n.d.
Cu	n.d.	13	26	6	n.d.	n.d.	11	n.d.
Mn	9	19	400	105	25	n.d.	125	85
Ni	n.d.	8	18	n.d.	n.d.	n.d.	n.d.	n.d.
Pb	7	13	16	n.d.	n.d.	n.d.	n.d.	n.d.
Zn	n.d.	12	23	1053	756	608	204	265
V	n.d.	n.d.	n.d.	n.d.	n.d.	n.d.	n.d.	n.d.

n.d. non detected

Phosphorus analysis

Phosphorus (P) is one of the elements that interferes most in the silicon production process when present at concentrations > 100 mg kg^{-1}, as PO_4 has a similar tetrahedral structure to SiO_4, and thus competes with Si in the crystalline structure. The total P content measured in sub-bituminous coal was 151.7 mg kg^{-1} whereas the P content of the biochars varied from 32.9 mg kg^{-1} in BAcHw-1 to 1204 mg kg^{-1} in Bbark (Table 7.2). For the acacia samples, the P content was highest in the bark, and

decreased through the sapwood and heartwood. The P content of the acacia heartwood (BAcHw-1) was four times lower than that of the coal sample.

The inorganic P (Pi) was fractionated in order to obtain a better understanding of its distribution. The results of organic and inorganic P distribution are reported in Figure 7.9. The proportion of Pi in biochars varied from 20% in BSd-1 to more than 96% in BAcHw-1 of the total P content. In the latter, the total P content was low and almost all of it corresponded to inorganic forms. The inorganic P content of coal was around 10% of the total P.

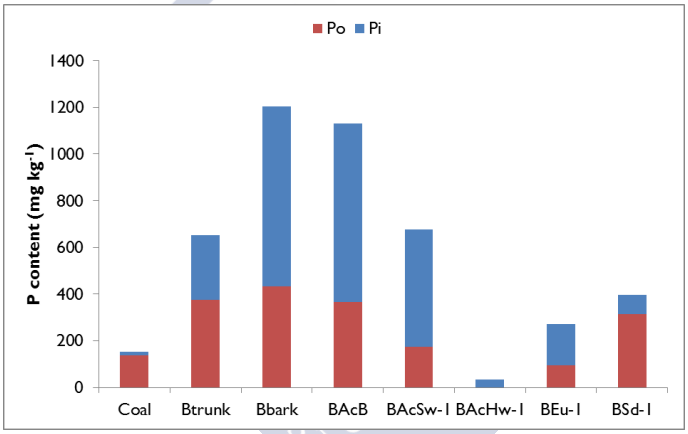

Figure 7.9 P content of different carbonaceous samples analysed: organic P (Po) and inorganic P (Pi).

The distribution of the different Pi fractions (soluble/loosely bound P, Al-P, Fe-P, reductant soluble P, Ca-P and occluded P) varied widely in the different samples (Figure 7.10). In coal, almost all the inorganic fractions were below the detection limits or present at very low concentrations, with a predominance of Al-P (~30%). In the biochar samples, Ca-P varied between 3 and 322 mg kg^{-1}; this was the predominant form in BAcB, BAcSw-1 and Bbark. The next abundant inorganic form was occluded P, which varied from 3.6 to around 216 mg kg^{-1}, with values below detection

limits in BAcHw-1. The highest concentration of this form was found in both of the bark samples and the concentration was lowest in sawdust and heartwood biochars. By contrast, the predominant Pi forms in BacHw-1 were reductant soluble P and Al-P, with 45.7% and 30.9% of the total Pi, respectively (Figure 7.11). The Fe-P fraction was below 10% in most of the samples, except BEu-1 and BSd-1, in which it represented > 50% of total Pi. Finally, soluble/loosely bound P varied between below detection limits (8.16 mg kg^{-1}) in BAcHw-1 to almost 114 mg kg^{-1} in Bbark; the percentage of soluble/loosely bound P was >10% of Pi in most of the samples.

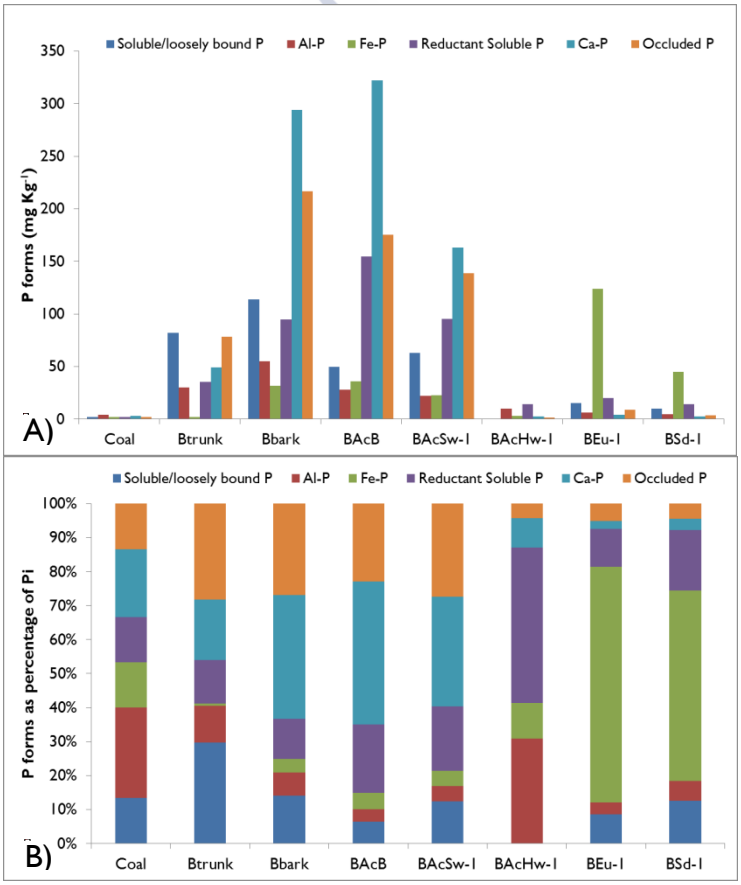

Figure 7.10 Inorganic P forms expressed as A) absolute values and B) the percentage of each form relative to the total amount of Pi.

Plant-available P, as estimated with 2% formic acid, was also measured (Figure 7.12), as small biochar pieces and the waste material generated by the silicon industry could be applied to soils as amendment. Available-P varied from 12 mg kg^{-1} in sawdust biochar to almost 300 mg kg^{-1} in acacia bark, with values below detection limits in coal and acacia heartwood biochar. In both biochars produced from bark and the Btrunk biochar, available P ranged between 21 and 27% of the total P content. By contrast, only around 3% of total P in BSd-1 was plant-available.

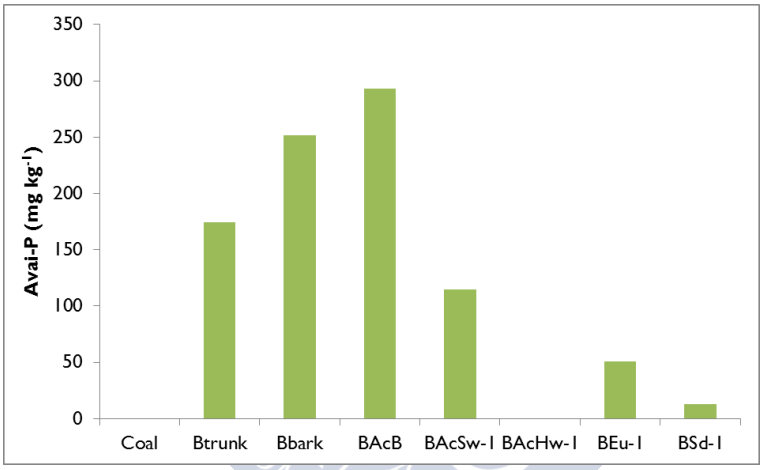

Figure 7.11 Plant-available P (Avai-P) content of the different carbonaceous materials analysed.

Biochar and coal samples were analysed by SEM to determine their morphology and structure (Figure 7.12). The SEM images showed that the biochar structure was more regular and conserved the vegetal cellular structure, providing micro and macroporosity, while coal was more amorphous (Figure 7.12A). Bark-derived biochars (Figure 7.12C and D) were more heterogeneous and irregular than those of trunk-derived biochars, and they were richer in inorganic constituents.

SEM-EDX analysis helped to clarify the distribution of P at the biochar surface and potentially enabled analysis detection of inorganic constituents.

No P was observed at the surface of the coal sample, and inorganic particles were mainly composed of Si, Al and K, with lower concentrations of S, Fe and Mg. Different particles, in addition to the carbonaceous matrix, were distinguished in biochars and mainly comprised calcium carbonate and Si and, to a lesser extent, Fe, Al and K. These particles were more abundant in bark biochar. In the trunk biochars, such as eucalyptus, inorganic particles were also more abundant in the bark than in the heartwood (Figure 7.13) consistent with the larger ash content in the former. P was only detected in bark samples, as shown in the specific surface analysis of Bbark (Figure 7.14) and the mapping of BAcB surface (Figure 7.15), in which P was found to be distributed across the whole surface analysed.

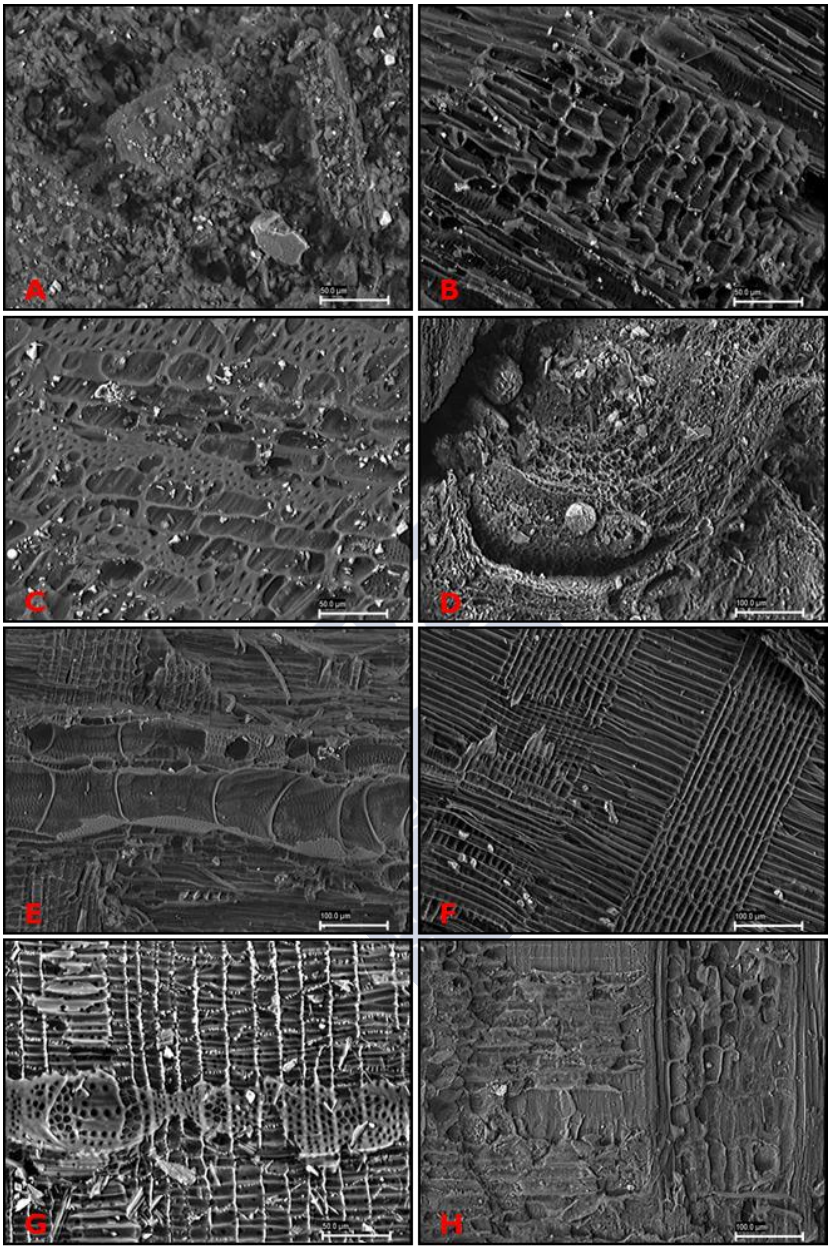

Figure 7.12 SEM images of (A) sub-bituminous coal, (B) Btrunk, (C) Bbark, (D) BAcB, (E) BAcSw, (F) BAcHw, (G) BEu-1, (H) Bsd-1.

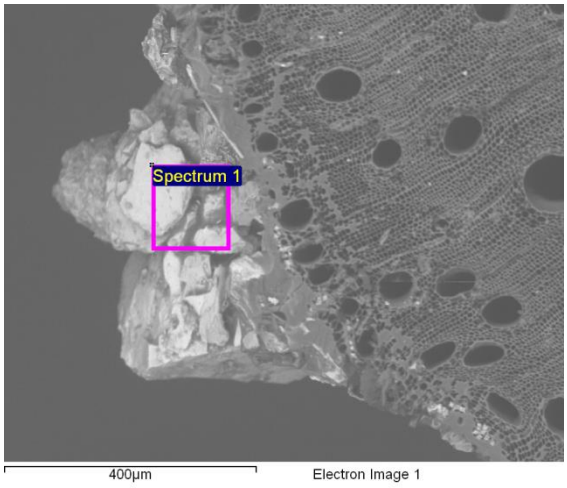

Element	Conc.	%Weight
C K	10.72	32.19
O K	17.53	41.42
Mg K	1.33	2.79
Al K	2.28	4.34
Si K	4.76	8.62
K K	1.36	1.97
Ca K	0.83	1.28
Ti K	0.21	0.38
Mn K	0.10	0.18
Fe K	3.68	6.82

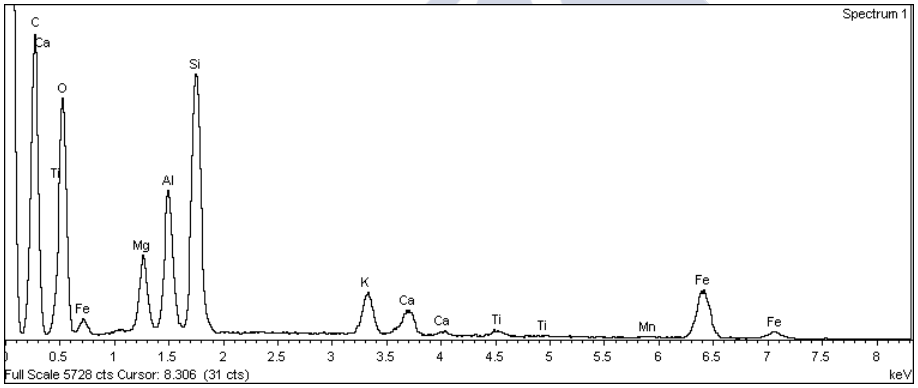

Figure 7.13 SEM-EDX analysis of eucalyptus biochar (BEu-1). Surface analysis was done in the square area denoted Spectrum 1.

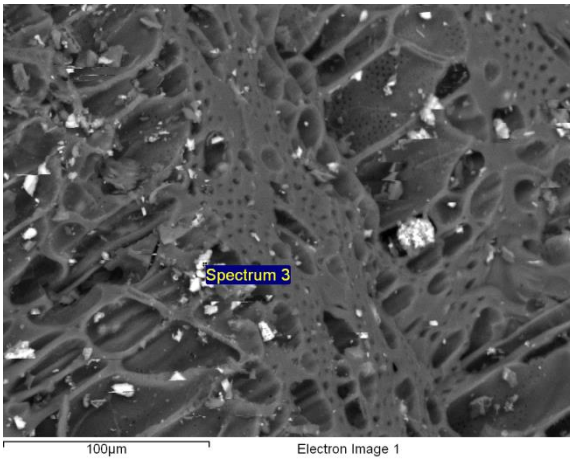

Element	Conc.	%Weight
C K	23.47	29.15
O K	20.90	45.65
Mg K	0.26	0.36
Al K	0.72	0.87
Si K	1.68	1.85
P K	1.45	1.10
S K	0.46	0.47
Cl K	0.09	0.11
K K	0.52	0.45
Ca K	19.46	18.84
Mn K	0.50	0.62
Fe K	0.43	0.53

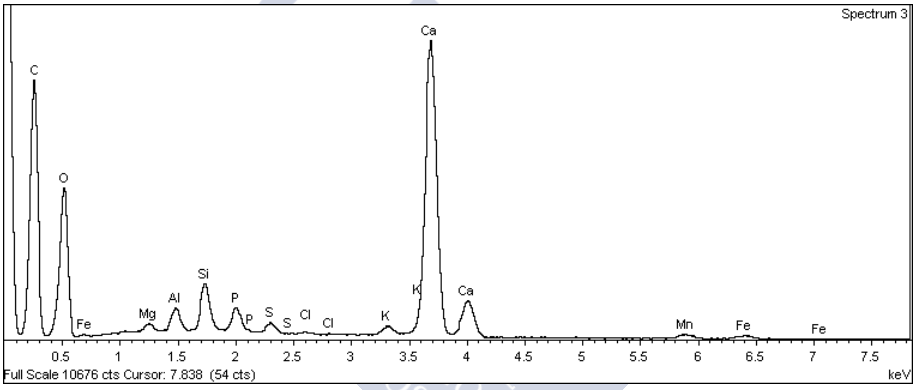

Figure 7.14 SEM-EDX analysis of Bbark obtained in the area denoted Spectrum 3 of the Electro Image.

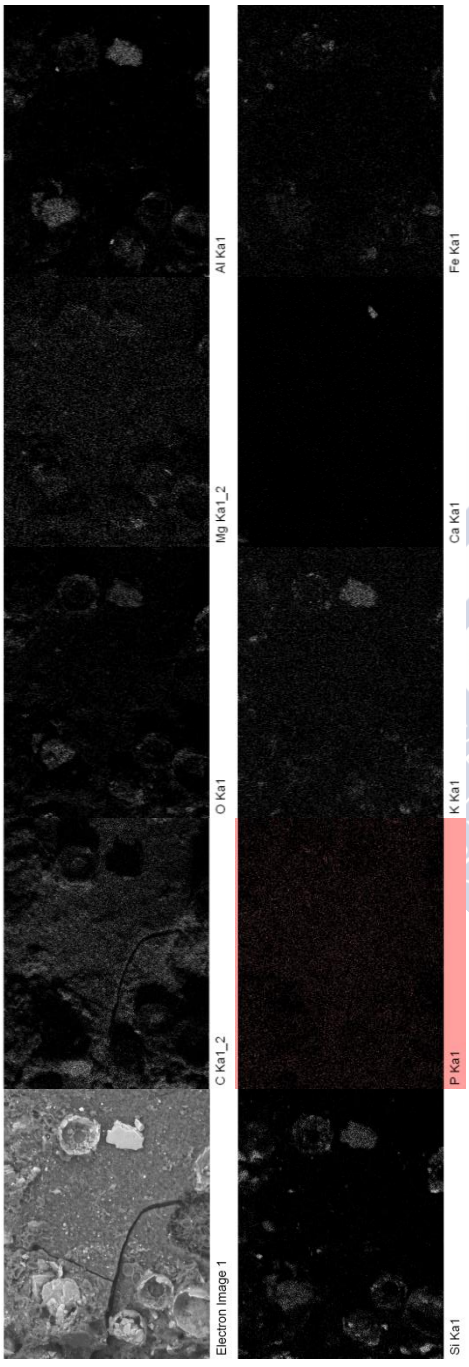

Figure 7.15 Mapping of BAcB surface were can be seen as P is distributed on the surface.

DISCUSSION

The potential use of biochar to produce silicon was evaluated, with the overall aim of using the biochar to replace the non-renewable resource (i.e. coal) currently used in the process. Feedstocks that are widely available in Galician forests were evaluated (i.e. pine, eucalyptus and acacia), so that the demands of the production company (Ferroatlántica S.A.) would be ensured. The moisture content of all the samples was below the 15% limit established for coal. The proximate analysis revealed that FixC was slightly below the process requirements (>60%) in most of the biochars studied, except Btrunk and BAcHw-1. This parameter can be easily improved by increasing the pyrolysis temperature, as all the samples produced at LTA-USC were pyrolysed at low temperature (HHT ≤ 400 °C). However, the ash content (and the dominant ions present in the ash) increases with pyrolysis temperature (Antal & Gronli, 2003) and must be retested accordingly. In addition, the biochar yield will decrease, and this should be taken into account for maximising the benefits of the use of these charcoals (Spokas et al., 2012; Brewer et al., 2012; Antal & Gronli, 2003). It is possible that a trade-off between yield, FixC and ash content will be obtained at temperatures around 450-500 °C. This was the case of eucalyptus biochar BEu-2 (see chapter 4), which was produced at 500 °C and yielded a FixC content of 79%. Given the importance of reducing the ash content, the use of bark as a feedstock (as well as any other biochar rich in ash) for silicon production is discouraged. On the other hand, ash can be removed from biochar by a simple mechanical process (shaking). This step can reduce the P content, considering that most of the nutrients remain in ash.

The elemental composition of biochars was found to be different from that of coal. For example, all biochars except Bbark, contained significantly less Fe and Al than coal. The presence of these metals can generate impurities in the silicon produced, and the use of these biochars instead of coal could therefore improve the quality, and thus the economic value of the silicon. Silicon is considered first class when the Fe content is below

0.56% (SilicioFerroSolar S.L., 2016), whereas when the final product contains more than 5% Fe, it is considered ferrosilicon (FeSi), which is of lower value. Macronutrients, such as Ca can also interfere in silicon formation, and the Ca content of biochar was higher than that of coal. However, Ca is easily oxidised, together with Al, in liquid silicon and removed in the slag as calcium aluminates.

The study of phosphorus focused on inorganic P forms, as organic P volatilises at temperatures around 700 °C (De Luca et al., 2009; Bissolino & Dagnino, 2007), and it will therefore disappear in electric arc furnaces operating at higher temperatures (around 2000 °C). The total P content and the inorganic fractions present in the biochar varied with the feedstock. The bark samples were enriched in P (which decreased through heartwood). Madgwick & Frederick (1988) also concluded that the P concentration in *Pinus radiata* was highest in bark and decreased through heartwood, with the nutrient content being inversely correlated with the stem diameter. A similar nutrient distribution was observed for wild cherry (*Prunus avium* L.) (Morhart et al., 2016), for different eucalyptus subspecies (Judd et al., 1996) and for silver birch (*Betula pendula*), in which P enrichment was also observed in branches relative to stems (Uri et al., 2007). These results are consistent with the higher P content in BEu-1 than in BAcHw-1, as small branches that included a thin layer of bark were used to produce BEu-1, while acacia trunk was wider. Phosphorus is taken up from soil by the roots and transported through the xylem to the foliage and younger parts of the plant (Schachtman et al., 1998), which are richest in P. When the plant is deficient in P or is about to lose its leaves, translocation of Pi occurs from the old leaves to the young leaves or to the growing roots via the phloem (Schachtman et al., 1998). Of the different inorganic P forms, Fe-P is the least desirable as both Fe and P prevent the production of high quality silicon. The concentration of Fe-P was low in all the samples, despite being the predominant form in biochar derived from eucalyptus and from pine sawdust. By contrast, both samples contained relatively low

amounts of inorganic P (178.6 and 80.5 mg kg^{-1}, respectively), and it is assumed that their contribution is not relevant. In other biochars (Bbark, BAcB and BAcSw-1), the most abundant P form was that associated with Ca, which is less detrimental in the production process, as it will remain in the slag. On the basis of the results obtained, with exception of bark samples, biochar obtained from pine, acacia and eucalyptus trunk or branches could be used to substitute coal in the silicon production process. The use of biochar derived from sawdust is hampered by the small particle size, which is well below optimal for silicon production, which is that of the "cigarette box". Although pelletizing is a possible option, this would increase the production costs of the biochar.

The phosphorus content of feedstock is influenced by the P concentration in soils and its availability to plants (Gil-Sotres, 1980). Thus, even if the same tree species are used to produce biochar, the total composition will vary depending on the type of soil in which the trees grow. The P enrichment of soils depends on the lithology or the original soil material, as well as factors that contribute to rock weathering such as climate, biota, and duration of weathering (Gil-Sotres, 1980). In acidic soils, the P is mainly associated with reactive Al and Fe as a surface complex, while at higher pH, Ca-P precipitates predominate. In light of the results described above, future research should focus on the effects of the different lithological zones in Galicia (Figure 7.16) on the elemental composition of wood (pine, eucalyptus, acacia and scrub), to enable the selection of the best area for obtaining the feedstock for large scale biochar production.

On the other hand, phosphorus is the most limiting macronutrient (after N) for plants. Biochars produced from bark are enriched in P, of which 21-27% is plant-available, and they are thus not suitable for silicon production. Likewise, this biochars discarded to produce silicon, including small-sized biochars, resulting from the charcoal making process for silicon production could be applied to forest soils as an amendment to improve soil properties, thus contributing to closing biogeochemical cycles while

promoting the revalorisation of waste products. This could help to enhance timber production and ensure the supply of timber for the Si production company (Ferroatlántica S.A). Galician forest land includes for 600000 ha of unproductive land, which could be transformed into productive woodland and thus contribute to generating revenue for the owners. If biochar production would provide a new market for forest owners, thereby reducing forest abandonment, improving woodland management and decreasing the incidence of wildfires.

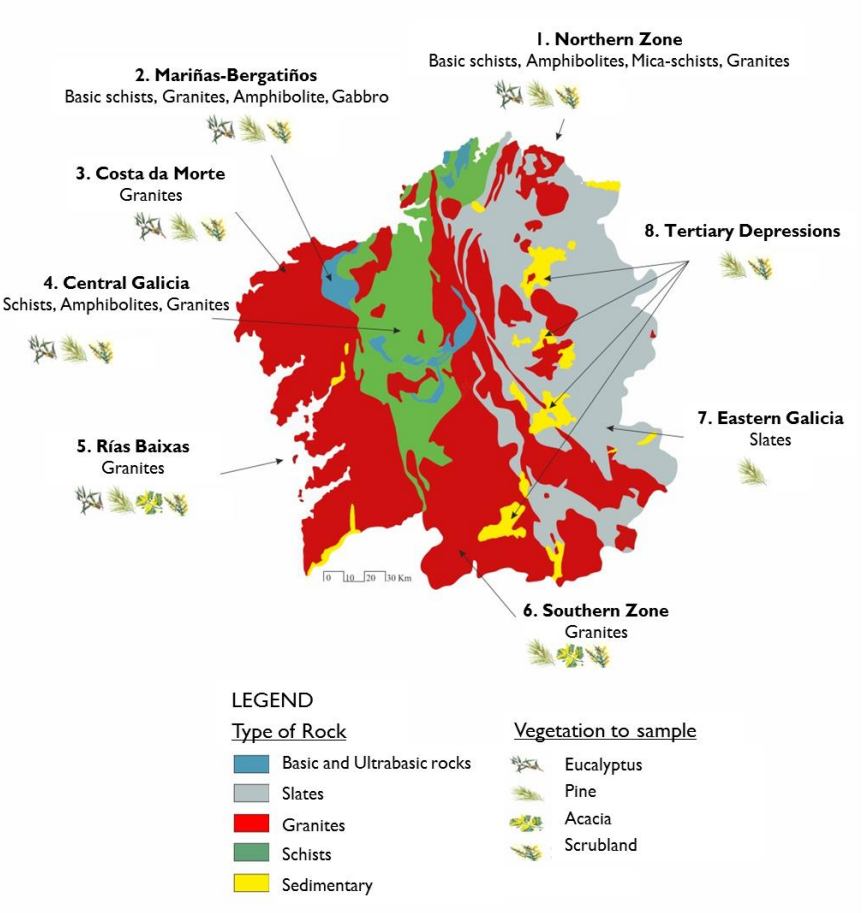

Figure 7.16 Map of the different lithological areas in Galicia (Macías & Calvo de Anta, 2001), indicating possible biomass sampling locations for future research.

CONCLUSIONS

This research was carried out to determine the potential use of different biochars to substitute coal in the silicon production process. The results revealed that biochars derived from pine, eucalyptus and acacia trunk and branches comply with the requirements of elemental composition, size and humidity, and with that of FixC for pyrolysis temperatures of 400-500 °C. Thus, bark-derived biochars are unsuitable due to their high ash content, and specifically the high concentration of P, which is known to interfere in the silicon production. Thus, bark-derived biochars are proposed as soil amendments in the sites where the original trees were grown, thus closing the biogeochemical cycle of the elements involved and enhancing wood production. Further research is recommended in order to establish the influence of parent material on the P content of feedstock and biochar.

ACKNOWLEDGEMENTS

I would like to thank Ferroatlántica S.A. for the technical and economic support provided, and for providing access to the facilities on several occsions. I am also grateful to CVAN supplying the biochar samples evaluated in this study.

USC
UNIVERSIDADE
DE SANTIAGO
DE COMPOSTELA

8. Final Conclusions

USC
UNIVERSIDADE
DE SANTIAGO
DE COMPOSTELA

CONCLUSIONES

La presente Tesis Doctoral ha estudiado el potencial de biocarbones producidos a partir de distintos residuos mediante un reactor experimental de bajo coste para distintas aplicaciones de carácter ambiental como son: (i) el secuestro de C como herramienta para luchar contra el cambio climático; (ii) la mejora de las propiedades de suelos degradados o contaminados; (iii) su uso como adsorbente de contaminantes orgánicos derivados del petróleo; (iv) la sustitución del carbón fósil en el proceso de producción de silicio ultrapuro. Las siguientes conclusiones resumen los principales resultados obtenidos:

- Es posible obtener biocarbón con un reactor experimental de bajo coste en cantidades y calidad suficientes para distintas aplicaciones ambientales. El control de las condiciones de pirólisis con este tipo de sistema no es exhaustivo; sin bien, se pudo predecir la máxima temperatura alcanzada durante la pirolisis mediante análisis de espectroscopía de infrarrojo próximo (NIRS), clasificando las muestras en biocarbones obtenidos a baja temperatura (HHT ≤ 400 °C) o a alta temperatura (HHT > 400 °C).
- Los diferentes métodos utilizados para analizar la estabilidad de los biocarbones determinaron un aumento de la recalcitrancia con el incremento de la temperatura de pirólisis. La mayoría de las muestras producidas a baja temperatura se clasificaron como "material carbonoso pirogénico" (PCM) al presentar un ratio H/C_{org} > 0.7.
- De todas las muestras analizadas las que mayor potencial presentaron para el secuestro de C (Clase 5) fueron los derivados de corteza de pino (BPb), miscanthus (BMis), carozo de maíz (BCc) y eucalipto (BEu-2), todos ellos producidos a más de 400 °C. Mientras que las muestras con mayor componente inorgánico o cenizas (e.g. el biocarbón de estiércol de pollo (BCm) o el de

compost de alperujo (BOpc)) presentaron menor proporción en carbono recalcitrante.

- En cuanto al potencial fertilizante de los biocarbones estudiados, el de cáscara de arroz (BRh) presentó la mayor capacidad (Clase 4), seguido del biocarbón de estiércol de pollo (BCm) con Clase 3 y del compost de alperujo (BOpc) y astilla de pino (BSdG), con Clase 2. Además, 10 de los biocarbones analizados presentaron una disponibilidad de nutrientes correspondiente a la Clase 1, lo que indica que presentan capacidad para satisfacer los requisitos del cultivo de maíz para al menos uno de los nutrientes considerados. Por otra parte, los biocarbones derivados de madera o herbáceas, ricos en C recalcitrante (BEu-2, BPb o BMis), son los que presentaron el menor potencial fertilizante. Además de aportar nutrientes, los biocarbones presentan capacidad de retención de agua, capacidad de intercambio catiónico y capacidad de aportar estructura y porosidad al suelo, propiedades que será necesario estudiar en profundidad y seguir sus variaciones una vez sean aplicados al suelo.
- Se descarta la aplicación al suelo de biocarbones hechos con neumáticos usados, a pesar de su alto contenido en C recalcitrante, por ser potencialmente peligrosos debido a su composición en metales pesados (en especial Co y Zn) y PAHs, superando los niveles establecidos por el IBI y EBC. El resto de biocarbones estudiados no presentan toxicidad respecto a metales pesados o PAHs.
- Los biocarbones analizados presentaron potencial para ser utilizados como adsorbentes de bajo coste de contaminantes orgánicos en sistemas acuosos, variando su capacidad en función de las condiciones de pirólisis, la materia prima y la naturaleza del contaminante. Se demostró que cuanto más volátil e hidrofílico es un compuesto (e.g., ETBE, MTBE o benceno), más baja es su retención en el biocarbón. Los biocarbones producidos una

temperatura de pirólisis alta (HHT > 400 °C), como BEu-2, presentaron una mayor capacidad de retención para compuestos volátiles (MTBE, ETBE y BTEX) e hidrocarburos totales del petróleo (TPH), debido a su alto contenido en C aromático y su elevada superficie específica. La adsorción reflejó un comportamiento en multicapa y una mayor capacidad de adsorción en los biocarbones que en los PCMs. Los modelos empíricos de Langmuir y Freundlich fueron adecuados para describir los resultados experimentales y para detectar diferencias generales en el comportamiento de adsorción de los distintos compuestos orgánicos por los diferentes biocarbones.

- Además de las aplicaciones tradicionales de los biocarbones de fijación de C, mejora de las propiedades del suelo y agente adsorbente, se ha evaluado su potencial para sustituir al carbón en aplicaciones industriales como la producción de silicio con calidad fotovoltaica. El estudio indicó que los biocarbones derivados de maderas de pino, acacia y eucaliptus descortezadas producidos a temperaturas 450-500 °C cumplen con los requisitos que exige el proceso de producción del silicio.
- Se descartan para este uso los biocarbones producidos a partir de corteza, debido principalmente a su alto contenido en cenizas y en fósforo, ya que pueden interferir en la producción del silicio. Sin embargo, estos biocarbones de corteza son ricos en nutrientes, por lo que pueden ser aplicados a los suelos forestales de los que se extrae la madera, cerrando así el ciclo biogeoquímico de los elementos que contienen, mejorando las propiedades del suelo y, por consiguiente, aumentando la producción de la biomasa forestal.

Los estudios realizados revelan que cada biocarbón presenta una composición y unas propiedades físico-químicas variables. Esta variabilidad los hace adecuados para diferentes aplicaciones, permitiendo resolver distintas problemáticas medioambientales. Sin embargo es necesario un

análisis completo, tanto de las características de cada biocarbón, como de la aplicación deseada, con el objetivo de detectar el biocarbón más adecuado para cada uso. Además, siempre se tendrá en cuenta que se cumplan los valores críticos de concentración de contaminantes que aseguren la ausencia de toxicidad para el medio ambiente al aplicar un biocarbón.

CONCLUSIONS

Overall, this thesis describes the potential production of biochar from different types of waste in a low-cost experimental reactor and its use to address different environmental applications: (i) as C sink to mitigate global change; (ii) as an amendment to improve the properties of degraded or contaminated soils; (iii) as a sorbent of fuel organic pollutants; (iv) as an alternative to the use of coal in the ultrapure silicon production process.

The main results obtained can be summarized as follows:

- Biochar was produced in a low-cost experimental reactor, with satisfactory results in terms of yield and quality. Control of pyrolysis conditions in this type of system was not exhaustive; however, the highest heating temperature reached during pyrolysis was successfully estimated using near infrared spectroscopy (NIRS). This simple method enabled classification of biochars into two groups: biochars produced at low temperature (HHT ≤ 400 °C) and those produced at high temperature (HHT > 400 °C).
- The different methods used to determine the C stability of biochars showed an increase in recalcitrant C with increasing pyrolysis temperature. Most of the samples produced at low temperature were classified as "Pyrogenic carbonaceous material" (PCM) with a H/C_{org} ratio > 0.7.
- The samples with the greatest potential for C sink (Class 5) were those produced over 400 °C and derived from pine bark (BPb), miscanthus (BMis), corncob (BCc) and eucalyptus (BEu-2); while samples with higher contents of inorganic components, such as chicken manure biochar (BCm) and olive pomace compost biochar (BOpc), contained a lower proportion of recalcitrant C.
- Regarding the fertiliser value of the biochars, rice husk biochar (BRh) was categorised as having the highest fertiliser capacity

(Class 4), followed by chicken manure biochar (BCm) (Class 3) and olive pomace compost (BOpc) and pine sawdust (BSdG) biochars (Class 2). In addition, 10 out of the 23 biochars analysed were categorised as having Class 1 fertiliser value, indicating that they are capable of satisfying the requirements of a corn crop for at least one of the available nutrients considered. On the contrary, wood derived biochars rich in recalcitrant C (BEu-2, BPb or BMis) showed the lowest fertilising potential. Besides providing nutrients, biochar displays water retention capacity, cation exchange capacity and can provide structure and porosity to soils. Biochar production could thus be presented to farmers as a low-cost tool for disposing of waste and improving land while also capturing C from the atmosphere. However, the latter properties must be studied in further depth after application of biochar to soils for a better understanding of the interactions and changes that take place in the field.

- Tyre derived biochar should be completely disregarded for use as soil amendments because of the concentration of heavy metals (Co and Zn) and PAHs, which exceed the levels established by the IBI and EBC. The other samples analysed do not show toxicity regarding the heavy metals or PAHs contents.

- All biochars tested in this study could be used as low-cost sorbents to remove fuel-based organic compounds from aqueous systems. As expected, not all biochars presented the same sorption capacity, and the characteristics of the contaminant, the pyrolysis conditions (especially HHT) and the nature of the feedstock material were the main factors affecting the sorption behaviour and capacity. The most volatile and hydrophilic organic compounds such as MTBE, ETBE and benzene were poorly sorbed on biochar. Samples obtained at high pyrolysis temperatures (> 400 °C), i.e. BEu-2, performed better in removing of organic compounds from aqueous

solutions: sorption was favoured by higher aromatic carbon content and specific surface area. The sorption of fuel organic compounds on biochar reflected a multilayer behaviour and a relatively high sorption capacity of the biochar produced at high temperatures (> 400 °C). Moreover, Langmuir and Freundlich empirical models adequately described the experimental results and detected general differences in the sorption behaviour of volatile organic compounds and TPHs by the different biochars.

- In addition to the conventional applications of biochar as a soil amendment, C sink and sorbent material, its potential use as a substitute for coal in industrial applications, such as in the production of high quality silicon, has been demonstrated. The study revealed that biochars derived from wood without bark (such as eucalyptus, acacia or pine) meet the requirements for silicon production when produced at 450-500 °C.

- Bark-derived biochars are unsuitable due to their high ash content, and specifically the high concentration of P, which is known to interfere in the silicon production. Bark-derived biochars are proposed as soil amendments in the sites where the original trees were grown, thus closing the biogeochemical cycle of the elements involved and enhancing wood production.

The different studies conducted within this doctoral research confirm that the physico-chemical composition of biochar depends on feedstock and production conditions. This variability enables the production of different types of biochar applicable to diverse environmental problems. Nevertheless, a comprehensive study of each situation, including the biochar and application area, is required in order to determine the most suitable biochar in each case. In addition, the absence of toxic effects on the the environment must be ensured before biochar can be applied to soil.

USC
UNIVERSIDADE
DE SANTIAGO
DE COMPOSTELA

9. References

USC
UNIVERSIDADE
DE SANTIAGO
DE COMPOSTELA

REFERENCES

Ackerman, F. (2000). Waste management and climate change. *Local Environment,* 5, 223-229.

Agudo López, R., Aguirre Royuela, M., Cueto Asín, A., Herranz Baquero, O., Mullor Parrondo, A., Olande Vegas, A., Requejo Sánchez, C., & Tourné Whyte, M. (2010). *Perfil Ambiental de España 2010. Informe basado en indicadores.* Madrid: Ministerio de Medio Ambiente, y Medio Rural y Marino (MARM).

Ahmad, M., Ok, Y., Kim, B.-Y., Ahn, J., Lee, Y., Zhang, M., Moon, M., Al-Wabe, M. I., & Lee, S. (2016). Impact of soybean stover- and pine needle-derived biochars on Pb and As mobility, microbial community, and carbon stability in a contaminated agricultural soil. *Journal of Environmental Management*, 166, 131-139.

Ahmad, M., Rajapaksha, A., Lim, J., Zhang, M., Boland, N., Mohan, D., Vithnage, M., Lee, S. S., & Ok, Y. (2014). Biochar as a sorbent for contaminant management in soil and water: A review. *Chemosphere,* 99, 19-33.

Aivalioti, M., Vamvasakis, I., & Gidarakos, E. (2010). BTEX and MTBE adsorption onto raw and thermally modified diatomite. *Journal of Hazardous Materials, 178*, 136-143.

Alberdi, I., Hernández, L., Condés, S., & Cañellas, I. (2012). La estimación de la biodiversidad forestal en el Inventario Forestal Nacional. Aplicación en el IFN-4 en Galicia. *Foresta,* 54, 20-31.

Ali, I., & Gupta, V. (2007). Advances in water treatment by adsorption technology. *Nature protocols,* 1, 2661-2667.

Amonette, J. E., & Joseph, S. (2009). Characteristics of biochar: microchemical properties. In J. Lehmann, & S. Joseph, *Biochar for*

environmental management: science and technology (pp. 33-52). London: Earthscan.

Anderson, L., & Tillmann, D. (1977). *Fuels from waste.* London: Academic Press.

Antal, M., & Gronli, M. (2003). The art, science, and technology of charcoal production. *Industrial Engineering Chemistry Research,* 42, 1619-1640.

Baldock, J., & Smernik, R. (2002). Chemical composition and bioavailability of thermally altered *Pinus resinosa* (Red pine) wood. *Organic Geochemistry,* 33, 1093-1109.

Balseiro-Romero, M., Gkorezis, P., Kidd, P. S., Vangrosveld, J., & Monterroso, C. (2016). Enhaced degradation of diesel in the rhizosphere of *Lupinus luteus* after inoculation with diesel-degrading and plant growth-promoting bacterial strains. *Journal of Environmental Quality*, 45, 924-932.

Balseiro-Romero, M. (2014). *Behaviour of fuel organic compounds in contaminated soils and development of a phytoremediation procedure.* Tesis Doctoral. Universidade de Santiago de Compostela.

Balseiro-Romero, M., & Monterroso, C. (2013). A headspace-analysis approach to assess the sorption of fuel volatile compounds by soils. *Soil Science Society of America Journal,* 77, 800-808.

Balseiro-Romero, M., Kidd, P. S., & Monterroso, C. Influence of plant root exudates on the mobility of fuel organic compounds in contaminated soils. Phytotechnologies 9th International Conference. Hasselt, Belgium, September 2012.

Bascomb, C. (1986). Distribution of pyrophosphate extractable iron and Organic carbon in soils of various groups. *Journal of Soil Science*, 19, 251-256.

Bice, D. (n.d.). Overview of the carbon cycle from a systems perspective *Earth 103: Earth in the future*. College of Earth and Mineral

Science, Editor. Accessed: 03/22/2017, Available at: https://www.e-education.psu.edu/earth103/node/1019

Bissolino, P., & Dagnino, E. (2007). Estudio de la dinámica de las fracciones de fósforo orgánico e inorgánico en suelos de la región semiárida pampeana central del área del Caldenal sometidos a quemas controladas. *Revista de la Facultad de Agronomía, 18*, 79-80.

Boateng, A. A., Garcia-Perez, M., Masek, O., Brown, R., & del Campo, B. (2015). Biochar production technology. In J. Lehmann, & S. Joseph (Eds.), *Biochar for environmental management: science, technology and implementation* (pp. 63-87). London: Routledge.

Bornemann, L., Lookan, R. S., & Welp, G. (2007). Differential sorption behaviour of aromatic hydrocarbons on charcoals prepared at different temperatures from grass and wood. *Chemosphere,* 67, 1033-1042.

Breus, I., & Mishchenko, A. (2006). Sorption of volatile organic contaminants by soils (A review). *Eurasian Soil Science,* 39, 1271-1283.

Brewer, C., Hu, Y., Schmidt-Rohr, K., Loynachan, T., Laird, D. A., & Brown, R. (2012). Extent of pyrolysis impacts on fast pyrolysis biochar properties. *Journal of Environmental Quality,* 177, 1115-1122.

Brewer, C., Unger, R., Schmidt-Rohr, K., & Brown, R. (2011). Criteria to select biochars for field studies based on biochar chemical properties. *Bioenergy Research,* 4, 312-323.

Bridgwater, A. (2003). Renewable fuels and chemicals by thermal processing of biomass. *Chemical Engineering Journal,* 91, 87-102.

Brown, R. (2009). Biochar production technology. In J. Lehmann, & S. Joseph, *Biochar for environmental management: science and technology* (pp. 127-146). London: Earthscan.

Brown, R., del Campo, B., Boateng, A. A., García-Pérez, M., & Masek, O. (2015). Fundaments of biochar production. In J. Lehmann, & S. Joseph (Eds.),

Biochar for environmental management: science, technology and implementation (pp. 39-61). London: Earthscan.

Bruckman, V., Klinglmüller, M., & Milenkovic, M. (2016). Biochar in the view of climate change mitigation: the FOREBIOM experience. In V. J. Bruckman, E. A. Varon, B. B. Uzun, & J. Liu (Eds.), *Biochar: A regional supply chain approach in view of climate change mitigation* (pp. 1-22). Cambridge: Cambridge University Press.

Bucheli, T., Hilber, I., & Schmidt, H. (2015). Polycyclic aromatic hydrocarbons and polychlorinated aromatic compounds in biochar. In J. Lehmann, & S. Joseph (Eds.), *Biochar for environmental management: science, technology and implementation* (pp. 595-624). London: Earthscan.

Budai, A., Zimmerman, A., Cowie, A., Webber, J., Singh, B., Glaser, B., Masiello, C. A., Andersson, D., Shields, F., Williams, M., Sohi, S., & Joseph, S. (2013). *Biochar carbon stability test method: assessment of methods to determine biochar carbon stability.* (I. B. Initiative., Editor) Retrieved October 31, 2016, from IBI Document, Carbon Methodology.: http://www.biochar-international.org/

Buss, W., Graham, M., MacKinnon, G., & Masek, O. (2016). Strategies for producing biochars with minimum PAH contamination. *Journal of Analytical and Applied Pyrolysis,* 119, 24-30.

Calvelo Pereira, R., Kaal, J., Camps Arbestain, M., Pardo Lorenzo, R., Aitkenhead, W., Hedley, M., Macías, F., Hindmarsh, J., & Maciá-Agulló, J. (2011). Contribution to characterisation of biochar to estimate the labile fraction of carbon. *Organic Geochemistry*, 42, 1331-1342.

Camps-Arbestain, M., Amonette, J., Singh, B., Wang, T., & Schmidt, H. (2015). A biochar classification system and associated test methods. In J. Lehmann, & S. Joseph (Eds.), *Biochar for environmental management: science, technology and implementation* (pp. 167-193). London: Earthscan.

Camps-Arbestain, M., Madinabeitia, Z., Anza Hortalà, M., Macías-García, F., Virgel, S., & Macías, F. (2008). Extractability and leachability of heavy metals in technosols prepared from mixtures of unconsolidated wastes. *Waste Management,* 28, 2653-2666.

Camps-Arbestain, M., Shen, Q., Wang, T., van Zwieten, L., & Novak, J. (2017). Available nutrients in biochar. In B. Singh, M. Camps-Arbestain, & J. Lehmann (Eds.), *Biochar: a guide to analytical methods* (pp. 109-125). Clayton South: CSIRO publising.

Cao, X., & Harris, W. (2010). Properties of dairy-manure-derived biochar pertinent to its potential use in remediation. *Bioresource Technology*, 101, 5222-5228.

Carballo, J., & Picos, J. (2009). El sector forestal: problemática y alternativas. EGAP, Santiago de Compostela: Xornadas sobre Políticas Públicas en tempos de crise.

Carbunion. (2015). *Memoria anual.* Madrid: Federación Nacional de Empresarios de Minas de Carbón.

Case, S., McNamara, N., Ready, D., & Whitaker, J. (2012). The effect of biochar addition on N_2O and CO_2 emissions from a sandy loam soil – the role of soil aeration. *Soil Biology and Biochemistry,* 51, 125-134.

Cayuela, M., van Zwieten, L., Singh, B., Jeffery, S., Roig, A., & Sánchez-Monedero, M. (2014). Biochar's role in mitigating soil nitrous oxide emissions: A review and meta-analysis. *Agriculture, Ecosystems and Environment,* 191, 5-16.

Chan, K., van Zwieten, L., Meszaros, I., Downie, A., & Joseph, S. (2007). Agronomic values of greenwaste biochar as a soil amendment. *Australian Journal of Soil Research,* 45, 629-634.

Chang, S., & Jackson, M. (1957). Fractionation of soil phosphorus. *Soil Science*, 84, 133-144.

Chen, B., & Yuan, M. (2011). Enhanced sorption of polycyclic aromatic hydrocarbons by soil amended with biochar. *Journal of Soils and Sediments,* 11, 62-71.

Chen, B., Zhou, D., & Zhu, L. (2008). Transitional adsorption and partition of nonpolar and polar aromatic contaminants by biochars of pine needles with different pyrolytic temperatures. *Environmental Science & Technology,* 41, 5137-5143.

Chen, X., Chen, G., Chen, L., Chen, Y., Lehmann, J., McBride, M. B., & Hay, A. (2011). Adsorption of copper and zinc by biochars produced from pyrolysis of hardwood and corn straw in aqueous solution. *Bioresource Technology,* 102, 8877-8884.

Chen, Y., Camps-Arbestain, M., Shen, Q., Singh, B., & Cayuela, M. (2018). The role of organic amendments in building soil nutrient fertility: a meta-analysis and review. *Nutrient Cycling in Agroecosystems*, https://doi.org/10.1007/s10705-017-9903-5.

Chiou, C., Kile, D., Rutherford, D., Sheng, G., & Boyd, S. (2000). Sorption of selected organic compounds from water to a peat soil and its humic and humin fractions: potential sources of the sorption nonlinearity. *Environmental Science & Technology,* 33, 1637-1644.

Chun, Y., Sheng, G., Chiou, C., & Xing, B. (2004). Compositions and sorptive properties of crop residue-derived chars. *Environmental Science & Technology,* 38, 4669-4555.

Compton, H., Prince, G., Fredericks, S., & Gussman, C. (2003). Phytoremediation of dissolved phase organic compounds: Optimal site considerations relative to field case studies. *Remediation,* 13, 21-37.

CONCAWE. (2017). *Performance of European cross-country oil pipelines. Statistical summary of reported spillages in 2015 and since 1971*. Brussels: CONCAWE Oil Pipelines Management Group.

Confemadera Galicia & UVigo. (2015). *Informe resultados Confemadera Galicia - Universidad de Vigo.* http://clustermadeira.com/wp-content/uploads/2012/06/Informe-de-Resultados-2015.pdf.

Cordella, M., Torri, C., Adamiano, A., Fabbri, D., Barontini, F., & Cozzani, V. (2012). Bio-oils from biomass slow pyrolysis: A chemical and toxicological screening. *Journal of Hazardous Materials*, 231-232, 26-35.

Cornelissen, G., & Hale, S. (2017). Polycyclic aromatic hydrocarbons in biochar. In B. Singh, M. Camps-Arbestain, & J. Lehmann (Eds.), *Biochar: a guide to analytical methods* (pp. 126-131). Clayton South: CSIRO Publisher.

Cornelissen, G., Gustafsson, O., Bucheli, T. D., Jonker, M. T., Koelmans, A. A., & Van Noort, P. C. (2005). Extensive sorption of organic compounds to black carbon, coal, and kerogen in sediments and soils: Mechanisms and consequences for distribution, bioaccumulation and biodegradation. *Environmental Science & Technology,* 39, 6881-6895.

Cornelissen, G., Rutherford, D., Arp, H., Dörsch, P., Kelly, C., & Rostad, C. (2013). Sorption of pure N_2O to biochars and other organic and inorganic materials in anhydrous systems. *Environmental Science & Technology,* 47, 7704-7712.

Cowie, A., Woolf, D., Gaunt, J., Brandao, M., Anaya de la Rosa, R., & Cowie, A. (2015). Biochar, carbon accounting and climate change. In J. Lehmann, & S. Joseph (Eds.), *Biochar for environmental management: science, technology and implementation* (pp. 763-794). London: Earthscan.

Crombie, K., Masek, O., Sohi, S., & Brownsort, P. (2013). The effect of pyrolysis conditions on biochar stability as determined by three methods. *GCB Bioenergy,* 5, 122-131.

De Luca, T., MacKenzie, M., & Gundale, M. (2009). Biochars effects on soil nutrient transformations. In J. Lehmann, & S. Joseph (Eds.), *Biochar for environmental management: science and technology* (pp. 251-270). London: Earthscan.

De Muñiz, G., Carneiro, M., Nisgoski, S., Ramirez, M., & Magalhães, W. (2013). SEM and NIR characterisation of four forest species charcoal. *Wood Science and Technology, 47*, 815-823.

Demirbas, A. (2006). Production and characterization of bio-chars from biomass via pyrolysis, energy sources. *Energy Sources, Part A: Recovery, Utilization, and Environmental Effects*, 28, 413-422.

Donahue, C., & Rais, E. (2009). Proximate analysis of coal. *Journal of Chemical Education*, 86, 222-224.

EBC (2012). *European biochar certificate - Guidelines for a sustainable production of biochar. Version 6.2E of 4th February 2016,* Arbaz (Switzerland): European biochar Foundation, doi:10.13140/RG.2.1.4658.7043

ECOREGA. (2013). *Sistemas de gestión de los residuos orgánicos en las explotaciones ganaderas: Ecogestión de los residuos orgánicos ganaderos y su repercusión en la emisión de gei.* Unións Agrarias-Upa.

Eden, M., Bray, W., Herrera, L., & McEwan, C. (1984). *Terra preta* soils and their archaeological context in the caqueta basin of southeast Colombia. *American Antiquity*, 49, 125-140.

EFOA. (2010). *European Fuel Oxygenates Association*. Retrieved from http://www.efoa.eu/

Elias, X., & Velo, E. (2005). La gasificación. In X. E. Castells (Ed.), *Tratamiento y valorización energética de residuos* (pp. 413-477). Fundación Universitaria Iberoamericana: Ediciones Díaz de Santos.

Enders, A., & Lehmann, J. (2017). Proximate analyses for characterising biochars. In B. Singh, M. Camps-Arbestain, & J. Lehmann (Eds.), *Biochar: a guide to analytical methods* (pp. 9-22). Clayton South: CSIRO Publishing.

Enders, A., Hanley, K., Whitman, T., Joseph, A., & Lehmann, J. (2012). Characterization of biochars to evaluate recalcitrance and agronomic performance. *Bioresource Technology,* 114, 644-653.

Enders, A., Sohi, S., Lehmann, J., & Singh, B. (2017). Total element analysis of metals and nutrients in biochars. In B. Singh, M. Camps-Arbestain, & J. Lehmann (Eds.), *Biochar: a guide for analytical methods* (pp. 95-108). Clayton South: CSIRO Publishing.

EPA, U. E. (2013). *Clean water act priority pollutants*. Retrieved 03/28/ 2017, from http://water.epa.gov/scitech/methods/cwa/pollutants.cfm

Fakhru'l-Razi, A., Pendashteh, A., Abdullah, L., Biak, D., Madaeni, S., & Abidin, Z. (2009). Review of technologies for oil and gas produced water treatment. *Journal of Hazardous Materials,* 170, 530-551.

FAO. (1987). *Simple technologies for charcoal making* (Second ed.). Rome: FAO Forestry Paper 41.

FAOSTAT. (2014). *Food and agriculture organization of the United Nations*. Retrieved 01/31/2018, from http://www.fao.org/faostat/en

Farrell, J., Cernansky, N., Dryer, F., Friend, D., Hergart, C., Law, C., McDavid, R. M., Patel, A. K., Mueller, C. J., & Pitsh, H. (2007). Development of an experimental database and kinetic models for surrogate diesel fuels. *Society of Automotive Engineers, SAE Paper 2007-01-0201*.

Fernández Marcos, M., Fuentes Colmeiro, R., & López Mosquera, M. (1994). Los suelos de Galicia. Problemas de fertilidad y corrección. *Agricultura: Revista Agropecuaria*, 742, 388-391.

Fingas, M. (2012). *Oil spills in the basic of oil spill clean-up*. Boca Raton: CRC Press.

Fries, M., Zhou, J., Chee-Sanford, J., & Tiedje, J. M. (1994). Isolation, characterization and distribution of denitrifying toluene degraders from a variety of habitats. *Applied and Environmental Microbiology,* 60, 2802-2810.

Fuertes, A. B., Camps-Arbestain, M., Sevilla, M., Maciá-Angulló, J. A., Fiol, S., López, R., Smernik, R. J., Aitkenhead, W. P., Arce, F., & Macías, F. (2010). Chemical and structural properties of carbonaceous products

obtained by pyrolysis and hydrothermal carbonisation of corn stover. *Australian Journal of Soil Research,* 48, 618-626.

Galinato, S., Yoder, J., & Granatstein, D. (2011). The economic value of biochar in crop production and carbon sequestration. *Energy Policy*, 39, 6344-6350.

García-Ares, M. (2015). *Los biochar: propiedades, producción y aplicaciones.* Tesis doctoral, Universidade de Santiago de Compostela.

Gaunt, J., & Lehmann, J. (2008). Energy balance and emissions associated with biochar sequestration and pyrolysis production. *Environmental Science & Technology,* 42, 4152-4158.

Gil-Sotres, F. (1980). *Estudio de los suelos de la Sierra del Barbanza.* Tesis doctoral, Universidade de Santiago de Compostela.

Glaser, B. (2007). Prehistorically modified soils of central Amazonia: a model for sustainable agriculture in the twenty-first century. *Philosophical Transactions of The Royal Society,* 362, 187-196.

Glaser, B., & Birk, J. J. (2012). State of scientific knowledge on properties and genesis os Anthropogenic Dark Earths in Central Amazonia (terra preta de Índio). *Geochimica et Cosmochimica Acta,* 82, 39-51.

Glaser, B., Balashov, E., Haumaier, L., Guggenberger, G., & Zech, W. (2000). Black carbon in density fractions of anthropogenic soils of the Brazilian Amazon region. *Organic Geochemistry, 31*, 669-678.

Glaser, B., Haumaier, L., Guggenberger, G., & Zech, W. (2001). The 'Terra Preta' phenomenon: a model for sustainable agriculture. *Naturwissenschaften,* 88, 37-41.

González Laxe, F. (2013). Galicia, una potencia forestal sin explotar. *La Voz de Galicia*. 5/5/2013.

Goss, K., & Schwarzenbach, R. (2003). Rules of thumb for assessing equilibrium partitioning of organic compounds; success and pitfalls. *Journal of Chemical Education,* 80, 450-455.

Graber, E., Tsechansky, L., Gerstl, Z., & Lew, B. (2012). High surface area biochar negatively impacts herbicide efficacy. *Plant Soil,* 353, 95-106.

Guerrero, C. (2010). Espectroscopía de infrarrojo cercano (NIR) para la estimación de las temperaturas alcanzadas en suelos quemados. In A. Cerdá, & A. Jordán (Eds.), *Actualización en métodos y técnicas para el estudio de los suelos afectados por incendios forestales* (pp. 259-288). Valencia: Cátedra de Divulgación de la Ciencia.

Gupta, R., & Kulkarni, G. (2011). Removal of organic compounds from water by using a gold nanoparticle–poly(dimethylsiloxane) nanocomposite foam. *ChemSusChem,* 4, 737-747.

Haefele, S. M. (2007). Black soil, green rice. *Rice Today*, 6, 26-27.

Hale, S., Lehmann, J., Rutherfor, D., Zimmerman, A., Bachmann, R., Shitumbanuma, V., & Cornelissen, G. (2012). Quantifying the total and bioavailable polycyclic aromatic hydrocarbons and dioxins in biochars. *Environmental Science & Technology,* 46, 2830-2838.

Harvey, O. R., Kuo, L. J., Zimmerman, A. R., Louchouarn, P., Amonette, J. E., & Herbert, B. E. (2012). An index-based approach to assessing recalcitrance and soil carbon sequestration potential of engineered black carbons (biochars). *Environmental Science & Technology,* 46, 1415-1421.

Hedges, J., Eglinton, G., Hatcher, P., Kirchman, D., Arnosti, C., Derenne, S., & Rullkötter, J. (2000). The molecularly-uncharacterised component of nonliving organic matter in natural environments. *Organic Geochemistry,* 31, 945-958.

Hina, K., Bishop, P., Camps Arbestain, M., Calvelo-Pereira, R., Maciá-Angulló, J., Hindmarsh, J., Hanly, J. A., & Hedley, M. J, (2010). Producing

biochars with enhanced surface activity through alkaline pretreatment of feedstocks. *Australian Journal of Soil Research,* 48, 606-617.

Hung Chia, C., Munroe, P., Joseph, S., & Lin, Y. (2010). Microscopic characterisation of synthetic Terra preta. *Australian Journal of Soil Research,* 48, 593-605.

IBI (2015). *Standardized product definition and product testing guidelines for biochar that is used in soil. Version 2.1*. Retrieved 16/03/2017, from International Biochar Initiative: http://www.biochar-international.org

IHS Markit. (2016). *SiC and GaN power semiconductors device report.* IHS Technology.

INE (2006). *Estadísticas sobre la generación de residuos en la agricultura 2003-2006.* Madrid: Instituto Nacional de Estadística.

IPCC (2005). IPCC Special report on *carbon dioxide capture and storage.* Prepared by Working group III of the Intergovernmental Panel on Climate Change. In B. Metz; O. Davidson; H. Coninck; M. Loos; & L. Meyer (Eds.). Cambridge: Cambridge University Press.

IPCC (2007). Climate change 2007: Impacts, adaptation and vulnerability. Contribution of working group II to the fourth assessment report of the intergovernmental panel on climate change. In M. Parry, O. Canziani, J. Palutikof, P. van der Kinden & C. Hanson (Eds.). Cambridge: Cambridge University Press.

IPCC (2014). *Climate change 2014: synthesis report. Contribution of working groups I, II and III to the fifth assessment report of the intergovernmental panel on climate change.* Core Writing Team, R.K. Pachauri & L.A. Meyer Geneva, Switzerland.

Ippolito, J., Spokas, K., Novak, J., Lentz, R., & Cantrell, K. (2015). Biochar elemental composition and factors influencing nutrient retention. In J. Lehmann, & S. Joseph (Eds.), *Biochar for environmental management: science, technology and implementation* (pp. 139-163). London: Earthscan.

ITOF (2017). *Oil tanker spill statistics 2016.* Canterbury, UK: Impact PR & Design Limited.

Jecu, L., Gheorghe, A., Popea, F., Rosu, A., Stoica, A., & Stroescu, M. (2008). Potential of microbial species in biodegradation of volatile organic compounds from waters. *Chemical Engineering Transactions,* 14, 501-507.

Jeffery, S., Bezemer, M. C., Kuyper, T., Lehmann, J., Mommer, L., Sohi, S., van de Voorde, T. F. J., Wardle, D. A., & van Groeningen, J. (2015). The way forward in biochar research; targeting trade-offs between the potential wins. *GCB Bioenergy,* 7, 1-13.

Jestel, N. (2010). Raman Spectroscopy. In K. Bakeev (Ed.), *Process analytical technology: Spectroscopic tools and implementation strategies for the chemical and pharmaceutical industries.* (p. 195-243). Online: John Wiley & Sons, Ltd.

Joseph, S., Camps-Arbestain, M., Lin, Y., Munroe, P., Chia, C., Hook, J., Van Zwieten, L., Kimber, S., Cowie, A., Singh, B.P., Lehmann, J., Foidl, N., Smernik, R.J., & Amonette, J. E. (2010). An investigation into the reactions of biochar in soil. *Australian Journal of Soil Research,* 48, 501-515.

Judd, T. S., Attiwill, P. M., & Adams, M. A. (1996). Nutrient concentration in Eucalyptus: a synthesis in relation to differences between taxa, sites and components. In P. M. Attiwill, & M. A. Adams (Eds.), *Nutrition of Eucalyptus (*pp. 123-153). Collingwood: CSIRO Australia.

Kan, T., Strezov, V., & Evans, T. (2016). Lignocellulosic biomass pyrolysis: A review of product properties and effects of pyrolysis parameters. *Renewable and Sustainable Energy Reviews,* 57, 1126-1140.

Kanai, H., Inouye, V., Goo, R., Chow, R., Yazawa, L., & Maka, J. (1994). GC/MS analysis of MTBE, ETBE and TAME in gasolines. *Analytical Chemistry,* 66, 924-927.

Karhu, K., Mattila, T., Bergström, I., & Regina, K. (2011). Biochar addition to agricultural soil increased CH_4 uptake and water holding

capacity – Results from a short-term pilot field study. *Agriculture, Ecosystems & Environment,* 140, 309-313.

Kim, D., Song, W., & Lu, J. C. (2011). Interdisciplinary investigation of contaminants fate and transport at a former UST site (10 years case study). *Environmental Earth Sciences,* 64, 277-291.

Kinney, T., Masiello, C., Dugan, B., Hockaday, W., & Dean, M. (2012). Hydrologic properties of biochars produced at different temperatures. *Biomass and Bioenergy,* 41, 34-43.

Klason, P., Heidenstam, G., & Norlin, E. (1909). Untersuchungen zur holzverkohlung. I. Die trockene destillation der cellulose. *Angewandte Chemie*, 25, 1205-1214.

Klason, P., Heidenstam, G., & Norlin, E. (1910). Untersuchungen zur holzverkohlung. II. Die trockene destillation des Holzes von Kiefer, Fichte, Birke und Buche. *Angewandte Chemie*, 25, 1252-1257.

Kleber, M., Hockaday, W., & Nico, P. (2015). Characteristics of biochar: macro-molecular properties. In J. Lehmann, & S. Joseph (Eds.), *Biochar for environmental management: science, technology and implementation.* (pp. 111-137). London: Earthscan.

Knicker, H. (2011). Solid state CPMAS ^{13}C and ^{15}N NMR spectroscopy in organic geochemistry and how spin dynamics can either aggravate or improve spectra interpretation. *Organic Geochemistry,* 42, 867-890.

Komang Ralebitso-Senior, T., & Orr, C. (2016). Microbial ecology analysis of biochar-augmented soils: setting the scene. In T. Komang Ralebitso-Senior, & C. Orr (Eds.), *Biochar application: Essential soil microbial ecology* (pp. 1-40). Amsterdam: Elsevier.

Kookan, R., Graber, E., & Smernik, R. (2017). Guiding principles for measuring sorption of organic compounds on biochars. In B. Singh, M. Camps-Arbestain, & J. Lehmann (Eds.), *Biochar a guide to analytical methods* (pp. 141-150). Clayton South: CSIRO Publishing.

Kookana, R. S. (2010). The role of biochar in modifying the environmental fate, bioavailability, and efficacy of pesticides in soils: a review. *Australian Journal of Soil Research,* 48, 627-637.

Krull, I. E., Baldock, J., Skjemstad, J., & Smernik, R. (2009). Characteristics of biochar: organo-chemical properties. In J. Lehmann, & J. Joseph (Eds.), *Biochar for environmental management: science and technology* (pp. 53-66). London: Earthscan.

Kuppussamy, S., Thavamani, P., Megharaj, M., Venkateswarlu, K., & Naidu, R. (2016). Agronomic and remedial benefits and risks of applying biochar to soil: Current knowledge and future research directions. *Environment International,* 87, 1-12.

Kupryianchyk, D., Hale, S., Zimmerman, A., Harvey, O., Rutherford, D., Abiven, S., Knicker, H., Schmidt, H. P., Rumpel, C., & Cornelissen, G. (2016). Sorption of hydrophobic organic compounds to a diverse suite of carbonaceous materials with emphasis on biochar. *Chemosphere,* 144, 879-887.

Kurchania, A. (2012). Biomass Energy. In C. Baskar, S. Baskar, & R. Dillon (Eds.), *Biomass conversion* (pp. 91-122). Verlag Berlin Heidelberg: Springer.

Kusumo, B., Arbestain, M., Mahmud, A., Hedley, M., Hedley, C., Pereira, R., Wang, T., & Singh, B. (2011). Assessing biochar stability indices using near infrared spectroscopy. *Plant and Soil,* 338, 233-245.

Laird, D. A. (2008). The charcoal vision: A win–win–win scenario for simultaneously producing bioenergy, permanently sequestering carbon, while improving soil and water quality. *Agronomy Journal,* 100, 178–181.

Laird, D., Fleming, P., Wang, B., Horton, R., & Karlen, D. (2010). Biochar impact on nutrient leaching from a Midwestern agricultural soil. *Geoderma,* 158, 436-442.

Lal, R. (2007). Carbon sequestration. *Philosophical Transactions of the Royal Society B: Biological Sciences,* 363, 815-830.

Lattao, C., Cao, X., Mao, J., Schmidt-Rohr, K., & Pignatello, J. (2014). Influence of molecular structure and adsorbent properties on sorption of organic compounds to a temperature series of wood chars. *Environmental Science & Technology,* 48, 4790-4798.

Lehmann, J. (2007). A handful of carbon. *Nature*, 447, 143-144.

Lehmann, J. (2009). Terra Preta Nova - Where to from here? In W. I. Woods, W. G. Teixeira, J. Lehmann, C. Steiner, A. M. G. A. WinklerPrins, & L. Rebellato (Eds.), *Amazonian Dark Earths: Wim Sombroek's Vision* (p. 473-486). Dordrecht: Springer.

Lehmann, J., & Joseph, S. (2009). *Biochar for environmental management: science and technology*. London: Earthscan.

Lehmann, J., & Joseph, S. (2015). *Biochar for environmental management: science, technology and implementation*. London: Earthscan.

Lehmann, J., Abiven, S., Kleber, M., Pan, G., Singh, B. P., Sohi, S., & Zimmerman, A. R. (2015). Persistence of biochar in soil. In J. Lehmann, & S. Joseph (Eds.), *Biochar for environmental management: science, technology and implementation* (pp. 235-282). London: Earthscan.

Lehmann, J., Rilling, M., Thies, J., Masiello, C. A., Hockaday, W., & Crowley, D. (2011). Biochar effects on soil biota – A review. *Soil Biology and Biochemistry,* 43, 1812-1836.

Leifeld, J. (2007). Thermal stability of black carbon characterised by oxidative differential scanning calorimetry. *Organic Geochemistry*, 38, 112-127.

Liang, B., Lehmann, J., Solomon, D., Kinyangi, J., Grossman, J., O'Neill, B., Neves, E. (2006). Black carbon increases cation exchange capacity in soils. *Soil Science Society of America Journal,* 70, 1719-1730.

Liao, R., Gao, B., & Fang, J. (2013). Invasive plants as feedstock for biochar and bioenergy production. *Bioresource Technology*, 140, 439-442.

Limousin, G., Gaudet, J. P., Charlet, L., Szenknect, S., Barthès, V., & Krimissa, M. (2007). Sorption isotherms: A review on physical bases, modelling and measurement. *Applied Geochemistry,* 22, 249-275.

Lorenz, K., & Lal, R. (2016). *Soil organic carbon – An appropriate indicator to monitor trends of land and soil degradation within the SDG framework?* Dessau-Roßlau: Umweltbundesamt. German Environment Agency.

Lorenzo, P., & Rodríguez-Echeverría, S. (2015). Cambios provocados en el suelo por la invasión de acacias australianas. *Ecosistemas,* 24, 59-66.

Lorenzo, P., Rodríguez, J., González, L., & Rodríguez-Echeverría, S. (2016). Changes in microhabitat, but not allelopathy, affect plant establishment after *Acacia dealbata* invasion. *Journal of Plant Ecology,* 10, 610-617.

Lormas, J., Urbano, C., Merino, T., & Camarero, E. (2001). *Valorización de Biomasa en el País Vasco.* Bilbao: Ente Vasco de la Energía.

Macías, F., & Calvo de Anta, R. (2001). Los suelos. In A. Precedo Ledo & J. Sancho Comíns (Eds.), *Atlas de Galicia* (pp. 173-218). Santiago de Compostela: Xunta de Galicia.

Macías, F., & Camps Arbestain, M. (2010). Soil carbon sequestration in a changing global environment. *Mitigation and Adaptation Strategies for Global Change*, 15, 511-529.

Macías, F., Calvo de Anta, R., Rodríguez-Lado, L., Verde, R., Pena-Pérez, X., & Camps-Arbestain, M. (2004). El sumidero de carbono de los suelos de Galicia. *Edafología,* 11, 341-376.

Macías, F., Camps-Arbestain, M., & Rodríguez-Lado, L. (2005). Alternativas de secuestro de carbono orgánico en suelos y biomasa de Galicia. *Recursos Rurais,* 1, 71-85.

Macías, F., Macías-García, F., Nieto, C., Verde, J., Pérez, C., Bao, M., & Camps-Arbestain, M. (2011). Gestión de residuos y cambio climático. In M. López Mosquera, & M. Sainz Osés (Eds.), *Gestión de residuos orgánicos de uso agrícola* (pp. 11-24). Santiago de Compostela: Servizo de Publicacións e Intercambio Científico, Universidade de Santiago de Compostela.

Mackay, D., Shiu, W. Y., Ma, K. C., & Lee, S. (2006). *Handbook of physical-chemical properties and environmental fate for organic chemicals.* Boca Raton: CRC Press.

Madgwick, H. A., & Frederick, D. J. (1988). Nutrient concentration within stems of *Pinus radiata*. *New Zealand Journal of Forestry Science,* 18, 221-225.

Mahmud, A., Hedley, M., Kusumo, B., & Camps Arbestain, M. (in preparation). Near-infrared Spectroscopy (NIRS) for predicting the maximum pyrolysis temperature of biochar.

MAPAMA. (2008). *Anuario Estadística Forestal*. Retrieved 01/2018, from http://www.mapama.gob.es/es/desarrollo-rural/temas/politica-forestal/inventario-cartografia/inventario-forestal-nacional/default.aspx

Mašek, O., Brownsort, P., Cross, A., & Sohi, S. (2011). Influence of production conditions on the yield and environmental stability of biochar. *Fuel,* 103, 151-155.

Masiello, C. (2004). New directions in black carbon organic geochemistry. *Marine Chemistry,* 92, 201-213.

Masiello, C., Dugan, B., Brewer, C., Spokas, K., Novak, J. M., Liu, Z., & Sorrenti, G. (2015). Biochar effects on soil hydrology. In J. Lehmann, & S. Joseph (Eds.), *Biochar for environmental management: science, technology and implementation* (pp. 543-562). London: Earthscan.

McBeath, A., Smernik, R., Krull, E., & Lehmann, J. (2014). The influence of feedstock and production temperature on biochar carbon chemistry: A solid-state ^{13}C NMR study. *Biomass and Bioenergy,* 60, 121-129.

McDonald-Wharry, J., Manley-Harris, M., & Pickering, K. (2013). Carbonisation of biomass-derived chars and the thermal reduction of a graphene oxide sample studied using Raman. *Carbon,* 59, 383-405.

Méndez, A., Gómez, A., Paz-Ferreiro, J., & Gascó, G. (2012). Effects of sewage sludge biochar on plant metal availability after application to a Mediterranean soil. *Chemosphere,* 89, 1354-1359.

Ministerio de Agricultura, Alimentación y Medio Ambiente. (2012). *Producción y consumo sostenibles y residuos agrarios.* Madrid: M.A.P.A.

Ministerio de Agricultura, Pesca y Alimentación (M.A.P.A.). (1986). *Métodos oficiales de análisis. Tomo III, Secretaría General Técnica.* Madrid: M.A.P.A.

Miramontes, A. (2009). *La industria de la madera en Galicia. La significación del subsector del mueble.* Tesis doctoral*, Universidade de* Santiago de Compostela.

Monlau, F., Francavilla, M., Sambusiti, C., Antoniou, N., Solhy, A., Libutti, A., Zabaniotou, A., Barakat, A., & Monteleone, M. (2016). Toward a functional integration of anaerobic digestion and pyrolysis for a suitable resource management. Comparison between solid-digestate and its derived pyrochar as soil amendment. *Applied Energy,* 169, 652-662.

Morhart, C., Sheppard, J. P., Schuler, J. K., & Spiecker, H. (2016). Above-ground woody biomass allocation and within tree carbon and nutrient distribution of wild cherry (*Prunus avium* L.) - a case study. *Forest Ecosystems,* 3, 1-15.

Morillo, E., & Villaverde, J. (2017). Advanced technologies for the remediation of pesticide-contaminated soils. *Science of the Total Environment,* 586, 576-597.

Müller, A., Schmidhuber, J., Hoogeveen, J., & Steduto, P. (2008). Some insights in the effect of growing bio-energy demand on global food security and natural resources. *Water Policy*, 10, 83-94.

Murphy, J., & Riley, J. (1962). A modified single solution method for the determination of phosphate in natural waters. *Analytica Chimica Acta, 27*, 31-36.

NASA. (2017). *Global climate change. Vital signs of the Planet*. Retrieved 11/12/2017, from https://climate.nasa.gov/

Navarro-Pedreño, J., Moral, R., Gómez Lucas, I., & Mataix, J. (1995). *Residuos orgánicos y agricultura.* Alicante: Universidad de Alicante.

Novak, J., & Busscher, W. (2013). Selection and use of designer biochars to improve characteristics of South-eastern USA Coastal Plain degraded soils. In J. Lee (Ed.), *Advanced Biofuels and Bioproducts* (pp. 69-96). New York: Springer.

Novak, J., Busscher, W., Laird, D., Ahmedna, M., Watts, D., & Niandou, M. (2009). Impact of biochar amendment on fertility of a south-eastern coastal plain soil. *Soil Science,* 174, 101-112.

Oleszczuk, P., Cwikła-Bundyra, W., Bogusz, A., Skwarek, E., Ok, Y. S., & Sik, J. (2016). Characterization of nanoparticles of biochars from different biomass. *Journal of Analytical and Applied Pyrolysis,* 121, 165-172.

Peech, M., Alexander, L., Dean, L., & Reed, J. (1947). Methods of soil analysis for soil fertility investigations. *USDA Circular,* 757, 7-25.

Pointner, M., Kuttner, P., Obrlik, T., Jäger, A., & Kahr, H. (2014). Composition of corncobs as a substrate for fermentation of biofuels. *Agronomy Research,* 12, 391-396.

Pratt, K., & Moran, D. (2010). Evaluating the cost-effectiveness of global biochar mitigation potential. *Biomass and Bioenergy,* 34, 1149-1158.

Qian, K., Kumar, A., Zhang, H., Bellmer, D., & Huhnke, R. (2015). Recent advances in utilization of biochar. *Renewable and Sustainable Energy Reviews,* 42, 1055-1064.

Rajapaksha, A., Mohan, D., Igalavithan, A., Lee, S., & Ok, S. Y. (2015). Definitions and fundamentals of biochar. In Y. S. Ok, S. Uchimiya, S. Chang, & N. Bolan (Eds.), *Biochar: production, characterization and applications* (pp. 4-16). Boca Raton: CRC Press.

Rao, M., Sultana, R., & Kota, S. (2017). *Solid hazardous waste management.* Singapore: Butterworth-Heinemann.

Ripberger, G. D. (2016) *A study of the importance of secondary reactions in char formation and pyrolysis.* PhD Thesis. Massey University.

Riuji Lohri, C., Mtoro Rajabu, H., Sweeney, D. J., & Zurbrügg, C. (2016). Char fuel production in developing countries - A review of urban biowaste carbonization. *Renewable and Sustainable Energy Reviews*, 59, 1514-1530.

Rodríguez, J., Lorenzo, P., & González, L. (2017). Different growth strategies to invade undisturbed plant communities by *Acacia dealbata* link. *Forest Ecology and Management,* 399, 47-53.

Sander, M., & Pignatello, J. (2005). Characterization of charcoal adsorption sites for aromatic compounds: Insights drawn from single-solute and bi-solute competitive experiments. *Environmental Science & Technology,* 39, 1606-1615.

Sano, T., Hasegawa, M., Kawakami, Y., & Yanigishita, H. (1995). Separation of methanol/mmethyl-tert-butyl ether mixture by pervaporation using silicalite membrane. *Journal of Membrane Science,* 107, 193-196.

Sanz, M., Dana, E. D., & Sobrino, E. (2004). *Atlas de las plantas alóctonas invasoras en España.* Madrid: Ministerio de Medio Ambiente.

Savitzky, A., & Miller, J. (1964). Smoothing and differentiation of data by simplified least squares procedure. *Analytical Chemistry,* 36, 1627-1639.

Schachtman, D., Reid, R. J., & Ayling, S. (1998). Phosphorus uptake by plants: from soil to cell. *Plant Physiology,* 116, 447-453.

Schimmelpfennig, S., & Glaser, B. (2012). One step forward toward characterization: Some important material properties to distinguish biochars. *Journal of Environmental Quality,* 41, 1001-1013.

Serrano, A., & Gallego, M. (2006). Sorption study of 25 volatile organic compounds in several Mediterranean soils using headspace-gas chromatography-mass spectrometry. *Journal of Chromatography A,* 1118, 261-270.

Shackley, S., Clare, A., Joseph, S., McCarl, B., & Schmidt, H. (2015). Economic evaluation of biochar systems: current evidence and challenges. In J. Lehmann, & S. Josehp (Eds.), *Biochar for environmental management: science, technology and implementation* (pp. 813-851). London: Earthscan.

Shareef, T. M. E. S., & Zhao, B. (2017). Review Paper: The fundamentals of biochar as a soil amendment tool and management in agriculture scope: An overview for farmers and gardeners. *Journal of Agricultural Chemistry and Environment*, 6, 38-61.

SilicioFerroSolar S.L. (2016). *Data sheet solar grade silicon.* Technical Report. Grupo FerroAtlántica.

Silvani, L., Vrchotova, B., Kastanek, P., Demnerova, K., Pettiti, I., & Papini, M. P. (2017). Characterizing biochar as alternative sorbent for oil spill remediation. *Scientific Reports,* 7(43912), 1-10.

Sipilä, K., Kuoppala, E., Fagernäs, L., & Oasmaa, A. (1998). Characterization of biomass-based flash pyrolysis oils. *Biomass and bioenergy,* 2, 103-111.

Site, A. (2001). Factors affecting sorption of organic compounds in natural sorbent/water systems and sorption coefficients for selected pollutants. A Review. *Journal of Physical and Chemical Reference Data,* 30, 187-439.

Smernik, R. (2009). Biochar and sorption of organic compounds. In J. Lehmann, & S. Joseph (Eds.), *Biochar for environmental management: science and technology* (pp. 289-300). London: Earthscan.

Sohi, S., Krull, E., Lopez-Capel, E., & Bol, R. (2010). A review of biochar and its use and function in soil. *Advances in Agronomy* 105, 47-82.

Sombroek, W., Kern, D., Rodrigues, T., Cravo, M., Cunha, T., Woods, W., & Glaser, B. (2002). *Terra Preta* and *Terra Mulata*: pre-Columbian Amazon kitchen middens and agricultural fields, their sustainability and their replication. 17th World Congress of Soil Science, Bangkok: Contribution to Symposium 18 - Anthropogenic factors of soil formation.

Sparkes, J., & Stoutjesdijk, P. (2011). *Biochar: implications for agricultural productivity.* Canberra: ABARES technical report 11.6, Australian Bureau of Agricultural and Resource Economics and Science.

Speller, C. (1993). The potential for growing biomass crops for fuel on surplus land in the UK. *Outlook on Agriculture,* 22, 23-29.

Spokas, K. A. (2010). Review of the stability of biochar in soils: predictability of O:C molar ratios. *Carbon Management,* 1, 289-303.

Spokas, K. A., Cantrell, K. B., Novak, J. M., Archer, D. W., Ippolito, J. A., Collins, H. P., Boateng, A. A., Lima, I. M., Lab, M. C., McAloon, A. J., Lentz, R. D., & Nichols, K. A. (2012). Biochar: A synthesis of its agronomic impact beyond carbon sequestration. *Journal of Environmental Quality*, 41, 973-989.

Sposito, G. (1984). *The surface chemistry of soils.* New York: Oxford University Press.

Steiner, C. (2016). Considerations in biochar characterization. In M. Guo, Z. He, & M. Uchimiya (Eds.), *Agricultural and Environmental Applications of Biochar: Advances and Barriers* (pp. 87-100). Madison, USA: Soil Science Society of America Special Publication 63.

Steiner, C., Bayode, A., & Komang Ralebitso-Senior, T. (2016). Feedstock and production parameters: Effects on biochar properties and microbial communities. In T. Komang Ralebitso-Senior, & C. Orr (Eds.), *Biochar application: Essential soil microbial ecology* (pp. 41-54). Amsterdam: Elsevier.

Suárez-Abelenda, M., Kaal, J., Camps-Arbestain, M., Knicker, H., & Macías, F. (2014). Molecular characteristics of permanganate- and dichromate oxidation-resistant soil organic matter from a black-C-rich colluvial soil. *Soil Research,* 52, 164-179.

Sun, K., Jin, J., Keilweit, M., Kleber, M., Wang, Z., Pan, Z., & Xing, B. (2012). Polar and aliphatic domains regulate sorption of phthalic acid esters (PAEs) to biochars. *Bioresource Technology,* 140, 120-127.

Syuhada, A., Shamshuddin, J., Fauziah, C., Rosenani, A., & Arifin, A. (2016). Biochar as soil amendment: Impact on chemical properties and corn nutrient uptake in a Podzol. *Canadian Journal of Soil Science,* 96, 400-412.

Ter Braak, C., & Šmilauer, P. (2002). CANOCO reference manual and CanoDraw for Windows User's guide: Software for Canonical Community Ordination (version 4.5). *Microcomputer Power.*

Tirol-Padre, A., & Ladha, J. (2004). Assessing the reliability of permanganate oxidizable carbon as an index of soil labile carbon. *Soil Science Society of America Journal*, 68, 969-978.

Uchimiya, M., Wartelle, L., Klasson, K., Fortier, C., & Lima, I. (2011). Influence of pyrolysis temperature on biochar property and function as a heavy metal sorbent in soil. *Journal of Agriculture and Food Chemistry,* 59, 2501-2510.

United Nations (2009). *United Nations framework convention on climate change*. (U. Nations, Ed.) Retrieved 03/09/2017, from http://unfccc.int/essential_background/glossary/items/3666.php#C

United Nations, Department of Economic and Social Affairs, Population Division. (2015). *World population prospects: The 2015 revision, key finding and advance tables.* Working Paper N ESA/WP.241.

Uri, V., Vares, A., Tullus, H., & Kanal, A. (2007). Above-ground biomass production and nutrient accumulation in young stands of silver birch on abandoned agricultural land. *Biomass and Bioenergy,* 31, 195-204.

USEPA, (2010). *Waste and clean-up risk assessment glossary*. Retrieved 07/01/2015, from http://www.epa.gov/oswer/riskassessment/glossary.htm

Van de Velden, M., Baeyens, J., Brems, A., Janssens, B., & Dewil, R. (2010). Fundamentals, kinetics and endothermicity of the biomass pyrolysis reaction. *Renewable Energy,* 35, 232-242.

Van Zwieten, L., Kimber, S., Morris, S., Chan, K., Downie, A., Rust, J., Joseph, S., & Cowie, A. (2010). Effects of biochar from slow pyrolysis of papermill waste on agronomic performance and soil fertility. *Plant Soil,* 327, 235-246.

Viscarra Rossel, R. (2008). ParLeS: Software for chemometric analysis of spectroscopic data. *Chemometrics and Intelligent Laboratory Systems,* 90, 72–83.

Visioli, G., Conti, D., Menta, C., Bandiera, M., Malcevschi, A., Jones, D. L., & Vamerali, T. (2016). Assessing biochar ecotoxicology for soil amendment by root phytotoxicity bioassays. *Environmental Monitoring and Assessment*, 188: 166.

Walkley, A., & Black, I. (1934). An examination of Degtjareff Method for determining soil organic matter and a proposed modification of the chromic acid tiration method. *Soil Science,* 63, 251-264.

Wang, J., Xiong, Z., & Kuzyakov, Y. (2016). Biochar stability in soil: meta-analysis of decomposition and priming effects. *Global Change and Biology Bioenergy,* 8, 512-523.

Wang, T., Camps-Arbestain, M., Hedley, M., & Bishop, P. (2012a). Chemical and bioassay characterisation of nitrogen availability in biochar produced from dairy manure and biosolids. *Organic Geochemistry,* 51, 45-54.

Wang, T., Camps-Arbestain, M., & Hedley, M. (2012b). The fate of phosphorus of ash-rich biochars in a soil-plant system. *Plant and Soil,* 375, 61-64.

Wang, T., Camps-Arbestain, M., Hedley, M., & Bishop, P. (2012c). Predicting phosphorus bioavailability from high-ash biochars. *Plant and soil*, 357, 173-187.

Wang, T., Camps-Arbestain, M., Hedley, M., Pal Singh, B., Calvelo-Pereira, R., & Wang, C. (2014). Determination of carbonate-C in biochars. *Soil Research*, 52, 495-504.

Weidenhamer, J., & Callaway, R. (2010). Direct and indirect effects of invasive plants on soil chemistry and ecosystem function. *Journal of Chemical Ecology,* 36, 5-69.

Wijmans, J., Kamaruddin, H., Segelke, S., Wessling, S., & Baker, R. (2006). Removal of dissolved VOCs from water with an air stripper/membrane vapor separation system. *Separation Science and Technology,* 32, 2267-2287.

Wilbur, S., & Bosch, S. (2004). *Interaction profile for: Benzene, Toluene, Ethylbenzene, and Xylenes (BTEX).* US Agency for Toxic Substances and Disease Registry.

WMO (2017). T*he state of greenhouse gases in the atmosphere based on global observations through 2016. Greenhouse Gas Bulletin,* World Meteorological Organization.

Woods, W., Teixeira, W., Lehmann, J., WinklerPrins, A. M. G. A., & Rebellato, L. (2009). *Amazonian dark earths: Wim Sombroek´s Vision.* Dordrecht: Springer.

Woolf, D., Amonette, J., Street-Perrott, A., Lehmann, J., & Joseph, S. (2010). Sustainable biochar to mitigate global climate change. *Nature Communications,* 1, 56.

WRB, IUSS Grupo de Trabajo. (2007). *Base Referencial Mundial del Recurso Suelo. Primera actualización 2007.* FAO, Roma: Informes sobre Recursos Mundiales de Suelos N° 103.

Xiao, L., Bi, E., Du, B., Zhao, X., & Xing, C. (2014). Surface characterization of maize-straw-derived biochars and their sorption performance for MTBE and benzene. *Environmental Earth Sciences,* 71, 5195-5205.

Xiao, X., Chen, Z., & Chen, B. (2016). H/C atomic ratio as a smart linkage between pyrolytic temperatures, aromatic clusters and sorption properties of biochars derived from diverse precursory materials. *Nature Scientific reports,* 6, (22644), 1-13.

Xie, T., Sadasivam, B. Y., Reddy, K. R., Wang, C., & Spokas, K. (2010). Review of the effects of biochar amendment on soil properties and carbon sequestration. *Journal of Hazardous, Toxic, and Radioactive Waste,* 20, 04015013.

Yamauchi, S., & Kurimoto, Y. (2003). Raman spectroscopic study on pyrolysed wood and bark of Japanese cedar: Temperature dependence of Raman parameters. *Journal of Wood Science,* 49, 235-240.

Yan, R., Yang, H., Chin, T., Liang, D. T., Chen, H., & Zheng, C. (2005). Influence of temperature on the distribution of gaseous products from pyrolyzing palm oil wastes. *Combustion and Flame*, 142, 24-32.

Yang, H., Yan, R., Chen, H., Lee, D., & Zheng, C. (2007). Characteristics of hemicellulose, cellulose and lignin pyrolysis. *Fuel,* 86, 1781-1788.

Yoder, J., Galinato, S., Granatstein, D., & Garcia-Pérez, M. (2011). Economic tradeoff between biochar and bio-oil production via pyrolysis. *Biomass and Bioenergy,* 35, 1851-1862.

Yuan, J.-H., Xua, R.-K., & Zhang, H. (2011). The forms of alkalis in the biochar produced from crop residues at different temperatures. *Bioresource Technology,* 102, 3488-3497.

Zadaka-Amir, D., Nasser, A., Nir, S., & Mishael, Y. (2012). Removal of methyl tertiary-butyl ether (MTBE) from water by polymer–zeolite composites. *Microporous and Mesoporous Materials,* 151, 216-222.

Zaib, Q., Aina, O., & Ahmad, F. (2014). Using multi-walled carbon nanotubes (MWNTs) for oilfield produced water treatment with environmentally acceptable endpoints. *Environmental Science: Processes & Impacts,* 16, 2039-2047.

Zhang, A., Liu, Y., Pan, G., Hussain, Q., Li, L., Zheng, J., & Zhang, X. (2012). Effect of biochar amendment on maize yield and greenhouse gas emissions from a soil organic carbon poor calcareous loamy soil from Central China Plain. *Plant Soil,* 351, 263-265.

Zhang, G., Zhang, Q., Sun, K., Liu, X., Zheng, W., & Zhao, Y. (2011). Sorption of simazine to corn straw biochars prepared at different pyrolytic temperatures. *Environmental Pollution,* 159, 2594-2601.

Zhang, H., & Kovar, J. (2009). Fractionation of soil phosphorus. In J. Kovar, & G. Pierzynski (Eds.), *Methods for P analysis for soils, sediments, residuals, and waters* (pp. 50-60). Manhattan: Southern Cooperative Series Bulletin.

Zhang, M., & Lu, L. (2015). Biochar for organic contaminant management in water and wastewater. In Y. S. Ok, S. Uchimiya, S. X. Chang, & N. Bolan (Eds.), *Biochar: Production, characterization and applications* (pp. 221-244). Boca Raton: CRC Press.

Zhang, X., Gao, B., Zhen, Y., Hu, X., Creamer, A., Annable, M., & Li, Y. (2017). Biochar for volatile organic compound (VOC) removal: Sorption performance and governing mechanisms. *Bioresource Technology,* 245, 606-614.

Zhang, X., McGrouther, K., He, L., Huang, H., Lu, K., & Wang, H. (2015). Biochar for organic contaminant management in soil. In Y. S. Ok, S. M. Uchimiya, S. X. Chang, & N. Bolan (Eds.), *Biochar: production, characterization and applications* (pp. 140-165). Boca Raton: CRC Press.

Zhao, L., Cao, X., Masekb, O., & Zimmerman, A. (2013). Heterogeneity of biochar properties as a function of feedstock sources and production temperatures. *Journal of Hazardous Materials,* 256–257, 1-9.

Zwetsloot, M., Lehmann, J., Taryn, B., Vanek, S., Hestrin, R., & Nigussie, A. (2016). Phosphorus availability from bone char in a P-fixing soil influenced by root-mycorrhizae-biochar interactions. *Plant Soil,* 408, 95-105.

USC
UNIVERSIDADE
DE SANTIAGO
DE COMPOSTELA

Supporting Information

USC
UNIVERSIDADE
DE SANTIAGO
DE COMPOSTELA

A. Supporting Information Chapter 4

Table S A.1 Results of TGA-DSC following the method established by Harvey et al. (2012). The temperature at 50% weight loss (Temp W50%) and R50 Index were calculated from the corrected TGA curve. The peak temperature of uppermost peak and its contribution to the total heat (calculated as explained by Leifeld, 2007) were obtained from the DSC curve.

TGA			DSC			
Name	**Temp W 50% (°C)**	**R50**	**Temp 1st Peak (°C)**	**Temp Last Peak (°C)**	**Contribution to total heat (%)**	**dH (kJ g^{-1})**
BAcB	501.5	0.57	494.4	561.0	2%	13.8
BAcSw-1	493.3	0.56	367.4	625.4	6.9%	13.1
BAcSw-2	496.5	0.56	356.5	588.4	2%	15.3
BAcSw-3	509.5	0.58	370.5	632.9	18%	13.6
BAcHw-1	521.5	0.59	384.7	657.2	9%	12.4
BAcHw-2	509.2	0.57	368.1	677.1	19%	12.5
BEu-1	458.0	0.52	368.5	515.0	12%	13.4
BEu-2	527.4	0.60	576.4	618.8	2%	16.9
BSd-1	457.8	0.52	377.7	465.6	1%	10.5
BSd-2	482.8	0.54	436.4	645.5	2%	11.4
BCm	409.4	0.46	340.9	555.7	43%	7.7
BOpc	500.3	0.56	315.6	487.4	58%	7.6
BCc-1	487.1	0.55	426.7	555.8	2%	15.0
BCc-2	568.5	0.64	456.9	683.0	11%	21.1
BCc-3	489.3	0.55	489.2	592.5	2%	17.4
BCn	533.5	0.60	447.1	704.0	22%	15.4
BMis	574.3	0.65	612.4	612.4	100%	16.4
BVs	537.6	0.61	442.7	660.4	19%	16.9
BTy	656.4	0.74	616.2	783.3	7%	17.1
BPl	581.8	0.66	479.8	785.7	21%	13.5
BSdG	474.7	0.54	438.5	573.8	9%	14.1
BPb	616.1	0.70	564.8	693.2	1%	19.2
BRh	528.2	0.60	438.4	593.8	6%	11.9

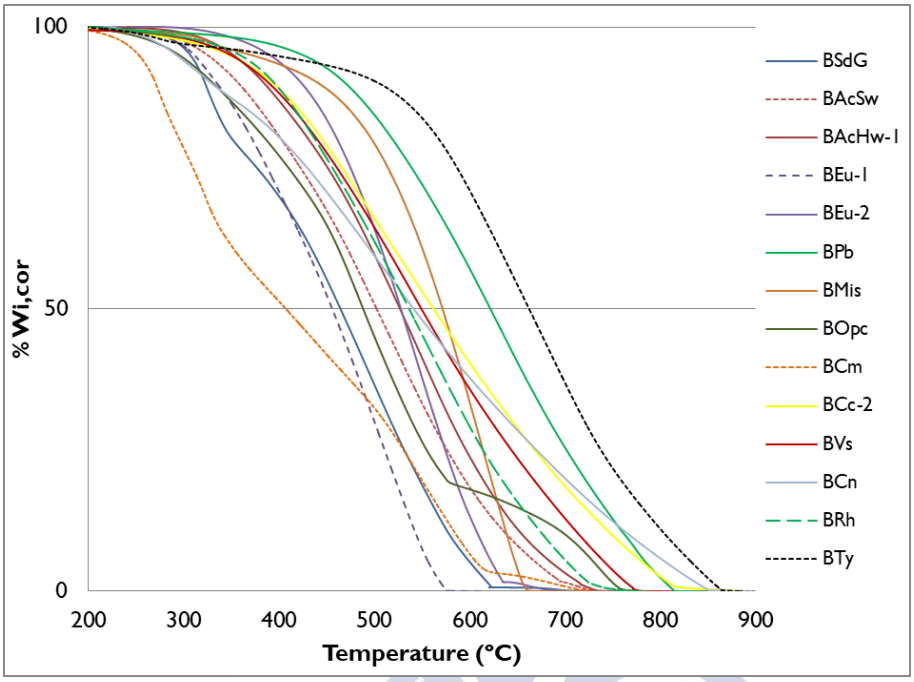

Figure S A.1 Corrected thermogravimetry patterns of biochars derived from different feedstocks according to the procedure of Harvey et al. (2012).

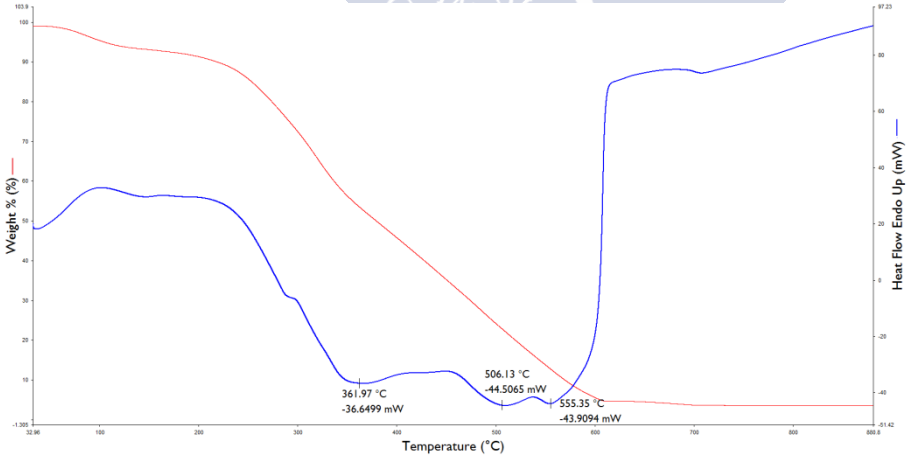

Figure S A.2 Thermogram of acacia bark feedstock (AcB) obtained with method (i). Weight loss (%) is represented in red and heat flow in blue. Peak height is shown in blue curve.

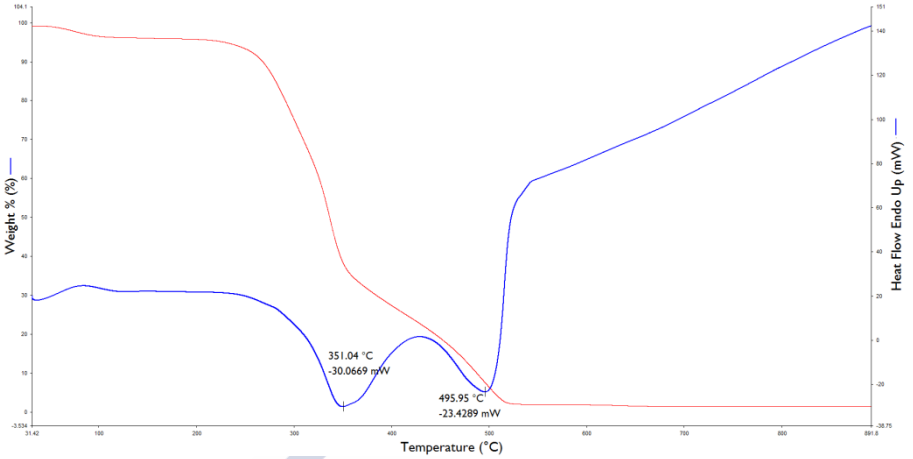

Figure S A.3 Thermogram of acacia sapwood feedstock (AcSw) obtained with method (i). Weight loss (%) is represented in red and heat flow in blue. Peak height is shown in blue curve.

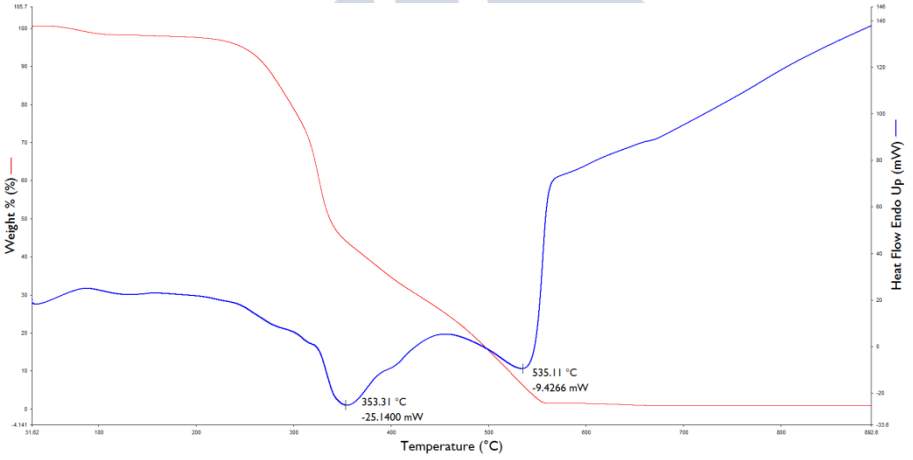

Figure S A.4 Thermogram of acacia heartwood feedstock (AcHw) obtained with method (i). Weight loss (%) is represented in red and heat flow in blue. Peak height is shown in blue curve.

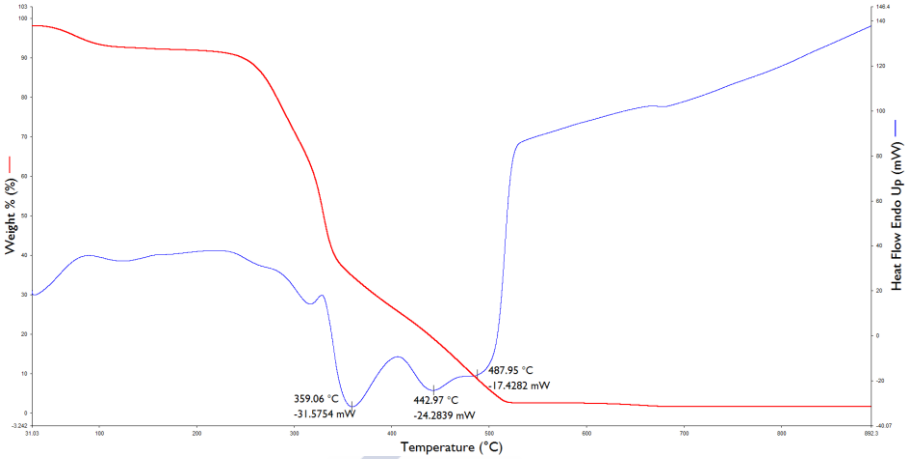

Figure S A.5 Thermogram of eucalyptus feedstock obtained with method (i). Weight loss (%) is represented in red and heat flow in blue. Peak height is shown in blue curve.

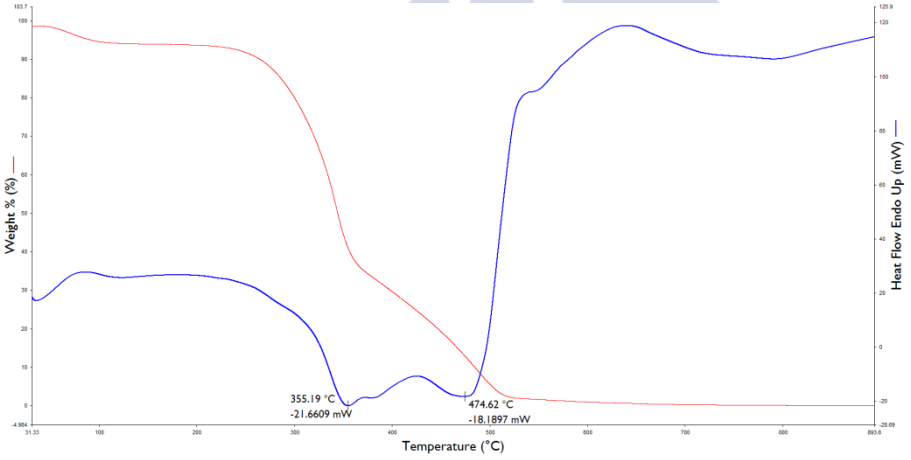

Figure S A.6 Thermogram of sawdust (Sd) obtained with method (i). Weight loss (%) is represented in red and heat flow in blue. Peak height is shown in blue curve.

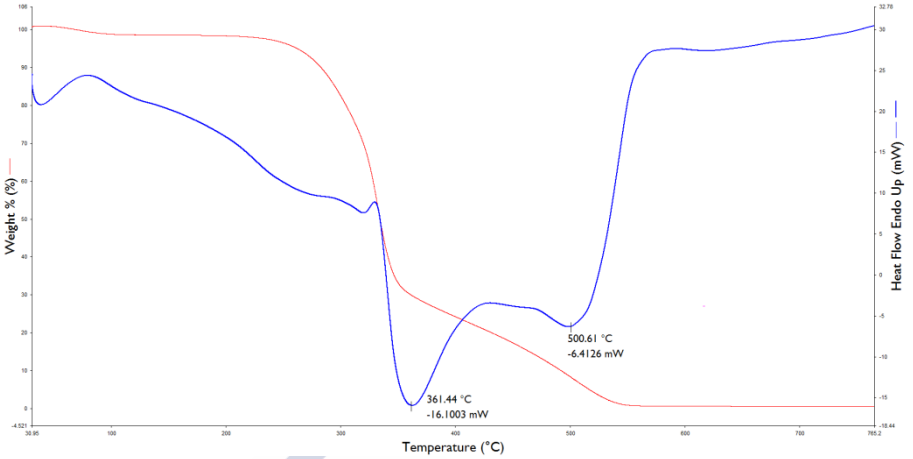

Figure S A.7 Thermogram of miscanthus raw material (Mis) obtained with method (i). Weight loss (%) is represented in red and heat flow in blue. Peak height is shown in blue curve.

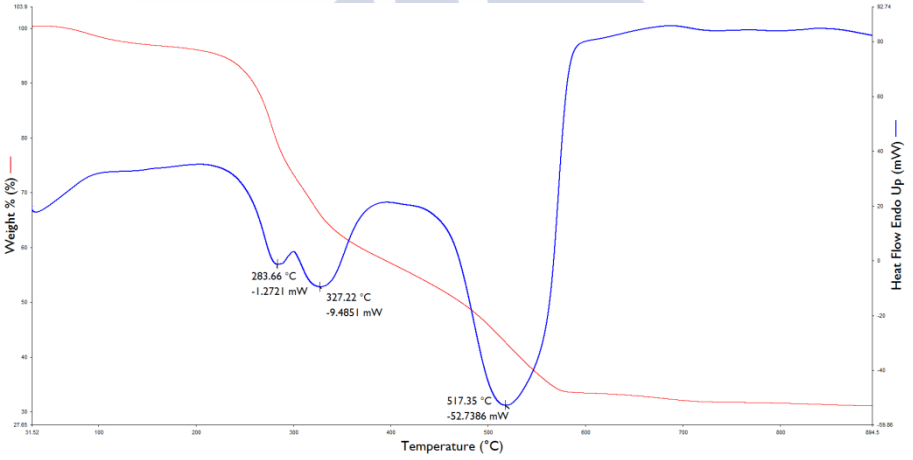

Figure S A.8 Thermogram of chicken manure feedstock (Cm) obtained with method (i). Weight loss (%) is represented in red and heat flow in blue. Peak height is shown in blue curve.

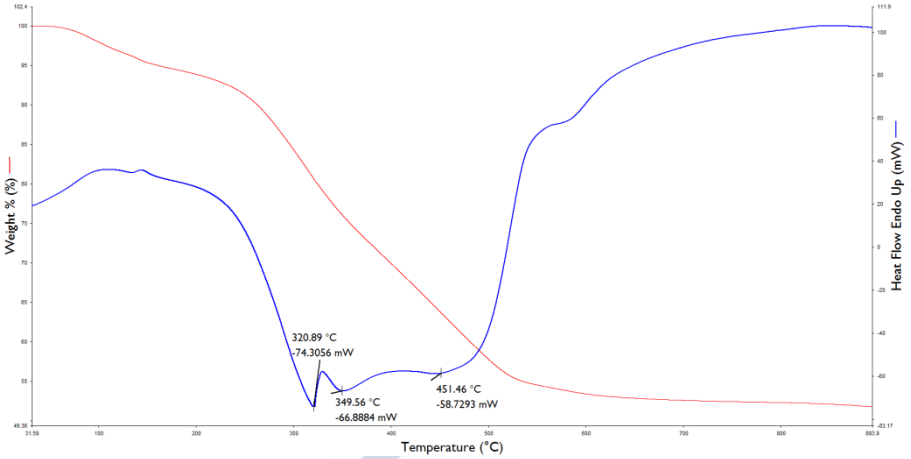

Figure S A.9 Thermogram of olive pomace compost feedstock (Opc) obtained with method (i). Weight loss (%) is represented in red and heat flow in blue. Peak height is shown in blue curve.

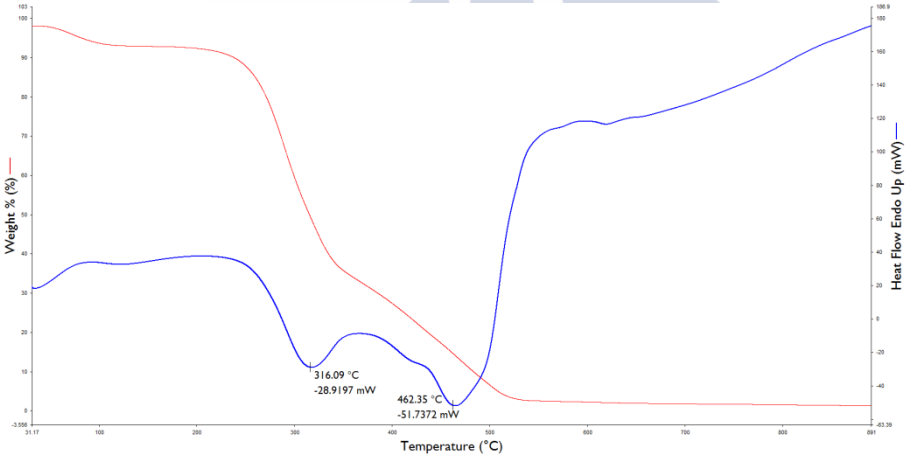

Figure S A.10 Thermogram of corncob feedstock (Cc) obtained with method (i). Weight loss (%) is represented in red and heat flow in blue. Peak height is shown in blue curve.

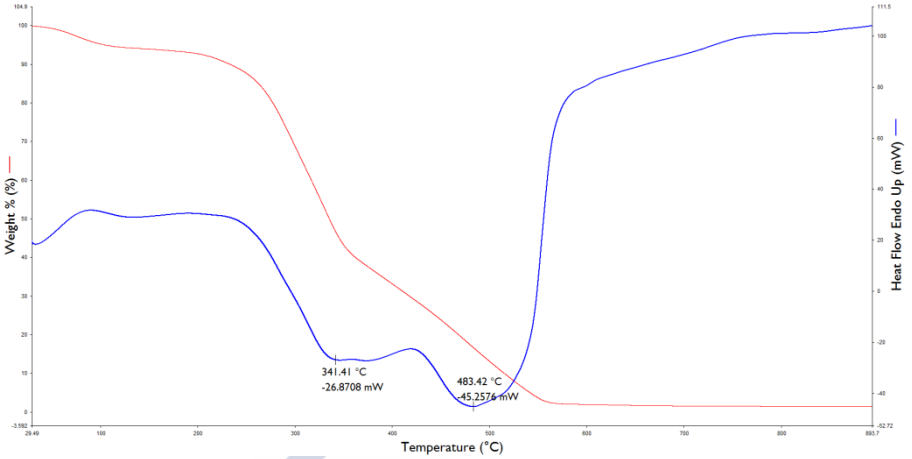

Figure S A.11 Thermogram of vine shoot feedstock (Vs) obtained with method (i). Weight loss (%) is represented in red and heat flow in blue. Peak height is shown in blue curve.

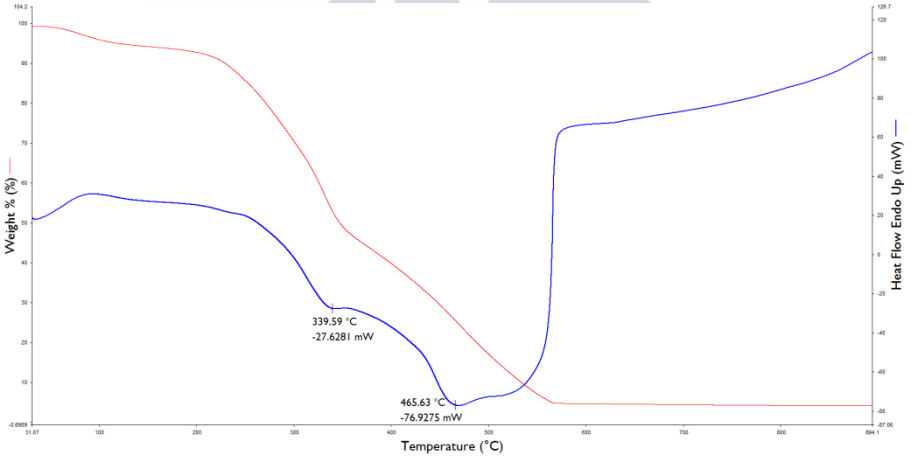

Figure S A.12 Thermogram of chestnut (Cn) obtained with method (i). Weight loss (%) is represented in red and heat flow in blue. Peak height is shown in blue curve.

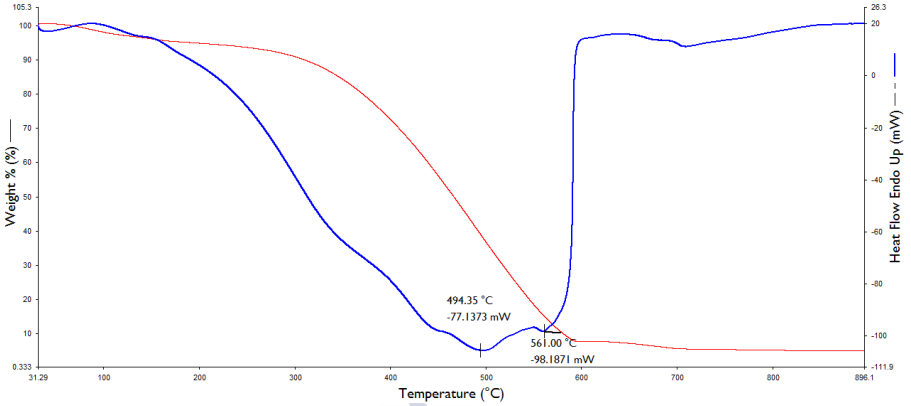

Figure S A.13 Thermogram of BAcB obtained with method (i). Weight loss (%) is represented in red and heat flow in blue. Peak height is shown in blue curve.

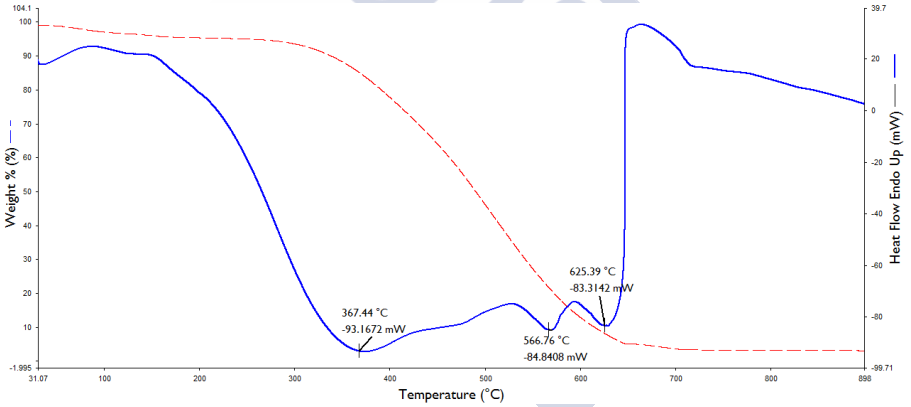

Figure S A.14 Thermogram of BAcSw-1 obtained with method (i). Weight loss (%) is represented in red and heat flow in blue. Peak height is shown in blue curve.

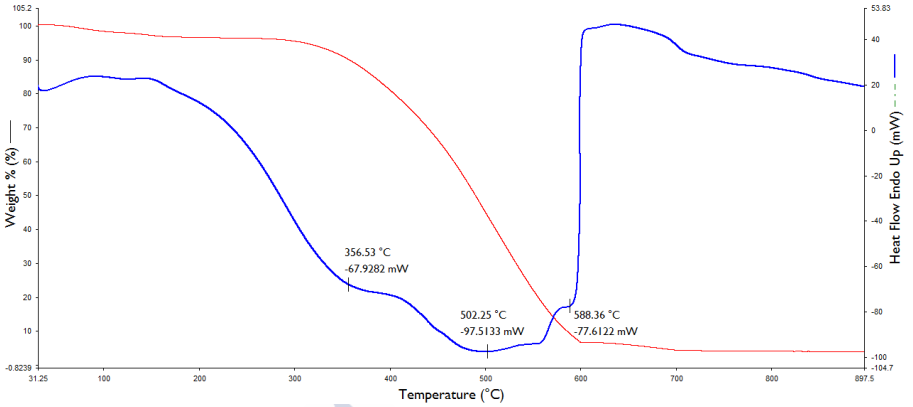

Figure S A.15 Thermogram of BAcSw-2 obtained with method (i). Weight loss (%) is represented in red and heat flow in blue. Peak height is shown in blue curve.

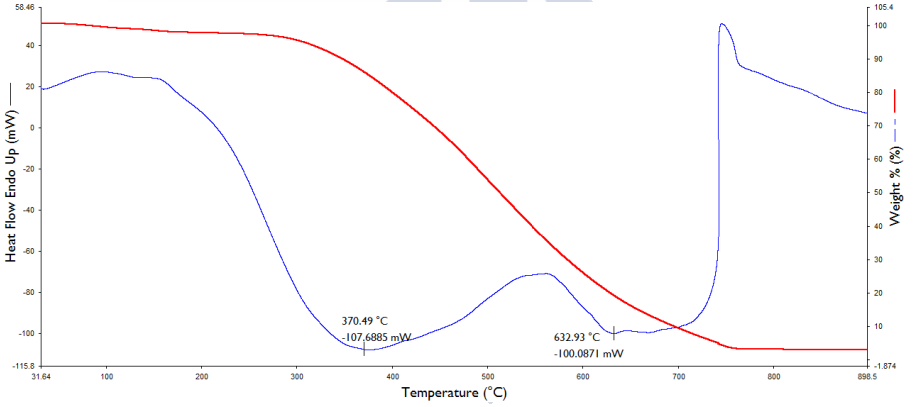

Figure S A.16 Thermogram of BAcSw-3 obtained with method (i). Weight loss (%) is represented in red and heat flow in blue. Peak height is shown in blue curve.

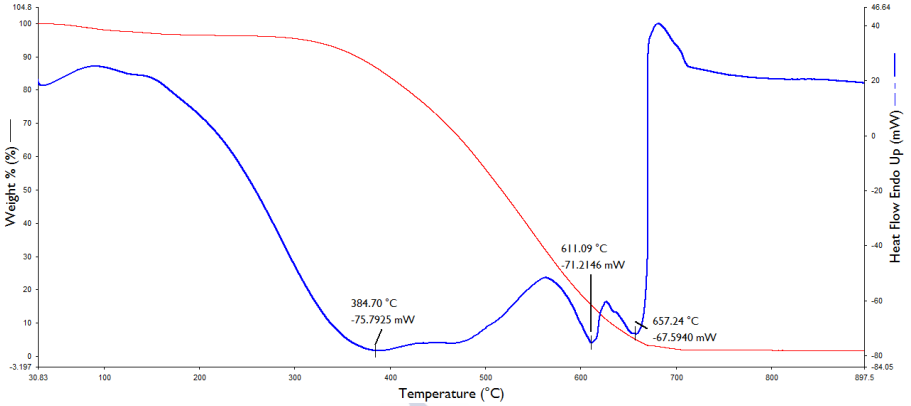

Figure S A.17 BAcHw-1 thermogram obtained with method (i). Weight loss (%) is represented in red and heat flow in blue. Peak height is shown in blue curve.

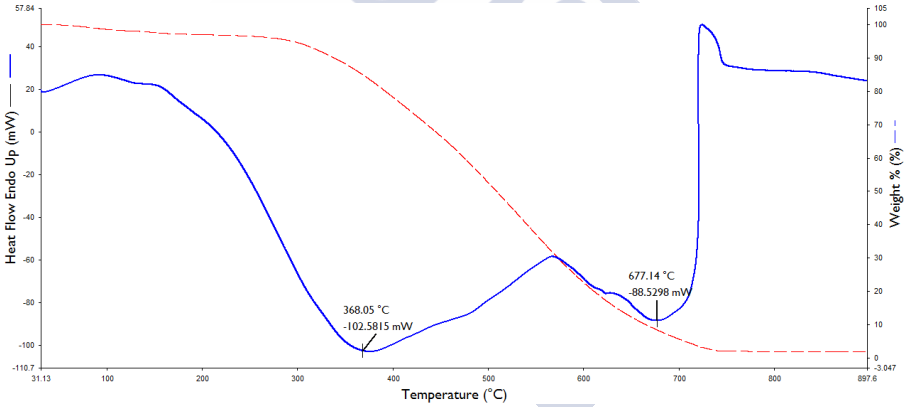

Figure S A.18 BAcHw-2 thermogram obtained with method (i). Weight loss (%) is represented in red and heat flow in blue. Peak height is shown in blue curve.

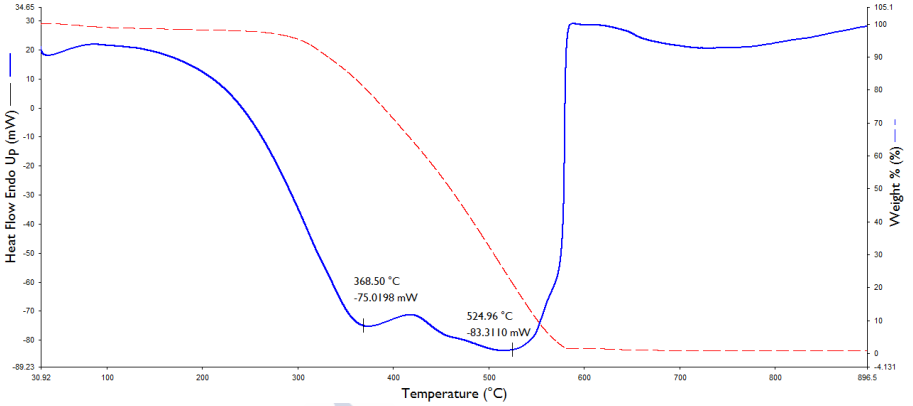

Figure S A.19 Thermogram of BEu-1obtained with method (i). Weight loss (%) is represented in red and heat flow in blue. Peak height is shown in blue curve.

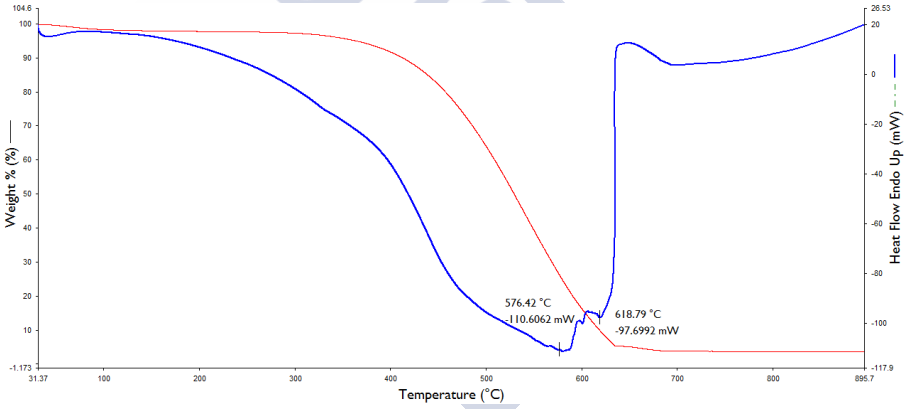

Figure S A.20 BEu-2 thermogram obtained with method (i). Weight loss (%) is represented in red and heat flow in blue. Peak height is shown in blue curve.

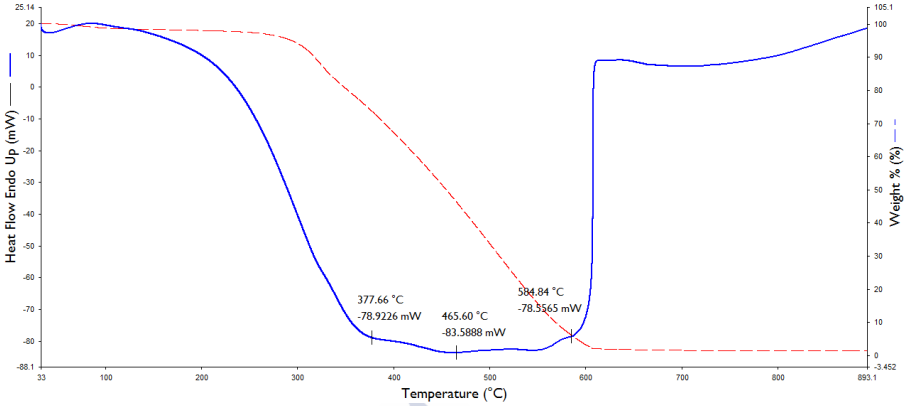

Figure S A.21 Thermogram of BSd-1 obtained with method (i). Weight loss (%) is represented in red and heat flow in blue. Peak height is shown in blue curve.

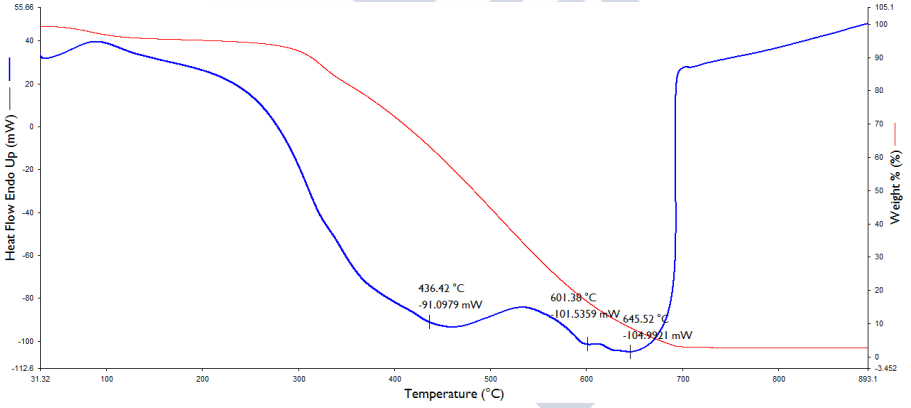

Figure S A.22 BSd-2 thermogram obtained with method (i). Weight loss (%) is represented in red and heat flow in blue. Peak height is shown in blue curve.

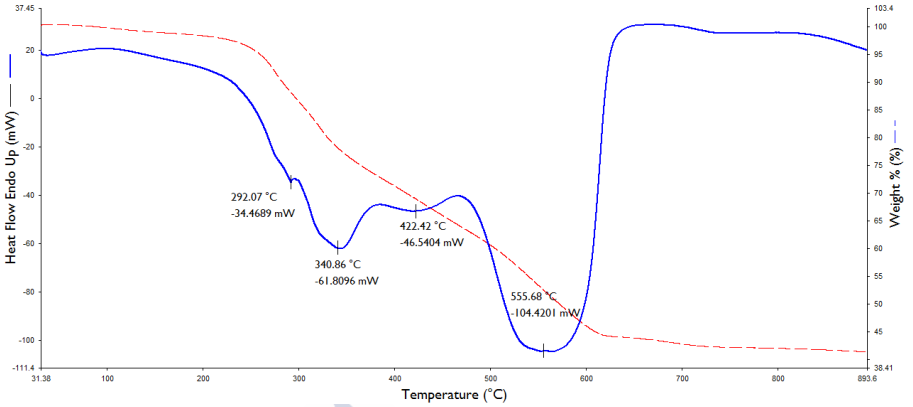

Figure S A.23 Thermogram of BCm obtained with method (i). Weight loss (%) is represented in red and heat flow in blue. Peak height is shown in blue curve.

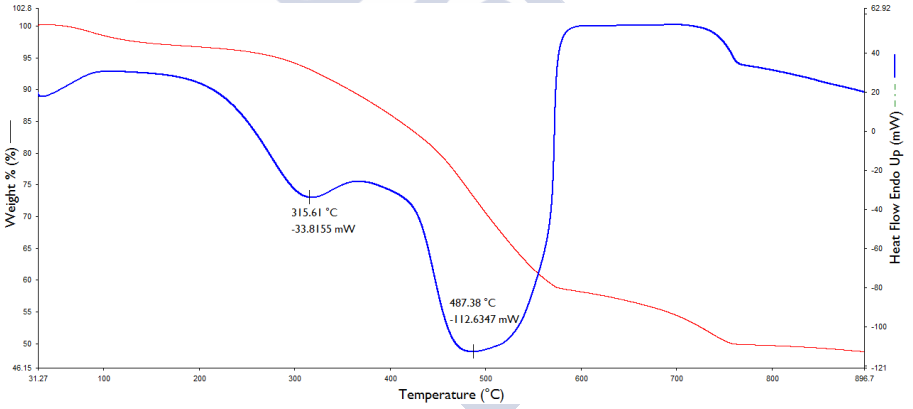

Figure S A.24 Thermogram of BOpc obtained with method (i). Weight loss (%) is represented in red and heat flow in blue. Peak height is shown in blue curve.

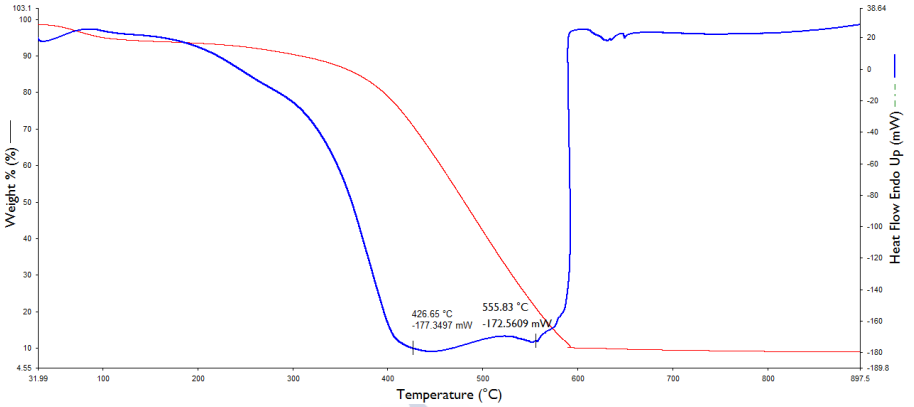

Figure S A.25 Thermogram of BCc-1obtained with method (i). Weight loss (%) is represented in red and heat flow in blue. Peak height is shown in blue curve.

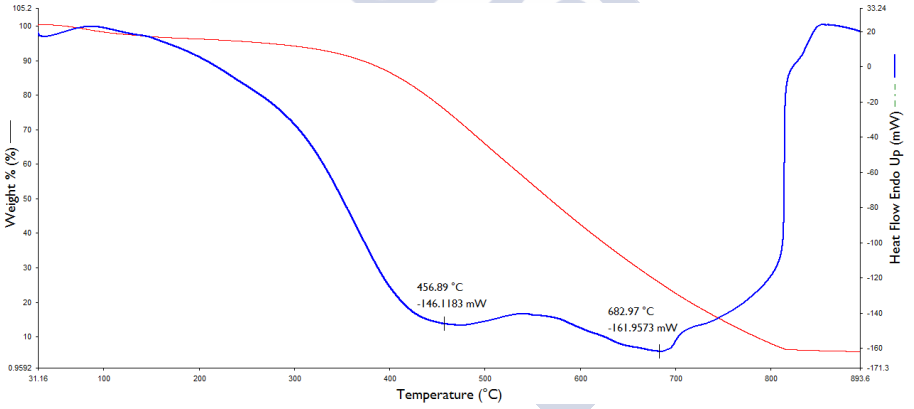

Figure S A.26 Thermogram of BCc-2 obtained with method (i). Weight loss (%) is represented in red and heat flow in blue. Peak height is shown in blue curve.

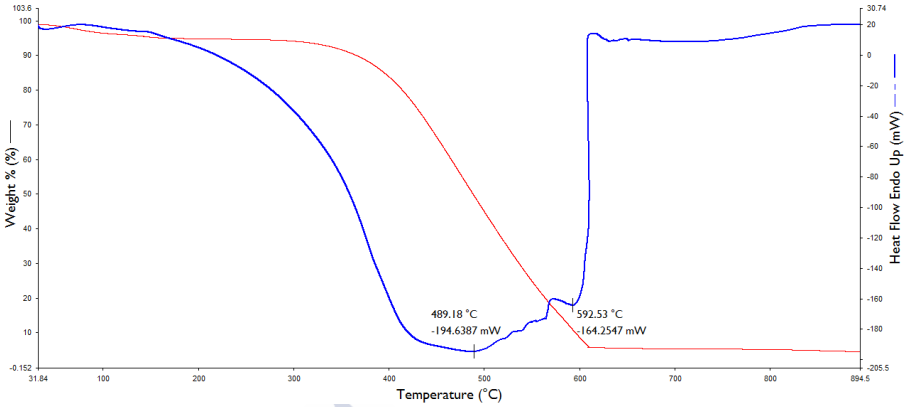

Figure S A.27 BCc-3 thermogram obtained with method (i). Weight loss (%) is represented in red and heat flow in blue. Peak height is shown in blue curve.

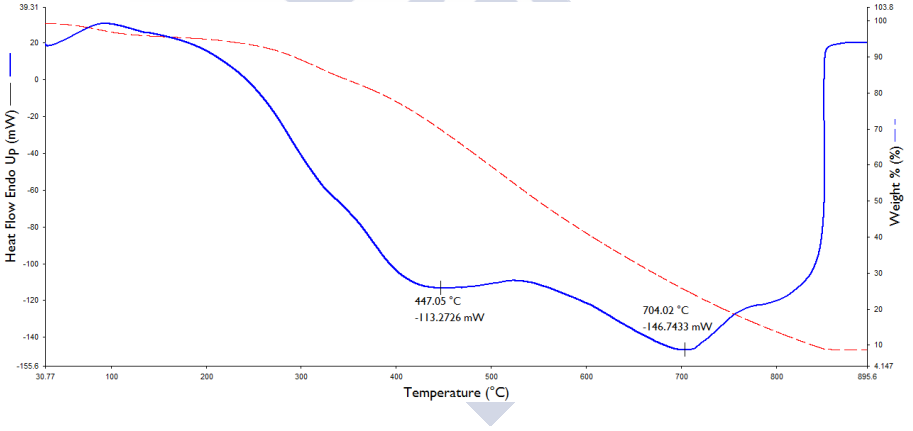

Figure S A.28 BCn thermogram obtained with method (i). Weight loss (%) is represented in red and heat flow in blue. Peak height is shown in blue curve.

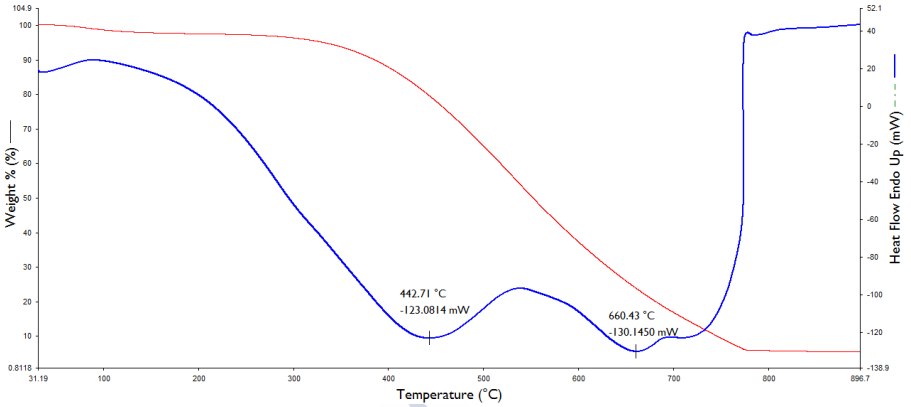

Figure S A.29 BVs thermogram obtained with method (i). Weight loss (%) is represented in red and heat flow in blue. Peak height is shown in blue curve.

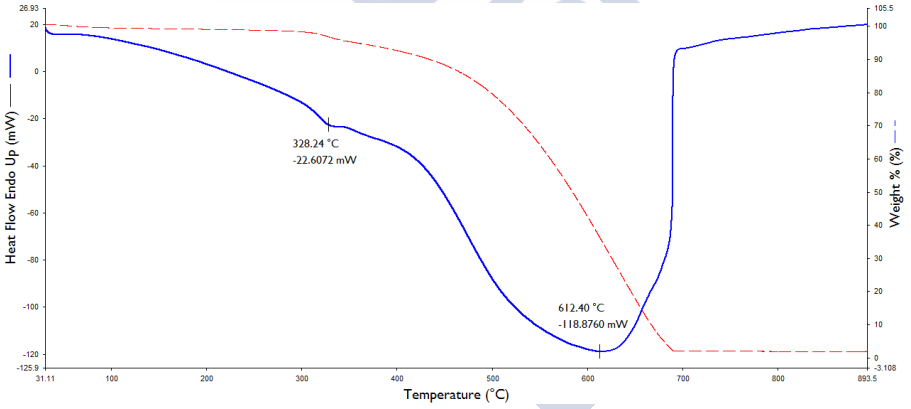

Figure S A.30 BMis thermogram obtained with method (i). Weight loss (%) is represented in red and heat flow in blue. Peak height is shown in blue curve.

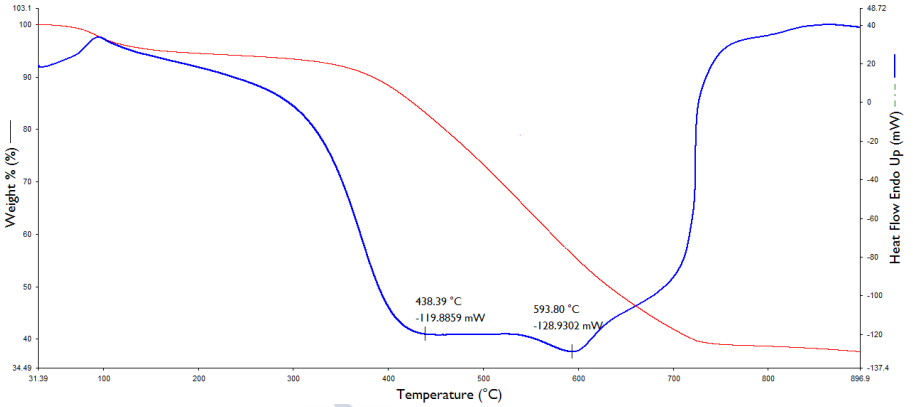

Figure S A.31 BRh thermogram obtained with method (i). Weight loss (%) is represented in red and heat flow in blue. Peak height is shown in blue curve.

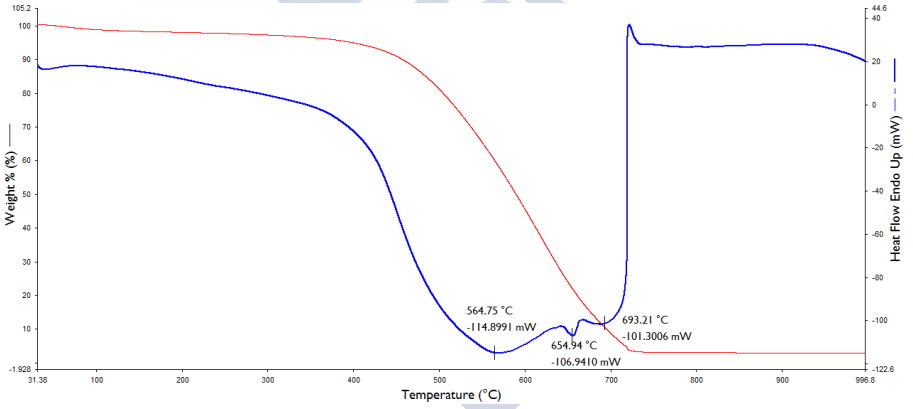

Figure S A.32 Thermogram of BPb obtained with method (i). Weight loss (%) is represented in red and heat flow in blue. Peak height is shown in blue curve.

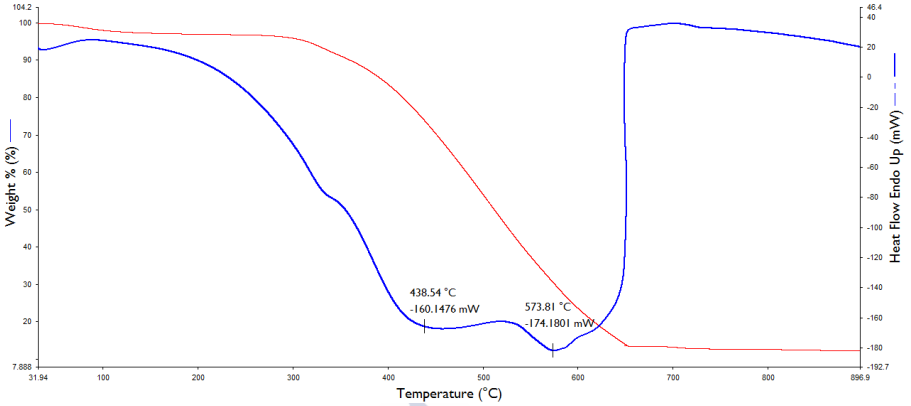

Figure S A.33 Thermogram of BSdG obtained with method (i). Weight loss (%) is represented in red and heat flow in blue. Peak height is shown in blue curve.

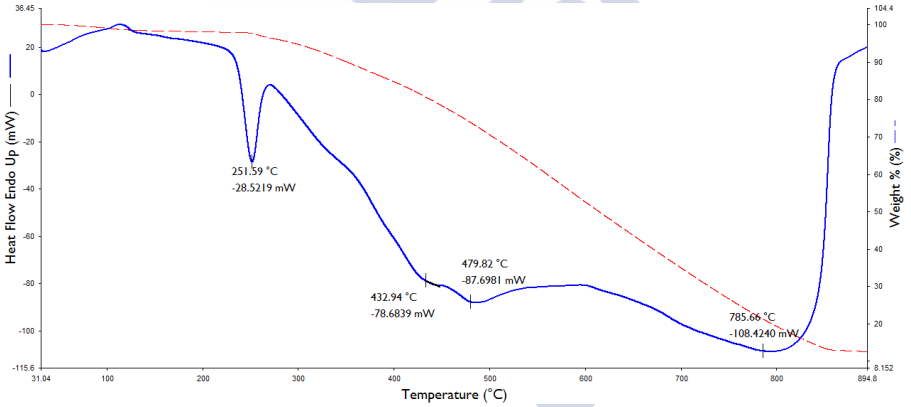

Figure S A.34 BPI thermogram obtained with method (i). Weight loss (%) is represented in red and heat flow in blue. Peak height is shown in blue curve.

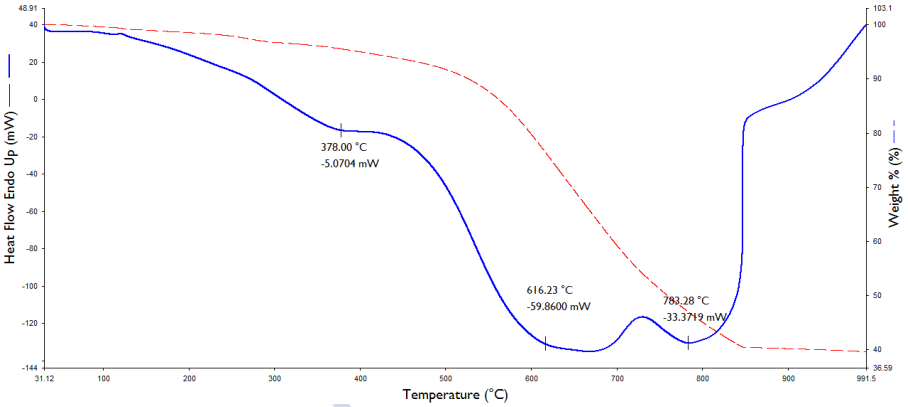

Figure S A.35 Thermogram of BTy obtained with method (i). Weight loss (%) is represented in red and heat flow in blue. Peak height is shown in blue curve.

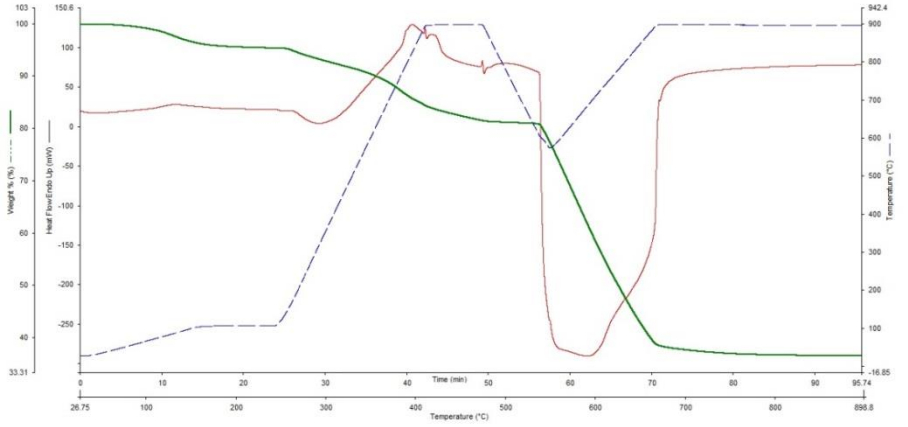

Figure S A.36 Example of TGA-DSC curve obtained with method (ii) for BPb. The blue curve represents the temperature ramp; the green curve the weight loss, and the red curve the heat flow.

Table S A.2 Moisture, volatile matter and fixed carbon determined by proximate analysis and TGA (expressed as average ± standard deviation).

		Dry basis		
Sample	**%Moisture**	**% VM**	**% Ash**	**%FixC**
BAcB	5.05 ± 0.43	42.92 ± 0.25	5.25 ± 0.23	51.83 ± 0.02
BAcSw-1	3.01 ± 0.33	39.37 ± 2.26	2.65 ± 0.17	57.98 ± 2.43
BAcSw-2	2.72 ± 2.27	37.31 ± 2.81	3.62 ± 0.40	59.06 ± 2.81
BAcSw-3	2.09 ± 0.64	39.63 ± 0.63	2.88 ± 0.29	57.49 ± 0.71
BAcHw-1	3.17 ± 0.72	37.63 ± 0.15	1.61 ± 0.06	60.76 ± 0.21
BAcHw-2	2.65 ± 0.58	1.98 ± 4.03	1.98 ± 0.02	51.60 ± 4.01
BEu-1	2.14 ± 0.58	47.62 ± 0.11	0.77 ± 0.30	51.61 ± 0.19
BEu-2	2.41 ± 0.42	22.17 ± 1.90	3.92 ± 0.34	73.91 ± 1.57
BSd-1	2.39 ± 0.06	52.10 ± 0.88	1.37 ± 0.02	46.53 ± 0.90
BSd-2	4.26 ± 0.13	47.58 ± 0.45	2.76 ± 0.07	49.66 ± 0.48
BCm	2.49 ± 0.26	46.08 ± 0.08	39.69 ± 0.30	14.23 ± 0.38
BOpc	2.65 ± 0.89	29.41 ± 1.31	49.49 ± 0.16	21.10 ± 1.48
BCc-1	3.49 ± 1.76	16.03 ± 2.11	9.09 ± 0.35	74.88 ± 2.45
BCc-2	4.94 ± 1.19	15.78 ± 3.64	5.33 ± 0.05	78.90 ± 3.59
BCc-3	3,47 ± 0.80	20.89 ± 7,42	3,99 ± 0,91	75,12 ± 8,33
BCn	4.55 ± 1.98	25.70 ± 2.57	9.07 ± 0.22	65.23 ± 2.35
BMis	1.30 ± 0.07	24.39 ± 5.85	1.40 ± 0.42	74.21 ± 5.43
BVs	2.86 ± 0.55	23.01 ± 2.46	5.45 ± 0.05	71.54 ± 2.50
BPl	2.31 ± 0.32	35.12 ± 0.26	13.09 ± 0.45	51.79 ± 0.19
BPb	2.58 ± 1.55	14.91 ± 2.83	2.82 ± 0.18	82.27 ± 2.65
BRh	4.25 ± 0.38	16.67 ± 2.97	38.66 ± 0.48	44.66 ± 3.45
BSdG	2.09 ± 0.06	22.26 ± 2.83	11.15 ± 0.65	66.59 ± 3.48
BTy	1.14 ± 0.14	10.73 ± 0.69	36.17 ± 3.32	53.10 ± 4.01

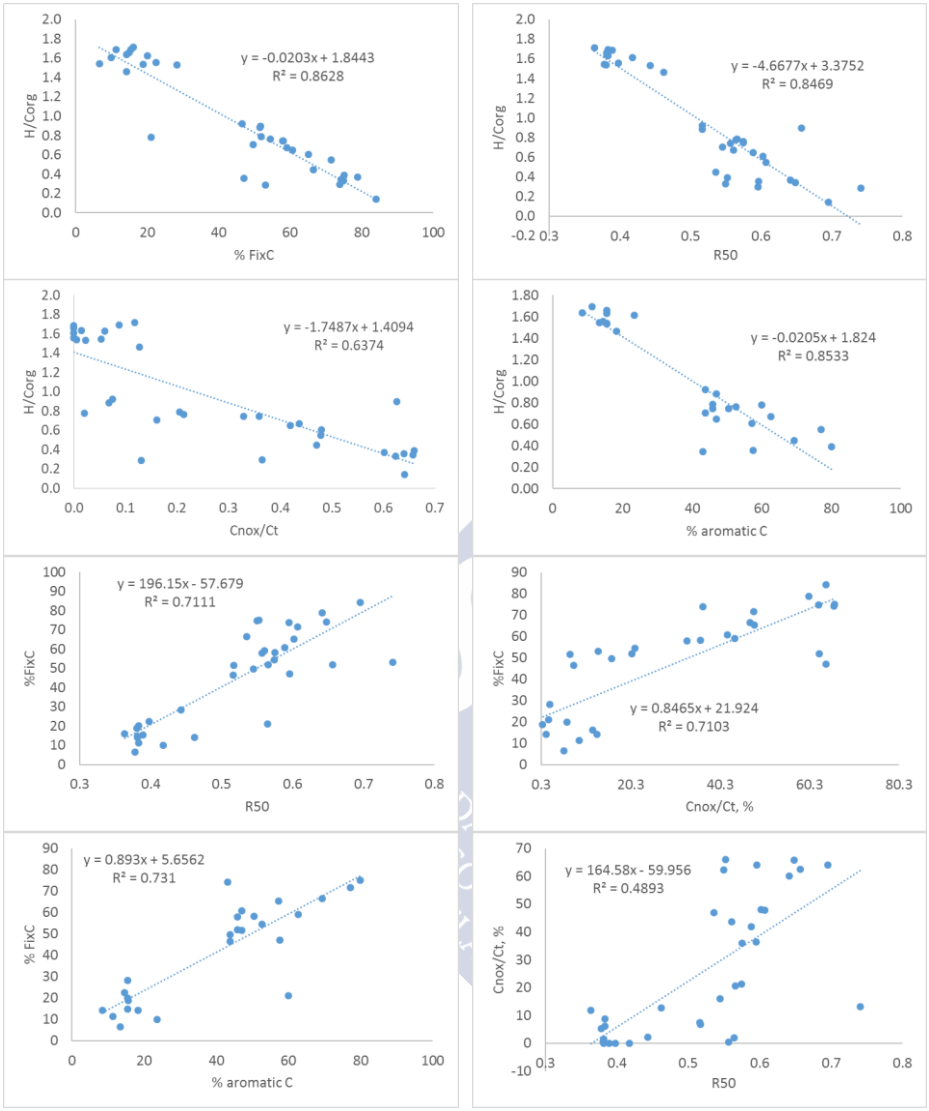

Figure S A.37 Correlations between H/C_{org} and the other parameters associated with carbon stability and recalcitrance (Include data from feedstock, PCM and biochar).

B. Supporting Information Chapter 5

Table S B.1 Total elemental analysis of different feedstock: acacia bark, sapwood and heart wood (AcB, AcSw, AcHw, respectively), eucalyptus (Eu), sawdust (Sd), miscanthus (Mis), vine shoot (Vs), corncob (Cc), chestnut (Cn), chicken manure (Cm) and olive pomace compost (Opc).

	Fe	Ca	Mg	Na	K	Al	Co	Cr	Cu	Mn	Ni	Pb	Zn
Sample	g/kg						mg/kg						
AcB	0.3	9.3	1.6	0.6	4.6	0.7	< 5	< 5	5.0	60.0	< 5	< 25	618.0
AcSw	0.2	4.3	0.3	0.3	1.0	0.3	< 5	< 5	< 5	10.0	< 5	< 25	292.0
AcHw	0.0	4.3	0.0	0.2	0.0	0.1	< 5	< 5	< 5	< 5	< 5	< 25	171.0
Eu	0.2	13.6	0.7	0.1	0.3	0.1	< 5	< 5	< 5	116.0	7.0	< 25	8.0
Sd	0.2	1.6	0.3	0.1	0.7	0.1	< 5	< 5	< 5	42.0	< 5	< 25	18.0
Mis	0.3	0.6	0.3	0.1	0.1	0.1	< 5	10.0	6.0	67.0	< 5	< 25	15.0
Vs	0.1	5.6	0.9	0.1	5.0	0.1	< 5	6.0	11.0	94.0	< 5	< 25	24.0
Cc	0.1	0.1	0.2	0.0	5.9	0.0	< 5	< 5	5.1	< 5	6.7	< 25	0.0
Cn	1.0	1.8	1.0	0.1	4.1	0.4	< 5	< 5	8.0	11.0	196.2	< 25	0.6
Cm	9.8	32.6	5.0	2.8	12.4	10.5	6.0	23.0	40.0	460.0	19.0	< 25	274.0
Opc	7.4	74.4	5.4	2.3	17.1	9.8	7.0	28.0	41.0	176.0	15.0	< 25	59.0

Table S B.2 Macronutrient content of biochars, expressed in g kg^{-1}.

Sample	P	Ca	Mg	Na	K	Fe	Al
BAcB	1.13	21.70	2.20	1.05	7.33	0.20	0.24
BAcSw-1	0.68	16.00	0.80	0.76	3.10	0.05	<0.05
BAcSw-2	0.77	2.04	1.04	0.89	3.69	0.04	<0.05
BAcSw-3	0.62	14.82	0.76	0.78	3.02	0.13	<0.05
BAcHw-1	0.03	11.74	0.42	0.61	0.39	0.03	<0.05
BAcHw-3	0.02	12.02	0.34	0.63	0.29	0.05	0.07
BEu-1	0.27	4.52	0.44	0.20	0.50	0.26	0.14
BEu-2	1.25	23.26	1.07	0.34	3.08	0.99	0.50
BSd-1	0.40	4.34	0.46	0.27	1.61	0.46	0.44
BSd-2	0.25	5.26	0.84	0.40	1.95	1.32	0.43
BCm	15.35	47.80	7.20	3.97	16.82	14.58	14.00
BOpc	3.84	124.20	8.60	3.38	24.00	10.78	11.80
BCc-1	2.31	1.64	1.40	0.17	17.12	3.98	1.07
BCc-2	2.78	1.30	0.63	0.19	21.84	5.20	0.40
BCc-3	1.32	0.79	1.04	1.91	21.52	0.47	0.15
BCn	1.85	7.90	2.40	0.20	14.42	2.28	1.48
BMis	0.25	2.66	1.80	0.11	0.34	0.82	0.33
BVs	3.91	13.56	2.20	0.47	14.82	0.69	0.28
BPb	0.48	11.62	1.28	0.66	2.90	0.54	0.90
BRh	17.22	20.14	8.40	4.70	35.92	3.70	0.84
BSdG	6.70	20.80	5.40	1.80	15.50	2.54	0.56
BPl	2.99	17.82	0.85	1.45	1.92	5.99	3.99
BTy	0.37	5.78	0.68	0.56	0.67	211.96	0.96

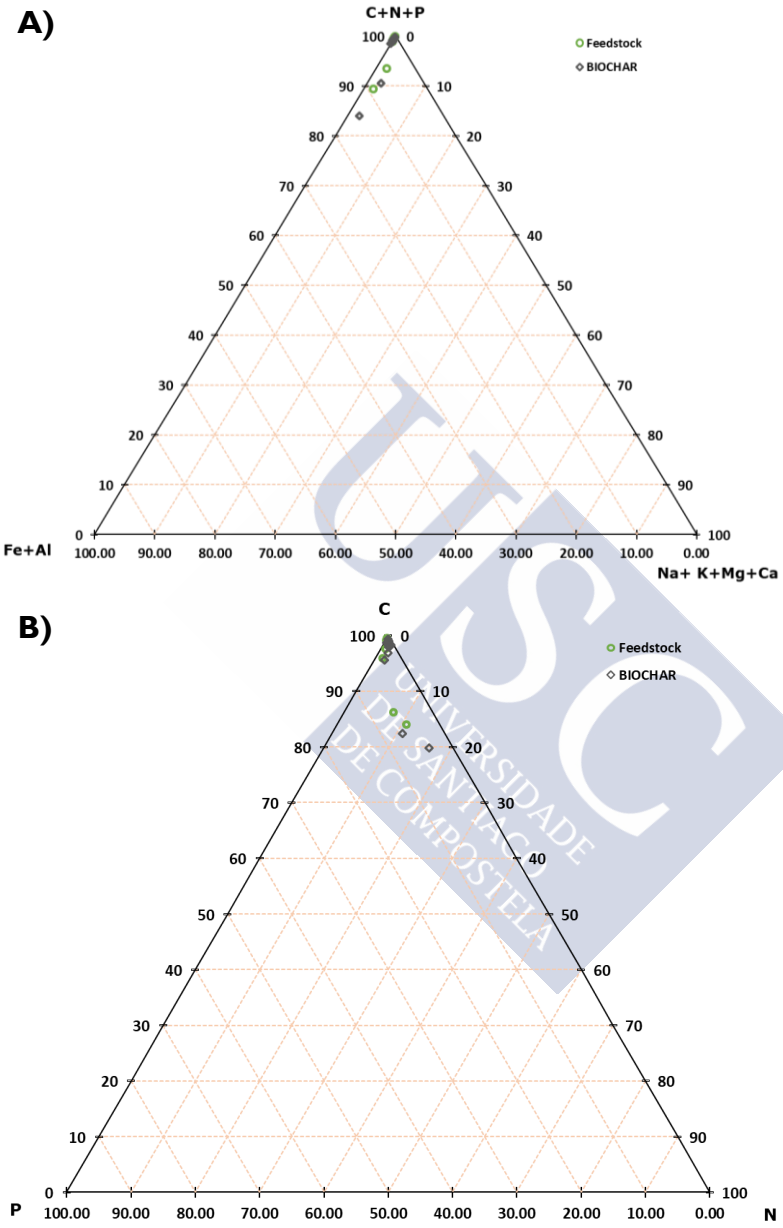

Figure S B.1 Ternary diagram for nutrient content in (A) feedstock and biochar grouped in biogenic nutrients (C+N+P), alkaline and earth-alkaline metals (Na+K+Mg+Ca) and Fe+Al, and (B) the individual changes in C, P and N.

Table S B.3 Trace metal content of biochars, expressed in mg kg^{-1}.

Sample	Co	Cr	Cu	Mn	Ni	Pb	Zn
BAcB	<5	<5	6	105	<5	<25	1053
BAcSw-1	<5	<5	<5	25	<5	<25	756
BAcSw-2	<5	<5	<5	27	<5	<25	885
BAcSw-3	<5	<5	<5	26	<5	<25	781
BAcHw-1	<5	<5	<5	<5	<5	<25	608
BAcHw-3	<5	<5	<5	5	<5	<25	631
BEu-1	<5	<5	11	125	<5	<25	204
BEu-2	<5	10	20	138	26	<25	42
BSd-1	<5	<5	<5	85	<5	<25	265
BSd-2	<5	6	7	137	8	<25	55
BCm	10	24	55	720	23	<25	400
BOpc	11	25	60	234	28	39	76
BCc-1	<5	46	22	78	140	<25	440
BCc-2	<5	62	15	68	79	<25	620
BCc-3	7	28	16	36	28	<25	81
BCn	6	11	30	700	18	<25	32
BMis	<5	11	13	520	53	<25	123
BVs	6	21	34	235	39	<25	187
BPb	<5	8	9	61	9	<25	5
BRh	<5	25	108	800	24	<25	400
BSdG	<5	23	55	446	20	<25	860
BPl	<5	20.5	46.5	60.3	41.1	48.2	651.7
BTy	352	21	201	1380	55	42	35000

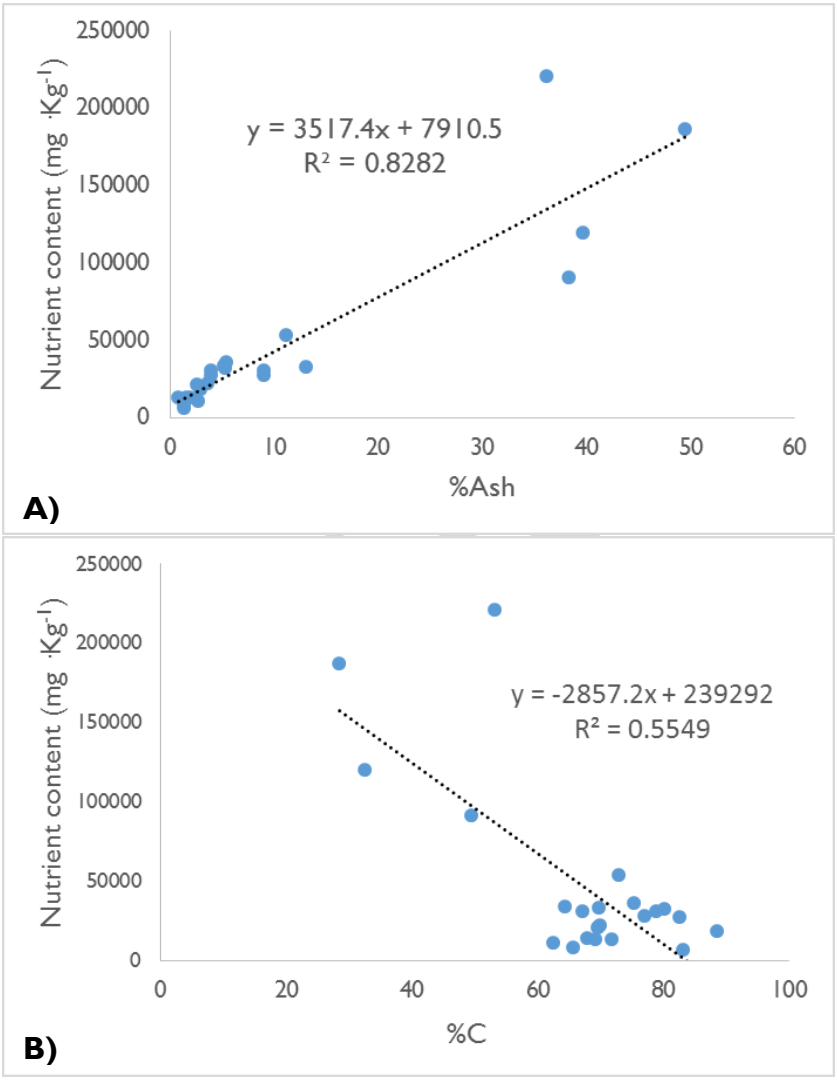

Figure S B.2 Correlation between nutrient concentration (expressed as the sum of P, Fe, Ca, Mg, Na, K and Al total contents in mg kg^{-1}) and (A) % ash and (B) total C content.

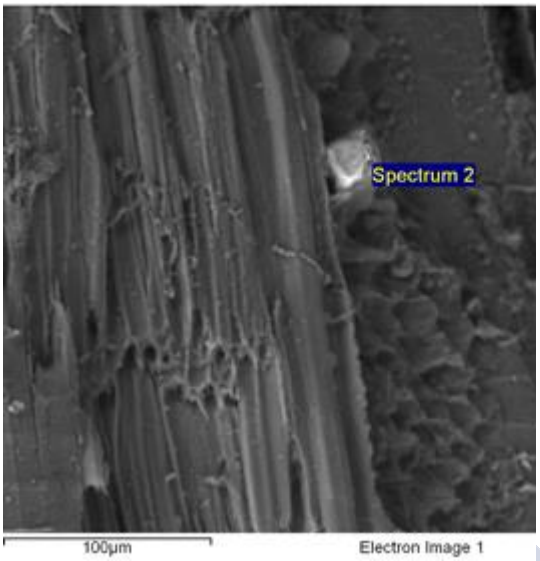

Element	Weight%	Atomic%
C K	48.30	59.27
O K	39.22	36.14
Ca K	12.48	4.59

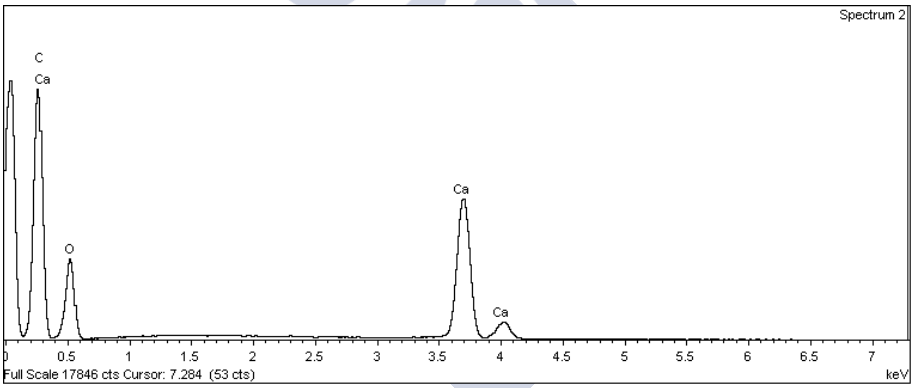

Figure S B.3 SEM-EDX microanalysis for BSd-1. The results of the surface analysis were consistent with the total analysis, and Ca was found to be the most abundant nutrient in the carbon matrix.

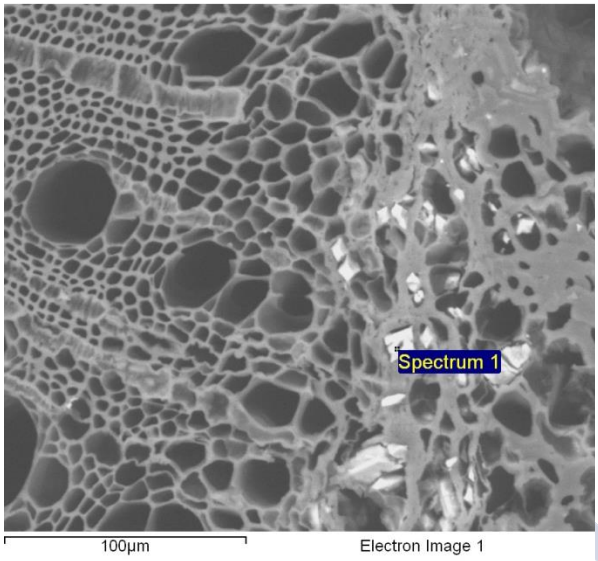

Element	Weight %	Atomic %
C K	17.87	28.22
O K	46.15	54.74
K K	0.40	0.20
Ca K	35.58	16.84

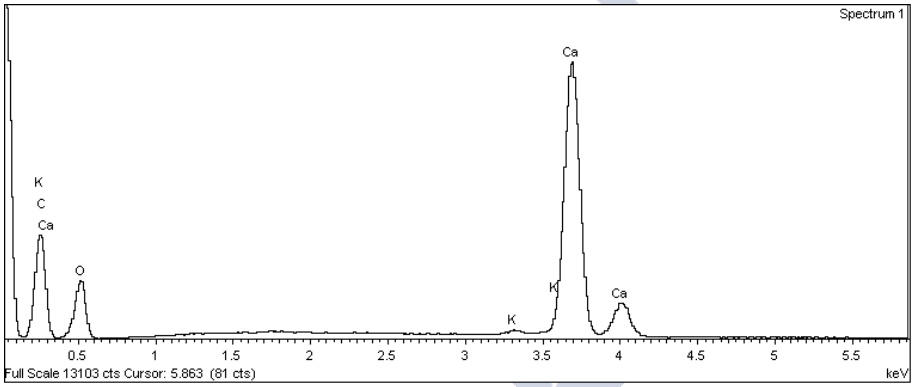

Figure S B.4 Backscattered electron image of eucalyptus biochar. EDX analysis was conducted at the point marked as Spectrum 1. Both the spectrum and composition table show that Ca is the major element, with small amounts of K.

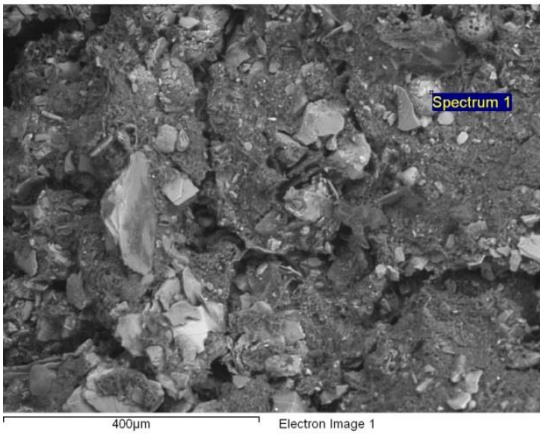

Element	Weight%	Atomic%
C K	19.63	32.71
O K	27.31	34.17
Mg K	1.11	0.92
Al K	10.86	8.06
Si K	21.09	15.03
P K	0.39	0.25
S K	0.29	0.18
K K	10.54	5.40
Ca K	0.69	0.34
Ti K	0.71	0.30
Fe K	7.37	2.64

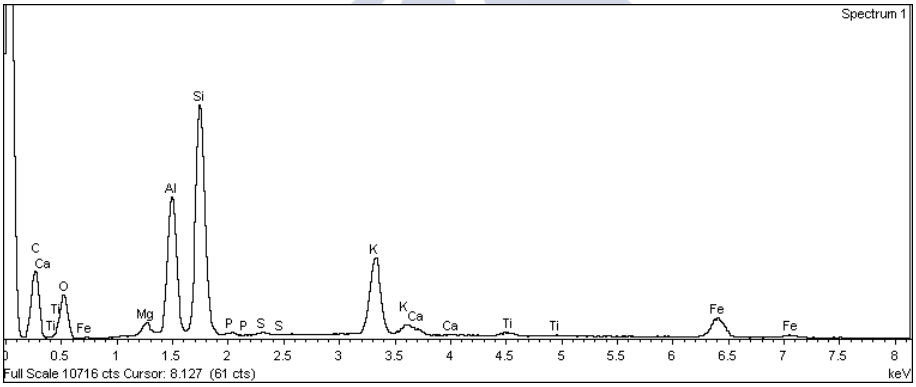

Figure S B.5 BAcB SEM-EDX microanalysis of a surface particle. Acacia bark is rich in mineral salts in the carbon structure, such as Si, Ca, P, K, Al, Fe, etc.

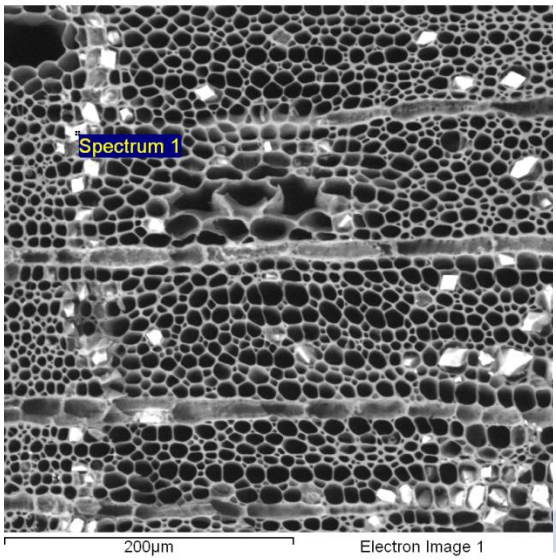

Element	Weight%	Atomic%
C K	17.76	25.92
O K	57.89	63.43
K K	0.10	0.04
Ca K	24.24	10.60

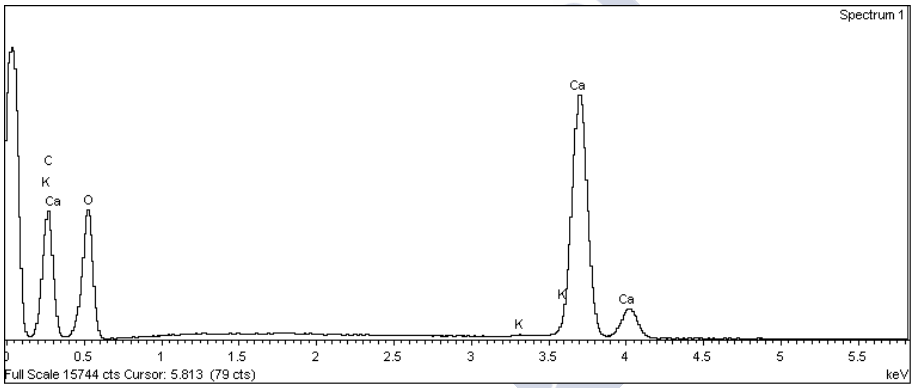

Figure S B.6 SEM image of acacia trunk PCM (BAcSw-3) with the EDX spectrum of the area of salt accumulation (Spectrum1). Particles mainly comprised calcium carbonate.

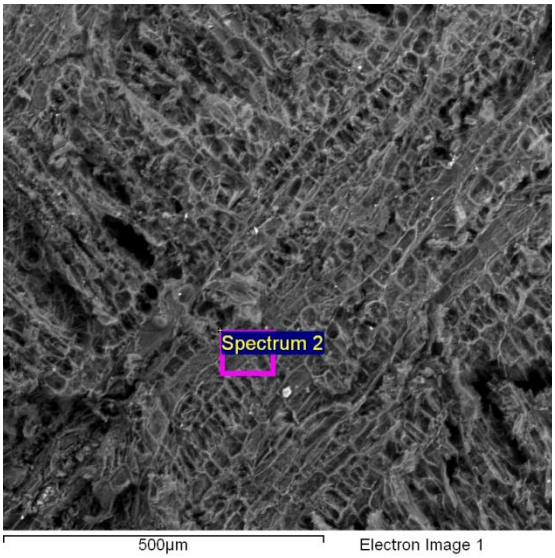

Element	Weight%	Atomic%
C K	43.27	52.31
O K	49.41	44.84
Mg K	0.45	0.27
P K	0.46	0.21
S K	0.23	0.10
K K	2.87	1.06
Ca K	3.33	1.20

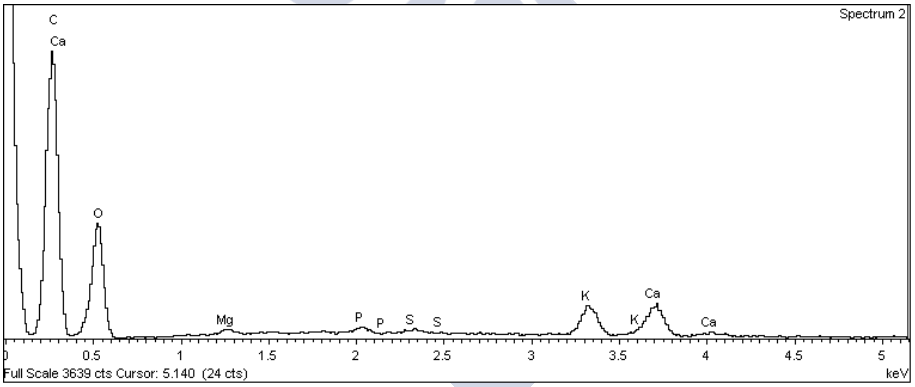

Figure S B.7 SEM image of corncob biochar with its EDX spectra taken in the area delimited as Spectrum 2. There carbonaceous matrix is rich in K and Ca, with lower concentrations of Mg, P and S.

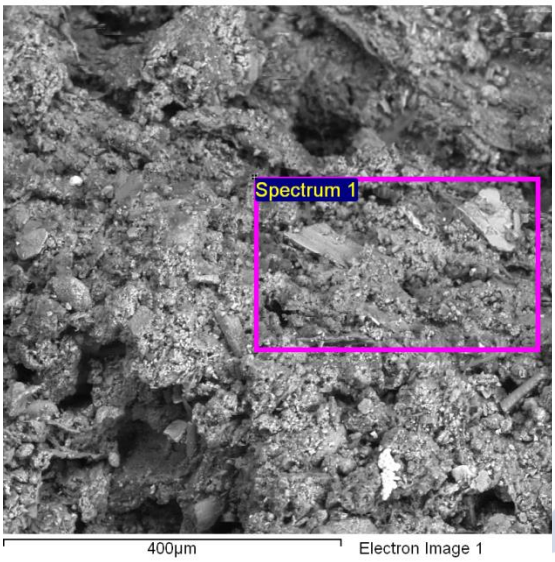

Element	Weight%	Atomic%
C K	26.35	38.22
O K	42.07	45.82
Mg K	0.95	0.68
Al K	1.46	0.94
Si K	9.25	5.74
P K	0.68	0.38
Cl K	1.32	0.65
K K	4.02	1.79
Ca K	11.66	5.07
Fe K	2.25	0.70

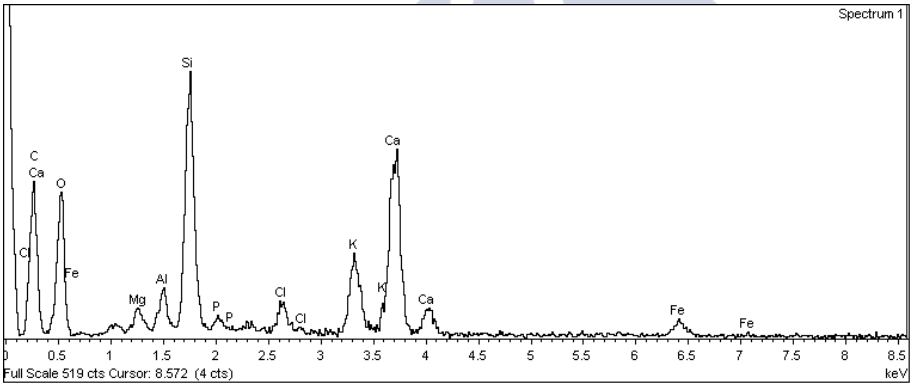

Figure S B.8 SEM-EDX microanalysis of a surface area of pyrolysed olive pomace compost (BOpc) (Marked with a square as Spectrum I). This sample shows an irregular surface, rich in mineral salts, such as Si, Ca, P, K, Al, Fe, etc.

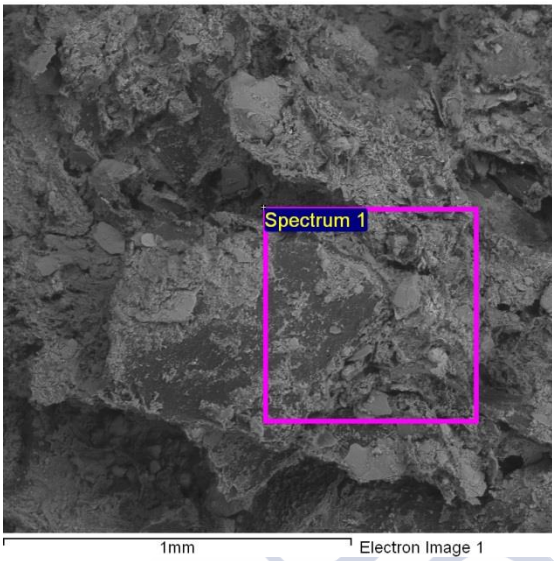

Element	Weight%	Atomic%
C K	29.20	41.58
O K	40.07	42.84
Na K	0.97	0.72
Mg K	1.10	0.77
Al K	3.22	2.04
Si K	5.32	3.24
P K	2.40	1.32
S K	0.39	0.21
Cl K	2.58	1.25
K K	6.37	2.79
Ca K	5.57	2.38
Fe K	2.82	0.86

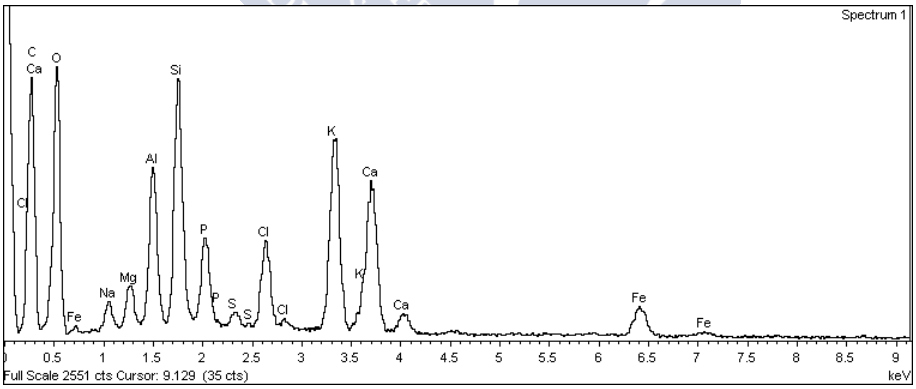

Figure S B.9 Pyrolysed chicken manure sample (BCm) SEM image with EDX surface microanalysis.

Table S B.4 Hydrological behaviour of pyrolysed materials, expressed as % of dry sample.

	Field capacity		Wilting Point	
Sample	Mean	Sd	Mean	Sd
BAcB	42.59	6.61	29.02	2.85
BAcSw-1	68.99	4.83	54.63	6.02
BAcSw-2	93.54	56.38	68.96	43.44
BAcSw-3	86.23	15.57	67.76	13.43
BAcHw-1	49.64	14.26	36.18	13.01
BAcHw-2	45.14	6.06	35.19	6.10
BEu-1	107.74	34.71	84.92	23.92
BEu-2	176.81	6.44	96.53	31.61
BSd-1	131.57	50.59	84.02	4.44
BSd-2	122.73	7.06	66.07	4.24
BOpc	63.26	1.54	47.30	1.76
BCm	66.46	0.09	58.20	1.14
BPb	125.82	21.21	115.56	18.88
BRh	128.17	1.55	96.16	1.36
BCc-1	153.28	3.26	138.25	0.86
BCc-2	121.07	3.80	108.85	2.97

Table S B.5 The 16 PAH priority compounds tested on biochar samples (units: µg kg^{-1}).

Sample	Acenaphthene	Acenaphthylene	Anthracene	Benzo(a)anthracene	Benzo(a)pyrene	Benzo(b)fluoranthene	Benzo(g,h,i)perylene	Benzo(k)fluoranthene	Chrysene	Dibenzo(a,h)anthracene	Fluoranthene	Fluorene	Indene(1,2,3-cd)pyrene	Naphthalene	Phenanthrene	Pyrene
BCc-1	21.8	19.8	7.0	0.5	97.0	1.3	9.0	1.5	102.5	41.2	6.5	23.2	22.2	81.2	17.7	10.2
BCc-2	7.8	6.6	2.0	0.3	105.0	1.7	6.3	1.5	101.4	49.8	1.3	4.3	25.8	26.5	<0.017	3.1
BCc-3	6.0	3.0	4.7	0.8	128.5	1.2	1.3	1.0	111.6	60.3	1.2	5.7	33.8	112.1	<0.017	3.0
BAcB	10.0	6.3	10.4	<0.001	54.7	4.2	16.9	3.4	64.7	154.8	7.1	34.0	31.4	111.6	23.2	12.3
BAcSw-1	2.7	5.0	5.7	1.2	98.0	2.0	3.5	1.7	139.5	67.3	4.3	15.0	49.7	20.0	<0.017	11.8
BAcSw-2	5.3	5.6	5.9	0.7	47.6	0.7	1.3	0.8	87.2	22.0	1.3	12.3	16.9	107.4	<0.017	2.8
BAcSw-3	9.9	<0.08	7.9	0.7	111.7	1.8	0.2	1.8	158.4	47.5	5.1	25.2	47.5	243.4	<0.017	10.8
BAcHw-1	0.9	2.4	4.3	<0.001	121.4	6.4	44.0	7.7	91.2	159.8	3.7	3.7	96.9	3.4	<0.015	5.7
BAcHw-3	6.1	<0.08	7.1	1.5	107.1	1.2	0.3	1.3	124.4	27.3	6.6	26.2	13.2	57.4	14.8	11.0
BEu-1	5.3	<0.08	6.0	0.3	75.4	1.5	0.7	1.3	128.7	51.4	4.0	13.7	24.3	11.8	12.8	11.0
BEu-2	8.3	5.7	2.4	0.7	108.9	3.1	19.7	3.2	92.2	90.6	1.5	1.9	20.1	8.6	<0.017	2.8
BSd-1	4.3	<0.08	5.9	0.7	93.5	2.0	1.4	3.9	153.7	25.7	12.3	8.4	25.7	27.6	13.7	14.1
BSd-2	<0.01	2.7	5.5	0.3	94.5	0.2	1.8	1.3	121.3	53.8	0.7	1.3	22.1	31.6	<0.017	4.3
BCm	165.1	85.5	47.3	302.3	31.8	4.8	7.2	7.4	23.4	165.4	11.9	31.6	2165.3	25.4	20.5	11.1
Bopc	5.3	3.5	10.5	1.2	108.8	3.3	13.1	3.5	143.6	68.5	8.7	8.2	23.0	9.7	23.5	25.8
BVs	10.5	17.6	17.9	0.7	135.2	3.1	2.6	1.8	115.7	69.0	24.7	25.6	33.2	134.9	55.7	39.6
BPb	24.2	14.0	2.3	0.8	121.2	1.6	0.7	2.1	101.5	121.7	1.8	2.6	26.7	241.1	<0.017	3.6
BRh	3.2	5.3	3.6	0.7	107.2	0.2	1.7	1.2	142.1	40.3	0.8	2.0	13.4	43.9	<0.017	4.8
BTy	1055.7	1763.7	861.0	340.6	119.4	110.9	357.7	108.0	179.8	2431.1	1097.4	1300.9	455.4	2997.7	1541.7	1724.5
BPl	102.1	82.7	240.3	483.0	85.4	105.2	103.1	109.4	219.0	584.3	172.0	362.6	56.2	532.7	414.6	331.7

C. Supporting Information Chapter 6

Table S C.1 Main properties of volatile organic compounds (VOC) (Balseiro-Romero, 2014).

	Benzene	Toluene	Ethyl-benzene	o-Xylene	m-Xylene	p-Xylene	MTBE	ETBE
Formula	C_6H_6	C_7H_8	C_8H_{10}	C_8H_{10}	C_8H_{10}	C_8H_{10}	$C_5H_{12}O$	$C_6H_{14}O$
Molecular weight (g mol^{-1})	78.11	91.14	106.17	106.17	106.17	106.17	88.15	102.18
Melting point (°C)	5.9	-95.0	-95.0	-25.2	-47.8	13.2	-108.6	-94.0
Boiling point (°C)	80.1	110.6	136.2	144.5	139.1	138.4	55.0	69.0
Density (g cm^{-3}, 20 °C)	0.8765	0.8669	0.8670	0.8802	0.8842	0.8611	0.7578	0.7450
Water solubility (g L^{-1}, 25 °C)	1.80	0.47	0.14	0.20	0.17	0.20	51.6	26.0
Log Kow	2.16	2.69	3.15	3.15	3.20	3.15	1.06	1.48
Log Koc	1.92	2.39	1.98	2.35	2.11	2.52	1.05	1.57
Vapour pressure (Pa, 25 °C)	12654	3786	1546	767	833	787	31156	28000
Henry's law constant (Pa m^3 mol^{-1}, 25 °C)	576	474	559	542	731	762	59	166

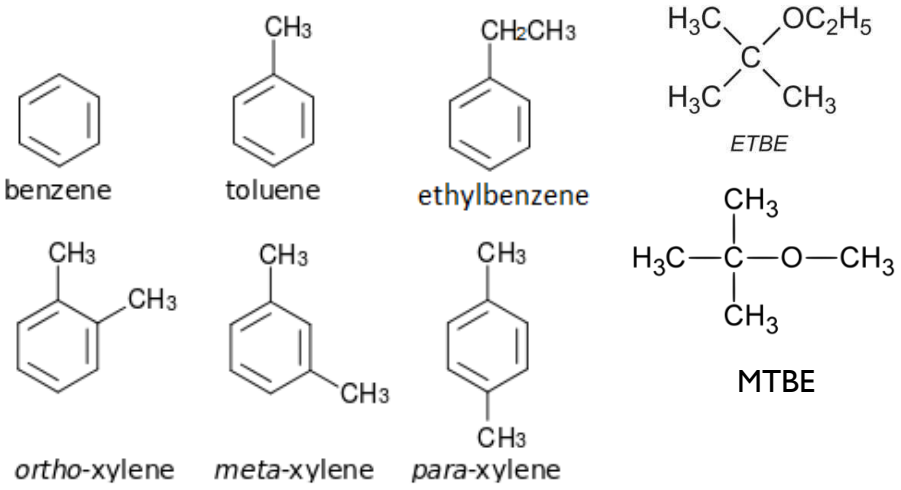

Figure S C.1 BTEX and FO molecular structure.

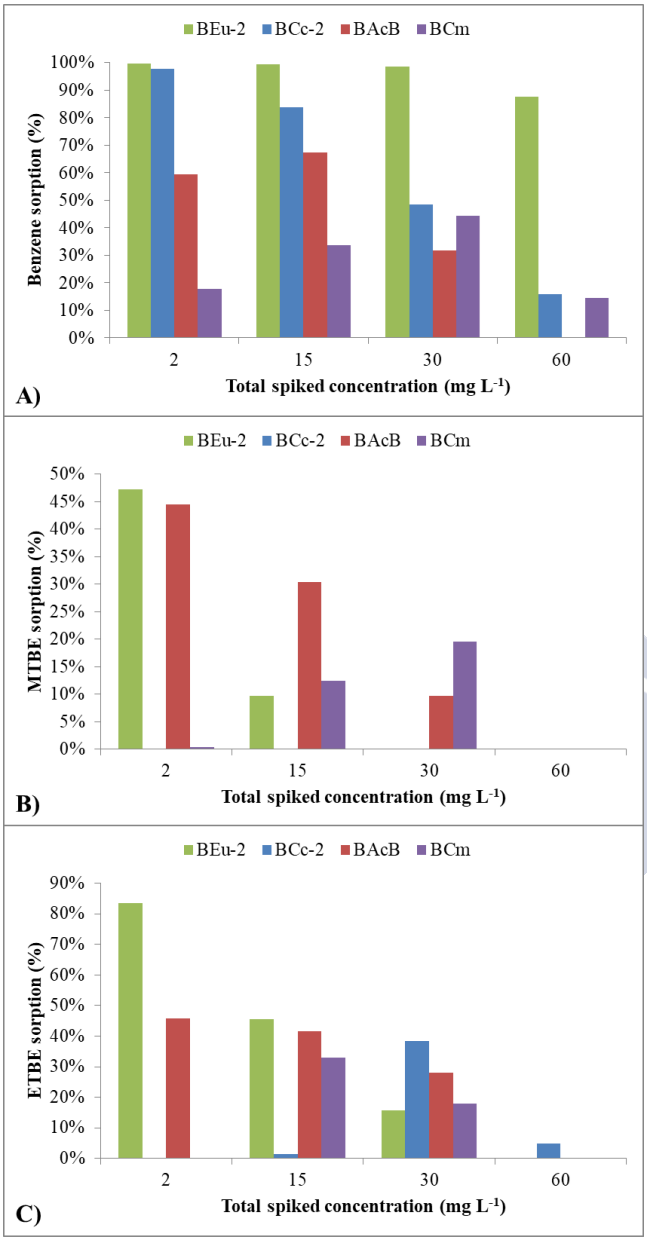

Figure S C.2 Sorption of benzene, ETBE and MTBE by the biochars at different initial spiked concentrations (concentrations above 60 mg L^{-1} yield to +95% recovery).

D. Supporting Information Chapter 7

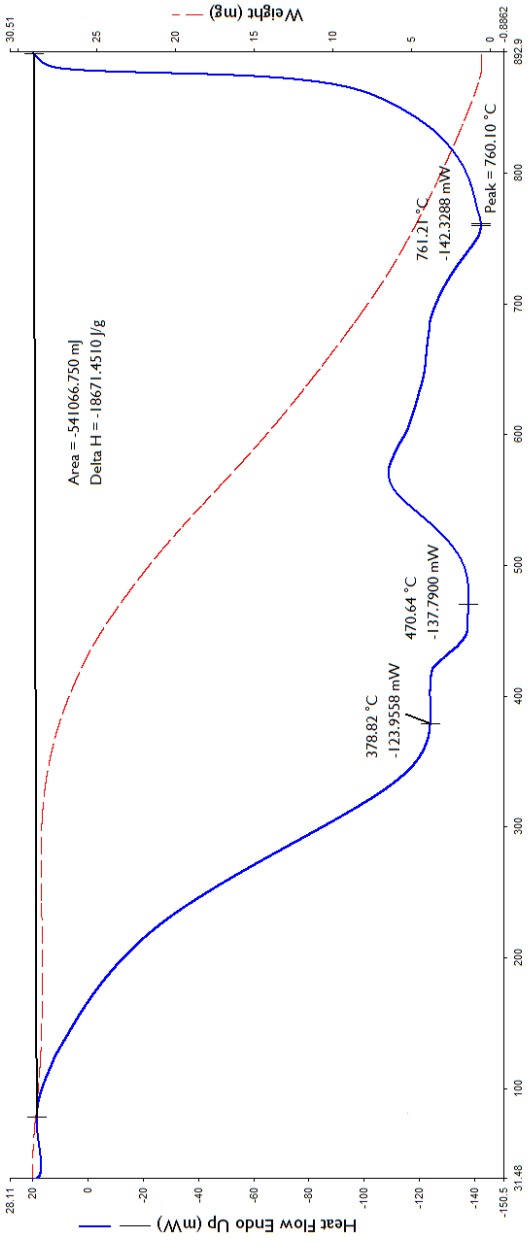

Figure S D.1 Coal TGA-DSC thermograph obtained with procedure developed by Harvey et al. (2012)

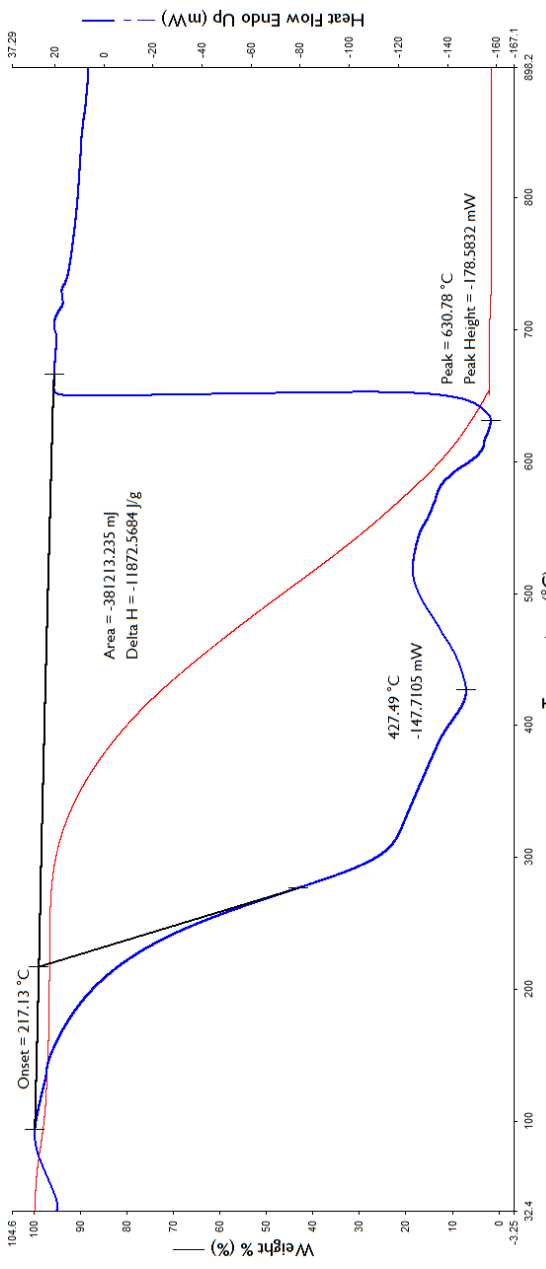

Figure S D.2 BtrunkTGA-DSC thermograph obtained with procedure developed by Harvey et al. (2012).

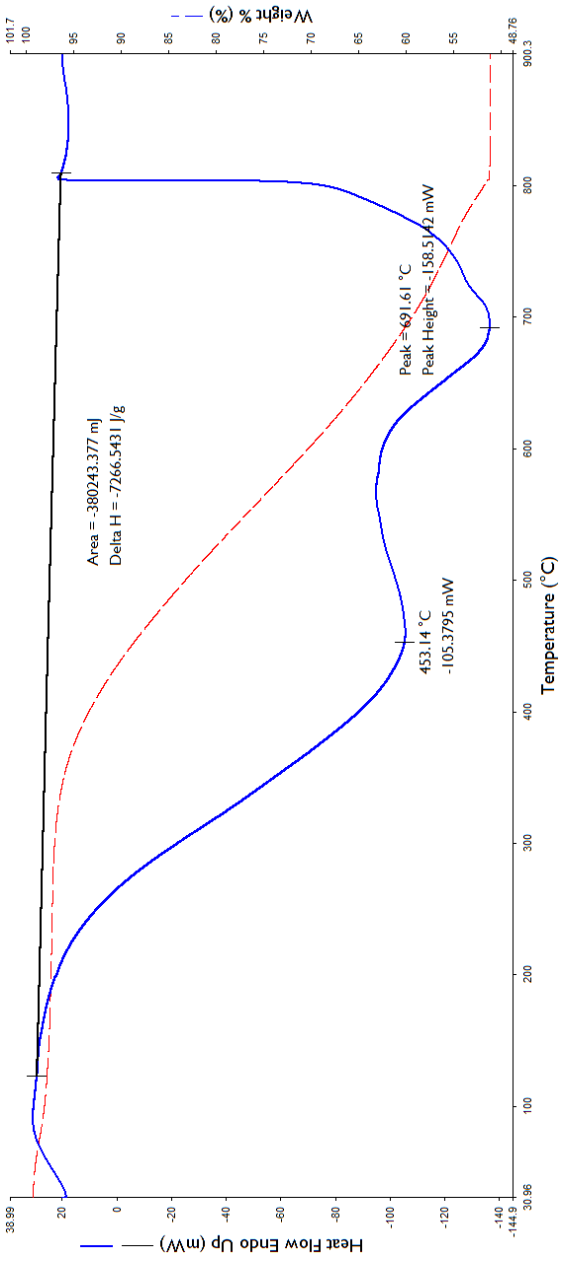

Figure S D.3 Bbark TGA-DSC thermograph obtained with procedure developed by Harvey et al. (2012).

USC
UNIVERSIDADE
DE SANTIAGO
DE COMPOSTELA

AGRADECIMIENTOS

Como dice el refrán "de bien nacido es ser agradecido" y esta tesis no existiría sin la ayuda de mucha gente. En primer lugar quiero agradecer a mi director Felipe Macías por ofrecerme la oportunidad de formar parte de su equipo. Gracias por tu ayuda, por recibirme siempre con una sonrisa entrañable y con un "por supuesto" a toda petición, pero sobre todo me gustaría agradecerte que lleves la ciencia al mundo real y pongamos nuestro granito de arena (en forma de Tecnosol) para dejar la Tierra un poquito mejor.

En segundo lugar quiero agradecer a mi directora neozelandesa Marta Camps. Gracias por acogerme en Nueva Zelanda y convertirte en mi tutora en la parte final de la tesis, fuiste el empujón indispensable para que este libro cogiera forma. I want to take the opportunity to acknowledge the rest of Massey team. Thank you very much to Roberto and Quinhua, not only for the unconditional help in the lab, but also for opening the doors of your houses to us and made really nice my internship in New Zealand. Thanks also to all my lab colleagues and soils PhD students for being really kind and for the good moments we passed. I cannot forget Ian, Glenys, Bob and the other lab technicians always ready to help.

A Felipe Macías García, a Clara y José por los momentos que compartimos en Touro y por convertirse en expertos productores de biochar.

Un millón de gracias a todos y cada uno de los técnicos del laboratorio de edafología: Carmen, Paco, David, María, gracias por ayudarme, enseñarme y sobre todo por vuestra paciencia para responder una y mil veces todas mis preguntas.

Gracias a los vecinos de laboratorio, Juan, Sara y Rocío por ofrecer siempre vuestra ayuda incondicional aun cuando no os correspondía y por todo lo que me habéis enseñado.

Gracias a mis compañeros del Instituto: Maca, Ramón, María, Elena, Bea, Pepe, Andrés, Carmina, Luis, Darío, Adriana, Tere, Raiana, … por los momentos compartidos dentro y fuera del laboratorio, por escuchar y ayudar en los momentos de estrés, por las cañas, celebraciones, excursiones etc. etc. etc. En especial me gustaría agradecer a María y Elena, sois las mejores compañeras que nadie puede pedir, siempre dispuestas a ayudar en lo que sea, sin una mala cara ni una mala contestación. Y gracias por tener una cama para mí en los "building team time".

Thanks to my flatmates in New Zealand, you were our family there, for your crazy behaviour, our conversations to change the world and your encouragement.

A los nuevos amigos que han ido apareciendo durante estos años Esther, Marta, Joan, Marina, Monchi, Cuca, Ángela, Elena, los "in-extremidos", las leopardo, Gabi y Libia, Tamara, mi familia Blablacar… y todos los que aunque no nombre me habéis acompañado durante este periodo, gracias por ejercer de válvula para liberar presión, por las risas, los buenos momentos y por ser mi familia en el norte.

A mi "Burbuja", porque en contra de los pronósticos, la distancia no es el olvido. Los años pasan, la familia crece, pero vosotros siempre estáis ahí.

A mi familia política, gracias por vuestro apoyo y Antero gracias por tus enseñanzas, las visitas a la central y las analíticas.

A mi familia, por ser siempre mi pilar y mi referencia. En primer lugar quiero agradecer a mi hermana Mirian por leerse la tesis y hacer de correctora nativa, deberían darte la doble titulación en biomedicina y biochar! Y por ponerme un reto muy difícil con la brillante presentación de tu tesis, a pesar de ser mi hermana pequeña eres, has sido y serás mi ejemplo a seguir. A mi hermana Ana, por tomarnos siempre de referencia y querer seguir nuestros pasos, gracias por todas tus visitas que hacen más llevaderas la distancia. A mis padres, por apoyarnos siempre, por ser un ejemplo de fuerza y sacrificio, por enseñarme que con trabajo todo se

puede conseguir y nunca poner limitaciones a nuestra formación y carrera profesional aunque ello supusiera volar del nido. A mis yayos, mis segundos padres, siempre orgullosos de sus nietas, yayo gracias por ser el vivo ejemplo de la lucha continua, el afán de superación y de que aunque uno se caiga se puede levantar.

A ti, por estar siempre ahí, en la salud y en la enfermedad, en las alegrías y en las penas… Gracias por enseñarme a hacer estadística, a mejorar gráficos, pero sobre todo por tu paciencia infinita, que si es difícil terminar una tesis más lo es cuando tu compañera también lo está haciendo y ser capaz de atemperar los nervios de ambos. Juntos empezamos esta aventura de hacer una tesis y juntos la terminamos "más sabios", con más experiencias vividas y más unidos que nunca.

"No tiene ningún sentido que la criatura con el mayor desarrollo intelectual que haya caminado sobre el planeta esté destruyendo su única casa", Jane Goodall, primatóloga y antropóloga